IN THE UNITED STATES PATENT AND TRADEMARK OFFICE

Applicants:	Richard James Lewis, et al.	**Examiner:**	Hugh Parker Young
Serial No:	10/537,704	**Art Unit:**	1654
Filed:	December 12, 2005	**Docket:**	16095
For:	NOVEL χ-CONOTOXIN PEPTIDES (-1)		
Confirmation No:	6539		

Commissioner for Patents
P. O. Box 1450
Alexandria, VA 22313-1450

DECLARATION OF DR. RICHARD J. LEWIS UNDER 37 C.F.R. §1.132

Sir:

I, Richard J Lewis, hereby declare as follows:

1. I am a co-inventor named in the above-identified application. I hold a joint appointment as Chief Scientific Officer (CSO) with Xenome Ltd. and Group Leader (Molecular Pharmacology) with the Institute for Molecular Bioscience (IMB), University of Queensland.

2. I have over 20 years experience in the isolation, purification, structure elucidation and pharmacology of marine toxins, particularly those acting at ion channels and transporters. I currently head an NHMRC Program Grant focused on dissecting pain pathways using conotoxins. I have established a strong international reputation in the field of venom peptides, and am considered as a major contributor to the emergence of venom peptides as a new source of therapeutics for intractable diseases such as chronic pain. I have over 160 publications, including over 130 original research articles in peer reviewed journals such as *Nature Neuroscience, EMBO Journal, Journal of Biological Chemistry, Structure,*

Journal American Chemical Society and *PNAS*, and numerous review articles in prestigious journals including *Nature Reviews Drug Discovery*. I have been named as a co-inventor on 9 patent applications. I was the Chair of the Gordon Research Conference on Mycotoxins and Phycotoxins. Presently I am a member of the Editorial Board of *Biochemical Pharmacology, Toxicon and Current Molecular Pharmacology.*

3. I am familiar with the subject matter disclosed and claimed in the above-identified application (" the '704 application"). In general, the '704 application is directed to novel χ-conotoxin peptides, which are useful as inhibitors of neuronal amine transporters. I have also read the Office Action dated November 1, 2007, issued in the '704 application. I understand that the Examiner has cited U.S. Patent No. 6,767,896 to McIntosh et al. ("the '896 patent") and U.S. 2005/0271589 A1 by Jones et al. ("the '589 publication") as prior art against the '704 application. I have been asked to comment on these cited references and their relevance to the χ-conotoxin peptides claimed in the '704 application.

4. It is my understanding that the Examiner is of the opinion that the conotoxin peptide claimed in the '704 application, particularly, the χ-conotoxin peptide having the sequence, pGluGlyValCysCysGlyTyrLysLeuCysHisHypCys (SEQ ID NO: 4), is obvious to the skilled artisan in light of the teaching of the '896 patent, alone or in combination with the '589 publication. Specifically, the Examiner has made the following statement on page 4 of the Office Action:

> "[T]he issue presented is whether one of ordinary skill in the art at the time of the invention would have been motivated by the teachings/suggestions of McIntosh et al. alone or in view of Jones et al. to select pGlu in position 1 of same conotoxin peptide (over native Asn) of McIntosh et al. ... from a Markush group of ONLY three amino acid options (Asn, Gln, pGlu) – 1 of which, Asn, is the native amino acid." (Emphasis in original).

5. Based on my review of the '896 patent and the '589 publication, it is my opinion that in the first instance, there is no basis in these references that would suggest to one to select the Mar1 peptide specifically, and then the N-terminus of Mar1, as the basis of modification in order to obtain SEQ ID NO: 4 of the '704 application. Further, I find no basis in these references that would suggest to one to substitute the N-terminal Asn of Mar1 with

pGlu. pGlu is disclosed in the '896 patent as an alternative to Gln, which is found in the native peptide designated as Q819. It is my opinion that such disclosure is limited and unrelated to Mar1, especially considering that a Asn-pGlu substitution had never been documented in the literature and is considered to be a non-conservative substitution. The applicant of the '704 application was the first to make such a substitution and to demonstrate the superior, unexpected properties of the resulting peptide (SEQ ID NO: 4).

6. The '896 patent discloses conotoxin peptides characterized by a general formula I, as set out in SEQ ID NO: 1:

Xaa-Xaa_0-Xaa_1-Cys-Cys-Gly-Xaa_2-Xaa_3-Xaa_4-Cys-Xaa_5-Xaa_6-Cys-Xaa_7 (SEQ ID NO: 1)

According to the '896 patent, each of Xaa, Xaa_1, Xaa_2, Xaa_3, Xaa_4, Xaa_5, Xaa_6, and Xaa_7 (i.e., nine out of the fourteen amino acid positions) can be selected from a group of possible amino acid residues.

7. The '896 patent further discloses several sub-generic peptides that fall "within general formula I":

Asn-Gly-Val-Cys-Cys-Gly-Xaa_1-Xaa_2 -Leu-Cys-His-Xaa_3 -Cys	(SEQ ID NO:2);
Gly-Val-Cys-Cys-Gly- Xaa_1-Xaa_2-Leu-Cys-His-Xaa_3-Cys	(SEQ ID NO:3);
Gly-Ile-Cys-Cys-Gly-Val-Ser-Phe-Cys- Xaa_1- Xaa_3 -Cys	(SEQ ID NO:4);
Ala-Cys-Cys-Gly- Xaa_1-Xaa_2-Leu-Cys-Ser-Xaa_3 -Cys	(SEQ ID NO:5);
Xaa_4-Thr-Cys-Cys-Gly-Xaa_1-Arg -Met- Cys-Val- Xaa_3-Cys-Gly	(SEQ ID NO:6);
Ser-Thr-Cys-Cys-Gly-Phe-Xaa_2-Met-Cys-Ile- Xaa_3-Cys-Arg	(SEQ ID NO:7).

Each of Xaa_1, Xaa_2, Xaa_3, Xaa_4 in SEQ ID NOS: 2-7 is also selectable from a group of amino acids. When certain amino acid is selected for each of the Xaa's in SEQ ID NOS: 2-7, the following six specific conotoxin peptides are derived, which, according to the '896 patent, represent native conotoxin peptides from various Conus species (see col. 4 and col. 22 of the '896 patent):

Mar 1: Asn-Gly-Val-Cys-Cys-Gly-Tyr-Lys-Leu-Cys-His-Hyp-Cys

Mar 2: Gly-Val-Cys-Cys-Gly-Tyr-Lys-Leu-Cys-His-Hyp-Cys

U036: Gly-Ile-Cys-Cys-Gly-Val-Ser-Phe-Cys-Tyr-Hyp -Cys

Q818: Ala-Cys-Cys-Gly-Tyr-Lys-Leu-Cys-Ser-Hyp -Cys

Q819: Gln-Thr-Cys-Cys-Gly-Tyr-Arg-Met-Cys-Val-Hyp-Cys-Gly

Q820: Ser-Thr-Cys-Cys-Gly-Phe-Lys-Met-Cys-Ile-Hyp-Cys-Arg

8. The Examiner has provided the following assessment of the '896 patent on page 3, bottom paragraph of the Office Action:

> "As to the modified conotoxin peptide formula of McIntosh et al., the native conotoxin peptide options are fixed as the first option of each Xaa option of the formula. And specifically, as to Xaa1 (Asn, Gln, pGlu) and Xaa6 (Pro, hydroxyl-Pro (e.g., 4-hydroxyproline) or g-Hyp) – there are ONLY three amino acid options thereto, one of which is the native amino acid. As to the latter, hydroxyl-Pro is a known modified amino acid version of Pro. It is the Xaa1 position that is primarily at issue here and discussed in detail below." (Emphasis in original).

9. By "formula", I believe the Examiner is referring to formula I of the '896 patent. In my review of the '896 patent, there is no teaching for a preference to select native amino acid options over non-native amino acid options. Further, as discussed above, the '896 patent discloses six (6) specific native conotoxin peptides (Table on col. 4 of the '896 patent). Although these six specific peptides all fall within general formula I, the amino acid sequences of these peptides vary significantly. Thus, even if one were to select each Xaa option of formula I based on amino acids found in a native conotoxin peptide, there are multiple options to select. For example, among the choices provided for each of the Xaa's in formula I, there are three to five possible amino acid options for each of the following seven Xaa positions, all representing amino acids found in a native conotoxin peptide:

Xaa: des-Xaa, Asn, Gln
Xaa0: des-Xaa, Gly, Ala, Ser
Xaa1: Val, Ala, Thr, Ile
Xaa2: Phe, Tyr, Val
Xaa3: Lys, Arg, Ser
Xaa4: Leu, Phe, Met
Xaa5: His, Tyr, Ser, Ile, Val

10. Even if one were to select amino acids based on the first choice given for each Xaa's in the '896 patent, one would arrive at the sequence, Val-Cys-Cys-Gly-Phe-Lys-Leu-Cys-His-Hyp-Cys, which would miss two amino acids (pGlu-Gly) at the N-terminus and have a "Phe" instead of "Tyr", as compared to SEQ ID NO: 4 of the '704 application.

11. Based on my review, I find no basis in the '896 patent for the selection of the Mar1 peptide, or any other of the six native peptides, as a basis for further modification. Stability has been one of the key advantages of disulfide-rich conotoxins, having evolved to remain intact in venom for months and perhaps longer before being deployed in prey capture and defense. The chi conotoxins such as Mar1 are highly networked with four of 13 residues involved in disulfide bridges, and like other disulfide-rich conotoxins, stability was considered to be an already inherent advantage of this family. The '896 patent does not disclose any need or advantage for further modifying any of the six native peptides.

12. Furthermore, I find no basis in the '896 patent for specifically selecting the N-terminal residue of Mar1 (Asn) as a basis for further modification. Based on formula I, theoretically, seven out of the thirteen amino acids of Mar1 can be substituted with a different amino acid residue, which again, can be selected from a group of amino acid options. Moreover, the '896 patent discloses Mar1 as fitting the sub-generic sequence of SEQ ID NO: 2. Based on SEQ ID NO: 2, theoretically, three amino acid positions of Mar1 can be modified, each position having several choices of amino acid residues. Notably, none of these three amino acid positions is the N-terminal residue.

13. With respect to pGlu, I have noticed only two mentions of pGlu in the '896 patent. The first mention appears in the context of formula I (col. 3, line 23), where pGlu is listed as one of four possible choices for the N-terminal amino acid of formula I. Again, this formula will not give rise to SEQ ID NO: 4 of the '704 application unless each of the remaining eight Xaa residues is specifically selected to correspond to the native Mar 1 or Mar 2 amino acid residues. The second mention of pGlu appears on column 4, line 16-17 of the '896 patent. Here, pGlu is disclosed as a possible alternative for Gln as the N-terminal

residue of SEQ ID NO: 6. SEQ ID NO: 6 of the '896 patent differs from instant SEQ ID NO: 4 in several other amino acid positions.

14. It is my opinion that the inclusion of pGlu in the list of options in formula I relates directly to SEQ ID NO: 6, and that the limited disclosure relating to pGlu in the '896 patent would not be understood as suggesting to one to make the Asn to pGlu substitution in the Mar1 peptide specifically. In fact, focusing on the N-terminus, I am unaware of any precedent in conotoxin research, nor indeed in the much wider field of peptides, for such a substitution, nor was there previously any recognized need for such a substitution. To the best of my knowledge, and despite extensive literature searching to locate another example, the substitution of Asn by pGlu is not a previously known substitution, and SEQ ID NO: 4 of the '704 application represents the first example of such a substitution. Experimental results to date demonstrate a number of unprecedented advantages conferred by this substitution. Preclinical animal studies demonstrate efficacy, a good safety profile and a long duration of action in hard to treat pain conditions. Below I have summarized experimental data and discussed the results of literature searches in support of my position.

Literature Searches:

15. *The Pyroglutamate Residue: Natural Derivation Solely From Gln And Glu.* The natural formation of the pyroglutamate residue occurs **exclusively** when an N-terminal glutamine (Gln) or glutamic acid (Glu) residue cyclizes, i.e., the free amino group condenses with the amide group to form a lactam covalent link. While the mechanism for the Gln-pGlu conversion is well characterized[1], the mechanism for the rearrangement of Glu to pGlu is still not well understood.[2] Rearrangements to pGlu occur spontaneously when Gln and Glu are in the N-terminal position. The formation of pGlu effectively 'caps' or blocks the N-terminus allowing no more amino acid additions.[2,3] Importantly, there are **no** known cases of pGlu residues formed by rearrangement of other amino acid residues. Thus, nature provides no clue that a pGlu residue could be used to improve a peptide's characteristics, unless that peptide already possesses either N-terminal Glu or Gln residue.

---

[1] Abraham, GN& Podell, DN (1981) *Mol Cell Biochem 38*: 181-190 (attached hereto as **Exhibit 1**).
[2] Yu, L. et al (2006) *J Pharm Anal 42(4)*: 455-463 (**Exhibit 2**).
[3] Garden RW *et al.*, (1999) *Journal of Neurochemistry 72*, 676-681 (**Exhibit 3**).

16. *Previous Studies On pGlu-Containing Peptides: No Known Asn To pGlu Substitutions.* There are a number of literature examples of peptides where the pGlu residue is used in structure activity relationship (SAR) studies. However, despite extensive searching, I have not been able to locate **any** example of peptide where a N-terminal residue Asn has been replaced by a pGlu, and extremely few examples where the pGlu replacement is for any other residue than Glu or Gln. In many cases, even when the N-terminal **is** a Glu or Gln, the replacement by pGlu does not necessarily provide a genuine advantage. For example, Beck et al (2001)[4] replaced N-terminal Gln by a pGlu and although the resulting peptides demonstrated higher chemical stability than the parent peptides, they were less active. Therefore, in that case, the replacement of Glu by pGlu resulted in a net disadvantage. In another study, Tekiran et al (1999)[5] found no difference in the activity of their N-terminal glutamate and pyroglutamate amyloid peptides. In a different study, **addition** of pGlu to an N-terminus conferred some advantages, but, unlike SEQ ID NO: 4 of the '704 application, this was not an example of amino acid replacement.[6] Of note, the same peptides were later found to be insufficiently stable *in vivo* to be useful, thus demonstrating that the addition of pGlu by no means confers predictable advantages to a peptide.[7]

17. While the presence of pGlu in naturally occurring peptides is not rare (for example pGlu occurs in Eledoisin, crab hyperglycaemic neuropeptides, some conotoxins and many other peptides), it exists as a post translational modification (PTM) of Gln or Glu, not of any other amino acid. While the substitution of these particular residues by pGlu in SAR studies has precedence, there is no general rule that identifies this particular form of N-terminal blocking as conferring special advantages over other forms such as simple N-terminal acetylation. Indeed, pGlu is not considered to be a particularly stable entity and there has been a long recognized need for a means of stabilizing the pGlu residue from enzymatic degradation (pyroglutamyl aminopeptidase) in a drug development context.[8] For example, Irwin et al (2005)[8] used palmitate-derivatized analogues of pGlu-containing peptides to

---

[4] Beck, A. *et al.*, (2001) *J Pept Res 57(6)*: 528-538 (**Exhibit 4**).
[5] Tekiran, TL *et al* (1999) *J. Neurochem 73(4)*: 1584-1589 (**Exhibit 5**).
[6] Harte, FPM *et al* (2002) *Diabetologica 45*: 1281-1291(**Exhibit 6**).
[7] Irwin N. *et al* (2005) *J Med Chem 48(4)*: 1244-50 (**Exhibit 7**).
[8] Moss J & Bundgaard H (1992) *Acta Pharm Nord 4(4)*: 301-8 (**Exhibit 8**).

extend their biological half lives, the pGlu-peptides being insufficiently stable to be considered viable drug candidates. Thus, in general, while N-terminal blocking is a useful strategy for improving peptide stability, a more conservative approach is usually adopted (i.e., N-acetylation of existing residues), to avoid reducing or changing the activities inherent in a parent peptide. pGlu blocking strategies have previously been utilized in a pre-emptive sense in N-Glu or N-Gln cases (i.e. because these residues would naturally cyclize to form pGlu), but this is also a conservative approach. There has been no known advantage demonstrated for pGlu substitutions outside of this limited field of use.

18. Furthermore, N-terminal capping can seriously disrupt the structure (and hence activity) of a peptide. For instance, N-capping provides improved helical propensity. The helix capping propensity are ranked amongst amino acids as Asn > Ser, Gly > Thr, Leu, Ile > Pro, Met > Val > Ala > Gln. It is evident that Asn and Gln/pGlu are at opposing ends of the helical propensity scale, indicating that replacing Asn by a Gln/pGlu may have non-conservative structural ramifications. Thus, from a N-terminal capping perspective, a Gln/pGlu residue is the LEAST likely replacement for Asn as it would have the greatest disruptive potential on a native structure.

19. Of particular relevance, is that pGlu-substitution has previously been applied only in the case of linear peptides which are generally unstable. There have been no known cases of the application of this form of N-capping to stabilized peptides with strong disulfide bridge networks. Stability has been one of the key advantages of disulfide-rich conotoxins, having evolved to remain intact in venom for months and perhaps longer before being deployed in prey capture and defense.[9] The chi conotoxins such as MrIA are highly networked with four of 13 residues involved in disulfide bridges, and like other disulfide-rich conotoxins, stability was considered to be an already inherent advantage of this family. The applicant of the '704 application was the first to recognize a need for further stabilization of this class, and also to explore beyond the traditional bounds of simple N-terminal acetylation to seek a successful solution.

[9] Adams, D *et al.*, (1999) *Drug Discovery Research 46*, 219-234 (**Exhibit 9**).

Conotoxins and pGlu.

20. Conotoxins are peptides discovered in the venoms of cone snail. There are potentially as many as 50000+ peptides belonging to many different classes.[10] Conotoxins are classified by their primary structure, pharmacological activity and, where present, their disulfide pairings. Examples include omega conotoxins (3 disulfide bridges, blocks voltage-sensitive calcium channels), mu conotoxins (3 disulfide bridges, blocks voltage-sensitive sodium channels), alpha conotoxins (2 disulfide bridges, blocks nicotinic acetylcholine ion channels) and chi conotoxins (2 disulfide bridges, blocks Norepinephrine Transporter). It is important to note that SAR studies for one conotoxin class generally have no relevance to those of a different class. Quite rationally, SAR studies for each conotoxin class are determined on a case-by-case basis.

21. Post-translational modifications have been identified on conotoxins, but surprisingly few examples of pGlu formation – and again, those that exist are formed exclusively from N-terminal Glu or Gln residues. The occurrence of an N-terminal Gln rearranging to a pyroglutamate is cited in Shon et al.,[11] for a mu conotoxin. This peptide has no similarity in sequence, structure or function to peptides of the chi-conotoxins (MrIA or related peptides). Further mention of pyroglutamate and conotoxins is made in the '589 publication (e.g., in Paragraph [0014]), cited by the Examiner, and related applications in describing the beta-superfamily family of conotoxins, a superfamily that is not classified according to standard conotoxin nomenclature and is not characterized in any manner that would link such members into an organized family (unlike other conotoxin families). Furthermore, a review of the sequences the beta-superfamily family of conotoxins makes it evident that many of the peptides belong to other conotoxin superfamilies. There is, in short, no evidence to support the existence of a B-superfamily. In any case, the subject matter of these applications is broad and not well-defined, but clearly pertains to a different class of peptide than the chi conotoxins, which is tightly defined in terms of structure and pharmacology and belongs to the T-superfamily of conotoxins. What is relevant or desirable for one set of class of peptides is not necessarily translatable to another class, let alone another

[10] Olivera, B. & Cruz, L. (2001) *Toxicon 39*, 7-14 (**Exhibit 10**).
[11] Shon *et al.*, (1998). *The Journal of Neuroscience 18 (12)*, 4473 – 4481 (**Exhibit 11**).

superfamily. In these applications, the mention of pGlu is in mere passing and, significantly, limited to the following: "The N-terminal Gln may be substituted with pyro-glutamate (Z)." Paragraph [0014] of the '589 application. This sole mention of pGlu reflects the spontaneous rearrangement that occurs in nature, and is not a recognition of the need for N-terminal stabilization. Despite a long list of potential substitutions, there is no mention of an Asn-pGlu conversion or replacement. There is no recognition of any advantage in making such a substitution in the '589 publication.

22. The '896 patent relates to peptides that are structurally similar to MrIA and could conceivably belong to the same class (chi conotoxin), had they had similar primary structure **and** demonstrated activity at the same pharmacological target (NET). As discussed above, there are only two mentions of pGlu in this patent – once being in the list of options for the N-terminal residue in formula I; the other time being the alternative of Gln as the N-terminal residue of SEQ ID NO: 6. The '896 patent also discloses Q819, which is a specific native peptide that falls within formula I and also fits the subgeneric formula of SEQ ID NO: 6. Q819 has a Gln at its N-terminus. Studies conducted under my supervision (see Example 4 below) have confirmed that Q819 is likely to belong to a different and as yet unidentified class as it displays no activity at the norepinephrine transporter (NET), even at high concentrations (unlike SEQ ID NO: 1 and SEQ ID NO: 4 of the '704 application). It is unreasonable to translate the effects of amino acid substitutions across classes, because the SAR studies will invariably be different across different pharmacological targets. Thus, even assuming that the '896 patent may have suggested making a substitution of Gln with pGlu in Q819, such disclosure is, in my opinion, not relevant to assessing possible substitutions in Mar1 because (1) peptides of the chi conotoxin class are a different class of conotoxin peptides, and (2) a substitution of Asn in Mar1 with pGlu is a non-conservative substitution, in contrast to a Gln-pGlu substitution. There is simply no recognition in the '896 patent that peptides of the chi conotoxin class would require further stabilization than that already provided by nature in the form of disulfide bridges and the native venom peptide sequence.

23. *One additional modification in Xen2174* - It is important to note that a specific peptide disclosed in the '704 application, Xen2174, is a peptide having the amino acid

sequence of SEQ ID NO: 4 and having its C-terminus amidated. The C-terminus amidation is believed to provide additional advantages in stability.

Experimental Data On Xen2174 And Other MrIA Analogues

24. It is my contention that the N-terminal residue of chi-conopeptides plays a determining role in several key features of the class. The following examples are provided to support the case that Xen2174 has clear and unexpected advantages over SEQ ID NO: 1 (also known as Mar1 or χ-MrIA) and other chi conotoxins, which make Xen2174 an exceptional candidate for drug development. To focus on the advantages of the pGlu residue alone, comparisons have been made between C-terminally amidated analogues. However, it should be noted that MrIA/Mar1 (SEQ ID NO;1) is in fact the free acid and that Xen2174 differs from MrIA in having pGlu instead of Asn at the N-terminus and being amidated at the C-terminus.

25. *Example 1 – Chemical Stability.* Chemical stability is an important requirement for any compound, but particularly so for medicinal products. To test for chemical stability, compounds were placed in various buffers and temperatures with the rate of breakdown monitored. 37°C was used to mimic the temperature that the compound would be exposed to as a therapeutic. The buffer was also chosen to match an acceptable buffer for the intended application – in this case human intrathecal (IT) administration. The chemical stabilities of Xen2174 and Mar1 (or χ-MrIA) were determined in 10 mM acetate/0.9% saline buffer. Stability was measured at 4°C and 37°C (body temperature). Both peptides show good stability at 4°C and good short-term stability even at 37°C. However, the stability of Mar1 is less than that of Xen2174 at all time points measured out to at least 31 days (see Fig. 1, attached as **Exhibit 12**). Mar 1 degraded by a small amount almost immediately whereas Xen2174 did not. In practical terms, these results indicate that Mar1 would **not** be suitable for use in chronic conditions that would require the peptide to be stored in an implantable pump or other delivery device at body temperature. On the other hand, these results strongly support the suitability of Xen2174 for chronic and long-term use. Thus, Xen2174 offers a significant advantage over Mar1 for long-term use in an implanted delivery device.

26. *Example 2 – Plasma Stability.* In addition to chemical stability, it is also important to assess how the compound would behave exposed to enzymes present in plasma. To understand this in a laboratory environment rat plasma is used – again the temperature was 37°C to mimic body temperature. Plasma is typically a harsher environment than buffer alone, having many components able to either breakdown peptide bonds (e.g. enzymes) or scramble the disulphide bonds (e.g. free thiols). For these studies, 50 µL of 1 mg/mL peptide was added to 50 µL of rat plasma. The samples were vortexed and incubated at 37°C before 500 µL 10% MeOH/2% TFA was added to stop the reaction at specific time points. The fixed sample was vortexed and centrifuged for 1 min. The sample was subsequently analyzed on LC/MS (Zorbax 300SB C18, 4.6 x 250 mm, flow rate 1 mL/min @ 50°C: MS – 300 – 2200 amu, DP48, FP315, 350°C, 60 µL injection volume). In terms of rat plasma stability at 37°C, the stability of Mar1 is again poor relative to Xen2174 at all time points out to at least 2 hr (see Fig. 2, attached as **Exhibit 13**). Xen2174 has a longer plasma half life, and as such, is expected to support a longer duration of action in humans.

27. *Example 3 – Therapeutic Index: Side Effects Vs Efficacy.* In terms of efficacy relative to side effects (otherwise known as the therapeutic index, a critical predictor of product clinical safety), it is my opinion that the effects of N-terminal residue substitution are unpredictable for this class of peptide. For example, several peptides having only one amino acid difference from Xen2174 display significantly narrower therapeutic indices. Noticeably, these substitutions are at the N-terminus. Examples of these include SEQ ID NO: 11 where Xaa1 refers to D-arg (rGVCCGYKLCHOC-NH_2), D-asn (nGVCCGYKLCHOC-NH_2) or norleucine ([NLE]GVCCGYKLCHOC-NH_2). Each of these peptides has a narrow therapeutic window in a rat model of neuropathic pain (~ 3), despite having similar affinities at NET. By comparison, Xen2174 has a wide therapeutic index in this model (~30-fold). These data are summarized in Table 1 (**Exhibit 14**). Thus the choice of N-terminal residue for this peptide class is critical to avoid unwanted side effects in animals. The pGlu residue at the N-terminus provides a wide therapeutic index, whereas other amino acid substitutions at this position do not. This benefit was entirely unexpected at the time the '704 application was filed.

28. *Example 4 – Comparison Of Binding Affinity Of Mar1 And Q819 For The Human Noradrenaline Transporter (HNET).* Conotoxin classification is based on both sequence and function. There is no disclosure in the '896 patent that Q819 belonged to the chi conotoxin family, as no data were presented showing that Q819 bound to hNET or was effective in treating pain. It is my opinion that due to significant differences in primary sequence between Q819 and Mar1 (or MrIA), Q819 is not a chi conotoxin and belongs to an as yet unidentified but different class. My opinion is supported by experiments conducted under my supervision, in which a number of Q819-related peptides were tested for binding to NET, the chi conotoxin target. The results (Table 2, **Exhibit 15**) show that Q819 is not active at hNET even at high concentrations. A modification of Q819 was also made to substitute the N-terminal Gln with pGlu. This derivative was also found to be inactive at hNET. It is therefore my conclusion that Mar1 and Q819 belong to different classes of conotoxins, and therefore the range of substitutions available for one class (Q819) is not relevant to a different class (Mar1). Furthermore, it is my opinion that even if these two peptides did belong to the same class, a pGlu substitution occurs naturally as a Gln rearrangement in Q819, and therefore bears no direct relevance to the substitution of Asn-pGlu in Mar1, proposed by the Examiner.

29. Therefore, given that the N-terminal residue of chi-conopeptides can independently affect each of the criteria by which a drug is judged (efficacy, safety, and stability) and from the little that was known about chi conotoxin SAR at the date of filing the '704 application, it was not possible to predict which of many different possible N-terminal substitutions, in combination with the C-terminal amidation, would satisfy each of these criteria simultaneously. Therefore, the superior properties of Xen2174 were clearly unexpected.

30. To conclude, it is my opinion that there is no suggestion in the '896 patent or the '589 publication for selecting the Mar1 peptide, and then selecting the N-terminal amino acid position of this peptide, as the basis for further modification. Further, it is my opinion that there is no suggestion in the '896 patent or the '589 publication for substituting Asn of

Mar1 with pGlu. The '704 application provides the first example of a peptide having an Asn to pGlu substitution, that has been shown to possess superior, unexpected properties.

31. I declare further that all statements made herein of our own knowledge are true and that all statements made on information and belief are believed to be true; and further that these statements were made with the knowledge that willful false statements and the like so made are punishable by fine or imprisonment; or both, under Section 1001 of Title 18 of the United Stated Code, and that such willful false statements may jeopardize the validity of the application or any patent issuing thereon.

Dated: 10/4/2008

R. Lewis

Richard J. Lewis

EXHIBIT 1

Pyroglutamic acid

Non-metabolic formation, function in proteins and peptides, and characteristics of the enzymes effecting its removal

George N. Abraham and David N. Podell

Depts. of Medicine and Microbiology, and the Center for Interdisciplinary Research in Immunologic Diseases of the University of Rochester School of Medicine and Dentistry, Rochester, NY 14642, U.S.A.

Summary

The formation of pyrrolidone carboxylic acid (PCA, pGlu) during protein biosynthesis is discussed. Studies are summarized which demonstrate that PCA is formed during the later stages of biosynthesis at the terminal phases of translation or as a post-translational event, just prior to cellular secretion of protein with amino-terminal PCA. Of the studies cited, the most convincing evidence suggests that PCA is derived from glutamine. Enzymes which selectively remove PCA from the N-terminus, and of benefit in amino-acid sequence analysis, have been isolated and shown to have a ubiquitous distribution in various animal and plant cells. The investigations which lead to the isolation of these enzymes and the procedures for their use in removing amino-terminal PCA from proteins, are described. Finally, the biologic function of PCA and the effects of its chemical modification are discussed using the neuropeptide Thyrotropin Releasing Factor (TRF) as a specific example.

Introduction

Pyroglutamic acid (pGlu)*, also termed pyrrolidone carboxylic acid (PCA, pyr) or 5-oxo-L-proline, is an interesting cyclical amino acid. It may be formed either enzymatically as an intermediate in amino acid metabolic and transport pathways, or during protein biosynthesis during which it becomes the amino-terminal residue of many biologically significant peptides and proteins. Structurally, it may be considered to be internally cyclized glutamic acid. Although occasionally referred to as 5-oxo-L-proline, the designation may imply a possible derivation from this amino acid rather than from glutamic acid or glutamine and will not be utilized here.

In essence, the presence of the internal amide bond which forms between nitrogen -1 and carbon -5 produces unique properties for this common amino acid, and chemically defines PCA as 2-carboxy γ-butyrolactam. The interal linkage is neutral and functionally acts as an amide. The basic electron pair of nitrogen -1 is in resonance with and attracted toward carbon -5 by the presence of the double-bonded oxygen. Thus, unlike proline, PCA will not react with substances such as phenylisothiocyanate. Shown below are the formulas of PCA, and its two possible amino acid precursors, glutamine and glutamic acid.

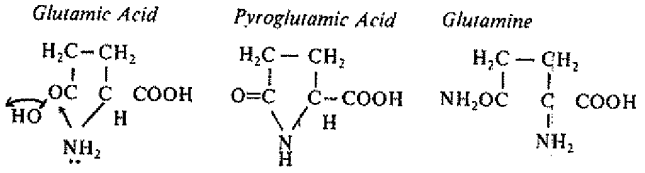

*The following terms and abbreviations are synonymous and will be utilized interchangeably throughout the text: pyroglutamic acid, pyrrolidonyl carboxylic acid, PCA, pGlu, pyr

Molecular and Cellular Biochemistry 38, 181–190 (1981). 0300–8177/81/0381–0181/$ 2.00.

The purpose of this review will be to (a) summarize studies which demonstrate how and at what stage PCA is formed during protein biosynthesis, (b) summarize the characteristics of the non-energy dependent enzymes which remove pGlu from proteins or transport forms of amino acids, (c) mention the various methods in primary amino acid sequence analysis and some of the types of proteins on which the non-energy dependent enzyme may be used, and (d) show in the instances studied how this unusual amino acid may impart activity to an important and biologically active peptide.

Pyroglutamic acid formation

The metabolic formation and utilization of pyroglutamate as an intermediate in the gamma-glutamyl amino acid transport cycle has been superbly reviewed by Van der Werf & Meister (1). The biochemical relationship between pyrrolidone carboxylic acid derived from the energy-dependent, enzyme-catalyzed reactions of this metabolic pathway and PCA which is formed as the amino terminus of many proteins and peptides has not been established. Briefly, in the gamma-glutamyl cycle, pyroglutamic acid is formed after the enzymatic removal (see below) of the N-terminal gamma-glutamate residue bonded to any one of a number of amino acids by the cytoplasmic enzyme gamma-glutamyl cyclotransferase (GCT). The pyroglutamate formed is then converted to L-glutamic acid by 5-oxo-L-prolinase. This latter enzyme, originally isolated from rat kidney and other tissues by Van der Werf *et al.* (1971), is unusual in that it instigates reactions which involve the co-hydrolysis of both the ATP and internal amide bonds. The reactions may be summarized as follows:

(a) gamma-glutamyl amino acid $\xrightarrow{\text{GCT}}$ pyroglutamate + amino acid

(b) pyroglutamate + L-glutamate $\xrightarrow[\text{ATP} \quad \text{ADP} + \text{Pi}]{\text{5-oxo-prolinase} + \text{Mg}^{++} + \text{k}^{+}}$

It has not been experimentally shown that the enzymes which catalyze the formation of pGlu in this pathway participate individually at some phase in biosynthesis of pGlu in proteins. It has been clearly demonstrated that ^{14}C-pyrrolidone carboxylic acid in culture medium is not utilized in protein biosynthesis. Kitos & Waymouth (5) added ^{14}C-pyrrolidone carboxylic acid (PCA) to culture media containing clone 929 mouse cells. After 4 days of culture the nutrient media, extracts of the cultured cells, and the atmosphere above the media were analyzed for ^{14}C. Nearly all of the radioactivity was recovered in the culture medium. This was then fractionated on cation exchange columns, and individual column fractions were subjected to paper chromatography in order to identify whether breakdown of (^{14}C) PCA had occurred. All radioactivity was obtained in a pool which migrated with an R_f identical to the pyrrolidone carboxylic acid standard. The authors concluded that the exogenous PCA was not taken up or utilized by murine L cells.

Subsequently, Moav & Harris (6) showed that addition of L-pyroglutamic acid (PCA) to cultures of rabbit lymph node cells did not affect the rate of cellular protein synthesis, nor was exogenous PCA incorporated into the rabbit immunoglobulin heavy chains which were synthesized and known to have this residue at the amino terminus. In an attempt to determine at what stage in protein synthesis PCA was incorporated, charged amino-acylated transfer RNAs were isolated from the lymph node cells and the acylated amino acids released and identified. The results suggested that PCA was bound to tRNA, and the authors speculated that the PCA-tRNA complex was most likely formed by cyclization of a glutamic-acid-tRNA-complex precursor.

Experimental support for this notion was provided by demonstrating that glutaminyl-tRNA can be converted *in vitro* to pyrrolidonyl carboxyl-tRNA. Bernfield & Nestor (7) isolated aminoacyl-tRNA synthetase and the pool of tRNAs from E. coli. Amino acids were then added to the tRNA pool using conditions which would acylate the tRNAs. Selectively labeled C^{14}-glutaminyl-tRNA was then isolated and treated with glutamine cyclotransferase (GCT) obtained from papaya latex (8). The acyl-amino acid was removed from the tRNA complex and shown to be pyrrolidone carboxylic acid. While the investigators did not rule out the possibility that glutamine might be converted to glutamic acid as an intermediate in the conversion

to pyrrolidonyl carboxyl-tRNA, they did provide some evidence which suggested that the action of GCT was specific for glutamine on the transfer RNA. Thus, it was not determined whether amino-terminal PCA was formed at the polypeptide or tRNA level.

Baglioni (9) extended these observations by using mouse myeloma cells whose predominant protein synthetic product was a monoclonal immunoglobulin with heavy chains containing amino-terminal PCA. Addition of radiolabeled glutamine, glutamic acid and PCA to culture media substantiated the earlier observations (5) that free PCA was not utilized or taken up by cells. Myeloma producing cells were incubated in the presence or (^{14}C) glutamine. Membrane bound polyribosomes from and immunoglobulin secreted by, these cells were isolated so that amino-terminal analysis could be performed on nascent and secreted radiolabeled proteins. The aminoterminal peptides were produced by pronase digestion and isolated by cation exchange chromatography of the digested proteins. Nascent protein was shown to contain predominantly N-terminal glutamic acid and secreted protein pyrrolidone carboxylic acid. Other data mentioned by the investigator were that (a) no PCA-tRNA was found in the cytoplasm of cells incubated with ^{14}C glutamine and (b) ^{14}C-PCA could not be charged to tRNAs extracted from these myeloma producing cells. Thus, the conclusion was reached that PCA must be formed by cyclization of an amino terminal glutamine most likely *after* conversion to glutamic acid on the polyribosome or just prior to secretion of the completed protein.

While the above data suggested that PCA could not be directly incorporated into protein, Rush & Starr (10) and Rush *et al.* (11) demonstrated that pyrrolidone carboxylic acid may nevertheless be converted into a form which could be utilized in protein synthesis by a 'decyclase' enzyme found in the human myeloma line which they studied. Murine plasmacytomas assayed simultaneously lacked the enzyme and were unable to utilize PCA directly in protein synthesis but nevertheless secreted immunoglobulin with PCA as the amino-terminal residue. Decyclase activity was, however, detected in murine-liver extracts.

Twardzik & Peterkofsky (12) attempted to determine whether glutamine or glutamic acid was the more direct precursor of pyroglutamic acid. By use of the mouse plasmacytoma RPC-20, which contained glutaminase but not glutamine synthetase, these investigators were able to obviate the conversion of glutamic acid to glutamine. When cultures of cells were incubated in media containing ^{3}H-glutamic acid and cold glutamine, only glutamic and pyroglutamic acid were detected in pronase hydrolysates of synthesized protein. When ^{14}C-glutamine and cold glutamic acid were utilized, amino-terminal peptides were shown to contain amino-terminal glutamic acid, glutamine, and pyrrolidonyl carboxylic acid, a result which suggested that PCA was derived from (^{14}C) glutamine after its conversion to glutamic acid. The investigators took care to utilize experimental conditions which prevented the spontaneous cyclization of glutamine to PCA which can occur at elevated temperatures in mildly acid or alkaline solutions.

Stott & Munro (13), building on previous studies, undertook a comprehensive approach toward determining the post-translational step in protein biosynthesis at which PCA is formed. Mouse-myeloma IgG was isolated as nascent protein on the polyribosome and as completed *intracellular* and mature secreted protein. When (^{3}H) nascent peptides and (^{14}C)-labeled intact heavy chains were co-digested with pronase and the amino terminal peptides isolated and analyzed, it was shown that less than 10% of the amino termini of the peptides contained PCA. When similar co-labeling and digestion experiments were performed to compare the ratio of amino-terminal PCA in intracellular to extracellular heavy chains, 60 to 70% of intracellular protein was shown to have N-terminal PCA. From these results, the investigators concluded that cyclization of the aminoterminal residue (i.e., glutamine or glutamic acid) to PCA occurs inside the cell prior to the secretion of the completed protein. In addition, they were unable to detect PCA-tRNA in cultures of rat liver cells incubated in the presence of radiolabeled glutamine, PCA, or glutamic acid.

Jones (14) examined the cell-free synthesis of immunoglobulin lambda light chains with amino-terminal PCA produced by the murine myeloma RPC-20. Microsomes, tRNA pools and appropriate initiating enzymes purified from the RPC-20 plasmacytoma were utilized to effect conditions of

cell-free protein synthesis in which the incorporation of radiolabeled glutamic acid was maximized. The microsomal proteins were precipitated, reduced, digested with subtilisin, and the acidic subtilopeptides purified. These were subjected to high voltage electrophoresis and produced 2 major peaks of radioactivity which were abolished after treatment of the peptide pools with bacterial pyrrolidonyl carboxyl peptidase. The results demonstrated conclusively that in this system pyroglutamate can be formed while protein is still bound to microsomes. In order to determine if a specific glutamyl-tRNA was involved in pyroglutamate synthesis, the pool of RPC-20 tRNAs was subjected to reverse-phase chromatography, and 2 isoaccepting species of glutamyl-tRNAs were isolated. Addition of either to the cell-free system allowed synthesis of light chain-containing amino-terminal pyroglutamic acid. Finally, since the RPC-20 plasmacytoma line lacks the enzyme catalyzing glutamic acid to glutamine conversion, all pGlu synthesized must have been derived from glutamic acid. These results suggested that protein synthesis had been initiated prior to cyclization of glutamic to pyroglutamic acid.

Data which supported this notion were provided by Prasad & Peterkofsky (15), who synchronized RPC-20 plasmacytoma cells for initiation of protein synthesis. Light chain, produced at time intervals 2 and 60 min after protein synthesis was initiated, was immunoprecipitated with specific anti-lambda antiserum. By this method, it was shown the specific activity of methionine, but not other radiolabeled amino acids, was greatest in light chain isolated from the earliest (i.e., 2 min) cultures. This was interpreted as indicated the presence of a methionine-initiated peptide precursor on the light chain which required processing (i.e., removal prior to cyclization of amino terminal glutamate to pyroglutamate).

Burstein *et al.* (16) extended these studies and demonstrated conclusively that a short-lived precursor peptide of 19 residues is formed early in light chain synthesis. Cleavage of this extra peptide was necessary before the cyclization of amino-terminal glutamic acid or glutamine could occur to form the pyrrolidonyl carboxyl group. The experiments were performed using the mouse plasmacytoma MOPC-315 which produces type lamda light chains with an amino-terminal PCA. Light chain-specific mRNA was prepared from the plasmacytoma polysome pool by immunoprecipitation with specific anti-murine light chain antibody, purified by oligo-DT chromatography, and the L chain-specific mRNAs translated in a wheat germ cell-free protein synthesis system. Protein was synthesized numerous times and in each instance (^{3}H)- or (S^{35})-labeled amino acid was added. By SDS polyacrylamide gel electrophoresis, an elongated light chain was found which in some instances contained amino-terminal ^{35}S-methionine. This was shown in other experiments to be a short-lived initiator residue. In addition to demonstrating the existence of a precursor molecule, the data assisted in defining the stage in biosynthesis at which pyroglutamic acid is formed and established that it could not be an initiator of protein synthesis.

Burstein & Schechter (17) extended these observations to 3 lambda light chain-producing mouse plasmacytomas utilizing similar conditions of cell-free mRNA translation. The focus of the study was to establish whether N-terminal glutamine or glutamic acid was the pyrrolidone carboxylic acid precursor. Light chains containing the octadecapeptide leader sequence (i.e., the precursor peptide less the cleaved initiator methionine) were subjected to automated sequence analysis for up to 40 residues. This allowed alignment of the identified residues after position 18 with those of mature light chain. When either (^{3}H) glutamic acid or (^{3}H) glutamine was utilized for protein synthesis, only glutamine was noted at position 19 (i.e., residue 1 of the mature light chain) and no redundancy was noted at any position. Identical results were noted for all 3 plasmacytoma lambda chains. Since no interconversions of glutamic acid to glutamine and vice versa are found in the cell-free system, the results clearly indicate that glutamine is the precursor for pyrrolidone carboxylic acid in this system.

Of some pertinence is the fact that of over 200 human and murine immunoglobulin heavy *or* light chains thus far subjected to amino terminal sequence analysis (18), only one human heavy chain isolated from a native protein contains an initial amino-terminal glutamine residue (19). Perhaps all amino terminal glutamine residues undergo enzymatic cyclization to form PCA prior to secretion from immunoglobulin-producing cells.

Pyrrolidonyl carboxy peptidase

Pyrrolidonyl carboxyl groups are present on numerous naturally occurring, biologically active proteins and peptides. In many instances, PCA inhibits the determination of primary structure at the amino terminus since one is unable to use biochemical methods, either automated or manual, which require a reactive primary amine group for sequential identification of amino acids carboxy distal to pGlu.

In some instances, chemical reduction of the pyrrolidone ring will permit sequence analysis. As one example, Takahaski & Cohen (20) have utilized diborane in tetrahydrofuran or tetramethylurea to reduce the pyrrolidone ring. Although this particular method allows simple and relatively rapid identification of PCA residues at the amino terminus of proteins, it is a qualitative technique, shows limited selectivity and only partially reduces carboxyl groups and peptide bonds. Further, there is less than 50% conversion of pyroglutamic acid into proline with simultaneous loss of peptide bonds by reduction. Thus, the procedure has restricted uses, especially when proteins or peptides are available in limited quantities.

Armentrout & Doolittle (21) noted that Pseudomonas fluorescens was able to maintain growth on media which contained pyrrolidone carboxylic acid as the only source of carbon and nitrogen. These investigators observed that an extract of the organism, instead of opening the pyrrolidone ring, quantitatively cleaved the dipeptide pyrrolidonyl-L-alanine into free PCA and L-alanine. They effected on 100-fold partial purification of the enzyme by 2-step $(NH_4)_2SO_4$ precipitation of a departiculated sonicate of bacteria, followed by DEAE-Sephadex chromatography. However, the partially purified enzyme was unstable in either a frozen or salt precipitated state, and it was rendered inactive by sulfhydryl inhibitors such as iodoacetamide and p-mercuriphenylsulfonate in low concentrations. That the enzyme was specific for the peptide bond joining the pyrrolidonyl group (pyr) to its neighboring carboxy-distal amino acid was demonstrated by its action on dipeptides such as pyr-L-valine and pyr-L-alanine, as well as on fibrinopeptides B from various mammalian species with amino termini of pyr-his, pyr-ser, and pyr-phe. While the rate of release of PCA was sometimes influenced by the neighboring amino acid, the enzyme was highly specific for the pyr-amino acid peptidyl bond only and showed no other non-specific protease activity. The reaction of this enzyme is thus:

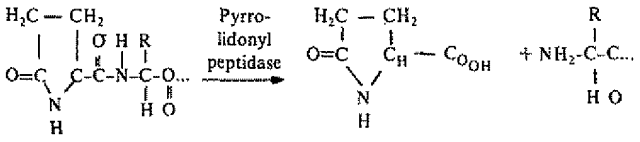

pyrrolidonyl-amino acid — pyrrolidone carboxylic acid — amino acid

The same investigators then developed isolation methods which enhanced the enzyme's stability, activity, and purity (22). Additional purification steps involved precipitation of nucleic acids from the bacterial sonicate, addition of 2-mercaptoethanol, EDTA and 2-pyrrolidone to all buffers utilized, and preparative polyacrylamide gel electrophoresis. They observed that, while the enzyme was unstable in solution alone, hydrolysis of the pyr-L-alanine dipeptide was maintained for nearly a day. They reasoned that addition of 2-pyrrolidone to enzyme solutions would enhance enzyme stability. It was also noted that lyophilized preparations which has lost enzymatic activity could be reactivated by addition of sulfhydryl protective agents.

Uliana & Doolittle (23) studied the influence of the amino acid which was bonded to amino-terminal PCA on its cleavage by the enzyme. The cleavage rates of the dipeptides which were examined comprised 3 groups: L-pyr-L-alanine being hydrolized at twice the rate of pyr-L-isoleucine, which was hydrolyzed nearly twice as fast as pyr-L-valine, leucine, phenylalanine *or* tyrosine (in decreasing order of the rate of reaction with enzyme). L-pyrrolidonyl-L-proline and D-pyrrolidonyl-L-alanine were not hydrolyzed, nor did dipeptides containing D-pyrrolidonyl carboxylic acid or D-alanine inhibit cleavage of the L-pyr-L-alanine bond. This demonstrated the stringent requirements of pyrrolidonyl peptidase for the L-optical isomers of amino acids.

Armentrout (24) was able to isolate pyrrolidonyl carboxy peptidase from rat liver cells. The rat liver enzyme, while slightly more labile than the bacterial product, was also stabilized in solution by 2-pyrrolidone and was likewise activated by reducing

agents. It was, however, of lower molecular weight, and while it hydrolyzed dipeptides in the same relative orders of structure as the bacterial product, there were minor differences in the relative rate relationships of peptide bond cleavage. The rat liver enzyme was more efficient in its removal of the pyrrolidonyl carboxyl group from fibrinopeptides B.

Almost concomitant with the above studies, Szewczuk & Mulczyk purified the peptidase activity from Bacillus subtilis (25) by use of a nearly identical purification procedure. The enzyme activity was assayed with the chromogenic substrate L-pyrrolidonyl-β naphthylamide, the percent of cleavage of the peptide bond being colorimetrically quantified by the amount of β-naphthylamide released. The bacillus enzyme was inactivated by mild heating (55 °C) and by the addition of Hg^{++} and Cu^{++}. Enzyme cleavage of the substrate was *competitively* inhibited by 2-pyrrolidone carboxylic acid. The ubiquitous nature of this enzyme was shown by finding peptidase activity in Streptococcus, Staphylococcus, Micrococcus, Sarcinia, and other Bacillus strains, as well as in several gram-negative bacterial strains such as Klebsiella, Neisseria, Enterobius and some strains of Escherichia.

Similar peptidase activity is also widely distributed in animal tissue and, remarkably, in plant cell extracts (26). Liver and kidney apparently contain the highest levels of this enzyme, but it is also found in spleen, lung, intestine, brain, heart and skeletal muscle of birds and mammals. Enzyme partially purified from pigeon liver, and with estimated molecular weights of 33 000 and 80 000 daltons, contained peptidase activity with nearly identical enzymatic and biochemical characteristics as that isolated from bacteria.

By use of the chromogenic L-pyr-β-naphthylamide substrate, Albert & Szewszuk (27) were able to determine the cellular localization of the pyrrolidonyl carboxy peptidase. Tissues which were snap-frozen immediately after sacrifice of the test animal were overlaid with L-pyrrolidone-β-naphthylamide at neutral pH, incubated at 37 °C, and then secondarily overlaid with tetraazotized O-dianizidine to colorimetrically localize free β-naphthylamide. Histochemical activity was assayed in numerous avian and rodent tissues. Since the kidney extracts and cells of all the species tested showed the greatest peptidase activity, cellular localization of the enzyme to the cytoplasm of endothelial cells of the proximal convoluted tubules was possible. Lesser amounts were histochemically detected in the cells of the distal convoluted tubules and no enzyme was detected in any cell nuclei or glomerular cells.

Curiously, pyrrolidonyl peptidase activity in bacteria is most likely membrane-associated. Exterkate (28) produced bacteria-burst spheroplasts by treatment of Streptococcus cremoris with lysozyme. The spheroplasts were lysed utilizing conditions which released intracellular marker enzymes and which allowed the conclusion that the pyrrolidonyl peptidase was associated with particulate cell structures. Further, since the enzyme was easily solubilized, it was inferred that it was weakly bonded by means of hydrophobic and/or electrostatic associations to the internal bacterial membrane.

Application of pyrrolidonyl carboxy peptidase (PCP) in protein sequencing

The knowledge that PCP is ubiquitous in its distribution and that it may be isolated from numerous sources to near homogeneity, as well as knowing the conditions for its storage with retention of enzyme activity (21, 22), were of considerable importance. With the advent of automated primary amino acid sequence technology which depends on a free amino terminal amino acid residue, it was apparent that a source of the enzyme would be required for the expeditious removal of amino-terminal amino acids blocked by the pyrrolindonyl group. Numerous attempts to effect large scale purifications of enzyme with retention of peptidase activity were, however, unsuccessful. By cell lysis combined with a gentle means of protein precipitation (presumed by the writer to be effected by either cold ethanol or 2-step ammonium sulfate), a preparation of enzyme has been obtained which may be stored in a lyophilized form at -70 °F with retention of activity for 3 years (29).

A general procedure for removal of pyrrolidone carboxylic acid from the amino terminus of proteins was devised by Podell & Abraham (30). The technique was influenced by obstacles encountered in previous studies, utilized portions of procedures devised by others (14, 21, 22, 25), and was success-

fully utilized on 3 immunoglobulin type lambda and 2 type gamma heavy chains. In brief, reduced and alkylated protein at 1 mg/ml concentrations (i.e., 2–4 $\times$ 10^{-4} mM/mL) in 0.1 M phosphate buffer at pH 8.0, containing *freshly added* dithiothreitol (5 mM), disodium EDTA (10 mM), and glycerin (5% v/v), is incubated under a nitrogen atmosphere with crude calf liver pyrrolidonyl carboxy peptidase (30, 31, 32) at 4 °C for 8–10 h. After this time, an equivalent quantity of enzyme is again added and the digest is incubated at 37 °C for up to 14 h. Essentially, quantitative removal of amino-terminal pyrrolidonyl carboxylic acid from each of the above proteins was possible. Yields of greater than 80% of the neighboring amino acid residue, i.e., residue 1 of the enzyme-treated protein, was obtained by automated sequence analysis. The identical conditions have been utilized by Franklin *et al.* (31) with equivalent results on an immunoglobulin heavy chain disease protein and by Chiu *et al.* (32) with intact heavy chain and a heavy chain fragment obtained after cyanogen bromide digestion. The procedure was devised on the assumption that the peptide bond between amino-terminal PCA and its carboxy-distal amino acid will be in the group shown by Uliana & Doolittle (23) to be most resistant to peptidase treatment, i.e., peptide bond cleavage proceeds quantitatively but at a slow rate. Thus, reducing conditions, a stabilizing reagent (glycerin), a double addition of crude enzyme, a metallic ion chelating agent, and a low concentration of protein (to minimize aggregation) were utilized. These conditions are of some importance when one suspects that leucine, valine, methionine, phenylalanine or tyrosine are peptide-bonded to PCA.

With experiences gained from immunoglobulins (29), it is apparent that for proteins comprised of multiple polypeptide chains, separation of these constituent subunits is necessary before efficient removal of the N-terminal pyrrolidone ring is possible.

There are experimental data which suggest that deblocking of soluble and purified peptides occurs more readily. Reid & Thompson (33) isolated the subcomponent C1q from the first component of complement. This was oxidized, subjected to limited pepsin digestion and the shortened β chain isolated. This 97 amino acid long fragment was dissolved in 0.1 M phosphate, pH 7.4, peptidase added, and incubated for 6 h at 37 °C without addition of reducing or chelating agents. Cleavage of the amino terminal pyrrolidonyl-leucine peptide bond was however effected. The conditions described will not render a similar bond in *intact* immuoglobulin heavy chains.

Bacterial enzyme (26) has been utilized by Gerber *et al.* (34) to cleave amino terminal PCA of a highly insoluble peptide derived from bacteriorhodopsin, a membrane protein. This 20-amino-acid-long peptide was produced by cyanogen bromide treatment of the parent protein, and after derivitization with 4-sulfophenylisothiocyanate, was treated with pyrrolidonyl peptidase under reducing conditions for 18 h, which effectively cleaved the amino terminal PCA-L-alanine bond.

Function of pyrrolidone carboxylic acid in proteins or peptides

The presence of an amino terminal pyroglutamic acid on a protein or peptide may in some instances enhance or be responsible for its biologic function or activity. A particularly well-studied example in the tripeptide thyrotropin releasing factor (TRF) which has the sequence pGlu-His-Pro. *In vivo*, this hypothalamic hormone mediates the release of thyrotropin by its action on the anterior pituitary gland (36) and *in vitro* has been shown to enhance prolactin synthesis and decrease growth hormone production in a cloned strain of rat pituitary cells (37, 38) possibly by its binding to cell-membrane receptors.

Hinkle *et al.* (37) have studied the effects of modification of each amino acid which comprises TRF, on its biologic activity, and affinity for the TRF receptor. They demonstrated that any structural substitution in the lactam ring of pyrrolidone carboxylic acid, effected both hormone synthesis and receptor binding. In instances simple modifications caused marked decreases in activity relative to parent TRF. As examples, shown below are TRF (a), and two analogs (b) and (c). In formula (b), carbon -4 is replaced by an oxygen linked both to carbon -3 and carbon -5. In formula (c) the oxygen of carbon -5 is replaced forming the amino acid proline, and producing the sequence Pro-His-Pro. These modifications produce compounds of diminished potency which show only 33% (b) and

0.8% (c) of the biologic activity of native TRF.

Of some interest was the finding that substitution of glutamic acid or glutamine for pGlu also causes a decrease in prolactin stimulating activity. However, because either residue may cyclize to pyroglutamate under the conditions of cell culture, any activity which was found was felt to be caused by the presence of native TRF.

Thyrotropin releasing factor (TRF) and 2 functional analogs

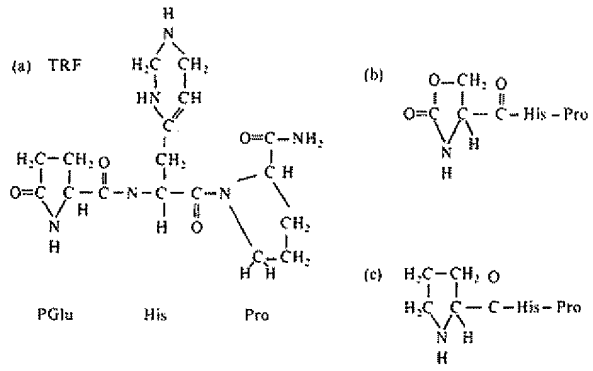

Similar modifications (39, 40) have also been shown to diminish the release of thyroid stimulating hormone from the anterior pituitary gland in an *in vivo* mouse model. As an example, substitution of the cyclopentane ring for the lactam ring caused greater than a 1000 fold decrease in TSH releasing activity.

The functional activity of pGlu on the amino terminus of immunoglobulins is less clear. The pyrrolidonyl group constitutes the amino-terminal residue of both the Mcg type lambda Bence-Jones dimer (41) and the heavy and light chain variable regions of the f(ab) fragment of IgG-New (32). The three-dimensional stucture of both molecules has been determined at the atomic level by x-ray crystallography (42, 43) and models constructed. Apparently the amino-terminal pGlu does not participate in binding of the antigen and no function has been ascribed to it by virtue of its three dimensional orientation which as shown, positions it away from the combining site cleft. The available data would suggest that the conversion of glutamine to pGlu in the immunoglobulin producing cell is a vestigial function.

Of particular interest are evolving but as yet preliminary data which suggest that free pyroglutamic acid may mediate particular neurobiologic functions. By use of paper chromatographic techniques, low levels of free pGlu were detected in normal human and guinea pig plasma (43) after treatment with perchloric acid to effect deproteination. By gas-liquid chromatography, micromolar concentrations of pGlu were determined for plasma, urine and cerebrospinal fluid (44). The pGlu found was assumed to be derived from the gamma glutamyl cycle (1, 2, 3) by the action of gamma-glutamylcyclotransferase on gamma-glutamyl-amino acids.

It is possible that PCA free in cerebral spinal fluid could exert some biologic effects. Lam *et al.* (45) demonstrated that free pyroglutamic acid in porcine hypothalamic tissue significantly inhibited prolactin release during prolactin purification. The mechanism of the inhibition was not determined. The study was well-controlled for spurious formation of PCA and its identification was accomplished by thin layer electrophoresis, and field desorption mass spectroscopy. Approximately 100 μg were detected in each 100 mg (dry weight) of hypothalamic tissue.

Conclusion

This review has focussed attention on aspects of pyroglutamic acid formation and function which have not been previously summarized. PCA is a crucial intermediate in the gamma-glutamyl metabolic cycle, and its function in this pathway has been very well delineated and reviewed by Meister and his colleagues (1, 2, 3).

The role of pyroglutamic acid in protein biosynthesis and in mediating the biologic function of proteins or peptides which contain it at the amino terminus, is less clear. This PCA is apparently not derived from that formed during the gamma-glutamyl cycle. As suggested by the above studies, PCA is most likely formed either late in protein translation by cyclization of N-terminal glutamine or may form just prior to secretion of completed protein from the cell. Regardless, all the experimental evidence cited conclusively shows that PCA formation occurs during the latter stages of protein biosynthesis and is apparently complete by the time

mature, extracellular protein is noted either in culture media of cells, or in the fluid phase of cell-free synthesis systems.

Once formed, amino-terminal pyrrolidone carboxylic acid may at times be an impediment to protein sequence determination since reactions which require a free amino terminus are not possible. However, a non-energy dependent enzyme has been described which has been utilized to effect quantitative removal of pGlu of many previously blocked proteins.

Pyroglutamic acid is present on proteins and peptides of very diverse biologic function. Studies cited above show that in the hormone TRF, this amino acid is responsible for a major portion of hormone activity by its binding to a TRF membrane receptor. However, in other instances PCA may not confer any apparent function. An example is PCA which forms the amino terminal residue of many immunoglobulin heavy and light chains. Aside from functions as an incorporated amino acid, free pyrrolidone carboxylic acid may possibly have biologic function as an inhibitor of cellular hormone release possibly by blockade of specific hormone receptors. While this has only been noted during hormone isolation, it is presumed that an *in vivo* correlate of this phenomenon will be found.

In terms of future areas of research concerning this amino acid, it would be of interest to find the unique enzyme(s) which is responsible for conversion of glutamic acid or glutamine to pyrroglutamic acid in protein biosynthesis or to unequivocally demonstrate if the enzymes of the gamma-glutamyl cycle can participate in this conversion. Finally, the experimental data mentioned which suggest that free pGlu may be inhibitory of hormone release and other studies (46, 47) which show that a substituted pyrrolidone ring may antagonize amino acid induced neuronal excitation, point to numerous other functions for this curious lactam at the internal or external cell membrane surface or cell-membrane receptor, levels.

Acknowledgements

The writing of this manuscript was performed utilizing facilities supported by U.S.P.H.S. research grant AI-11550, U.S.P.H.S. Training Grant 5 TO1 AI-00028, The David Welk Memorial Fund, Specialized Research Center Grant (CIRID) AI-15372, and the U.S.P.H.S. Medical Scientist Training Program (NIGMS).

The authors wish to thank Dr. Patricia Hinkle, Dept. Of Pharmacology, University of Rochester Medical Center for her helpful discussions concerning the role of PCA in TRF, and Dr. Kenneth Carle, Professor of Organic Chemistry, Hobart College, Geneva, New York for his elucidation of the resonant structure of PCA. Ms Nancy George edited and prepared this manuscript.

References

1. Van der Werf, P. & Meister, A., 1975. Adv. Enzymology 43: 519–566.
2. Meister, A., 1973. Science 180: 33–39.
3. Meister, A., 1974. Life Sciences 15: 177–190.
4. Van der Werf, P., Orlowski, M. & Meister, A., 1971. Proc. Natl. Acad. Sci. 68: 2982–2985.
5. Kitos, P. A. & Waymouth, C., 1966. J. Cell Physiology 67: 383–398.
6. Moav, B. & Harris, T. N., 1967. Biochem. Biophys. Res. Comm. 29: 773–776.
7. Bernfield, M. R. & Nestor, T., 1968. Biochem. Biophys. Res. Comm. 33: 843–848.
8. Messer, M. & Otteson, M., 1964. Biochem. Biophys. Acta 92: 409–412.
9. Baglioni, C., 1970. Biochem. Biophys. Res. Comm. 38: 212–219.
10. Rush, E. A. & Starr, J. L., 1970. Biochem. Biophys. Acta 199: 41–55.
11. Rush, E. A., McLaughlin, C. A. & Starr, J. L., 1971. Cancer Research 31: 1134–1139.
12. Twardzik, D. R. & Peterkofsky, A., 1972. Proc. Natl. Acad. Sci. 69: 274–277.
13. Stott, D. I. & Munro, A., 1972. Biochem. J. 128: 1221–1227.
14. Jones, G. H., 1974. Biochem. 13: 855–860.
15. Prasad, C. & Peterkofsky, A., 1975. J. Biol. Chem. 250: 171–179.
16. Burstein, Y., Kantor, F. & Schechter, I., 1976. Proc. Natl. Acad. Sci. 73: 2604–2608.
17. Burstein, Y. & Schechter, I., 1977. Biochem. J. 165: 347–354.
18. Kabat, E. A., Wu, T. T. & Bilofsky, H., 1979. In: Sequences of Immunoglobulin Heavy Chains. U.S. Department of Health, Education and Welfare, NIH publication No. 80–2008.
19. Kaplan, A. P., Hood, L., Terry, W. D. & Metzger, H., 1968. Immunochem. 8: 801–811.
20. Takahaski, S. & Cohen, L. A., 1966. Biochem. 5: 864–870.
21. Doolittle, R. F. & Armentrout, R. W., 1968. Biochem. 7: 516–521.
22. Armentrout, R. W. & Doolittle, R. F., 1969. Arch. Biochem. Biophys. 132: 80–90.

23. Uliana, J. A. & Doolittle, R. F., 1969. Arch. Biochem. Biophys. 131: 561–565.
24. Armentrout, R. W., 1969. Biochem. Biophys. Acta 191: 756–759.
25. Szewczuk, A. & Mulczyk, M., 1969. Eur. J. Biochem. 8: 63–67.
26. Szewczuk, A. & Kwiatkowska, J., 1970. Eur. J. Biochem. 15: 92–96.
27. Albert, Z. & Szewszuk, A., 1972. Acta Histochem. Bd. 44: 98–105.
28. Exterkate, F. A., 1977. J. Bacteriology 129: 1281–1288.
29. Abraham, G. N., unpublished data.
30. Podell, D. N. & Abraham, G. N., 1978. Biochem. Biophys. Res. Comm. 81: 176–185.
31. Franklin, E. C., Prelli, F., & Frangione, B., 1978. Proc. Natl. Acad. Sci. 76: 452–456.
32. Chiu, Y.-H., Lopez de Castro, J. A. & Poljak, R. J., 1979. Biochem. 18: 553–560.
33. Reid, K. B. M. & Thompson, E. O. P., 1978. Biochem. J. 173: 863–868.
34. Gerber, G., Anderegg, R. J., Herlihy, W. C., Gray, C. P., Biemann, K. & Khorana, H. G., 1979. Proc. Natl. Acad. Sci. 76: 227–231.
35. Jacobs, L. S., Snyder, P. J., Wilber, J. F., Utiger, R. D. & Daughaday, W. H., 1971. J. Clin. Endocrinol. 33: 996–998.
36. Hinkle, P. M. & Tashjian, A. H., Jr., 1973. J. Biol. Chem. 248: 6180–6186.
37. Dannies, P. S. & Tashjian, A. H., Jr., 1973. J. Biol. Chem. 248: 6174–6179.
38. Vale, W., Grant, G. & Guillemin, R., 1973. In: Frontiers in Neuroendocrinology (Ganong, W. F. & Martin, L., eds.), pp. 375–397. Oxford University Press, Toronto.
39. Goren, H. J., Baure, L. G. & Vale, W., 1977. Molecular Pharm. 13: 606–614.
40. Fett, J. W. & Deutsch, H. F., 1974. Biochem. 13: 4102–4114.
41. Schiffer, M., Girling, R. L., Ely, K. R., & Edmundson, A. B., 1973. Biochem. 12: 4620–4631.
42. Poljak, R. J., Amzel, L. M., Chen, B. L., Phizackerley, R. P. & Saul, F., 1974. Proc. Natl. Acad. Sci. 71: 3440.
43. Wolfersberger, M. G. & Tabachnik, J., 1973. Experientia 29: 346–347.
44. Wilk, S. & Orlowski, M., 1973. FEBS Letters 33: 157–160.
45. Lam, Y.-K., Knudsen, R., Folkers, K., Frick, W., Daves, G. D., Barofsky, D. F. & Bowers, C. Y., 1978. Biochem. Biophys. Res. Commun. 81: 680–683.
46. Stone, T. W., 1976. Experientia 32: 581–583.
47. Stone, T. W., 1976. J. Physiol. 257: 187–198.

Received January 30, 1981.

EXHIBIT 2

Available online at www.sciencedirect.com
ScienceDirect
Journal of Pharmaceutical and Biomedical Analysis 42 (2006) 455–463
JOURNAL OF PHARMACEUTICAL AND BIOMEDICAL ANALYSIS
www.elsevier.com/locate/jpba

Investigation of N-terminal glutamate cyclization of recombinant monoclonal antibody in formulation development

Lei Yu *, Alona Vizel, Mary Beth Huff, Meagan Young, Richard L. Remmele Jr., Bing He

Department of Pharmaceutics, Amgen Inc., One Amgen Center Drive, 2-2-A, Thousand Oaks, CA 91320, United States

Received 1 March 2006; received in revised form 2 May 2006; accepted 9 May 2006
Available online 7 July 2006

Abstract

The N-terminal glutamic acid (Glu) can be cyclized to form pyroglutamate (pGlu). Recent studies have suggested that N-terminal pGlu formation is an important posttranslational or co-translational event and is greatly facilitated by the enzyme glutaminyl cyclase, although the impact of the N-terminal cyclization on the potency and overall stability of mAbs is not been well known. Since most recombinant monoclonal antibodies (mAbs) contain glutamic acid and/or glutamine at their N-terminus, understanding the cyclization mechanisms may shed light on the factors that control the pGlu formation in therapeutic mAb development.

Here, two mass spectrometry-based techniques were developed to investigate *N*-pyroglutamyl formation and the high conversion rate to pGlu at the N-terminus of the mAb was reported in the formulation development. The pGlu formation is favored at pH 4 and 8, but is less common at the neutral pH that is optimum for the enzymatic Glu conversion. These observations suggest that pGlu formation can proceed non-enzymatically at mild conditions and that this cyclization is not driven by glutaminyl cyclase in non-physiological conditions. We also calculate the half-lives of the N-terminal Glu at different pH and temperatures from the kinetics data, which would be very helpful for predicting pGlu formation and for selecting proper formulation and storage conditions.

Keywords: Cyclization; *N*-Pyroglutamic acid; Glutamic acid; N-terminal; Monoclonal antibody; Peptide mapping; Liquid chromatography/mass spectrometry

1. Introduction

With the mastery of a robust cell line, large scale cell culture technology and highly efficient purification process, more and more recombinant monoclonal antibodies (mAbs) have been developed to fight diseases in many therapeutic areas [1,2]. Like other recombinant proteins, therapeutic mAbs are subject to a variety of chemical modifications that may occur during protein expression, purification, transportation and storage. These modifications include but are not limited to oxidation, deamidation, proteolysis cleavage, disulfide-bond scrambling, glycosylation and cyclization. These reactions, enzymatic or non-enzymatic, could affect the size or charge heterogeneity of mAbs, and may modify their antigen binding affinity. The impact of these modifications on the overall stability of the mAbs, their bioactivities, and therapeutic potency depends not only on just the modifications themselves but also on their locations [3–10]. Therefore, therapeutic mAbs also require extensive and stringent characterization of purity, structural integrity and stability. It is of a great interest to investigate the factors that affect these chemical modifications during therapeutic drug development.

It has been well known that the amino terminus of mAbs can be modified through acetylation, formylation and pyroglutamylation. Among them, pyroglutamate (pGlu) formation is of special interest because most mAbs have glutamine (Gln) or glutamic acid (Glu) at the amino terminus. Previous studies have shown that pGlu was almost exclusively formed in vivo by intramolecular Gln cyclization [11]. It was believed that the pGlu formation was an enzymatic reaction because Wilson and Cannan reported that the conversion of Glu to pGlu could only occur at relatively harsh incubation at 100 °C for 50 h [12,13]. The reaction is even slower in solutions of weak acids or weak bases. At strong acid or alkaline conditions the conversion of Glu to pGlu is rapid and practically complete. Other studies have reported that N-terminal pGlu can be derived from Glu without prior conversion to Gln and indicated that

* Tel.: +1 805 313 4773; fax: +1 805 375 5794.
E-mail address: leiy@amgen.com (L. Yu).

0731-7085/$ – see front matter © 2006 Published by Elsevier B.V.
doi:10.1016/j.jpba.2006.05.008

N-terminal pGlu formation from Glu must be an enzymatic reaction rather than a spontaneous chemical process [14]. The spontaneous cyclization of an N-terminal glutamine occurs only slowly under physiological conditions [15]. Recent studies have suggested that N-terminal pGlu formation is an important post-translational or co-translational event and is greatly facilitated by the enzyme glutaminyl cyclase [16,17]. If the above findings proved that the mechanism of N-terminal pGlu formation is an enzymatic reaction under physiological conditions, a non-enzymatic mechanism should be examined, which may occur in non-physiological conditions.

In this report, we have investigated the pGlu formation from Glu at the N-terminus of a mAb under weak acids or bases condition during therapeutic drug development. The mAb is different from other typical mAbs containing N-terminal Glu and its N-terminal Glu can be converted to pGlu non-enzymatically. The cyclization reaction is chemical process for the mAb during the formulation development. In this study, the two mass spectrometric-based methods were used to facilitate the investigation of the pGlu formation at the N-terminus of the mAb. The first method, a bottom-up method, is a proteolytic approach with trypsin digestion to identify the N-terminal pGlu by HPLC with electrospray ionization/ion trap mass spectrometry (ESI-MS trap). The second one uses high resolution ESI-QTOF MS to analyze the formation of pGlu at the N-terminus of the same mAb that is reduced but not further digested by protease to minimize sample treatment induced pGlu formation (a top-down method). The two methods gave comparable results: high percentage pGlu was observed for the studied mAbs of our formulated sample under high temperature shelf storage. These findings demonstrated that pGlu formation could occur under storage condition without facilitating by the enzyme.

2. Experimental

2.1. Materials

Recombinant mAb was produced and purified at Amgen Inc. The purified mAb was in 10 mM sodium acetate buffer with pH 5.2 and stored at −80 °C. Trypsin of sequencing grade was purchased from Promega and stored at −20 °C. All chemicals and reagents were of analytical grade and purchased from Sigma. Other formulated samples were prepared through dialyzing into the final formulation solutions using 10 MWCO Snakeskin dialysis bags.

2.2. Reduction, alkylation and tryptic digestion

Approximately 1 mg of the mAb was denatured with 6 M guanidine HCl, 0.25 M Tris–HCl, 1 mM EDTA, at pH 7.5. Ten microliters of 0.5 M dithiothreitol (DTT) was added to the solution and the reaction mixture was placed at 37 °C for 30 min. After the sample was cooled to room temperature, 24 μl of 0.5 M iodoacetamide (IAA) was added and the sample was incubated at room temperature in the dark for 30 min. Ten microliters of 0.5 M DTT was added to the samples in order to terminate the alkylation reaction. Approximately 500 μl of reduced and alkylated material was buffer exchanged with 950 μl of 0.1 M Tris–HCl to a final concentration of 1 mg/ml of antibody, using a NAP-5 column (Amersham BioSciences, Uppsala, Sweden) equilibrated with 10 ml of 50 mM Tris, 1 mM $CaCl_2$, pH 7.0. Tryptic digestion was performed for 5 h at 37 °C using an enzyme:protein ratio of 1:55. The digests were then refrigerated at 4 °C for analysis.

2.3. HPLC separation of tryptic peptides

The tryptic peptides were separated by reversed-phase HPLC using an Agilent 1100 HPLC equipped with a diode-array detector, autosampler, flow cell and temperature controlled column compartment (Agilent, Palo Alto, CA, USA). A Varian Metachem Polaris C18 column (150 mm × 2.1 mm i.d.) packed with a 3 μm nominal diameter, 300 Å pore size C_{18} resin (Varian, Torrance, CA, USA) was used for the separations. The solvents were—A: 0.1% trifluoroacetic acid (TFA; Pierce, Rockford, IL, USA) in water, and B: 0.1% TFA in 90% acetonitrile (Baker, Phillipsburg, NJ, USA). The column was equilibrated at 0% solvent B. The two-stage gradient was from 0 to 17% B within 17 min, then followed by a second gradient from 17 to 38% B within 90 min. A flush step was performed with 90% B for 10 min and the column was equilibrated with 0% B for 10 min. The column temperature was maintained at 40 °C. The absorbance of the eluent was monitored at 214 nm.

2.4. Mass spectrometry analysis of tryptic peptides

The HPLC was directly coupled to Agilent MSD ion trap mass spectrometer (Agilent, Palo Alto, CA, USA) equipped with an electrospray ionization source. The spray voltage was 4.5 kV and the capillary temperature was 350 °C. The fragmentation mass spectra were obtained using ion trap collision energies of 35%. Each full scan mass spectrum was followed by a zoom scan, followed by a data dependent MS/MS scan of the most intense peak. The Dynamic Exclusion feature was enabled (repeat counts, 2; repeat duration, 0.3 min; exclusion duration, 5 min and exclusion mass width, 2 Da).

2.5. HPLC separation of reduced antibodies

The reduced mAb was analyzed using an Agilent 1100 HPLC unit equipped with a diode-array detector, autosampler, micro flow cell and temperature controlled column compartment (Agilent, Palo Alto, CA, USA). Column was heated at 35 °C to enhance separation. Mobile phase A consisted of 0.1% formic acid in water and mobile phase B consisted of 80% *N*-propanol, 10% acetonitrile, 10% H_2O and 0.1% formic acid. Separation was performed on a Zorbax SB CN 150 mm × 1.0 mm 3.5 μm 300 Å (50 μl/min and 4 μg injection). The column was equilibrated at 10% solvent B. One minute after sample injection the concentration of buffer B was increase to 28% over 1 min followed by a linear gradient of 28% to 35% B over 33 min. The column was re-equilibrated by ramping up buffer B to 100% over

1 min, 5 min at 100% B, dropping down to 10% B over 1 min followed by 5 min at 10% B. UV absorption was monitored at 214 nm.

2.6. Mass spectrometry analysis of the reduced antibodies

Mass spectrometry was performed on a Micromass QTOF *Micro* mass spectrometer through an electrospray ionization (ESI) atmosphere–vacuum interface. The ESI-QTOF mass spectrometer was set to run in positive ion mode with a capillary voltage of 3400 V, sample cone voltage of 40 V, an *m/z* range of 1000–5500, with a mass resolution of 5000. The instrument was tuned and calibrated using multiply charged ions of antibody. The deconvolution of electrospray ionization mass spectra was performed using a MaxEnt1 algorithm, which is a part of the MassLynx software from Micromass.

2.7. Fourier transform infrared (FT-IR) spectroscopy

The cyclized mAb was analyzed by an ABB Bomem (Quebec, Canada) MB-series FT-IR spectrometer. The sample was prepared and infrared spectra were obtained according to published procedures [18]. The protein solution was loaded into a BioCell (Bio Tools) with CaF2 windows having a 6.5-μm fixed path length well. For each spectrum, a 128-scan interferogram was collected in a single-beam mode with a 4 cm^{-1} resolution. The reference spectrum was recorded under identical scan conditions. Second-derivative spectra were obtained with a seven-point Savitsky–Golay derivative function. Final spectra were treated with a 2× fast Fourier transform (FFT) interpolate function and plotted with SigmaPlot 8.0 software (Systat Software).

3. Results and discussion

The studied mAb contains Glu at N-terminus of both light chain (LC) and heavy chain (HC). The corresponding predicted peptides are EIVLTQSPGTLSLSPGER (LC) and EVQLVESGGGLVQPGGSLR (HC). N-terminal cyclization of Glu was observed at both LC and HC of the studied mAb, which was formulated at 30 mg/ml and stressed at pH 4.0–8.0 and several temperatures up to 45 °C for up to 3 months.

3.1. N-Pyroglutamate identification and confirmation

Tryptic digestion followed by HPLC separation and mass spectrometry analysis of peptides resulted in identification of *N*-pyroglutamyl formation. Fig. 1A gives the total ion chromatogram (TIC) of tryptic mapping. The mass spectra of the native N-terminal peptide peak and its modified peptide peak were shown Fig. 1B and C. The ion at *m/z* 942.7 is the doubly charged mass for the native tryptic peptide in Fig. 1B and the ion at *m/z* 933.8 corresponds to the cyclized tryptic peptide in Fig. 1C. Two doubly charged masses have a change of 9 Da in mass, indicating an 18 Da loss due to cyclization from Glu to pGlu. The cyclization occurred at the N-terminus of the LC and HC of the mAb. To verify these findings, tandem mass spectrometry analysis was performed to confirm the peptide containing pGlu on the LC and HC. Fig. 2 shows the MS/MS spectra of the four peptides, the native peptides and its pGlu containing peptides of the LC and HC. Fig. 2A and B show the tandem mass spectrum and the b, and y ion assignments for the native peptides of the LC and HC, which match the predicted masses. For pGlu containing peptides, Fig. 2C and D show that all y ions have the same mass as that of the native peptide, but all b ions lost 18 Da, resulting in the verification of pGlu and modification occurred at the N-terminus of the LC and HC.

Analyses also showed that the starting material of the studied mAb, purified bulk, did not contain detectable pGlu. Measurements have been taken to minimize sample handling induced pGlu formulation, such as the top-down method using high resolution ESI-QTOF MS with limited sample treatment. Analysis of control samples demonstrated that sample treatment, including tryptic mapping, did not contribute to pGlu formation at the N-terminus of LC. These experimental results showed that the N-terminal cyclization of LC and HC occurred in shelf storage, a non-physiological condition.

A top-down method was employed to demonstrate the formation of pGlu at the terminus of light LC. In Fig. 3, deconvoluted mass spectrum gives the mass 23,579 Da in the native LC peak and the mass 23,561 Da in the pGlu containing LC peak with 18 Da due to cyclization of the antibody. Data generated from the sample at different pH and buffers were analyzed by the bottom-up and top-down methods. In the peptide mapping method, the percentage of pGlu was determined from the integration of the extracted ion chromatogram (XIC) of the native peptide peak mass and pGlu peptide peak mass. The top-down method data was based upon the integration of two deconvoluted mass peak area of the native LC from the purified bulk and modified LC from the stressed samples. Table 1 listed the results from 3-month storage samples at different pH and buffers, showing a good correlation on the pGlu % of these mAb samples.

3.2. Effects of formulation conditions on N-pyroglutamyl formation and its rate

Temperature, pH and storage time were investigated on their impact on pGlu formation of the studied mAb. The pGlu formation at the N-terminus of the LC and HC increased with elevated temperature and lowered pH over 3 months (Fig. 4A and B). The pGlu formation of the HC was obviously slower than that of the LC no matter what pH, temperature and storage time levels. We could not detect any N-terminal pGlu formation on HC when temperature was at 29 °C or lower, even after 3-month storage. At the N-terminus, a significant amount of pGlu was observed on the LC when stored at 37 and 45 °C for 1 month, much faster than the HC. The mechanism that led to the difference is still to be explored. The extended pH effect data was collected from 3 months at 37 and 45 °C (Fig. 5). Within the pH range of 4–6, high amount of pGlu was generated at pH 4 and the minimal pGlu was formed at pH 6. Within the pH range of 6–8, the pGlu

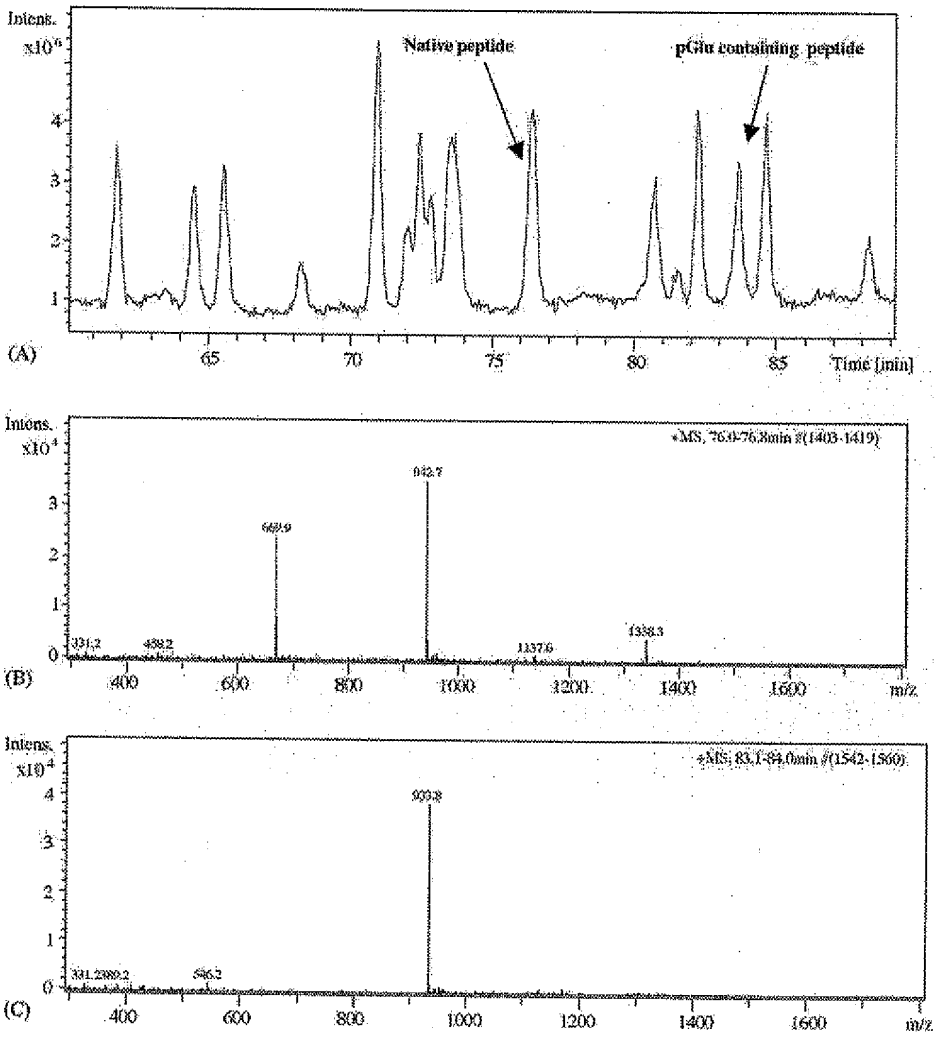

Fig. 1. Peak identification of *N*-pyroglutamyl formation from tryptic peptide mapping LC/MS trap. *N*-Pyroglutamte contained peak was found from stressed formulation sample.

Table 1
N-Pyroglutamate % determined by MSD trap and TOF MS

	Results (pGlu %)				
	pH 4.5	pH 4.7	pH 5.0	pH 5.2	pH 5.5
MSD trap[a]	50	42	38	30	20
QTOF MS[b]	49	43	39	33	27

	Results (pGlu %)					
	Acetate[c]	Propionate[c]	Glycolate[c]	Glutamate[c]	Histidine[c]	Succinate[c]
MSD trap[a]	35	33	40	40	46	45
QTOF MS[b]	33	33	37	37	40	40

Samples were stressed at 45 °C for 3 months.

[a] Data was obtained from peptide mapping by LC/MSD trap. The percentage of pGlu was determined from the integration of the extracted ion chromatogram (XIC) of the native peptide peak mass and pGlu peptide peak mass in the peptide mapping method.

[b] Data was obtained from reduced intact by QTOF MS and based upon the integration of two deconvoluted mass peak area of the native light chain from the purified bulk and modified LC from the stressed samples.

[c] The concentration is 10 mM for all buffers and pH is 5.2.

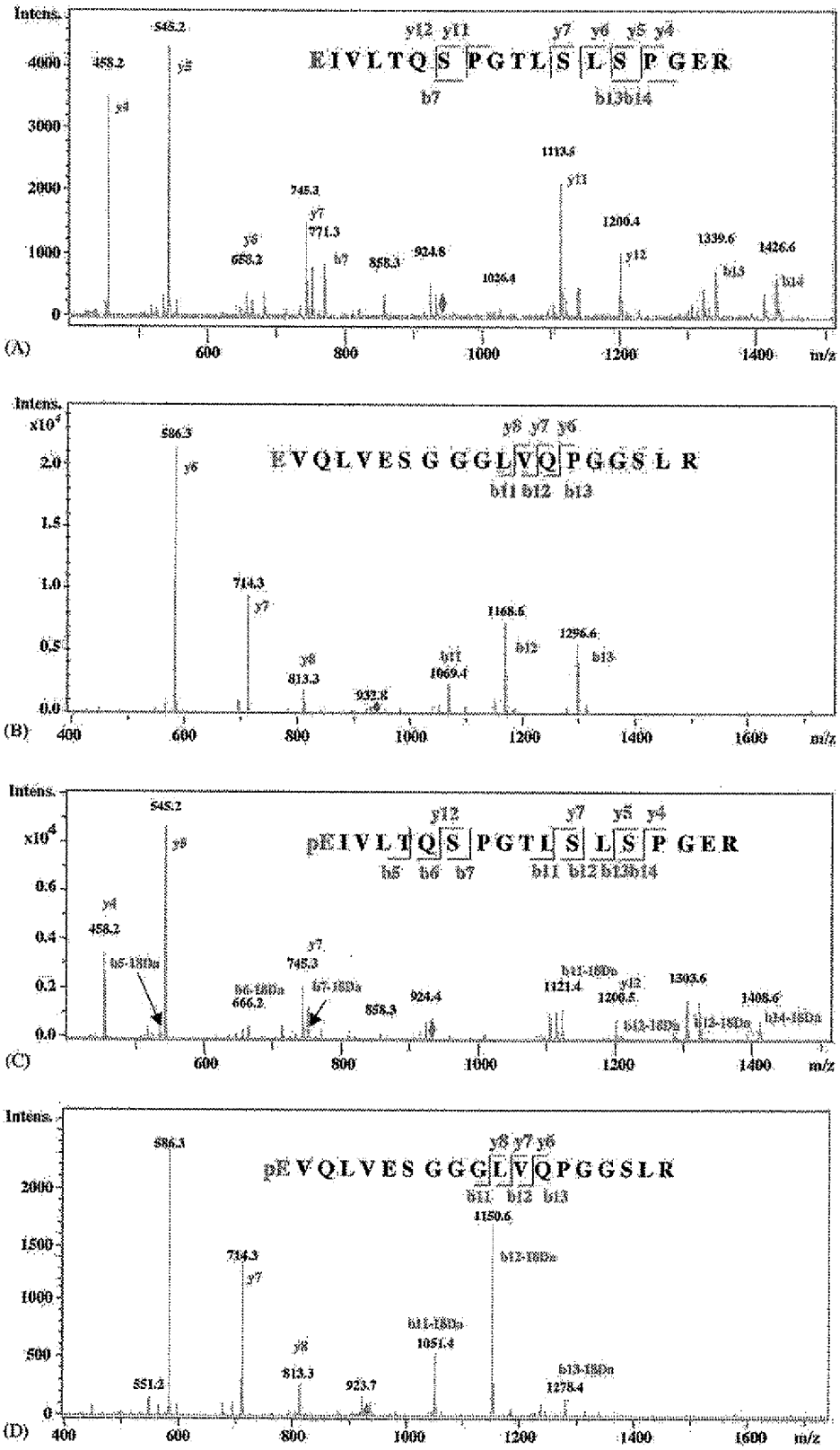

Fig. 2. Light chain and heavy chain MS/MS data of the native *N*-glutamate and *N*-pyroglutamate contained peptides. The native *N*-glutamate contained peptides of LC (A) and HC (B). The *N*-pyroglutamate contained peptides of LC (C) and HC (D).

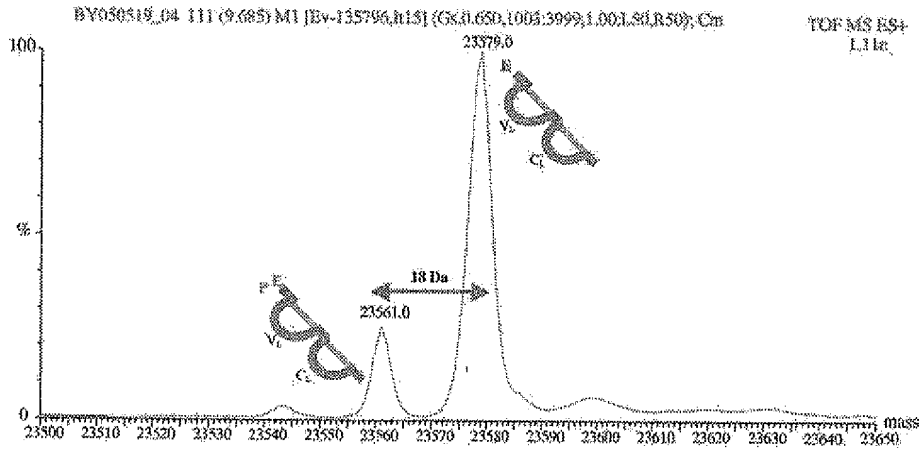

Fig. 3. Deconvoluted mass spectrum of reduced intact sample at 45 °C and 3 months by QTOF MS. Two peaks were determined to be light chain and *N*-pyro light chain that lost 18 Da due to cyclization.

increased with pH. This effect was demonstrated by the LC and HC data.

These data can be used to predict mAb N-terminal Glu storage half-life if the pGlu formation is assumed as a pseudo-first order rate reaction, the rate $[R]_c$ of the pGlu formation is proportional to the concentration of the native antibody.

$$[R]_c = d[pE]/dt = -d[E]/dt = k[E],$$

$$d[E]/([E] + [pE])/dt = -k[E]/[E] + [pE],$$

$$d[E]_r/dt = -k[E]r, \qquad [E]_r = A\exp(-kt),$$

$$\ln[E]_r = -kt + C \tag{1}$$

where $[E]_r$ is relative percentage of N-terminal Glu, [E] and [pE] are concentrations of Glu and pGlu derivatives, respectively. Eq. (1) was used to fit the data to obtain parameters of k (rate constant) and C (ln[percent of native mAb]) at time zero.

The plot of the logarithm of relative percent of N-terminal Glu as a function of time is linear and shown in Fig. 6. The linear regression fit predicts that slope (k) and the intercept (C) equal 0.0003 and equal 0.0101, respectively, for pH 4.5 and 45 °C. Based upon the above equation, the N-terminal Glu half-lives of LC and HC were calculated for other temperature and pH and tabulated in Table 2. Data was not shown for some temperatures since the pGlu formation was insignificant at 37 °C for HC and was undetectable for the LC and HC below 4 °C over 3 months. Data was also collected for 29 °C after 1-year observation with a half-life of 2 years at pH 5.

Buffer, excipient and surfactant were also studied to investigate the possible impact on pGlu formation. The 3-month data

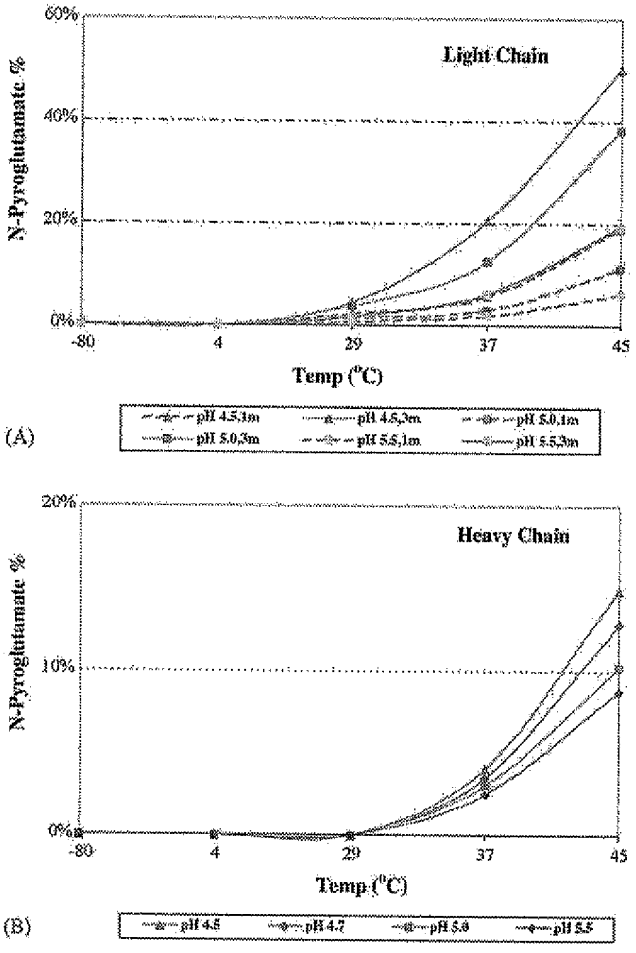

Fig. 4. *N*-Pyroglutamyl formation % of light chain (A) and heavy chain (B) from pH study at 1 and 3 months. Samples stressed at six temperatures, −80, 4, 29, 37 and 45 °C. Data was obtained from peptide mapping by LC/MSD trap.

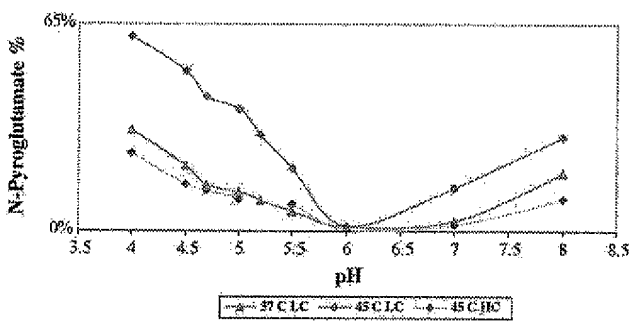

Fig. 5. pH effects on the pGlu formation of the LC and HC of the mAb.

Table 2
N-terminal Glu half-lives[a] of the mAb LC and HC vs. pH

	pH 4.0		pH 5.0		pH 6.0		pH 7.0		pH 8.0	
	LC	HC	LC	HC	LC	HC	LC	HC	LC	HC
37 °C	4.8	NA[b]	16	NA[b]	24	NA[b]	19	NA[b]	11	NA[b]
45 °C	2.4	9.6	4.9	19	9.6	481	9.6	96	4.8	19

The data was collected from the samples stressed at 37 and 45 °C over 3 months.
[a] Half-life ($t_{1/2}$, months) is calculated from linear regression data, the slope (k) and the intercept (C). Data was also obtained at 29 °C after 1-year observation with a half-life of 2 years for pH 5.
[b] Data was not available for the heavy chain at 37 °C since the pGlu formation was undetectable and insignificant.

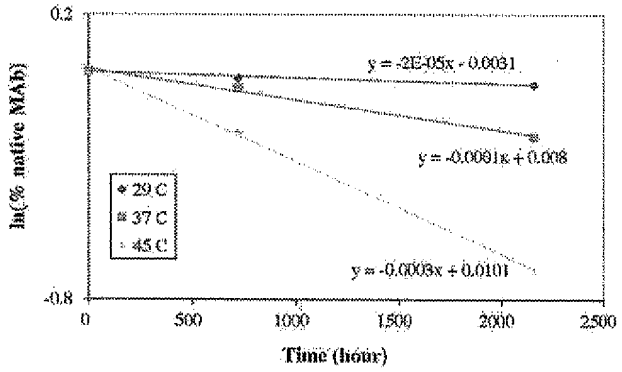

Fig. 6. Logarithm of the native mAb as a function of time at pH 4.5 and over 3 months.

did not show obvious effect as pH, temperature and storage time. Fig. 7 gave the buffer study result after 3-month storage. However, 1-year stability data from 29 °C and pH 5 showed that succinate buffer generated a relatively higher pGlu formation than acetate and histidine buffer. So far, it is unclear if the buffer pK_a and structure may impact the cyclization reaction. It has been reported that weak acids could catalyze the cyclization of Glu [19]. However, the buffer study indicates that the pGlu formation is slightly higher in histidine buffer than in sodium acetate at pH 5.0, suggesting that weak acids do not seem to accelerate the formation of pGlu. Further study may be needed to investigate this hypothesis. Both excipient and surfactant studies did not show any direct impact on pGlu formation with the exception for lactose (Fig. 8A and B). Lactose is a reducing sugar that can be reacted with lysine to form glycated lysine and this glycation was observed in our excipient screen study. This reaction can provide some information on mAb folding/unfolding status, indicating accessibility of a mAb surface. And more, lysine is the primary target for trypsin digestion and glycated lysine is almost non-reactive due to the hindering effect by the attached glycan on its side chain. However, glucose is also reducing sugar and its glycation was also found although glucose did not show significant impact on the cyclization of the mAb. This phenomenon is very interesting and also complicated. Further investigation may be needed to explore the impact of lactose on the cyclization.

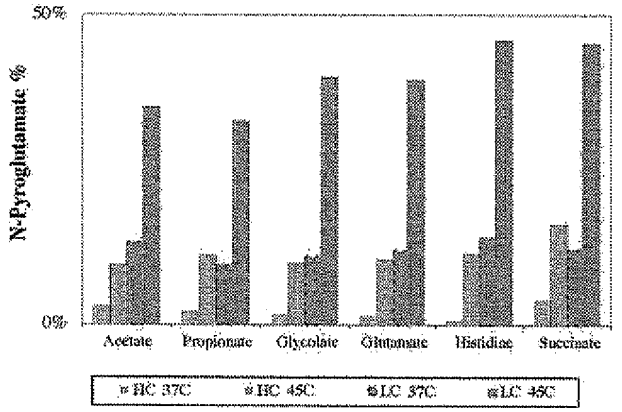

Fig. 7. *N*-Pyroglutamyl formation % of light chain and heavy chain from buffer study at 3 months. Data was calculated from stressed samples at 37 and 45 °C at 3 months.

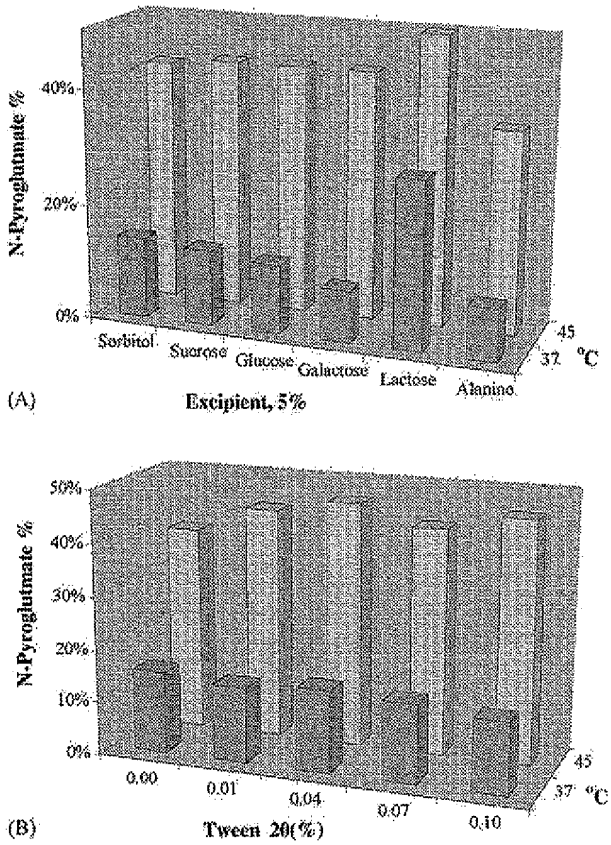

Fig. 8. *N*-Pyroglutamyl formation % of from excipient (A) and surfactant (B) studies at 3 months by LC/MSD trap. Data was calculated from stressed samples at 37 and 45 °C at 3 months.

3.3. Evaluation of IgG2 secondary structure and its biological activities

The literature has proposed that that pGlu from Glu can be an enzymatic reaction because the conversion of Glu to pGlu requires 50 h of incubation at 100 °C and at pH 4 and 10 [12,13]. The cyclization of Glu could hardly occur in relatively mild condition such as within cell culture and during purification and the formulation development process. The mAb in this study showed no detectable pGlu in the bulk materials after purification process. All conversion of Glu to pGlu occurred on shelf storage and grew with time, suggesting that pGlu can be formed under mild condition not through enzymatic reaction in a non-physiological condition. Moreover, this works proves that pGlu was derived from Glu without prior conversion to glutamine.

Both the N-terminus of the LC and HC are located in the framework region 1 and closed to CDR regions, and may potentially impact its bioactivity or potency after conversion to pGlu. If the binding epitope involves the N-terminus, such structural alteration may likely change the binding affinity directly. mAbs are densely packed molecules, cyclization, a modification involves the mAb peptide backbone on both LC and HC, can be reasonably anticipated certain impact on the local binding epitope environment indirectly. Such indirect impact can effect either through long range "linear" backbone adjustment or through the "3D" local bonding network at various levels, from H-bonding to covalent bonding. To isolate the impact of N-terminal cyclization from other physical and chemical degradations, some samples were treated to achieve about 50% N-terminal pGlu conversion with minimal physical and chemical degradations (i.e., aggregation, deamidation, oxidation). Since we did not see any significant tertiary structure change from our near-UV circular dichroism spectroscopy (data not shown), and the mAb contains predominantly β sheet, FT-IR is employed to determine whether or not the conformations of proteins with a broad range of secondary structural compositions are altered. FT-IR spectroscopy is one of the widely used vibrational spectroscopic methods in protein structural analysis, especially sensitive to the small secondary structure change. It is extremely sensitive to the conformational changes of proteins induced by various factors such as temperature, pH, and added chemicals and solvents. Fig. 9 compares the secondary structure of stressed mAb (red solid line) to the non-stressed mAb. A slight change was observed on some β turns around 1676 cm^{-1}. Since the tested sample was stored at 45 °C for 3 months, the β turn change might be caused by thermal stress. So far, we could not observe the significant structural change induced by cyclization. The impact evaluation of the N-terminal cyclization on the biological activity of the mAb remains challenging because it is hardly to obtain purely cyclized sample separately. Some conditions that favor N-terminal cyclization may also favor other physical and chemical degradations as well. This poses an intriguing challenge to isolate the impact of specific degradations on the activity of the affected therapeutic mAbs. Currently, other modifications such as oxidation have been observed in the stressed mAb. Considering that the objective is to minimize degradation of any kind, it immediately becomes clear that awareness of the properties that chemical modifications can have on activity and the ability to quantify them is of practical importance.

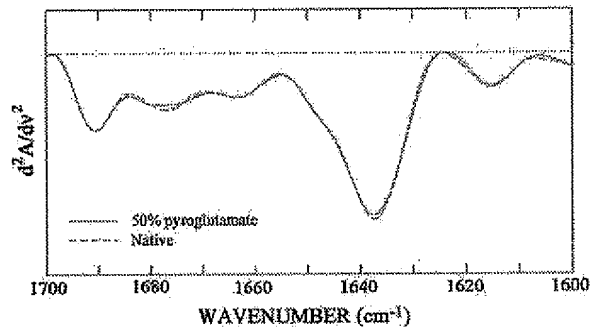

Fig. 9. Data from FT-IR secondary structure study. Comparison of the sample containing approximately 50% *N*-pyroglutamate (red solid line) to the native mAb (blue dotted line). (For interpretation of the references to colour in this figure legend, the reader is referred to the web version of the article.)

4. Conclusions

High conversion of N-terminal Glu to pGlu was observed on the studied mAb in assorted stability studies. This cyclization of Glu was observed and confirmed on the N-terminus of the LC and HC of the protein studied by the two mass spectrometry analytical techniques. Several formulation factors (temperature, time and pH) have been evaluated and the results showed that they significantly affected the formation of *N*-pyroglutamate. Based on the kinetic information presented in this study, the half-lives were calculated at pH 4.5–5.5 for LC and HC. Our data demonstrated that the pGlu of the mAb was formed non-enzymatically during stability studies. This non-enzymatic cyclization of Glu to pGlu of mAbs could be one of the major degradation pathways incurred in the mAb production and storage depending on pH and temperature conditions during the process development. The cyclization of Glu may not introduce significant conformational adaptation of the molecule based upon the preliminary structural change data. Whether or not it may induce further modifications and alter its bioactivity or therapeutic potency is unclear. Therefore, close monitoring of N-terminal pGlu formation can be critical to ensure quality of these mAb therapeutics with N-terminal Glu.

Acknowledgments

The authors would like to thank Aichun Dong for FT-IR work and Holly Huang for CD help. We appreciate David Brems for his comments and support.

References

[1] E. Andreakos, P.C. Taylor, M. Feldmann, Curr. Opin. Biotechnol. 13 (2002) 615–620.
[2] M. Trikha, L. Yan, L.M.T. Nakada, Curr. Opin. Biotechnol. 13 (2002) 609–614.
[3] F.J. Shen, M.Y. Kwong, R.G. Keck, R.J. Harris, in: D.R. Marshak (Ed.), Techniques in Protein Chemistry, Academic Press, San Diego, CA, 1996, pp. 275–285.

[4] R.J. Harris, B. Kabakoff, F.D. Macchi, F.J. Shen, M.Y. Kwong, J.D. Andya, S.J. Shire, N. Bjork, K. Totpal, A.B. Chen, J. Chromatogr. B 752 (2001) 233–245.
[5] R. Horejsi, G. Kollenz, F. Dachs, H.M. Tillian, K. Schauenstein, E. Schauenstein, W. Steinschifter, J. Biochem. Biophys. Meth. 34 (1997) 227–236.
[6] R.J. Harris, S.J. Shire, C. Winter, Drug Dev. Res. 61 (2004) 137–154.
[7] C.K. Verity, A. Loukas, D.P. McManus, P.J. Brindley, Parasitology 122 (2001) 415–420.
[8] P. Berasain, C. Carmona, B. Frangione, J.P. Dalton, F. Goni, Exp. Parasitol. 94 (2000) 99–106.
[9] E.M. Yoo, L.A. Wims, L.A. Chan, S.L. Morrison, J. Immunol. 170 (2003) 3134.
[10] R.G. Krishna, F. Wold, Methods in Protein Sequence Analysis, Plenum, New York, 1993, pp. 167–172.
[11] M. Messer, M. Ottersen, Compt. Rend. Trav. Lab. Carlsberg 35 (1965) 1–29.
[12] A. Bateman, S. Solomon, H.P.J. Bennett, J. Biol. Chem. 265 (1990) 22130–22136.
[13] H. Wilson, R.K. Cannan, J. Biol. Chem. 119 (1923) 309–331.
[14] D.R. Twardzik, A. Peterkofsky, Proc. Natl. Acad. Sci. 69 (1972) 274–277.
[15] W.H. Busby Jr., G.E. Quackbush, J. Humm, W.W. Youngblood, J.S. Kizer, J. Biol. Chem. 262 (1987) 8532–8536.
[16] S. Schilling, T. Hoffmann, S. Manhart, M. Hoffman, FEBS Lett. 563 (2004) 191–196.
[17] K.F. Huang, Y.L. Liu, W.J. Cheng, T.P. Ko, A.H.J. Wang, PNAS 102 (2005) 13117–13122.
[18] A.C. Dong, L.S. Jones, B.A. Kerwin, S. Krishnanc, J.F. Carpenter, Anal. Biochem. 351 (2006) 282–289.
[19] R.D. Dimarchi, J.P. Tam, S.B. Kent, R.B. Merrifield, Int. J. Pept. Protein Res. 19 (1982) 88–93.

EXHIBIT 3

Journal of Neurochemistry
Lippincott Williams & Wilkins, Philadelphia

Formation of *N*-Pyroglutamyl Peptides from *N*-Glu and *N*-Gln Precursors in *Aplysia* Neurons

Rebecca W. Garden, Tatiana P. Moroz, Juliann M. Gleeson, Philip D. Floyd, Lingjun Li, Stanislav S. Rubakhin, and Jonathan V. Sweedler

Department of Chemistry and Beckman Institute, University of Illinois, Urbana, Illinois, U.S.A.

Abstract: Matrix-assisted laser desorption/ionization with time-of-flight mass spectrometry is used to examine the formation of *N*-pyroglutamate (pGlu) in single, identified neurons from *Aplysia*. Six pGlu peptides are identified in the R3–14 and the R15 neurons that result from in vivo processing of peptides containing either Glu or Gln at their respective N-termini. Moreover, we show that Glu-derived pGlu is not a sample collection or measurement artifact. The pGlu peptides are detected in isolated cell bodies, regenerated neurites in culture, interganglionic connective nerves, cell homogenates, and collected releasates. We also demonstrate that R3–14 cells readily convert a synthetic *N*-Glu peptide to its pGlu analogue, indicating the presence of novel enzymatic activity. **Key Words:** Pyroglutamate—Neuropeptide—Matrix-assisted laser desorption/ionization mass spectrometry—Single cell—*Aplysia*—Abdominal ganglion.
J. Neurochem. **72,** 676–681 (1999).

Understanding neuropeptide function first requires information concerning the amino acid sequence and post-translational modification of the peptide. Often, terminal capping modulates a peptide's activity and/or resistance to degradation as in N-terminal acetylation, *N*-pyroglutamyl formation, and C-terminal amidation. *N*-Pyroglutamate (pGlu) is thought to be almost exclusively formed in vivo by intramolecular glutamine (Gln) cyclization (Messer and Ottesen, 1965; Busby et al., 1987; Fischer and Spiess, 1987). However, a few exceptions to Gln acting as the pGlu precursor have been reported. Bovine β-lipotropin(1–40) and joining peptides are pGlu modified to an extent of ~50%, although the precursor peptides have glutamic acid (Glu) at their respective N-termini (Bateman et al., 1990). Furthermore, multiple truncated forms of both water-soluble (Russo et al., 1997) and plaque-incorporated (Mori et al., 1992; Näslund et al., 1994) amyloid β-peptide contain pGlu derived from Glu. Such peptide heterogeneity may play a critical role in senile plaque formation and pathogenesis of Alzheimer's disease (Saido et al., 1995; Russo et al., 1997).

Formation of pGlu from N-terminal Glu is not a well-understood process. Mass spectrometry (MS) with fast-atom bombardment (Bateman et al., 1990), plasma desorption (Mori et al., 1992), and electrospray ionization (Näslund et al., 1994) has been used to identify the previously mentioned Glu-derived pGlu peptides. Although Gln cyclases, also described as Gln cyclotransferases, specifically convert Gln to pGlu (Messer and Ottesen, 1965; Gololobov et al., 1994), the Glu-converting analogue has not been identified. In fact, the possibility is often mentioned that Glu-derived pGlu is an acid-catalyzed artifact of peptide isolation (Nagle et al., 1989; Bateman et al., 1990; Saido et al., 1995). Unfortunately, conventional peptide extraction, purification, and sequencing techniques often yield ambiguous information concerning the nature of pGlu modifications.

We have used matrix-assisted laser desorption/ionization (MALDI) with time-of-flight MS (Kaufmann, 1995; Burlingame et al., 1998) to examine individual peptidergic neurons from the marine mollusk *Aplysia* (Scheller et al., 1984). We report that pGlu-containing peptides are found that arise from N-terminal processing of Glu as well as Gln. Twelve cells from the abdominal ganglion, the R3–14 cluster, synthesize a prohormone (Fig. 1A) that yields multiple peptides (Rothman et al., 1985; Kaldany et al., 1986; Newcomb and Scheller, 1987). The physiological significance of R3–14 peptides is uncertain except for histidine-rich basic peptide (HRBP), which mediates dose-dependent cardioexcitatory actions (Campanelli and Scheller, 1987). More than 90% of native HRBP contains Gln-derived pGlu; although, as is often the case, this finding has been ascribed to a possible acid-extraction artifact (Nagle et al., 1989). In addition to R3–14, the osmoregulatory neuron R15 synthesizes a prohormone that is cleaved as indicated in Fig. 1B (Buck

Received August 13, 1998; revised manuscript received September 24, 1998; accepted September 25, 1998.

Address correspondence and reprint requests to Dr. J. V. Sweedler at UIUC Department of Chemistry, 600 S. Mathews Ave., Box 63-5, Urbana, IL 61801, U.S.A.

Abbreviations used: antiANG-II, angiotensin II antipeptide; ASW, artificial sea water; DHB, 2,5-dihydroxybenzoic acid; HRBP, histidine-rich basic peptide; MALDI, matrix-assisted laser desorption/ionization; MS, mass spectrometry; PAC, pleural–abdominal connective; pGlu, pyroglutamate; TFA, trifluoroacetic acid.

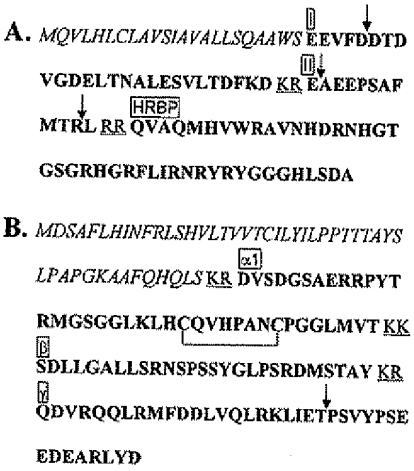

FIG. 1. Posttranslational processing of the *Aplysia* R3–14 (**A**) (Kaldany et al., 1985) and R15 (**B**) (Buck et al., 1987) prohormones. Putative signal and N-terminal sequences (not observed) are shown in italics, and dibasic cleavage sites are underlined. Previously identified peptides are shown in boldface, and unconventional cleavage sites described herein are indicated by arrows.

et al., 1987). Variant forms of the *N*-Gln peptide R15-γ have been observed (Weiss et al., 1989), although the exact nature of the modification has not been reported previously.

EXPERIMENTAL PROCEDURES

Chemicals

Hydrochloric acid, acetone, and acetonitrile were from Fisher Scientific (Pittsburgh, PA, U.S.A.), and 2,5-dihydroxybenzoic acid (DHB) was from ICN Pharmaceuticals (Costa Mesa, CA, U.S.A.). Trifluoroacetic acid (TFA), neurotensin, angiotensin II antipeptide (antiANG-II), poly-L-lysine hydrobromide (molecular weight, >300,000), and pGlu aminopeptidase (5-oxoprolyl-peptidase; EC 3.4.19.3) from *Bacillus amyloliquefaciens* were obtained from Sigma (St. Louis, MO, U.S.A.), as were the chemicals used to prepare artificial seawater (ASW) and culture media (Goldberg, 1991). Aqueous solutions were prepared with purified water (Millipore, Bedford, MA, U.S.A.).

Single-cell preparation

Aplysia californica (0.5–900 g) were obtained from Pacific Biomarine (Venice, CA, U.S.A.), Marinus Inc. (Long Beach, CA, U.S.A.), and the *Aplysia* Research Facility (Miami, FL, U.S.A.). Individual neurons were prepared for MALDI MS as previously described (Garden et al., 1996). In brief, after isolating and pinning each abdominal ganglion, the physiological saline was replaced by the aqueous DHB matrix solution (10 mg/ml). Neurons were identified based on their characteristic position, pigmentation, and morphology (Rittenhouse and Price, 1986), and tungsten needles were used to transfer each cell onto a MALDI sample plate containing ~0.5 μl of DHB.

Alternatively, mass spectra were obtained from R3–14 neurons that were cultured for 1–3 days. Established methods were used to isolate and maintain neurons in culture (Goldberg, 1991), and dissociated cells were transferred to a poly-L-lysine-coated glass coverslip (22 mm diameter) within a 35-mm Petri dish containing 2 ml of culture media. Before assay, the culture medium was replaced by DHB solution in a stepwise manner to reduce salt concentrations and to facilitate peptide ionization. After drying, each coverslip was attached to the machined inset of a modified MALDI sample plate so that the surface of the coverslip was even with the surface of the plate.

pGlu aminopeptidase treatment

R3–14 neurons from five *Aplysia* were dissected, pooled, and homogenized in 40:1:6 acetone/hydrochloric acid/water before freeze-drying and resuspension in ~10 μl of water. Mass spectra were obtained from this homogenate both before and after a 5-h incubation with pGlu aminopeptidase at 34°C. In both cases, 0.5 μl of homogenate was added to 0.5 μl of matrix on one spot of the MALDI sample plate. After mixing, 0.5 μl of this solution was combined with 0.5 μl of fresh matrix on a clean sample spot. Such spot-to-spot transfers were repeated until quality mass spectra were obtained (typically four transfers).

N-Glu peptide incubation

Individual R3–14 clusters were removed from four *Aplysia* abdominal ganglia in the presence of 15°C ASW containing a test *N*-glutamyl peptide, antiANG-II. The clusters were transferred into separate 500-μl polypropylene tubes. Cells within each cluster were disrupted with a tungsten needle before addition of 1 μl of water containing 4×10^{-5} *M* antiANG-II. Additional sample tubes consisted of antiANG-II (4×10^{-5} *M*) in ASW and water as controls. The volume occupied by each sample was ~10 μl. One set of samples (i.e., antiANG-II with cells, with ASW, and with water) was heated for 10 min at 95°C. All tubes were then maintained at 15°C, with periodic sampling for MS. MALDI sample spots were prepared as described in the previous section.

Microbore LC

Pleural–abdominal connectives (PACs) from 25 *Aplysia* were pooled for peptide extraction and LC separation as described recently (Floyd et al., 1999). A reversed-phase microbore LC (Magic 2002, Michrom BioResources, Auburn, CA, U.S.A.), consisting of a Reliasil C-18 column (0.5 × 150 mm) with 300 Å packing, was used at ambient temperature with a 50 μl/min flow rate. After column equilibration with solvent A (98% water, 0.1% TFA, and 1.9% acetonitrile), a gradient was developed from 0–80% solvent B (90% acetonitrile, 9.9% water, and 0.1% TFA) in 10 min. Fractions were collected and screened by MALDI MS; 0.5 μl of each fraction was deposited onto a MALDI sample plate followed by the same volume of DHB.

Release studies

The method for monitoring the peptides released from a cell cluster was similar to that previously described by our laboratory (Garden et al., 1998). For each experiment, a bag cell cluster (neuroendocrine cells adjacent to the R3–14 cells) with a 5-mm section of PAC was removed from the abdominal ganglion and placed to a small-volume release chamber. A pulled piece of polyethylene tubing was placed over the connective and served as a suction pipette electrode. One Ag/AgCl electrode was placed in the bath as a reference electrode, and another was positioned near the bag cells for recording and stimulation by an isolated pulse stimulator and a differential AC amplifier (A-M Systems, Carlsborg, WA, U.S.A.). To concentrate the peptides and to improve the salt removal, we modified our prior sampling procedure to include a microdi-

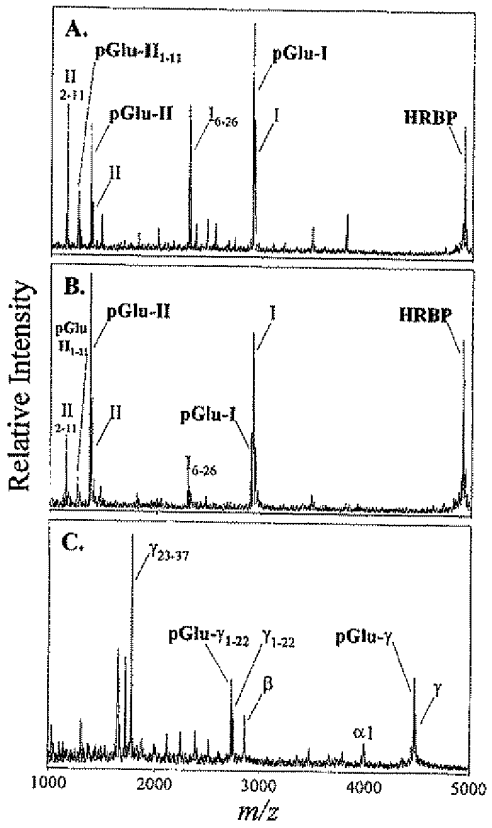

FIG. 2. MALDI peptide profiles of a single neuron from the R3–14 group (**A**), a regenerated process of a cultured R3–14 cell (**B**), and an isolated R15 cell (**C**). Labeled peaks correspond to $[M + H]^+$ where M is the molecular weight of each peptide. Those containing pGlu are indicated in boldface.

alysis step consisting of a hollow-fiber microdialysis tubing (Spectrum, Gardena, GA, U.S.A.) as used by Liu and coworkers (1996, 1997) for electrospray ionization MS. Each releasate sample (0.5–5 μl) was dialyzed for 30 min with acidified DHB matrix (10 mg/ml in 5% TFA) as the dialysate. The dialyzed releasate samples were then deposited directly onto a MALDI sample plate for subsequent analysis. To determine if detected peptides were released in a stimulation- and Ca^{2+}-dependent manner, this approach was repeated without electrical stimulation as well as with low-Ca^{2+} ASW (0.1 m*M* Ca^{2+} instead of the normal 10 m*M* Ca^{2+}).

MALDI MS

Mass spectra were obtained as described previously (Garden et al., 1998), using a Voyager Elite mass spectrometer (PerSeptive Biosystems, Framingham, MA, U.S.A.). It was necessary to independently optimize the laser power and delay time for each type of sample (i.e., single cells, cultured cells homogenates, LC fractions, and releasates). Care was used to avoid detector saturation and MALDI-induced fragmentation of peptides by working just above the threshold laser power required for ionization. Each representative mass spectrum shown is the unsmoothed average of 20–100 laser pulses, with mass calibration performed internally, using two peaks corresponding to previously identified peptides. Spectral peaks were assigned by comparing observed masses with those calculated from known amino acid sequences. Mass accuracy was typically better than 0.01%.

RESULTS

As shown in Fig. 2, mass spectra of freshly isolated and cultured cells from abdominal ganglia indicate the presence of previously characterized (Rothman et al., 1985; Kaldany et al., 1986; Weiss et al., 1989), as well as unidentified, peptides. Six of the detected peptides in R3–14 and R15 correspond, by mass, to pGlu-modified forms. The unexpected peaks were first assigned based on the observation of mass differences of 18.0 (Glu cyclization) or 17.0 (Gln cyclization). To confirm that these peptides actually contain N-terminal pGlu, we treated R3–14 extracts with pGlu aminopeptidase. Figure 3 shows an expanded view of pre- and postincubation mass spectra that confirms the identification of pGlu-II, as the peptide at *m/z* 1,363.6 (or any of its alkali metal adducts) is no longer detected after enzyme treatment. Instead, a peptide 111 Da lighter, corresponding to the removal of pGlu, is readily observed.

As expected from previous work (Kaldany et al., 1986; Nagle et al., 1989), essentially all HRBP in R3–14 neurons is in the pGlu form. The small peaks following HRBP (*m/z* 4,925.4) likely correspond to poorly resolved $[Gln - HRBP + H]^+$ (4,943.4) and $[HRBP + Na]^+$ (4,947.4). Besides the R3–14 precursor, one of the only other characterized *Aplysia* neuropeptide precursors containing peptides with N-terminal Glu or Gln is the R15 prohormone (Fig. 1B). We observe two pGlu peptides (Fig. 2C). Peptides α1, β, and γ_{23-37}, in addition to several currently unidentified peptides, are also detected.

An important question to address is whether the observed pGlu formation results from biological (i.e., enzymatic) modification or sampling and measurement effects. Two possible sources of artifacts are the drying of samples in acidic DHB matrix and the MS ionization process. To test for induced Glu and/or Gln cyclization, we performed several experiments. Mass spectra were obtained from synthetic peptides with N-terminal pGlu

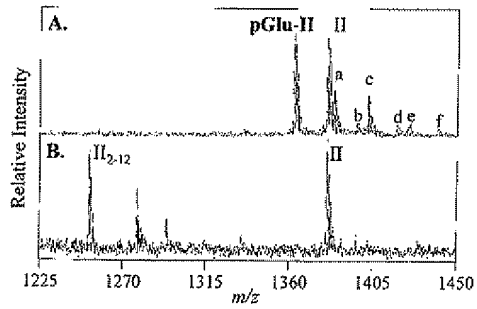

FIG. 3. Representative MALDI mass spectra acquired from an R3–14 homogenate both before (**A**) and after (**B**) incubation with pGlu aminopeptidase. Sodium and potassium adducts are indicated as follows: pGlu-II $[M + Na]^+$ (a); pGlu-II $[M + K]^+$ (b); II $[M + Na]^+$ (c); II $[M + K]^+$ (d); II $[M + 2Na - H]^+$ (e); II $[M + Na + K - H]^+$ (f).

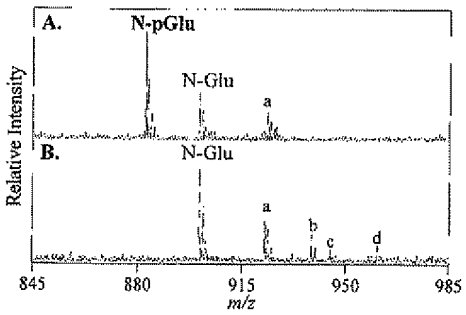

FIG. 4. Representative MALDI mass spectra acquired from R3–14 cluster homogenates that were incubated for 3 h with a synthetic *N*-glutamyl peptide (antiANG-II, designated *N*-Glu). **A:** Homogenates used to obtain the spectrum were maintained at 15°C throughout the dissection and incubation. **B:** These homogenates were heated at 95°C for 10 min before incubation. Peaks labeled as a, b, c, and d correspond to $[M + Na]^+$, $[M + K]^+$, $[M + 2Na - H]^+$, and $[M + Na + K - H]^+$, respectively, where M is the molecular weight of *N*-Glu.

(neurotensin) and N-terminal Glu (antiANG-II). When crystallized in the DHB matrix and ionized using MALDI, mass spectra contained only expected peaks corresponding to the sampled materials. As a further test, we separated and isolated HRBP, pGlu-I, pGlu-II, pGlu-II_{1-11}, pGlu-γ, and pGlu-γ_{1-22} from *Aplysia* PACs using microbore-LC. Significantly, the Glu and pGlu forms of R3–14 peptides I and II are well resolved, and once separated, the forms do not reequilibrate regardless of the sampling or measurement protocol (data not shown). Hence, for these synthetic and native peptides, N-terminal Glu/Gln cyclization is not an artifact. Our findings are consistent and expand on the previously documented cases of Glu-derived pGlu (Bateman et al., 1990; Mori et al., 1992; Näslund et al., 1994; Saido et al., 1995).

The next step is to determine if R3–14 cluster homogenates are capable of converting antiANG-II, a nonnative *N*-Glu peptide, into its pGlu form. No pGlu-antiANG-II is detected in the peptide-only controls, nor in the heat-treated homogenates; however, formation of pGlu-antiANG-II is observed in the R3–14 homogenates after several hours, with the intensity increasing throughout an 11-h incubation (Fig. 4). We then tested whether these pGlu modifications may be physiologically important by determining if the pGlu peptides are observed in stimulated release and whether the release is Ca^{2+} dependent. As shown in Fig. 5, we observe multiple bag cell peptides as well as significant amounts of I, II, and their modified forms in releasates. No detectable peptides are released without electrical stimulation of the PAC or in the presence of low-Ca^{2+} ASW (data not shown).

DISCUSSION

Single-cell MALDI provides a versatile alternative for accurate and precise mass-based profiling of peptidergic neurons (Jiménez et al., 1994; Garden et al., 1996). In fact, this approach detects novel processing of peptide precursors from some of the most well-characterized molluscan neurons (Garden et al., 1998; Jiménez et al., 1998). In the present study, we have used MALDI to detect peptides in a variety of cell preparations in order to investigate pGlu formation. Although spectral peak heights for different peptides and for different sample types cannot be quantitatively compared, MALDI provides a wealth of information concerning peptide distribution and processing. In fact, almost every reported case of single-cell MALDI reveals the presence of unexpected peptides, many of which result from unconventional processing of known prohormones. As summarized in Fig. 1, this is also the case with the R3–14 and R15 neurons from *Aplysia*.

R3–14 neurons are good candidates to use when examining for pGlu formation, because Nagle and coworkers (1989) demonstrated that significant portions of peptide I and HRBP were N-terminally blocked, yet they speculated that the cyclization could be an analytical artifact. Another R3–14 gene product, peptide II, has been sequenced (Rothman et al., 1985), and several shortened forms have been observed (Newcomb and Scheller, 1987). MALDI detects the previously isolated peptides I, II, II_{2-11}, and HRBP as well as three unexpected peptides corresponding to pGlu-modified forms (Fig. 2A and B). We confirm enzymatically that the blocked form of peptide II contains pGlu (Fig. 3). Furthermore, LC fractionation of the pGlu and Glu forms indicate that neither sampling nor MS is responsible for the cyclization.

We previously detected pGlu-II in releasates by electrically stimulating the PAC with attached bag cell neurons, although the peptide was not identified at that time (see Fig. 1 in Garden et al., 1998). To confirm and expand on this finding, we improved our collection and sampling of releasates from the sheath region surrounding the bag cell cluster by using microdialysis before MS. As shown in Fig. 5, pGlu-I, pGlu-II, as well as expected bag cell peptides are observed in a stimulation and Ca^{2+}-dependent manner. The R3–14 cluster projects

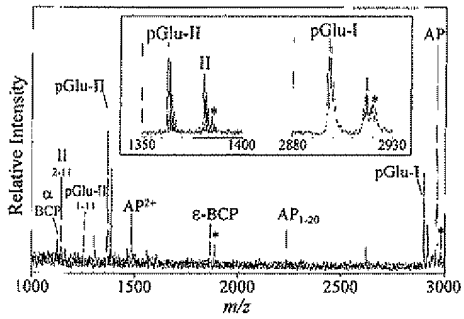

FIG. 5. Representative MALDI mass spectrum acquired from releasates from electrically stimulated bag cell clusters and the sheath area. The bag cell peptides (BCPs) detected include acidic peptide (AP), α-BCP, and ε-BCP. **Inset:** The expanded *m/z* regions show R3–14 peptides I, II, and their pGlu-modified forms. Sodium adducts are labeled with asterisks.

axons to the heart, the connective tissue sheath surrounding the abdominal ganglion, and other regions (Rittenhouse and Price, 1986). This likely explains why these abdominal ganglion peptides are released from the abdominal end of the PAC.

The detection of peptide α1, and not α2, in R15 supports the reports of differential and alternative splicing of RNA, which encodes the R15 precursor (Buck et al., 1987; Weiss et al., 1989). Moreover, two peptides separated by HPLC, yet having identical amino acid compositions, were previously isolated from 820 homogenized R15 neurons, and these peptides were suggested to represent slightly modified variants of R15-γ (Weiss et al., 1989). We also observe heterogeneity (Fig. 2C), as portions of R15-γ are not only pGlu modified, but are also further cleaved between Thr^{22} and Pro^{23} to yield γ_{1-22} and γ_{23-37}. The presence of both pGlu and Gln forms of R15-γ contrasts with the *N*-Gln peptide from R3–14, where most HRBP (>90%; Nagle et al., 1989) is pGlu modified.

When pGlu is derived from Glu, significant concentrations of both Glu and pGlu peptides are observed in single cells. This was also shown for peptides from pro-opiomelanocortin (Bateman et al., 1990) and from amyloid β-peptide (Mori et al., 1992; Näslund et al., 1994; Saido et al., 1995). However, in each of these cases, peptides were isolated and assayed primarily from somas; hence, they likely represent peptide-processing intermediates in addition to the final products. Likewise, the mass spectra acquired from isolated cell bodies represent snapshots of posttranslational processing. For example, MALDI of *Aplysia* bag cell somas often detects both unamidated and mature forms of egg-laying hormone, although only amidated egg-laying hormone is found in releasates (Garden et al., 1998). To determine if this explains the detection of both *N*-Glu and pGlu forms of the R3–14 peptides, we examined regenerated processes from cultured cells as well as cell releasates. However, as shown in Figs. 2B and 5, both forms were still observed in all cases with similar intensities. The importance of having appreciable amounts of the native and the cyclized pGlu peptides is unknown at this time.

Significantly, only unheated R3–14 homogenates can convert a nonnative *N*-Glu peptide into a pGlu peptide. This finding strongly indicates the presence of novel enzymatic activity. Previous characterization of Gln cyclase from papaya latex (Messer and Ottesen, 1965) and from porcine brain (Busby et al., 1987) indicates that *N*-Glu peptides do not act as inhibitors or substrates for pGlu formation. Furthermore, Gln cyclotransferase activity in *Streptococcus bovis* uses Gln, and not Glu, as a substrate for pGlu production (Chen and Russell, 1989). Although we do not know whether the Glu-to-pGlu conversion is caused by the same enzyme that catalyzes Gln-to-pGlu formation, this putative enzyme(s) has unique specificity and characteristics for *N*-Glu peptides.

In summary, we have used MALDI to characterize pGlu-modified peptides from isolated neurons, regenerated processes, LC fractions, cell homogenates, and releasates from electrically stimulated cells. Although one can envision other modifications producing the observed mass changes (e.g., amino acid substitutions), the combination of pGlu aminopeptidase and MALDI conclusively demonstrate the presence of pGlu peptides. The fidelity of synthetic standards and separated LC fractions demonstrates that pGlu formation is not a sample handling or measurement artifact. Release of at least two of the pGlu peptides in a physiological manner suggests a biological role, and the ability to modify nonnative *N*-Glu peptides suggests novel enzymatic activity. The presence of pGlu can have significant effects on neuropeptide function as encountered with thyrotropin-releasing hormone (Abraham and Podell, 1981) and adipokinetic hormone II (Stagg and Candy, 1998). We expect that formation of pGlu from *N*-Glu peptides will be found in many additional biological systems, as more are studied for this in vivo processing. MALDI is an excellent way to identify such modifications.

Acknowledgment: Stephen Martin at Perkin-Elmer Biosystems is acknowledged for assisting with custom-designed MALDI sample plates. This study was supported by NIH grant R01NS53030 and NSF grant CHE9622663. *Aplysia californica* were partially provided by National Resource for *Aplysia* at the University of Miami under NIH grant NCRR RR10294. R.W.G. acknowledges support from an Eastman Fellowship in Analytical Chemistry and Polymer Characterization.

REFERENCES

Abraham G. N. and Podell D. N. (1981) Pyroglutamic acid: nonmetabolic formation, function in proteins and peptides, and characteristics of the enzymes effecting its removal. *Mol. Cell. Biochem.* **38,** 181–190.

Bateman A., Solomon S., and Bennett H. P. J. (1990) Post-translational modification of bovine pro-opiomelanocortin: tyrosine sulfation and pyroglutamate formation, a mass spectrometric study. *J. Biol. Chem.* **266,** 22130–22136.

Buck L. B., Bigelow J. M., and Axel R. (1987) Alternative splicing in individual *Aplysia* neurons generates neuropeptide diversity. *Cell* **51,** 127–133.

Burlingame A. L., Boyd R. K., and Gaskell S. J. (1998) Mass spectrometry. *Anal. Chem.* **70,** 647R–716R.

Busby W. H., Quackenbush G. E., Humm J., Youngblood W. W., and Kizer J. S. (1987) An enzyme(s) that converts glutaminyl-peptides into pyroglutamyl peptides. *J. Biol. Chem.* **262,** 8532–8536.

Campanelli J. T. and Scheller R. H. (1987) Histidine-rich basic peptide: a cardioactive neuropeptide from *Aplysia* neurons R3–14. *J. Neurophysiol.* **57,** 1201–1209.

Chen G. and Russell J. B. (1989) Transport of glutamine by *Streptococcus bovis* and conversion of glutamine to pyroglutamic acid and ammonia. *J. Bacteriol.* **171,** 2981–2985.

Fischer W. H. and Spiess J. (1987) Identification of a mammalian glutaminyl cyclase converting glutaminyl into pyroglutamyl peptides. *Proc. Natl. Acad. Sci. USA* **84,** 3628–3632.

Floyd P. D., Li L., Moroz T. P., and Sweedler J. V. (1999) Characterization of peptides from *Aplysia* using microbore liquid chromatography with MALDI-TOF mass spectrometry guided purification. *J. Chromatogr. A* (in press).

Garden R. W., Moroz L. L., Moroz T. P., Shippy S. A., and Sweedler J. V. (1996) Excess salt removal with matrix rinsing: direct profiling of neurons form marine invertebrates using matrix-assisted laser desorption/ionization time-of-flight mass spectrometry. *J. Mass Spectrom.* **31,** 1126–1130.

Garden R. W., Shippy S. A., Li L., Moroz T. P., and Sweedler J. V. (1998) Proteolytic processing of the *Aplysia* egg-laying hormone prohormone. *Proc. Natl. Acad. Sci. USA* **95,** 3972–3977.

Goldberg D. J. (1991) Culturing the large neurons of *Aplysia*, in *Culturing Nerve Cells* (Banker G. and Goslin K., eds), pp. 155–175. MIT Press, Cambridge, Massachusetts.

Gololobov M. Y., Song L., Wang W., and Bateman R. C. Jr. (1994) Steady-state kinetics of glutamine cyclotransferase. *Arch. Biochem. Biophys.* **309,** 300–307.

Jiménez C. R., van Veelen P. A., Li K. W., Wildering W. C., Geraerts W. P. M., Tjaden U. R., and van der Greef J. (1994) Neuropeptide expression and processing as revealed by direct matrix-assisted laser desorption ionization mass spectrometry of single neurons. *J. Neurochem.* **62,** 404–407.

Jiménez C. R., Li K. W., Dreisewerd K., Spijker S., Kingston R., Bateman R. H., Burlingame A. L., Smit A. B., van Minnen J., and Geraerts W. P. M. (1998) Direct mass spectrometric peptide profiling and sequencing of single neurons reveals differential peptide patterns in a small neuronal network. *Biochemistry* **37,** 2070–2076.

Kaldany R. J., Campanelli J. T., Makk G., Evans C. J., and Scheller R. H. (1986) Proteolytic processing of a peptide precursor in *Aplysia* neuron R14. *J. Biol. Chem.* **261,** 5751–5757.

Kaufmann R. (1995) Matrix-assisted laser desorption ionization (MALDI) mass spectrometry: a novel analytical tool in molecular biology and biotechnology. *J. Biotechnol.* **41,** 155–175.

Liu C., Wu Q., Harms A. C., and Smith R. D. (1996) On-line microdialysis sample cleanup for electrospray ionization mass spectrometry of nucleic acid samples. *Anal. Chem.* **68,** 3295–3299.

Liu C., Muddiman D. C., Tang K., and Smith R. D. (1997) Improving the microdialysis procedure for electrospray ionization mass spectrometry of biological samples. *J. Mass Spectrom.* **32,** 425–431.

Messer M. and Ottesen M. (1965) Isolation and properties of glutamine cyclotransferase of dried papaya latex. *Compt. Rend. Trav. Lab. Carlsberg* **35,** 1–29.

Mori H., Takio K., Ogawara M., and Selkoe D. J. (1992) Mass spectrometry of purified amyloid β protein in Alzheimer's disease. *J. Biol. Chem.* **267,** 17082–17086.

Nagle G. T., Knock S. L., Painter S. D., Blankenship J. E., Fritz R. R., and Kurosky A. (1989) I. *Aplysia californica* neurons R3–14: primary structure of the myoactive histidine-rich basic peptide and peptide I. *Peptides* **10,** 849–857.

Näslund J., Schierhorn A., Hellman U., Lannfelt L., Roses A. D., Tjernberg L. O., Silverring J., Gandy S. E., Winblad B., Greengard P., Nordstedt C., and Terenius L. (1994) Relative abundance of Alzheimer Aβ amyloid peptide variants in Alzheimer disease and normal aging. *Proc. Natl. Acad. Sci. USA* **91,** 8378–8382.

Newcomb R. and Scheller R. H. (1987) Proteolytic processing of the *Aplysia* egg-laying hormone and R3–14 neuropeptide precursors. *J. Neurosci.* **7,** 854–863.

Rittenhouse A. R. and Price C. H. (1986) Electrophysiological and anatomical identification of the peripheral axons and target tissues of *Aplysia* neurons R3–14 and their status as multifunctional, multimessenger neurons. *J. Neurosci.* **6,** 2071–2084.

Rothman B. S., Sigvardt K. A., Hawke D. H., Brown R. O., Shively J. E., and Mayeri E. (1985) Identification and primary structural analysis of peptide II, an end-product of precursor processing in cells R_3–R_{14} of *Aplysia*. *Peptides* **6,** 1113–1118.

Russo C., Saido T. C., DeBusk L. M., Tabaton M., Gambetti P., and Teller J. K. (1997) Heterogeneity of water-soluble amyloid β-peptide in Alzheimer's disease and Down's syndrome brains. *FEBS Lett.* **409,** 411–416.

Saido T. C., Iwatsubo T., Mann D. M. A., Shimada H., Ihara Y., and Kawashima S. (1995) Dominant and differential deposition of distinct β-amyloid peptide species, $Aβ_{N3(pE)}$, in senile plaques. *Neuron* **14,** 457–466.

Scheller R. H., Kaldany R., Kreiner T., Mahon A. C., Nambu J. R., Schaefer M., and Taussig R. (1984) Neuropeptides: mediators of behavior in *Aplysia*. *Science* **225,** 1300–1308.

Stagg L. E. and Candy D. J. (1998) The effect of analogues of adipokinetic hormone II on second messenger systems in the fat body of *Schistocerca gregaria*. *Insect Biochem. Mol. Biol.* **28,** 59–68.

Weiss K. R., Bayley H., Lloyd P. E., Tenenbaum R., Kolks M. A. G., Buck L., Cropper E. C., Rosen S. C., and Kupfermann I. (1989) Purification and sequencing of neuropeptides contained in neuron R15 of *Aplysia californica*. *Proc. Natl. Acad. Sci. USA* **86,** 2913–2917.

EXHIBIT 4

A. Beck
M.-C. Bussat
C. Klinguer-Hamour
L. Goetsch
J.-P. Aubry
T. Champion
E. Julien
J.-F. Haeuw
J.-Y. Bonnefoy
N. Corvaia

Stability and CTL activity of N-terminal glutamic acid containing peptides

Authors' affiliations:
A. Beck, M.-C. Bussat, C. Klinguer-Hamour, L. Goetsch, J.-P. Aubry, T. Champion, E. Julien, J.-F. Haeuw, J.-Y. Bonnefoy and N. Corvaia,
BioMérieux-Pierre Fabre, Centre d'Immunologie Pierre Fabre (CIPF), Saint-Julien-en-Genevois, France.

Correspondence to:
Alain Beck
Department of Physico-Chemistry
Centre d'Immunologie Pierre Fabre (CIPF)
5 avenue Napoléon III
BP 497
F-74164 Saint-Julien-en-Genevois
Cedex
France
Tel.: 33-4-50-35-35-55
Fax: 33-4-50-35-35-90
E-mail: alain.beck@pierre-fabre.com
www.cipf.com

Dates:
Received 8 December 2000
Revised 22 January 2001
Accepted 11 February 2001

To cite this article:
Beck, A., Bussat, M.-C., Klinguer-Hamour, C., Goetsch, L., Aubry, J.-P., Champion, T., Julien, E., Haeuw, J.-F., Bonnefoy, J.-Y. & Corvaia, N. Stability and CTL activity of N-terminal glutamic acid containing peptides.
J. Peptide Res. 2001, 57, 528–538.

ISSN 1397-002X

Key words: clinical grade peptides; CTL epitopes; glutamic acid; melanoma; peptide vaccines; pyroglutamic acid

Abstract: Several cytotoxic T lymphocyte peptide-based vaccines against hepatitis B, human immunodeficiency virus and melanoma were recently studied in clinical trials. One interesting melanoma vaccine candidate alone or in combination with other tumor antigens, is the decapeptide ELA. This peptide is a Melan-A/MART-1 antigen immunodominant peptide analog, with an N-terminal glutamic acid. It has been reported that the amino group and γ-carboxylic group of glutamic acids, as well as the amino group and γ-carboxamide group of glutamines, condense easily to form pyroglutamic derivatives. To overcome this stability problem, several peptides of pharmaceutical interest have been developed with a pyroglutamic acid instead of N-terminal glutamine or glutamic acid, without loss of pharmacological properties. Unfortunately compared with ELA, the pyroglutamic acid derivative (PyrELA) and also the N-terminal acetyl-capped derivative (AcELA) failed to elicit cytotoxic T lymphocyte (CTL) activity. Despite the apparent minor modifications introduced in PyrELA and AcELA, these two derivatives probably have lower affinity than ELA for the specific class I major histocompatibility complex. Consequently, in order to conserve full activity of ELA, the formation of PyrELA must be avoided. Furthermore, this stability problem is worse in the case of clinical grade ELA, produced as an acetate salt, like most of the pharmaceutical grade peptides. We report here that the hydrochloride salt, shows higher stability than the acetate salt and may be suitable for use in man. Similar stability data were also obtained for MAGE-3, another N-terminal glutamic acid containing CTL peptide in clinical development, leading us to suggest that all N-terminal glutamic acid and probably glutamine-containing CTL peptide epitopes may be stabilized as hydrochloride salts.

Abbreviations: AAA, amino acid analysis; AcOH, acetic acid; B-ALL, B-cell acute lymphoblastic leukemia; CEA, carcinoembryonic antigen; CTL, cytotoxic T lymphocyte; DMEM, Dulbecco's modified Eagle's medium; DMSO, dimethylsulfoxide; EBNA, Epstein-Barr virus-encoded antigen; EBV, Epstein-Barr virus; EF2, elongation factor 2; ES-MS, electrospray-mass spectrometry; Fmoc, 9-fluorenylmethyloxycarbonyl; HCV, hepatitis C virus; HIV, human immunodeficiency virus; HLA, human leukocyte antigen; ICH, International Conference of Harmonization; MAGE, melanoma antigen; MART, melanoma antigen recognized by T cells; MFI, mean fluorescence intensity; MHC, major histocompatibility complex; MUM-1, melanoma ubiquitous mutated-1; PSA, prostate specific antigen; RP-HPLC, reverse phase-high performance liquid chromatography; tBu, tertiobutyl; TEAP, triethylammonium phosphate; TFA, trifluoroacetic acid; TIS, triisopropylsilane; TRP-2, tyrosinase-related protein-2; UV, ultraviolet.

Synthetic cytotoxic T lymphocyte (CTL) peptide epitope-based vaccines are being developed against a number of human pathogens including viruses (1) and tumors (2,3). The synthetic peptide approach has several advantages: (i) peptides are chemically well defined, (ii) they are often relatively stable, (iii) no infectious material is involved in their manufacture, (iv) they are relatively easy to manufacture, and (v) any potential oncogenic or deleterious biological activity associated with whole virus or recombinant vaccines is avoided (4). In the domain of tumor vaccines, melanoma is one of the main targets studied. Melanoma-associated antigens recognized by CTL from cancer patients (3) include, for example, proteins from the MAGE family (5,6) and melanoma-associated differentiation antigens such as Melan-A/MART-1 (7,8).

Interactions between peptides and major histocompatibility complex (MHC) have been studied extensively: MHC class I–peptide interactions involved recognition by CD8 CTL, while the interaction between peptides and MHC class II involved CD_4 helper T-cell recognition. The mechanisms of these interactions are comparable in some aspects but differ significantly in others, among them, the typical length of a class I ligand comprises 9–10 amino acids and contains two anchor residues, at positions 2 and 9, whereas class II peptides are 12–25 amino acids long. MHC class I- and class II-specific peptides are described extensively in on-line databases, such as SYFPEITHI (http://www.uni-tuebingen.de/uni/kxi) (9) or MHCPEP (http://wehih.wehi/edu/au/mhcpep) (10). Several CTL-peptide vaccines have been studied in clinical trials against melanoma (2,3,5,6), hepatitis B virus (1) or human immunodeficiency virus (HIV) (11). Many other CTL-epitopes have been identified and several are currently in preclinical development (9). One interesting melanoma antigen is the HLA-A2.1-restricted ELA decapeptide (ELAGIGILTV), which is a Melan-A/MART-$1_{(26-35)A27L}$ immunodominant peptide analog, shown to be more immunogenic than the parent EAA peptide (EAAGIGILTV) (8). This peptide is also better recognized than the parent Melan/MART-1_{26-35} peptide by tumor-infiltrating lymphocytes (TILs) as well as Melan-A-specific CTL clones derived from melanoma patients (7,8).

In contrast, rP40, the recombinant *Klebsiella pneumoniae* outer membrane protein A (kpOmpA), was shown to have good antigen-carrier properties for covalently coupled peptides (12). In addition, the ELA decapeptide, mixed or chemically conjugated to rP40 has been shown to induce a strong CTL response which makes the ELA/rP40 combination very promising as a candidate for further pharmaceutical development (13). As part of the preclinical development of a new ELA/rP40 melanoma vaccine candidate, we report here stability and CTL activity studies of ELA and two peptide derivatives (PyrELA and AcELA), as well as three different ELA salt formulations (trifluoroacetate, acetate, hydrochloride). Furthermore, in order to generalize our observations to other N-terminal glutamic acid-containing peptides, stability studies were also performed with MAGE-3, another melanoma-derived peptide of clinical interest, produced in the same three different salt formulations.

Results and Discussion

ELA, PyrELA and AcELA synthesis, characterization and CTL activity studies

ELA peptide possesses a glutamic acid at the N-terminal position. Recently, slow pyroglutamic acid formation was described on an influenza nonstructural protein (152–160)-derived mouse CTL epitope (EEGAIVGEI) which also contains a glutamic acid at the same position (4). This pyroglutamic acid formation occurred when the peptide was mixed in a water-in-oil adjuvant formulation. However, it is also known that the amino group and the carboxamide group of glutamine in the N-terminal position of peptides and proteins, easily condense to form pyroglutamate residues (<E or pGlu) in solution or in the dry state (14–16). Many peptides of pharmaceutical interest have a pyroglutamic

acid instead of N-terminal nonstable glutamine or glutamic acid: thyrotropin-releasing hormone (TRH), substance P (pGlu^6, Pro^9)-fragment 6–11, luteinizing hormone (LH-RH) and derivatives, bombesin, gastrin and sauvagin (16). Some of them, such as buserelin and gonadorelin, are already on the market (17). Pyroglutamic acid was shown to be extremely stable; it could be converted to glutamic acid only under very drastic conditions such as 2 M hydrochloric acid at 100°C for 2 h (15) making it an interesting building block for a pharmaceutical. In order to study ELA's potentially low stability and to investigate more stable analogs, we synthesized and tested an ELA pyroglutamic acid derivative (PyrELA, <ELAGIGILTV) as well as the N-terminal acetyl-capped derivative (AcELA, AcELAGIGILTV) for CTL activity. The purpose of this last modification of ELA was to block the N-terminal group to avoid cyclization with the γ-carboxylic group. This type of modification has recently been described for MART-1_{27-35} parent nonapeptide (AAGIGILTV) in order to improve its resistance to proteolytic degradation (18). In both cases, these minor modifications resulted in enhanced stability, with possibly no change in their immunological activity. The PyrELA peptide was obtained as the ELA peptide analog by solid-phase synthesis, except for the last coupling step in which glutamic acid was replaced by commercially available pyroglutamic acid to obtain the cyclic analog. The AcELA derivative was also obtained easily from the protected ELA peptide after a capping reaction using acetic anhydride at the last step. PyrELA and AcELA were slightly more difficult to handle than the ELA parent peptide probably because they were both more hydrophobic.

Each of the three peptides was mixed with the new adjuvant protein rP40 and the CTL activity measured as described previously, using a specific ^{51}Cr release assay (13). As expected, immunization of mice with ELA/rP40 complex generated ELA-specific CTLs (Fig. 1A), but surprisingly, compared with ELA, PyrELA (Fig. 1B) and AcELA (Fig. 1C) failed to elicit CTL activity. Despite the apparent minor modifications introduced in PyrELA and AcELA, these two derivatives probably have lower affinity than ELA for the specific HLA-A2.1 class I MHC molecule. This was clearly illustrated by the binding of the peptides to the HLA-A2.1 molecules present on 'T2 cells', performed as described previously (7) (Fig. 2): ELA showed much higher MHC binding stability than the PyrELA and AcELA derivatives. Taken together, both experiments show that formation of PyrELA has to be avoided in order to conserve ELA full CTL activity.

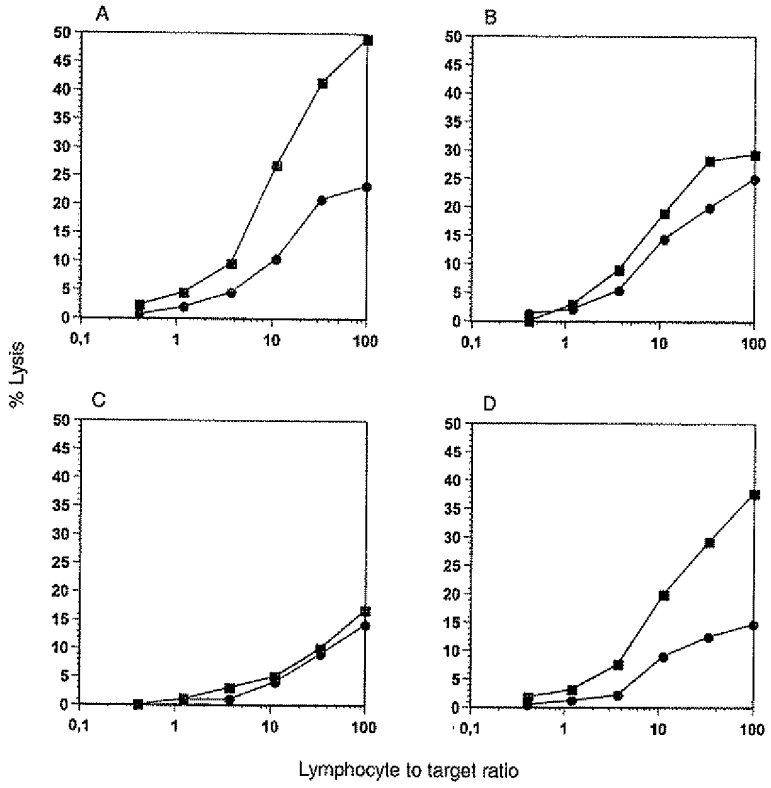

Figure 1. Specific CTL responses. HLA-A*0201/K^b mice were immunized subcutaneously with (A) rP40+ELA (TFA), (B) rP40+ PyrELA (TFA), (C) rP40+ AcELA (TFA) or (D) rP40+ELA (HCl). Lymph node cells were stimulated twice *in vitro* with EL4/A2K^b cells pulsed with ELA (TFA), PyrELA (TFA), AcELA (TFA) or ELA (HCl), respectively, and assayed for cytotoxic activity using ^{51}Cr-labeled target cells loaded (■) or not loaded (●) with the corresponding peptide.

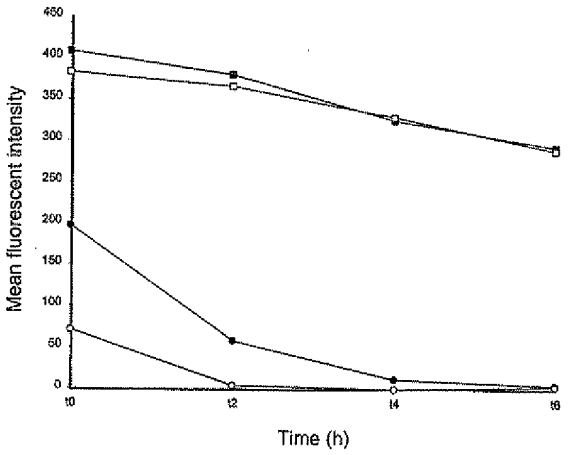

Figure 2. HLA-A2 stability studies with ELA (TFA), PyrELA (TFA), AcELA (TFA) and ELA (HCl). T2 cells were incubated overnight with ELA (TFA) (□), PyrELA (TFA) (●), AcELA (TFA) (○) and ELA (HCl) (■) peptides at 100 μg/mL. After removing the free peptides, cells were incubated at 37°C for 0, 2, 4 or 6 h. The amount of surface HLA-A2 molecules stabilized by the peptides (expressed as MFI) was monitored by flow cytometry after staining the cells with an anti-HLA-A2 monoclonal antibody.

ELA trifluoroacetate, acetate and hydrochloride salt preparation and stability studies

The majority of research grade peptides are produced as trifluoroacetate salts because the classical reverse-phase HPLC purification step is performed using trifluoroacetic acid (TFA) as a peptide-solubilizing and chaotropic agent (19,20). After freeze-drying, TFA binds to free amino group termini as well as to chain-exposed lysine, histidine and arginine residues. However, therapeutic peptides for human use which are on the market were not registered as trifluoroacetic salts but usually as acetate salts (European and US Pharmacopoeias) and in one case as a hydrochloride salt (21). Trifluoroacetic acid is classified in the International Conference for Harmonization guidelines for residual solvents as a class IV solvent, for which no adequate toxicological data are available (22). This acidic solvent is not recommended for the last purification step of active pharmaceutical ingredients and has to be avoided in drug master files. Furthermore, residual trifluoroacetate in peptides was recently shown to inhibit the proliferation of osteoblast and chondrocyte cell cultures (20). To investigate alternative solutions, we decided to prepare the ELA peptide as different salts [trifluoroacetate (TFA), acetate (AcOH) and hydrochloride (HCl)], and to study their physico-chemical stability (RP-HPLC), their *in vitro* CTL activity (^{51}Cr release assay) and also their MHC class I, binding ability (T2 cells assay).

ELA (TFA) in a freeze-dried form was shown to be stable at −20°C for at least 3 months and at 4°C for 3 months (Fig. 3A). At 37°C, under stress conditions, the stability decreased continuously and after 3 months the amount of ELA was only 76%, contaminated by 22% PyrELA. Degradation was much more important for ELA acetate (AcOH) (Fig. 3B), especially at 37°C corresponding to accelerated degradation conditions: 53% PyrELA was formed after 2 months (Fig. 4A). At the same temperature and over the same period, the hydrochloride (HCl) salt of ELA (Fig. 3C) gave five time less PyrELA cyclization (Fig. 4B). Furthermore, no PyrELA formation was observed for the hydrochloride salt after 3 months at 4°C, which corresponds to a suitable temperature for the conservation of a pharmaceutical. The explanation of these observations may be extrapolated from those given by Dimarchi *et al.* (14) for glutamine (Fig. 5): pyroglutamate formation is accelerated in weak acid medium (acetic acid) compared with stronger acids (trifluoroacetic or hydrochloride acids). This cyclization reaction is pH-, temperature- and time dependent and the data obtained at 37°C give a good idea of what would happen during long-term conservation at a lower temperature. A hydrochloride acid salt has clear pharmaceutical advantage over a trifluoroacetic acid salt because it is used in many marketed drugs bearing amino groups in order to yield a water-soluble quaternary ammonium derivative. In addition, a trifluoroacetic acid salt has to be avoided for a new drug to be registered for human use (22). Finally, acetic and hydrochloric acids are both referenced as acidifying agent excipients in the US Pharmacopoeia, whereas trifluoroacetic acid is not.

After mixing to the adjuvant protein rP40, ELA (TFA) (Fig. 1A) and ELA (HCl) (Fig. 1D) show similar CTL activities and MHC binding stability (Fig. 2). Consequently, we believe that the ELA hydrochloride salt is the formulation of choice for further preclinical and clinical development for a new ELA-based melanoma vaccine.

MAGE-3 trifluoroacetate, acetate and hydrochloride salt preparation and stability studies

MAGE-1 161–169 (EADPTGHSY) (23) and MAGE-3 168–176 (EVDPIGHLY) (24) are, like ELA, CTL epitopes of therapeutic interest for the development of melanoma vaccine. MAGE-1 and MAGE-3 are HLA-A1 restricted antigens. Both have a glutamic acid at the N-terminal position and probably the same propensity to form a pyroglutamic acid derivative. Recently, the MAGE-3 peptide was shown to induce tumor regression in a significant

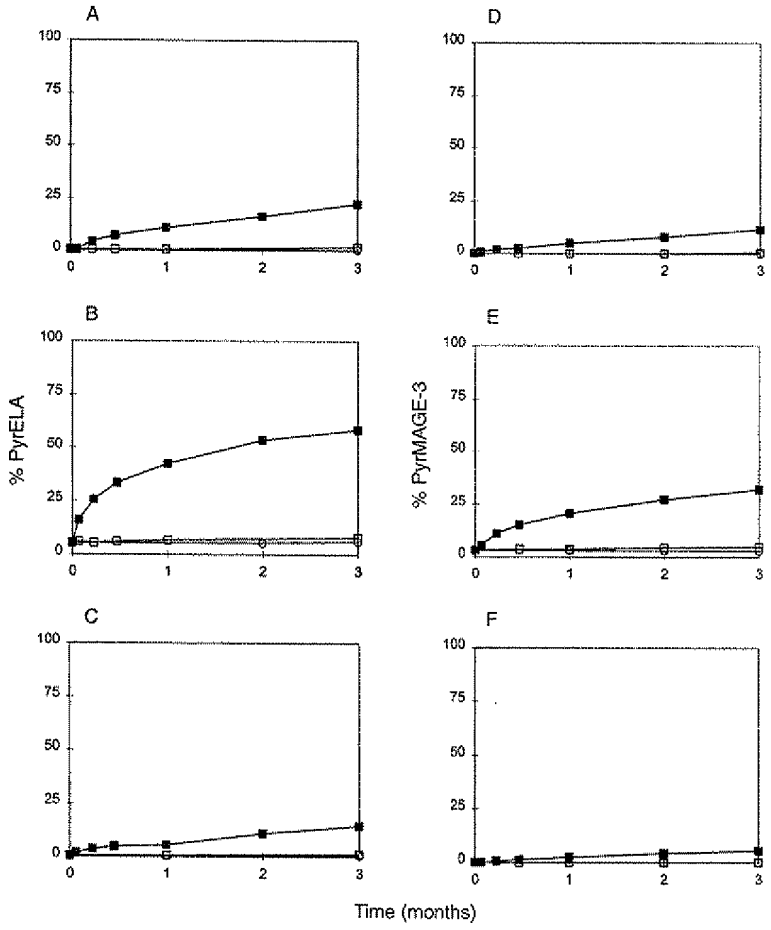

Figure 3. ELA and MAGE-3 stability studies. Percentage of PyrELA formation from ELA produced as (A) trifluoroacetate, (B) acetate, and (C) hydrochloride salt and percentage of PyrMAGE-3 formation from MAGE-3 produced as (D) trifluoroacetate, (E) acetate and (F) hydrochloride salt, analyzed by RP-HPLC after 1, 2 and 3 months at −20°C (○), 4°C (□) and 37°C (■).

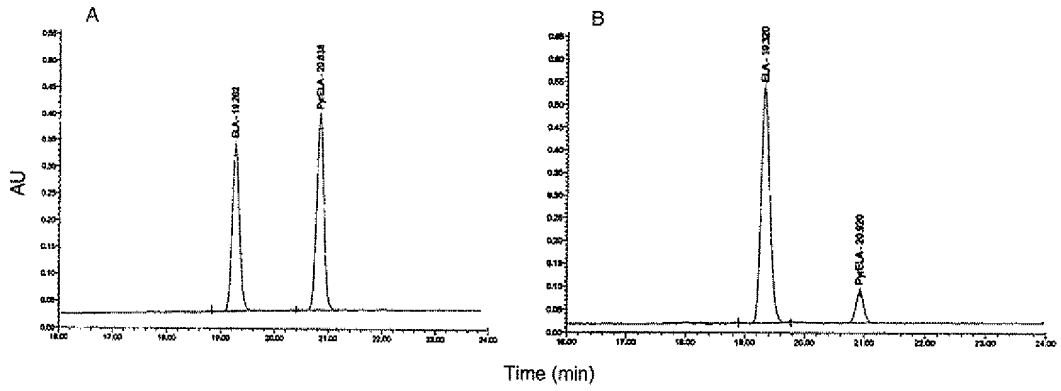

Figure 4. Representative RP-HPLC chromatograms of ELA as acetate or hydrochloride salts. (A) ELA (AcOH) after 2 months at 37°C is contaminated by 53% PyrELA; (B) ELA (HCl) after 2 months at 37°C is contaminated only by 10% PyrELA.

number of patients in clinical trials (5,6). The batch of peptide used in one of these studies (5) was produced according to current Good Manufacturing Practices (cGMP) as an acetate salt, as usual for clinical grade peptide. For this trial, vials were stored at −80°C, which is an exceptionally low temperature for pharmaceuticals, and thawed just before injection (5).

To investigate a potential stability problem due to the presence of a N-terminal glutamic acid, we synthesized the MAGE-3 peptide under the same three different salt forms

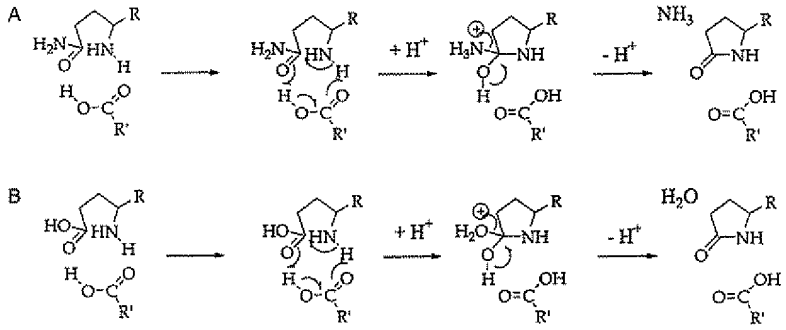

Figure 5. Proposed mechanism for weak acid catalyzed pyroglutamic acid formation: from (A) glutamine (14) which may be extrapolated to (B) glutamic acid with water formation instead ammoniac.

(trifluoroacetate, acetate and hydrochloride) and performed stability studies on the freeze-dried forms at −20, 4 and 37°C in order to check, as done for ELA, whether the hydrochloride salt would be more stable than the acetate one. The results shown in Fig. 3 were similar to those observed for ELA; the hydrochloride salt of MAGE-3 was more stable than the trifluoroacetate salt (Fig. 3D) and much more stable than acetate. After 3 months at 37°C for example, the amount of PyrMAGE-3 (<EVDPIGHLY) was 32% in the case of the acetate salt (Fig. 3E) and only 5% in the case of the hydrochloride salt (Fig. 3F). Producing and using MAGE-3 as a hydrochloride salt instead of an acetate salt for clinical trials would allow storage of the peptide at −20°C or even at 4°C, which is much more convenient in terms of 'cold chain', than the −80°C storage used by Marchand *et al.* (5).

Similar stabilization would probably also be obtained for N-terminal glutamine-containing peptides: taking glutamine as a model, Shih has shown that this amino acid was stable at pH 3 at 37°C for 24 h and that the cyclization occurred at higher pH (15).

As observed for ELA, MAGE-1 and MAGE-3, there are at least 30 known CTL peptides of therapeutic interest having a glutamic acid (Table 1) or a glutamine (Table 2) at the N-terminal position (9,10). Various types of HLAs (A1, A2, A3, B7, B8, B44...) are concerned, as well as a large number of tumor-associated antigens (MAGE (23–25), MART (7,8) GP100 (26), TRP-2, tyrosinase-related protein-2 (27) and MUM-1, melanoma ubiquitous mutated-1 (28), all involved in melanoma; HER-2/neu, a growth factor which is over-expressed in breast, ovarian and other adenocarcinomas (29); NY-ESO a cancer testis antigen (3,30); PSA, a prostate specific antigen (31); SART (32); CEA, a carcinoembryonic antigen (33); B-ALL, involved in B-cell acute lymphoblastic leukemia (34); EL2, squamous cell carcinoma of the lung (35)) and viruses (HIV (36–41), hepatitis C virus (42), Epstein-Barr virus – EBNA (43–47) and influenza (48,49).

***Table 1.* Example of human CTL epitopes with a glutamic acid at N-terminal position**

Antigens	Peptides	HLA restriction (Ref.)
MAGE-1 161–169	EADPTGHSY	A1 (23)
MAGE-3 168–176	EVDPIGHLY	A1 (24)
MART-1 26–35	EAAGIGILTV	A*0201 (50)
ELA (MART-1 26–35 A27L)	ELAGIGILTV	A*0201 (8)
HER-2/neu 971–979	ELVSEFSRM	A*0201 (29)
SART-1690–698	EYRGFTQDF	A24 (32)
HIV-1 gag p24 72–81	ETINEEAAEW	A25 (38)
MAGE-1 222–231	EVYDGREHSA	A28 (25)
TRP-2 222–231	EVISCKLIKR	A*3301/A*6801 (27)
EF2 581–589 squamous cell carcinoma	ETVSEQSNV	A*6802 (35)
EBV EBNA-1426–434	EPDVPPGAI	B7 (43)
Influenza NP 380–388	ELRSRYWAI	B8 (48)
HIV-1 gag p24 262–270	EIYKRWIIL	B8 (39)
HIV-1 gag p17 93–101	EIKDTKEAL	B8 (39)
HIV-1 RT 587–595	EPIVGAETF	B*3501 (41)
Influenza NP 339–347	EDLRVLSFI	B*3701 (49)
EBV EBNA 3C 281–290	EENLLDFVRF	B44 (47)
B-ALL (lymphoblastic leukemia)	EEKRGSLHVW	B44 (34)
MUM-1	EEKLIVVLF	B*4402 (28)

Unlike buserelin, gonadorelin and other peptides of therapeutic interest, the introduction of a pyroglutamic residue instead of the N-terminal glutamic acid or glutamine results, in the case of CTL peptide epitopes, in the loss of binding to the specific MHC class I molecules and loss of CTL activation capacity. As for ELA and MAGE-3, all these CTL peptides could certainly be efficiently stabilized as hydrochloride salts. This may reduce the formation of inactive pyroglutamate derivatives in the case of clinical development of synthetic CTL-peptide based vaccine.

Table 2. **Example of human CTL epitopes with a glutamine at N-terminal position**

Antigens	Peptides	HLA restriction (Ref.)
HCV-1 env E 257–266	QLRRHIDLLV	A*0201 (42)
NY-ESO-1 155–163 cancer testis Ag	QLSLLMWIT	A*0201 (30)
HIV-1 nef 73–82	QVPLRPMTYK	A3 (36)
PSA-9 162–170	QVHPQVTK	A3 (31)
GP100 551–559	QLVLHQILK	A*0301 (26)
HIV-1 nef 73–82	QVPLRPMTYK	A*1101 (37)
CEA 268–278	QYSWFVNGTF	A24 (33)
EBV EBNA-6 881–889	QPRAPIRPI	B*0702 (44)
EBV EBNA-3 158–166	QAKWRLQTL	B8 (45)
EBV EBNA-6B 213–222	QNGALAINTF	B*1501 (B62) (46)
HIV-1 nef 73–82	QVPLRPMTYK	B*3501 (40)

Materials and Methods

Chemicals

Fmoc-protected amino acid, 4-hydroxymethylphenoxy-methyle preloaded resins and peptide synthesis reagents were obtained from Perkin–Elmer (Norwalk, CT, USA). Organic solvents were HPLC grade from SDS (Peypin, France). Milli-Q water was used for aqueous solutions. Other solvents and chemicals were purchased from different commercial sources and were of the highest purity available. Pilot scale batches of ELA hydrochloride were produced by Neosystem (Strasbourg, France) and ELA acetate by Bachem (Basle, Switzerland).

Peptide synthesis

The protected peptide chain corresponding to ELA, PyrELA and MAGE-3 sequences were assembled using a solid-phase method on an Applied Biosystems 433A synthesizer using Fmoc/tBu chemistry at a 0.25-mmole scale. The side-chain protecting groups used were Glu(OtBu) and Thr(tBu) for ELA and AcELA; Thr(tBu) for PyrELA and Tyr(tBu), His(Trt), Asp(OtBu) and Glu(OtBu) for MAGE-3. Protected PyrELA was obtained by the same synthetic pathway as for ELA with the exception of the replacement of Fmoc-Glu(OtBu) by pyroglutamic acid at the last coupling step. Protected AcELA was obtained in a similar manner to ELA followed by capping with acetic anhydride. Resin-bound peptides (553 mg ELA; 549 mg PyrELA; 545 mg AcELA; 655 mg MAGE-3) were exposed to a mixture of TFA/anisole/water/thioanisole/TIS/phenol (20 mL : 1.5 mL : 1.0 mL : 1.0 mL : 0.5 mL : 1.5 g) and stirred at room temperature in a closed Falcon tube. After 3 h, the resin was filtered off and the crude peptide was precipitated in dry cold diethyl ether, centrifuged and washed several times with cold diethyl ether until scavengers were eliminated. The product was then dissolved in a mixture of H_2O/CH_3CN/TFA (50 : 50 : 0.1 v/v/v) and lyophilized to give 132 mg of ELA (40% yield), 250 mg of PyrELA (77% yield), 183 mg of AcELA (53% yield) and 290 mg of MAGE-3 (83% yield).

MAGE (AcOH) the acetate salt, was obtained by dissolving the MAGE (TFA) form in 0.1 M ammonium acetate (19) and purification by RP-HPLC with an 0.1-M ammonium acetate eluant. After freeze-drying the amount of acetic acid was 0.9% and residual TFA was 0.1%. MAGE-3 (HCl), the hydrochloride form, was obtained by dissolving the MAGE-3 (TFA) form in 50 mM HCl solution and purification by RP-HPLC using a 50-mM HCl eluant (20). After freeze-drying the amount of chloride was 5.2% and residual TFA was <0.1%.

Preparative HPLC

Purification was performed using a Waters Deltapak C_{18} 15 μm 300A column (100×25 mm) and a flow rate of 20 mL/min.

Characterization

RP-HPLC

RP-HPLC was performed on a Waters (Saint-Quentin, France) instrument controlled by MILLENIUM software equipped with UV detection. For method 1, the solvent system used was 0.1% aqueous TFA (buffer A) and 80% acetonitrile/0.1% TFA containing 20% buffer A (buffer B) on a C_{18} analytical column (Vydac 218TP, 5 μm, 250×4.6 mm) at a flow rate of 1 mL/min. For method 2, the solvent system used was 0.05 M pH 2.25 aqueous TEAP (buffer A) and 80% acetonitrile (buffer B) on a C_{18} analytical column (Interchrom Uptisphere, 5 μm, 250×4.6 mm) at a flow rate of 1.5 mL/min.

Electrospray-mass spectrometry

Electrospray-mass spectrometry (ES-MS) spectra were performed on a Bio-Q triple quadrupole mass spectrometer (Micromass, Manchester, UK) upgraded by the manufacturer so that the source had Quattro II performances, with a mass range of 4000. Samples were dissolved in aqueous 50% acetonitrile containing 1% formic acid at a final concentration of 2–5 pmol/μL. Aliquots (10 μL) were introduced into

the ion source at a flow rate of 6 μL/min. The extraction cone voltage was usually set to 50 V and the source temperature to 80°C. Data were acquired in the positive ionization mode from m/z=300 to m/z=1500 in 12 s per scan. Calibration was performed in the positive ionization mode using the multiply charged ions produced by a separate injection of horse heart myoglobin and the resolution adjusted so that the peak at m/z=998 was 1.2 Da wide at the half height.

Amino acid analysis

Crude samples were hydrolyzed for 1 h at 165°C using vapor phase hydrolysis in 6 N HCl and 2% saturated phenol. The sample was then analyzed using the Waters Picotag method on a Waters HPLC system equipped with an UV detector.

Anion analysis: anionic chromatography

The residual ions in the peptide were measured using a Dionex ion chromatograph equipped with an UV detector and automatic sampler. The particulars of the system settings used to evaluate the residual solvent in the peptide are the following: detector, inverse photometric detection at 263 nm; column, WESCAN anion column, 250×4 mm; elution buffer, 2 mM potassium hydrogen phthalate, pH 4.35; gradient, isocratic; flow rate, 3 mL/min; injection volume, 50 μL. A standard curve was constructed using key analytes in a series of concentrations. These samples were injected into the system and the resultant peak areas were measured. Area counts were plotted against the concentration of the standards and linear regression was used to determine the best-fit line. Peptide samples (1–2 mg) were dissolved, injected in the same manner and their area counts were used to calculate the amount of each ion present in the peptide sample by comparison with the calibration curve. The resulting value was further refined by adjustment with a recovery factor determined by spiking the peptide sample with an internal control of known concentration.

ELA (TFA) [ELAGIGILTV]. RP-HPLC purity: 96.8% (method 1)/95.8% (method 2); ES-MS, calculated mass: 985 Da/experimental mass: 985.01±0.06 Da; AAA: Glu (0.98/1), Gly (2.04/2), Thr (0.67/1), Ala (1.06/1), Val (1.04/1), Ile (2.03/2), Leu (2.13/2); TFA content: 11.0%; pH of reconstituted solution: 3.30.

PyrELA (TFA) [<ELAGIGILTV]. RP-HPLC purity: 99.4% (method 1); ES-MS, calculated mass: 967 Da/experimental mass: 967.21±0.37 Da; AAA: Glu (0.72/1), Gly (1.95/2), Thr (0.50/1), Ala (0.78/1), Val (0.79/1), Ile (1.92/2), Leu (1.63/2).

AcELA (TFA) [AcELAGIGILTV]. RP-HPLC purity: 86% (method 1); ES-MS: calculated mass: 1027 Da/experimental mass: 1026.80±0.16 Da; AAA: Glu (0.90/1), Gly (1.89/2), Thr (0.61/1), Ala (0.98/1), Val (1.02/1), Ile (1.91/2), Leu (1.99/2).

ELA (AcOH) [ELAGIGILTV]. RP-HPLC purity: 94.2% (method 1)/93.4% (method 2); AAA: Glu (1.17/1), Gly (2.41/2), Thr (0.81/1), Ala (0.98/1), Val (1.19/1), Ile (2.17/2), Leu (1.99/2); AcOH: 0.2%; TFA content: 0.04%; pH of reconstituted solution: 4.58.

ELA (HCl) [ELAGIGILTV]. RP-HPLC purity: 98.9% (method 1)/97.8% (method 2); AAA: Glu (0.97/1), Gly (2.02/2), Thr (0.94/1), Ala (1.01/1), Val (1.00/1), Ile (2.00/2), Leu (2.06/2); net peptide content (AAA): 98.3%; chloride content: 3.7%; TFA content: 0.1%; pH of reconstituted solution: 3.30.

MAGE-3 (TFA) [EVDPIGHLY]. RP-HPLC purity: 97.8% (method 1); ES-MS, calculated mass: 1042 Da/experimental mass: 1041.83±0.21 Da; AAA: Glu (1.02/1), Val (1.00/1), Asp (1.01/1), Pro (0.97/1), Ile (1.00/1), Gly (0.98/1), His (1.00/1), Leu (1.06/1), Tyr (0.91/1); TFA content: 18.1%; pH of reconstituted solution: 3.24.

PyroMAGE-3 [<EVDPIGHLY]. The peptide was obtained from MAGE-3 conserved at 37°C for 7 days. The peptide was isolated by RP-HPLC and identified by ES-MS, calculated mass: 1024 Da/measured mass: 1024.22±0.17 Da.

MAGE-3 (AcOH) [EVDPIGHLY]. RP-HPLC purity: 95.4% (method 1); AcOH content: 0.9%; TFA content: 0.1%; pH of reconstituted solution: 4.45.

MAGE-3 (HCl) [EVDPIGHLY]. RP-HPLC purity: 97.0% (method 1); chloride content: 5.2%; TFA content: 0.1%; pH of reconstituted solution: 3.28.

In vitro sensitization and cytolytic assays

Cytolytic activity of specific CTLs was determined in a ^{51}Cr release assay. HLA-A*0201/K^b transgenic mice were injected subcutaneously at the base of the tail with rP40 (300 μg) mixed with 50 μg of each peptides. Ten days after the injection, mice were sacrificed and lymphocyte suspensions from draining lymph nodes prepared for *in vitro* stimulation with ELA peptide or analogs. For *in vitro* stimulation, 4×10^6 cells were cultured for 7 days in 24-well costar plates, in complete DMEM medium with 4×10^5

irradiated (12 000 rad) EL-4/A_2K^b cells pulsed with 1 μM of the ELA peptide or analogs used for *in vivo* immunization.

After two *in vitro* stimulations, the cultured cells were tested for cytolytic activity determined in a ^{51}Cr-release assay. For cytolytic assays, EL-4/A_2K^b target cells pulsed or not with ELA or analogs, were incubated with 100 μL per 10^6 cells of ^{51}Cr for 1 h at 37°C and washed three times before use. Effector cells were then cultured with ^{51}Cr labeled target cells for 5 h at the indicated E:T ratio in 200 μL of complete DMEM in round plates (costar). After 5 h, 100 μL of supernatant from duplicate cultures was collected and counted. Data points are the mean percentage specific ^{51}Cr release from target cells calculated as follows: % specific lysis = (experimental release – spontaneous release/total release – spontaneous release)×100. Spontaneous release represents the counts obtained when the target cells were cultured in media in the absence of effector cells and full release represents the counts obtained when the target cells were lysed with 1% Triton X-100.

Measurement of the peptide/HLA-A2.1 complex stability (7).

T2 cells (10^6/mL) were incubated overnight with 100 μg/mL of each peptide in serum free OptiMEM medium (Gibco) supplemented with 100 ng/mL of β2m at 37°C.

Cells were then washed four times in order to remove free peptides, and resuspended in 1 mL RPMI-1640/10% fetal calf serum containing 10 μg/mL Brefeldin A (Sigma), in order to block cell-surface expression of newly synthesized HLA-A2.1 molecules. After 1 h incubation at 37°C, cells were washed and incubated at 37°C for 0, 2, 4, 6 or 8 h. Cells were subsequently stained with the MA2.1 antibody (ATCC, Manassas, VA, USA) to evaluate the HLA-A2.1 molecule expression, further revealed by an fluorescein isothiocyanate-labeled sheep antimouse immunoglobulin antibody (Dako, Glostrup, Denmark). After two washes cells analyzed by flow cytometry on a FACScan (BD Biosciences, San Jose, CA, USA). For each time point, peptide-induced HLA-A2.1 expression was evaluated by the formula: mean fluorescence intensity (MFI) of MA2.1 on peptide pre-incubated T2 cells – MFI of MA2.1 on T2 cells.

Acknowledgements: We thank Dr S. Plaue (Neosystem, Strasbourg, France) for helpful discussions, Dr A. Van Dorsselaer and N. Zorn (Université Louis Pasteur, Strasbourg, France) for performing mass spectrometry, Dr J.-F. Boé (Centre de Développement Pierre Fabre, Toulouse, France) for anion analysis, Dr U. F. Power (CIPF) for critical reading of the manuscript and A. Blaecke (CIPF) for excellent technical assistance.

References

1. Livingston, B.D., Alexander, J., Crimi, C., Oseroff, C., Celis, E., Daly, K., Guidotti, L.G., Chisari, F.V., Fikes, J., Chesnut, R.W. & Sette, A. (1999) Altered helper T lymphocyte function associated with chronic hepatitis B virus infection and its role in response to therapeutic vaccination in humans. *J. Immunol.* **162**, 3088–3095.
2. Rosenberg, S.A., Yang, J.C., Schwartzentruber, D.J., Hwu, P., Marincola, F.M., Topalian, S.L., Restifo, N.P., Dudley, M.E., Schwarz, S.L., Spiess, P.J., Wunderlich, J.R., Parkhurst, M.R., Kawakami, Y., Seipp, C.A., Einhorn, J.H. & White, D.E. (1998) Immunologic and therapeutic evaluation of a synthetic peptide vaccine for the treatment of patients with metastatic melanoma. *Nature Med.* **4**, 321–327.
3. Knuth, A., Jäger, D. & Jäger, E. (2000) Cancer immunotherapy in clinical oncology. *Cancer Chemother. Pharmacol.* **46**, S46–S51.
4. Elliott, S.L., Pye, S., Le, T., Mateo, L., Cox, J., Macdonald, L., Scalzo, A.A., Forbes, C.A. & Suhrbier, A. (1999) Peptide based cytotoxic T-cell vaccines; delivery of multiple epitopes, help, memory and problems. *Vaccine* **17**, 2009–2019.
5. Marchand, M., Van Baren, N., Weynants, P., Brichard, V., Dréno, B., Tessier, M.H., Rankin, E., Parmiani, G., Arienti, F., Humblet, Y., Bourlond, A., Vanwijck, R., Liénard, D., Beauduin, M., Dietrich, P.Y., Russo, V., Kerger, J., Masucci, G., Jäger, E., De Greve, J., Atzpodien, J., Brasseur, F., Coulie, P.G. & Van der Bruggen, P. (1999) Tumor regressions observed in patients with metastatic melanoma treated with an antigenic peptide encoded by gene *MAGE-3* and presented by HLA-A1. *Int. J. Cancer* **80**, 219–230.
6. Weber, J.S., Hua, F.L., Spears, L., Marty, V., Kuniyoshi, C. & Celis, E. (1999) A phase I trial of an HLA-A1 restricted MAGE-3 epitope peptide with incomplete Freund's adjuvant in patients with resected high-risk melanoma. *J. Immunother.* **22**, 431–440.
7. Romero, P., Gervois, N., Schneider, J., Escobar, P., Valmori, D., Pannetier, C., Steinle, A., Wolfel, T., Lienard, D., Brichard, V., Van Pel, A., Jotereau, F. & Cerottini, J.C. (1997) Cytolytic T lymphocyte recognition of the immunodominant HLA-A*0201-restricted Melan-A/MART-1 antigenic peptide in melanoma. *J. Immunol.* **159**, 2366–2374.
8. Valmori, D., Fonteneau, J.F., Lizana, C.M., Gervois, N., Lienard, D., Rimoldi, D., Jongeneel, V., Jotereau, F., Cerottini, J.C. & Romero, P. (1998) Enhanced generation of specific tumor-reactive CTL *in vitro* by selected Melan-A/MART-1 immunodominant peptide analogues. *J. Immunol.* **160**, 1750–1758.
9. Rammensee, H.G., Bachmann, J., Emmerich, N.P., Bachor, O.A. & Stevanovic, S. (1999) SYFPEITHI: database for MHC ligands and peptide motifs. *Immunogenetics* **50**, 213–219.
10. Brusic, V., Rudy, G. & Harrison, L.C. (1998) MHCPEP, a database of MHC-binding peptides: update 1997. *Nucleic Acids Res.* **26**, 368–371.

11. Gahery-Segard, H., Pialoux, G., Charmeteau, B., Sermet, S., Poncelet, H., Raux, M., Tartar, A., Levy, J.P., Gras-Masse, H. & Guillet, J.G. (2000) Multiepitopic B- and T-cell responses induced in human by a human immunodeficiency virus type 1 lipopeptide vaccine. *J. Virol.* **74**, 1694–1703.
12. Haeuw, J.F., Rauly, I., Zanna, L., Libon, C., Andreoni, C., Nguyen, T.N., Baussant, T., Bonnefoy, J.Y. & Beck, A. (1998) The recombinant *Klebsiella pneumoniae* outer membrane protein OmpA has carrier properties for conjugated antigenic peptides. *Eur. J. Biochem.* **255**, 446–454.
13. Jeannin, P., Renno, T., Goetsch, L., Miconnet, I., Aubry, J.P., Deloria, M.A., Herbault, N., Bay, C., Maguire, J.D., Soulas, C., Romero, P., Cerottini, J.C. & Bonnefoy, J.Y. (2000) OmpA targets dendritic cells, induces their maturation and antigen delivery into the MHC class I presentation pathway. *Nat. Immunol.* **1**, 502–509.
14. Dimarchi, R.D., Tam, J.P., Kent, S.B.H. & Merrifield, R.B. (1982) Weak acid-catalyzed pyrrolidon carboxylic acid formation from glutamine during solid phase peptide synthesis. *Int. J. Peptide Protein Res.* **19**, 88–93.
15. Shih, F.F. (1985) Analysis of glutamine, glutamic acid and pyroglutamic acid in protein hydrolysates by high-performance liquid chromatography. *J. Chromatogr.* **322**, 248–256.
16. Suzuki, Y., Motoi, H. & Sato, K. (1999) Quantitative analysis of pyroglutamic acid in peptides. *J. Food Chem.* **47**, 3248–3251.
17. Anonymous (2000) Gonadoreline (acétate de). In *Pharmacopée Européenne*, Strasbourg, France. 0827, pp. 1–5.
18. Brinckkerhoff, L.H., Kalashnikov, V.V., Thompson, L.W., Yamshchikov, G.V., Pierce, R.A., Galavotti, H.S., Engelhard, V.H. & Slingluff, C.L. Jr (1999) Terminal modifications inhibit proteolytic degradation of an immunogenic Mart-1, 27–35 peptide: implications for peptide vaccines. *Int. J. Cancer* **83**, 326–334.
19. Hoeger, C., Galyean, R., Boublik, J., McClintock, R. & Rivier, J. (1987) Preparative reversed phase high performance liquid chromatography: effects of buffer pH on the purification of synthetic peptides. *Biochromatography* **2**, 134–142.
20. Cornish, J., Callon, K.E., Lin, C.Q., Xiao, C.L., Mulvey, T.B., Cooper, G.J. & Reid, I.R. (1999) Trifluoroacetate, a contaminant in purified proteins, inhibits proliferation of osteoblasts and chondrocytes. *Am. J. Physiol. Endocrinol. Metab.* **277**, E779–E783.
21. Anonymous (2000) Gonadorelin. In *The United States Pharmacopeia: The National Formulary*. United States Pharmacopeial Convention, Inc, Rockville, MD, pp. 784–787.
22. Anonymous (1997) Guideline for residual solvents: ICH Q3C: Impurities. *Pharmeuropa* **9**, 498–506.
23. Van der Bruggen, P., Traversari, C., Chomez, P., Lurquin, C., de Plaen, E., Van den Eynde, B.J., Knuth, A. & Boon, T. (1991) A gene encoding an antigen recognized by cytolytic T lymphocytes on a human melanoma. *Science* **254**, 1643–1647.
24. Gaugler, B., Van den Eynde, B.J., Van der Bruggen, P., Romero, P., Gaforio, J.J., de Plaen, E., Lethé, B., Brasseur, F. & Boon, T. (1994) Human gene *MAGE-3* codes for an antigen recognized on a melanoma by autologous cytolytic T-lymphocytes. *J. Exp. Med.* **179**, 921–930.
25. Chaux, P., Luiten, R., Demotte, N., Vantomme, V., Stroobant, V., Traversari, C., Russo, V., Schultz, E., Cornelis, G.R., Boon, T. & Van der Bruggen, P. (1999) Identification of five Mage-A1 epitopes recognized by cytolytic T lymphocytes obtained by *in vitro* stimulation with dendritic cells transduced with Mage-A1. *J. Immunol.* **163**, 2928–2936.
26. Kawashima, I., Tsai, V., Southwood, S., Takesako, K., Celis, E. & Sette, A. (1998) Identification of gp100-derived, melanoma-specific cytotoxic T-lymphocyte epitopes restricted by HLA-A3 supertype molecules by primary *in vitro* immunization with peptide-pulsed dendritic cells. *Int. J. Cancer* **78**, 518–524.
27. Lupetti, R., Pisarra, P., Verrecchia, A., Farina, C., Nicolini, G., Anichini, A., Bordignon, C., Traversari, C. & Parmiani, G. (1998) Translation of a retained intron in tyrosinase-related protein (TRP)2 mRNA generates a new cytotoxic T-lymphocyte (CTL)-defined and shared human melanoma antigen not expressed in normal cells of the melanocytic lineage. *J. Exp. Med.* **188**, 1005–1016.
28. Coulie, P.G., Lehmann, F., Lethé, B., Herman, J., Lurquin, C., Andrawiss, M. & Boon, T. (1995) A mutated intron sequence codes for an antigenic peptide recognized by cytolytic T lymphocytes on a human melanoma. *Proc. Natl Acad. Sci. USA* **92**, 7976–7980.
29. Fisk, B., Savary, C., Hudson, J.M., 'Brian, C.A., Murray, J.L., Wharton, J.T. & Ioannides, C.G. (1996) Changes in an HER-2 peptide upregulating HLA-A2 expression affect both conformational epitopes and CTL recognition: implications for optimization of antigen presentation and tumor-specific CTL induction. *J. Immunother.* **18**, 197–209.
30. Jäger, E., Jäger, D. & Knuth, A. (1998) Strategies for the development of vaccines to treat breast cancer. *Recent Results Cancer Res.* **152**, 94–102.
31. Correale, P., Walmsley, K., Zaremba, S., Zhu, M.Z., Scholm, J. & Tsang, K.Y. (1998) Generation of human cytolytic T lymphocyte lines directed against prostate-specific antigen (PSA) employing a PSA oligoepitope peptide. *J. Immunol.* **161**, 3186–3194.
32. Kikuchi, M., Nakao, M., Inoue, Y., Matsunaga, K., Shichijo, S., Yamana, H. & Itoh, K. (1999) Identification of a SART-1-derived peptide capable of inducing HLA-A24-restricted and tumor-specific cytotoxic T lymphocytes. *Int. J. Cancer* **81**, 459–466.
33. Nukaya, I., Yasumoto, M., Iwasaki, T., Ideno, M., Sette, A., Celis, E., Takesako, K. & Kato, I. (1999) Identification of HLA-A24 epitope peptides of carcinoembryonic antigen which induce tumor-reactive cytotoxic T lymphocyte. *Int. J. Cancer* **80**, 92–97.
34. Dolstra, H., Fredix, H., Maas, F., Coulie, P.G., Brasseur, F., Mensink, E., Adema, G.J., de Witte, T.M., Figdor, C.G. & van de Wiel-van Kemenade, E. (1999) A human minor histocompatibility antigen specific for B cell acute lymphoblastic leukemia. *J. Exp. Med.* **189**, 301–308.
35. Hogan, K.T., Eisinger, D.P., Cupp, S.B. III, Lekstrom, K.J., Deacon, D.D., Shabanowitz, J., Hunt, D.F., Engelhard, V.H., Slingluff, C.L. Jr & Ross, M.M. (1998) The peptide recognized by HLA-A68.2-restricted, squamous cell carcinoma of the lung-specific cytotoxic T lymphocytes is derived from a mutated *Elongation Factor 2* gene. *Cancer Res.* **58**, 5144–5150.
36. Koenig, S., Fuerst, T.R., Wood, L.V., Woods, R.M., Suzich, J.A., Jones, G.M., de la Cruz, V.F., Davey, R.T. Jr, Venkatesan, S. & Moss, B. (1990) Mapping the fine specificity of a cytolytic T cell response to HIV-1 nef protein. *J. Immunol.* **145**, 127–135.
37. Couillin, I., Connan, F., Culmann-Penciolelli, B., Gomard, E., Guillet, J.G. & Choppin, J. (1995) HLA-dependent variations in human immunodeficiency viry Nef protein alter peptide/HLA binding. *Eur. J. Immunol.* **25**, 728–732.
38. Van Baalen, C.A., Klein, M.R., Huisman, R.C., Dings, M.E., Kerkhov Garde, S.R., Geretti, A.M., Gruters, R., Van Els, C.A., Miedema, F. & Osterhaus, A.D. (1996) Fine-specificity of cytotoxic T lymphocytes which recognize conserved epitopes of the Gag protein of human immunodeficiency virus type 1. *J. Gen. Virol.* **77**, 1659–1665.

39. DiBrino, M., Parker, K.C., Shiloach, J., Turner, R.V., Tsuchida, T., Garfield, M., Biddison, W.E. & Coligan, J.E. (1994) Endogenous peptides with distinct amino acid anchor residue motifs bind to HLA-A1 and HLA-B8. *J. Immunol.* **152**, 620–631.
40. Culmann, B., Gomard, E., Kieny, M.P., Guy, B., Dreyfus, F., Saimot, A.G., Sereni, D., Sicard, D. & Levy, J.P. (1991) Six epitopes reacting with human cytotoxic CD8+ T cells in the central region of the HIV-1 nef protein. *J. Immunol.* **146**, 1560–1565.
41. Shiga, H., Shioda, T., Tomiyama, H., Takamiya, Y., Oka, S., Yamaguchi, Y., Gojoubori, T., Rammensee, H.G., Miwa, K. & Takiguchi, M. (1997) Identification of multiple HIV-1 cytotoxic T-cell epitopes presented by human leucocyte antigen B35 molecules. *AIDS Res. Hum. Retroviruses* **10**, 1075–1083.
42. Shirai, M., Arichi, T., Nishioka, M., Nomura, T., Ikeda, K., Kawanishi, K., Engelhard, V.H., Feinstone, S.M. & Berzofsky, J.A. (1995) CTL responses of HLA-A2.1-transgenic mice specific for hepatitis C viral peptides predict epitopes for CTL of humans carrying HLA-A2-1. *J. Immunol.* **154**, 2733–2742.
43. Stuber, G., Dillner, J., Modrow, S., Wolf, H., Szekely, L., Klein, G. & Klein, E. (1995) HLA-A0201 and HLA-B7 binding peptides in the EBV-encoded EBNA-1, EBNA-2 and BZLF-1 proteins detected in the MHC class I stabilization assay. Low proportion of binding motifs for several HLA class I alleles in EBNA-1. *Int. Immunol.* **7**, 653–663.
44. Maier, R., Falk, K., Rotzschke, O., Maier, B., Gnau, S., Stevanovic, S., Jung, G., Rammensee, H.G. & Meyerhans, A. (1994) Peptide motifs of HLA-A3-A24, and -B7 molecules as determined by pool sequencing. *Immunogenetics* **40**, 306–308.
45. Burrows, S.R., Gardner, J., Khanna, R., Steward, T., Moss, D.J., Rodda, S. & Suhrbier, A. (1994) Five new cytotoxic T cell epitopes identified within Epsteins-Barr virus nuclear antigen 3. *J. Gen. Virol.* **75**, 2489–2493.
46. Kerr, B.M., Kienzle, N., Burrows, J.M., Cross, S.M., Silins, S.L., Buck, M., Benson, E.M., Coupar, B., Moss, D.J. & Sculley, T.B. (1996) Identification of type B-specific and cross-reactive cytotoxic T-lymphocyte responses to Epstein-Barr virus. *J. Virol.* **70**, 8858–8864.
47. Khanna, R., Burrows, S.R., Kurilla, M.G., Jacob, C.A., Misko, I.S., Sculley, T.B., Kieff, E. & Moss, D.J. (1992) Localization of Epstein-Barr virus cytotoxicity T cell epitopes using recombinant vaccinia: implications for vaccine development. *J. Exp. Med.* **176**, 169–176.
48. Sutton, J., Rowland-Jones, S., Rosenberg, W., Nixon, d., Gotch, F., Gao, X.M., Murray, A., Spoonas, A., Driscoll, P., Smith, M., Willis, A. & McMichael, A. (1993) A sequence pattern for peptides presented to cytotoxic T lymphocytes by HLA B8 revealed by analysis of epitopes and eluted peptides. *Eur. J. Immunol.* **23**, 447–453.
49. Townsend, A.R.M., Bastin, J., Gould, K. & Brownlee, G.G. (1986) Cytotoxic T lymphocytes recognize influenza haemagglutinin that lacks a signal sequence. *Nature* **324**, 575–577.
50. Kawakami, Y., Eliyahu, S., Sakaguchi, K., Robbins, P.F., Rivoltini, L., Yannelli, J.R., Appella, E. & Rosenberg, S.A. (1994) Identification of the immunodominant peptides of the MART-1 human melanoma antigen recognized by the majority of HLA-A2-restricted tumor infiltrating lymphocytes. *J. Exp. Med.* **181**, 347–352.

EXHIBIT 5

Journal of Neurochemistry
Lippincott Williams & Wilkins, Inc., Philadelphia

Toxicity of Pyroglutaminated Amyloid β-Peptides 3(pE)-40 and -42 Is Similar to That of Aβ1-40 and -42

*†T. L. Tekirian, ‡A. Y. Yang, ‡C. Glabe, and *†J. W. Geddes

**Sanders–Brown Alzheimer's Disease Research Center and †Department of Anatomy and Neurobiology, University of Kentucky, Lexington, Kentucky, and ‡Department of Molecular Biology and Biochemistry, University of California, Irvine, California, U.S.A.*

Abstract: An N-terminal truncated isoform of the amyloid β-peptide (Aβ) that begins with a pyroglutamate (pE) residue at position 3 [Aβ3(pE)-42] is the predominant isoform found in senile plaques. Based upon previous in vitro studies regarding Aβ N-terminal truncated isoforms, it has been hypothesized that Aβ3(pE)-x isoforms may aggregate more rapidly and become more toxic than corresponding Aβ1-x peptides. However, the toxicity and aggregation properties of Aβ3(pE)-42 and Aβ3(pE)-40 have not previously been examined. After initial solubilization and 1-week preaggregation of each peptide at 37°C and pH 7.4, the toxicity of 5–50 μ*M* Aβ3(pE)-42 was similar to that of Aβ1-42. Moreover, the toxicity of Aβ3(pE)-40 paralleled that induced by Aβ1-40 in both 1 day in vitro (DIV) cortical and 7 DIV hippocampal cells. Circular dichroism spectra did not reveal major differences in secondary structure between aged Aβ1-42, Aβ3(pE)-42, Aβ3(pE)-40, and Aβ1-40 or freshly solubilized forms of these peptides. Overall, the data indicate that the loss of the two N-terminal amino acids and the cyclization of glutamate at position 3 do not alter the extracellular toxicity of Aβ. **Key Words:** Alzheimer's disease—Amyloid β-peptide—Circular dichroism—Neurotoxins—Peptide fragments.
J. Neurochem. **73,** 1584–1589 (1999).

Amyloid β-peptide (Aβ) is a major component of senile plaques (Selkoe, 1989) and cerebrovascular angiopathy (Kalaria, 1996), histologic features strongly implicated in the pathogenesis of Alzheimer's disease (AD). The 4-kDa Aβ peptide is produced by proteolytic cleavage of the β-amyloid precursor protein by an unidentified β-secretase (cleaving at the N-terminus) and γ-secretase(s) (cleaving at the C-terminus) (Checler, 1995; Mills and Reiner, 1999). In addition, a 3-kDa peptide (p3), originating at Aβ amino acid 17(L), is generated by the combined action of α- and γ-secretases.

In addition to full-length Aβ1-42, there are several N- and C-terminal truncated Aβ isoforms; such heterogeneity affects the toxicity of Aβ peptides (Pike et al., 1993, 1995*a*). In vitro, truncation at the C-terminus diminishes Aβ aggregation and toxicity (e.g., Aβ1-40 vs. 1-42) (Pike et al., 1993). In contrast, several isoforms truncated at the N-terminus [Aβ4-42, Aβ8-42, Aβ12-42, and Aβ17-42(p3)] aggregate more readily and are more toxic than Aβ1-42 (Pike et al., 1995*a*). The secondary structure and aggregation state of Aβ appear to be directly related to its neurotoxicity in vitro (Simmons et al., 1994; Howlett et al., 1995).

A prevalent Aβ isoform in extracellular deposits within the human brain begins with a pyroglutamate (pE) at position 3 [Aβ3(pE)-x] (Mori et al., 1992; Saido et al., 1995; Russo et al., 1997; Tekirian et al., 1998). Pyroglutamic modification confers enhanced resistance to most aminopeptidases; thus, the abundance of Aβ3(pE)-x likely reflects decreased clearance. Aβ3(pE)-x is also abundant in the brains of other aged mammals (Tekirian et al., 1998) and may be the most abundant isoform in the AD brain (Russo et al., 1997; Tekirian et al., 1998). Previously, Saido and colleagues (1995) demonstrated that Aβ3(pE)-x forms stable aggregates similar to Aβ1-x. However, the toxicities of the two isoforms have not directly been compared. To examine the effects of Aβ3(pE)-x-associated toxicity in vitro, Aβ3(pE)-40 and Aβ3(pE)-42 peptides were compared with Aβ1-42 and Aβ1-40 in terms of toxicity and secondary structure.

Received March 5, 1999; revised manuscript received May 28, 1999; accepted May 31, 1999.

Address correspondence and reprint requests to Dr. J. W. Geddes at Sanders–Brown Center on Aging, University of Kentucky, 800 South Limestone, Lexington, KY 40536-0230, U.S.A.

The present address of Dr. T. L. Tekirian is Genetics and Aging Unit and Department of Neurology, Massachusetts General Hospital, Harvard Medical School, Boston, MA 02129, U.S.A.

The present address of Dr. A. Y. Yang is Dementia Research Program, Nathan Kline Institute, 140 Old Orangeburg Rd., Orangeburg, NY 10964, U.S.A.

Abbreviations used: Aβ, amyloid β-peptide; AD, Alzheimer's disease; DIV, days in vitro; DMEM, Dulbecco's modified Eagle medium; E-, embyonic day; HBSS, Hanks' balanced salt solution; p3, 3-kDa peptide; PBS, phosphate-buffered saline; pE, pyroglutamate.

MATERIALS AND METHODS

Aβ peptides

Aβ isoforms Aβ1-42 (DAEFRHDSGYEVHHQKLVFFAEDVGSNKGAIIGLMVGGVVIA), Aβ3(pE)-42, Aβ1-40, and Aβ3(pE)-40 were synthesized by solid-phase F-moc [*N*-(9-fluorenyl)methoxycarbonyl] amino acid chemistry using a continuous-flow semiautomatic instrument and purified by reverse-phase high performance liquid chromatography as described previously (Burdick et al., 1992; Jiang et al., 1994). Peptide purity was estimated to be 90–95% by electrospray mass spectrometry. Purified peptides were dissolved in 1 m*M* HCl and lyophilized in 1-mg aliquots for tissue culture treatments. Aβ peptides were resuspended in culture medium at a concentration of 5–50 μ*M* just prior to use ("freshly solubilized" peptide) or were prepared as a 250 μ*M* stock solution in phosphate-buffered saline (PBS; pH 7.4) and maintained at 37°C for 1 week ("aged" peptide) prior to dilution and addition into defined medium.

Cell culture

Primary cultures of fetal rat embryonic day (E) 18 hippocampal neurons were established according to the procedures of Brewer et al. (1993) with slight modifications. Timed pregnant Sprague–Dawley rats (Harlan, Indianapolis, IN, U.S.A.) were killed with halothane. Fetuses were removed using aseptic techniques. Fetal brains were removed and placed in Hanks' balanced salt solution (HBSS) without Ca^{2+} and Mg^{2+} (Life Technologies). Hippocampi were dissected and digested in HBSS containing 0.25% trypsin for 15 min at room temperature. Hippocampi were then washed with HBSS and incubated with mung bean trypsin inhibitor (1 mg/ml; Sigma) for 5 min. Tissues were dissociated by repeated trituration in HBSS (8 hippocampi/ml) with a fire-polished Pasteur pipette. Cells were seeded at 20,000 neurons/well in poly-D-lysine (50 μg/ml; Sigma)–coated Falcon four-chamber glass slides containing Neurobasal medium supplemented with 2% B27, 0.5 m*M* glutamine, and 25 μ*M* glutamate (Life Technologies). Cultures were maintained at 37°C in a humidified incubator with 6% CO_2 and 94% air. After 4 days in culture, one-third of the medium was replaced with medium without glutamate.

Primary cortical cultures were established from E18 Sprague–Dawley rat pups as described above. These cultures were maintained in serum-free Dulbecco's modified Eagle medium (DMEM) and N2 supplement (GibcoBRL; 1:100 dilution).

Treatment

Aged Aβ peptides were preincubated in PBS (pH 7.4) for 7 days at 37°C as a stock solution (250 μ*M*) prior to dilution and addition to cultures. Preincubation has previously been shown to result in enhanced cytotoxicity (Pike et al., 1991, 1993; Simmons et al., 1994). Freshly solubilized Aβ peptides were immediately diluted in culture medium to yield final concentrations of 5, 10, 25, or 50 μ*M* of each Aβ peptide. In each experiment, triplicate wells were treated at each concentration of a given Aβ peptide. Reported data indicate results obtained from six independent experiments in cortical cell culture and another six experiments in hippocampal cell culture.

Cell survival

A grid was etched on the bottom of each culture well. Prior to treatment with respective Aβ peptides, phase-contrast photomicrographs were taken, with ~30–50 neurons present in each field (4 fields/culture dish). Photos of the same 20× magnification fields (localized by the grid) were taken at various posttreatment timepoints (0, 3, 6, 12, 24 h). Morphological assessment of viable neurons was based upon somal appearance in which smooth, round, and vacuole-free neurons were scored as alive (Pike et al., 1991). Cell survival was then expressed as a percentage of initial neuron number.

Circular dichroism

Circular dichroism was used to evaluate the secondary structure of four synthetic Aβ peptides. The mean residue ellipticities of Aβ3(pE)-42, Aβ3(pE)-40, Aβ1-42, and Aβ1-40 were examined with a Jasco J-720 spectropolarimeter equipped with a computerized data processor. Peptide samples were either freshly solubilized at 25 μ*M* in PBS (pH 7.4) or aged overnight in 0.1 *M* sodium acetate buffer (pH 5.0) to induce Aβ assembly (Burdick et al., 1992) and then diluted to 25 μ*M* (from a 250 μ*M* stock solution) in PBS (pH 7.4). Samples were read at room temperature in a 1-mm path length quartz cell. Measurements were made over a 190- to 259-nm wavelength range, taken at 0.5-nm increments. Data from four scans were averaged and subtracted from baseline values. The instrument was calibrated with a 0.06% (wt/vol) solution of *d*-camphor sulfonate.

Statistics

Repeated-measure ANOVAs were used to test for significant differences between group means at different survival times. Post hoc analyses included two-tailed *t* tests with Bonferroni correction. In the results presented, error bars represent the SEMs.

RESULTS

The toxicity of aged (preaggregated) Aβ peptides was examined in both 1 day in vitro (DIV) cortical cultures and 7 DIV hippocampal cultures. Aβ1–40 toxicity was similar to that of Aβ3(pE)-40 at each of the concentrations examined (Fig. 1). For each peptide, toxicity was concentration dependent. Similarly, no differences were observed between the toxicity of aged Aβ1-42 as compared with Aβ 3(pE)-42 (Fig. 2). Despite the similar toxicities of preaggregated Aβx-40 and Aβx-42 peptides (Figs. 1 and 2), only the Aβx-42 peptides formed sodium dodecyl sulfate- and heat-stable high molecular mass aggregates (16 kDa) upon fresh solubilization as revealed by subsequent immunoblotting (results not shown).

In contrast to the similar toxicities of aged Aβx-40 and Aβx-42, freshly solubilized Aβx-40 revealed minimal toxicity, whereas the toxicity of freshly solubilized Aβx-42 was similar to that of the preaggregated peptide (Fig. 3). The lack of toxicity associated with freshly solubilized Aβ1-40 is consistent with previous observations (Harris et al., 1995). Thus, it appeared that the "aging" of Aβ1-40 and Aβ3(pE)-40 was required for cell death, whereas both aged and freshly solubilized Aβ1-42 and Aβ3(pE)-42 caused dose-dependent cell death.

Whereas freshly solubilized and aged 25 μ*M* Aβ3(pE)-42 and Aβ1-42 were neurotoxic, Aβ1-40 and Aβ3(pE)-40, at this same concentration, invoked minimal cell death (Fig. 3). Circular dichroism spectra of both "aged" (Fig. 4) and freshly solubilized (Fig. 5) Aβ

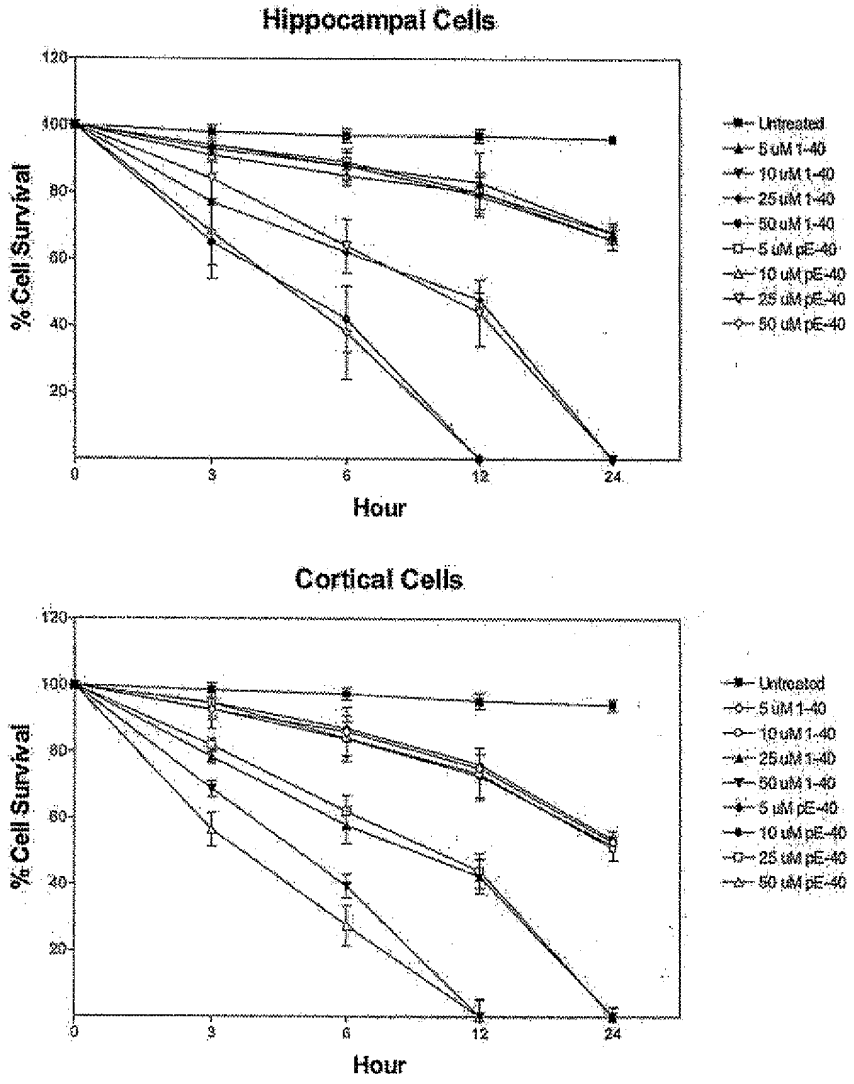

FIG. 1. Toxicity of "aged" Aβ3(pE)-40 pyroglutamate is similar to that of Aβ1-40 in both short-term cortical cultures and 7 DIV hippocampal cultures. Aβ1-40 and pyroglutaminated Aβ3(pE)-40, preincubated in PBS (pH 7.4) for 7 days at 37°C, were contrasted in terms of dose-dependent (5–50 *μM*) cell survival within 1 DIV E18-derived rat cortical cultures maintained in serum-free DMEM + N2 supplement as well as 7 DIV E18-derived hippocampal neurons maintained in Neurobasal medium + B27 supplement. The results demonstrate similar dose-dependent toxicities of the Aβ1-40 and Aβ3(pE)-40 peptides.

peptides exhibited positive peaks at 200 nm and negative peaks at 218 nm, indicative of β-pleated sheet secondary structure.

DISCUSSION

Aβ3(pE)-42 has been demonstrated as the predominant form of Aβ in extracellular deposits in the AD brain (Russo et al., 1997). However, the relative toxicity of this isoform had not previously been examined. The results of the present study demonstrate that Aβ3(pE)-40 is similar to Aβ1-40, and Aβ3(pE)-42 parallels Aβ1-42, in terms of extracellular neuronal toxicity in primary neuronal cultures and secondary structure analyses.

A study of N-terminal deletions by Pike et al. (1995*a*) demonstrated that N-terminal truncated isoforms of Aβ1-40 (Aβ4-40, Aβ8-40, Aβ12-40, and Aβ17-40) are more toxic than the full-length peptide immediately after and 7 days after solubilization. However, for the Aβx-42 peptides, N-terminal truncated isoforms (Aβ4-42, Aβ8-42, and Aβ12-42) exhibited similar or reduced toxicity as compared with full-length Aβ1-42 when the freshly solubilized peptides were examined and similar or greater toxicity when examined 7 days after solubilization. The results of the present study suggest that these observations cannot be extrapolated to the Aβ3(pE)-x isoforms. These data do not suggest that Aβ3(pE)-x isoforms are not important in AD pathogenesis. Instead, the results simply indicate that the loss of two amino acids at the N-terminus and cyclization of glutamate (E) to pyroglutamate (pE) does not alter extracellular Aβ toxicity, unlike the influence of the loss of two hydrophobic amino acids at the C-terminus.

In the present study, the toxicities of aged Aβ1-40 and Aβ1-42 were similar, whereas for the freshly solubilized

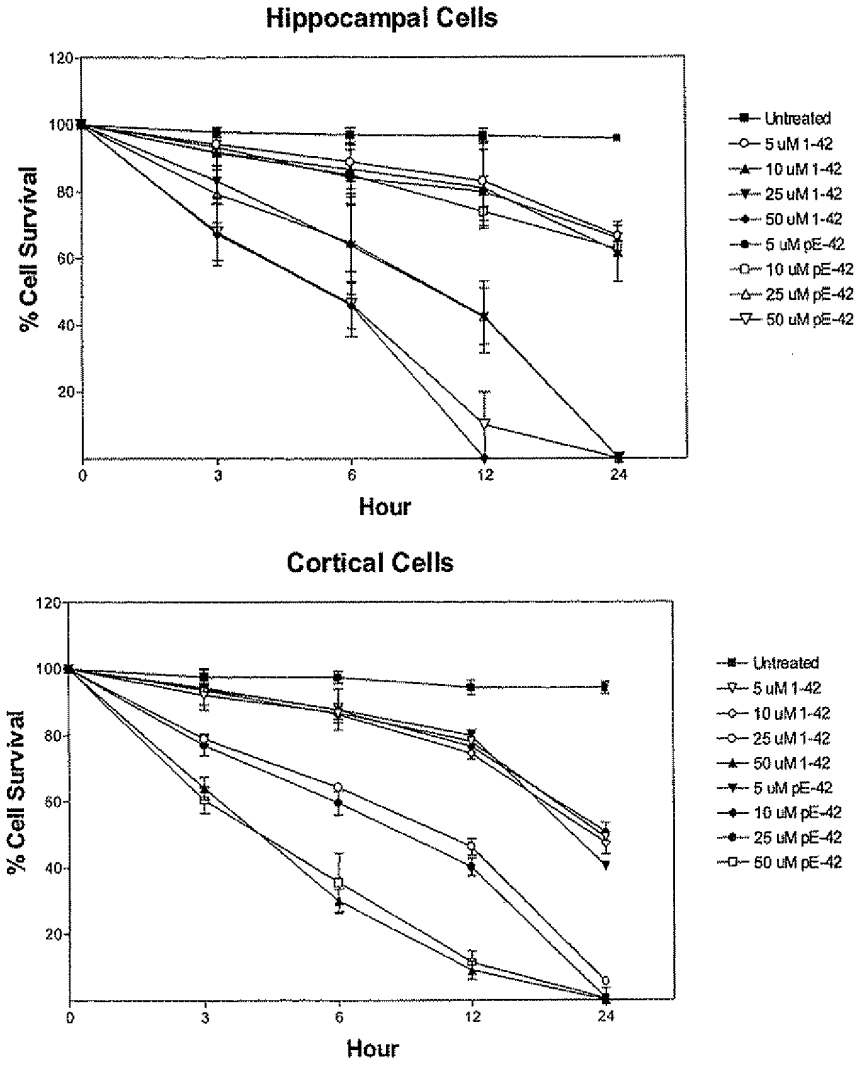

FIG. 2. Toxicity of "aged" Aβ3(pE)-42 pyroglutamate is similar to that of Aβ1-42 in both short-term cortical cultures and 7 DIV hippocampal cultures. Conditions for Aβ1-42 versus Aβ3(pE)-42 are as described in Fig. 1.

peptides, Aβ1-42 was much more toxic than Aβ1-40. In a previous study by Pike et al. (1993), aged Aβ1-39 and Aβ1-42 exhibited similar neurotoxicity, both resulting in almost 100% cell loss, but the aged Aβ1-42 was more toxic than freshly solubilized peptide. However, in other studies by the same group, aged Aβ1-42 was sometimes less toxic than freshly solubilized peptide (Pike et al., 1995*a*) or exhibited similar toxicity (Pike et al., 1995*b*). This observed inconsistency likely reflects variations in the purity and properties of the Aβ peptides (Simmons et al., 1994; Howlett et al., 1995). The 90% purity of the Aβ peptides used in the present study is greater than that which is available in most commercial preparations of Aβ peptide.

Circular dichroism spectra of aged pyroglutaminated and nonpyroglutaminated peptides indicate a similar extent of β-pleated sheet structure. This finding is consistent with the critical role of the hydrophobic C-terminus in influencing the solubility and aggregation properties of the Aβ peptide (Burdick et al., 1992), presumably independent of the loss of the two N-terminal amino acid residues and conversion of glutamate to pyroglutamate.

AβN3(pE)-x is thought to be formed by loss of the first two amino acids of Aβ1-x through aminopeptidase A activity, followed by glutamate cyclization at position 3. The conversion of L-glutamate to pyroglutamate protects the Aβ peptide from degradation through resistance to most extracytoplasmic (e.g., alanyl, arginyl, and glutamyl) aminopeptidases (McDonald and Barret, 1986). Moreover, pyroglutamyl aminopeptidase activity is very low in human cortical extracts (Kuda et al., 1997). Saido and colleagues have observed decreased aminopeptidase A (glutamyl aminopeptidase) activity in sporadic AD plasma as compared with age-matched controls (Kuda et al., 1997). These investigators further propose that this observation could account for Aβ3(pE)-x generation in AD brain by prolonging the in vivo life of the precursor [Aβ3(E)-x], thus allowing cyclization (Saido, 1998).

As a result of decreased catabolism, Aβ3(pE)-42 accumulates and becomes a predominant isoform associ-

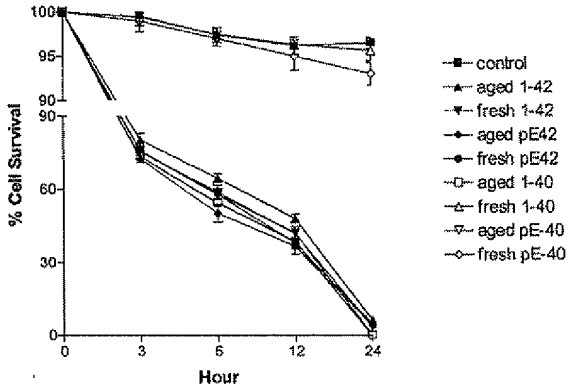

FIG. 3. Freshly solubilized Aβ3(pE)-40 and Aβ1-40 cause minimal cell death, whereas both freshly solubilized and aged Aβ3(pE)-42 and Aβ1-42 are neurotoxic. At 25 *μM*, aged and freshly solubilized Aβ1-40, Aβ3(pE)-40, Aβ1-42, and Aβ3(pE)-42 were compared in terms of relative toxicities within cortical cell cultures. Freshly solubilized peptides were suspended in culture medium just prior to use, whereas aged Aβ peptides were incubated as a 250 *μM* stock solution in PBS (pH 7.4) at 37°C for 1 week prior to dilution in cell culture medium and addition to the cultures.

ated with senile plaques (Saido et al., 1995, 1996; Tekirian et al., 1998). Aβ3(pE)-42 is not specific to AD or human brain as it is also found in senile plaques of nondemented human, canine, and polar bear brain as well as in cerebrovascular Aβ deposits in each of these species (Tekirian et al., 1998). Although not more toxic than Aβ1-42 in vitro, the abundance of Aβ3(pE)-42 in extracellular Aβ deposits and soluble Aβ peptides extracted from AD brains suggests that this isoform may play a critical role in plaque formation and AD pathogenesis.

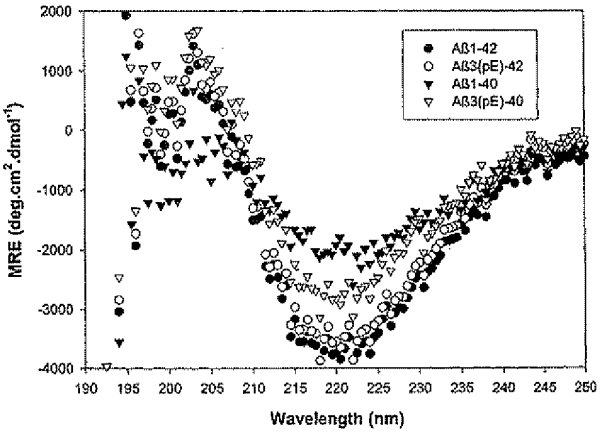

FIG. 4. Circular dichroism of "aged" Aβ peptides. For the circular dichroism studies, Aβ peptide "aging" or preaggregation was accelerated by overnight incubation in 0.1 *M* sodium acetate buffer (pH 5.0). All peptides [Aβ1-42, Aβ3(pE)-42, Aβ1-40, and Aβ3(pE)-40] revealed positive peaks at 200 nm and negative peaks at 218 nm, indicative of β-pleated sheet structure. MRE, mean residue ellipticity.

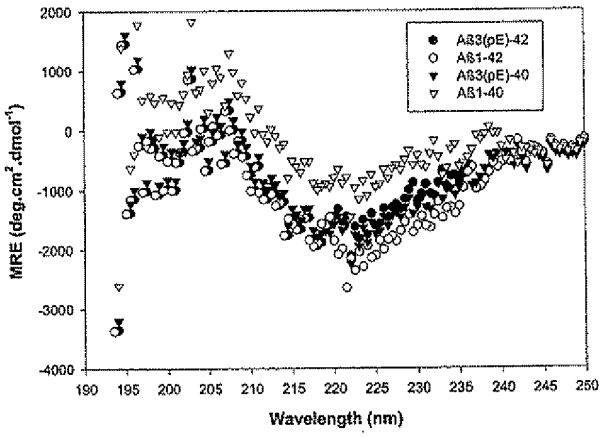

FIG. 5. Circular dichroism of freshly solubilized Aβ peptides. After fresh solubilization, the four Aβ peptides [Aβ1-42, Aβ3(pE)-42, Aβ1-40, and Aβ3(pE)-40] were suspended in PBS (pH 7.4) and assessed by circular dichroism analysis. All peptides revealed positive peaks at 200 nm and negative peaks at 218 nm, indicative of β-pleated sheet structure, although the negative 218-nm peak was not as pronounced as that observed with the aged Aβ peptides (Fig. 4). MRE, mean residue ellipticity.

Acknowledgment: This research was supported by NIH grants AG05144 (J.W.G.) and NS31230 (C.G.), NIMH grant F31 MH11650 (T.L.T.), American Health Assistance Foundation grant 22845 (A.Y.Y.), and an Alzheimer's Association Investigator Initiated Award (A.Y.Y.).

REFERENCES

Brewer G. J., Torricelli J. R., Evege E. K., and Price P. J. (1993) Optimized survival of hippocampal neurons in B27-supplemented Neurobasal, a new serum-free medium combination. *J. Neurosci. Res.* **35,** 567–576.

Burdick D., Soreghan B., Kwon M., Kosmoski J., Knauer M., Henschen A., Yates J., Cotman C., and Glabe C. (1992) Assembly and aggregation properties of synthetic Alzheimer's A4/beta amyloid peptide analogs. *J. Biol. Chem.* **267,** 546–554.

Checler F. (1995) Processing of the β-amyloid precursor protein and its regulation in Alzheimer's disease. *J. Neurochem.* **65,** 1431–1444.

Harris M. E., Hensley K., Butterfield D. A., Leedle R. A., and Carney J. M. (1995) Direct evidence of oxidative injury produced by the Alzheimer's beta-amyloid peptide (1-40) in cultured hippocampal neurons. *Exp. Neurol.* **131,** 193–202.

Howlett D. R., Jennings K. H., Lee D. C., Clark M. S., Brown F., Wetzel R., Wood S. J., Camilleri P., and Roberts G. W. (1995) Aggregation state and neurotoxic properties of Alzheimer beta-amyloid peptide. *Neurodegeneration* **4,** 23–32.

Jiang H., Burdick D., Glabe C. G., Cotman C. W., and Tenner A. J. (1994) Beta-amyloid activates complement by binding to a specific region of the collagen-like domain of the C1q A chain. *J. Immunol.* **152,** 5050–5059.

Kalaria R. N. (1996) Cerebral vessels in ageing and Alzheimer's disease. *Pharmacol. Ther.* **72,** 193–214.

Kuda T., Shoji M., Arai H., Kawashima S., and Saido T. C. (1997) Reduction of plasma glutamyl aminopeptidase activity in sporadic Alzheimer's disease. *Biochem. Biophys. Res. Commun.* **231,** 526–530.

McDonald J. K. and Barret A. J. (1986) *Mammalian Proteases.* Academic Press, London.

Mills J. and Reiner P. B. (1999) Regulation of amyloid precursor protein cleavage. *J. Neurochem.* **72,** 443–460.

Mori H., Takio K., Ogawara M., and Selkoe D. J. (1992) Mass spectrometry of purified amyloid beta protein in Alzheimer's disease. *J. Biol. Chem.* **267,** 17082–17086.

Pike C. J., Walencewicz A. J., Glabe C. G., and Cotman C. W. (1991) In vitro aging of beta-amyloid protein causes peptide aggregation and neurotoxicity. *Brain Res.* **563,** 311–314.

Pike C. J., Burdick D., Walencewicz A. J., Glabe C. G., and Cotman C. W. (1993) Neurodegeneration induced by beta-amyloid peptides in vitro: the role of peptide assembly state. *J. Neurosci.* **13,** 1676–1687.

Pike C. J., Overman M. J., and Cotman C. W. (1995*a*) Amino-terminal deletions enhance aggregation of beta-amyloid peptides in vitro. *J. Biol. Chem.* **270,** 23895–23898.

Pike C. J., Walencewicz-Wasserman A. J., Kosmoski J., Cribbs D. H., Glabe C. G., and Cotman C. W. (1995*b*) Structure–activity analyses of beta-amyloid peptides: contributions of the beta 25-35 region to aggregation and neurotoxicity. *J. Neurochem.* **64,** 253–265.

Russo C., Saido T. C., DeBusk L. M., Tabaton M., Gambetti P., and Teller J. K. (1997) Heterogeneity of water-soluble amyloid beta-peptide in Alzheimer's disease and Down's syndrome brains. *FEBS Lett.* **409,** 411–416.

Saido T. C. (1998) Alzheimer's disease as proteolytic disorders: anabolism and catabolism of beta-amyloid. *Neurobiol. Aging* **19,** S69–S75.

Saido T. C., Iwatsubo T., Mann D. M., Shimada H., Ihara Y., and Kawashima S. (1995) Dominant and differential deposition of distinct beta-amyloid peptide species, A beta N3(pE), in senile plaques. *Neuron* **14,** 457–466.

Saido T. C., Yamao-Harigaya W., Iwatsubo T., and Kawashima S. (1996) Amino- and carboxyl-terminal heterogeneity of beta-amyloid peptides deposited in human brain. *Neurosci. Lett.* **215,** 173–176.

Selkoe D. J. (1989) Amyloid beta protein precursor and the pathogenesis of Alzheimer's disease. *Cell* **58,** 611–612.

Simmons L. K., May P. C., Tomaselli K. J., Rydel R. E., Fuson K. S., Brigham E. F., Wright S., Lieberburg I., Becker G. W., Brems D. N., and Li W. Y. (1994) Secondary structure of amyloid beta peptide correlates with neurotoxic activity in vitro. *Mol. Pharmacol.* **45,** 373–379.

Tekirian T. L., Saido T. C., Markesbery W. R., Russell M. J., Wekstein D. R., Patel E., and Geddes J. W. (1998) N-Terminal heterogeneity of parenchymal and cerebrovascular Abeta deposits. *J. Neuropathol. Exp. Neurol.* **57,** 76–94.

EXHIBIT 6

Diabetologia (2002) 45:1281–1291
DOI 10.1007/s00125-002-0894-6

Diabetologia

Improved stability, insulin-releasing activity and antidiabetic potential of two novel N-terminal analogues of gastric inhibitory polypeptide: N-acetyl-GIP and pGlu-GIP

F. P. M. O'Harte[1], V. A. Gault[1], J. C. Parker[1], P. Harriott[2], M. H. Mooney[1], C. J. Bailey[3], P. R. Flatt[1]

[1] School of Biomedical Sciences, University of Ulster, Coleraine, N. Ireland, UK
[2] Centre for Peptide and Protein Engineering, School of Biology and Biochemistry, The Queen's University of Belfast, Belfast, N. Ireland, UK
[3] School of Pharmaceutical and Biological Sciences, Aston University, Birmingham, UK

Abstract

Aims/hypothesis. This study examined the plasma stability, biological activity and antidiabetic potential of two novel N-terminally modified analogues of gastric inhibitory polypeptide (GIP).
Methods. Degradation studies were carried out on GIP, N-acetyl-GIP (Ac-GIP) and N-pyroglutamyl-GIP (pGlu-GIP) in vitro following incubation with either dipeptidylpeptidase IV or human plasma. Cyclic adenosine 3′5′ monophosphate (cAMP) production was assessed in Chinese hamster lung fibroblast cells transfected with the human GIP receptor. Insulin-releasing ability was assessed in vitro in BRIN-BD11 cells and in obese diabetic (*ob/ob*) mice.
Results. GIP was rapidly degraded by dipeptidylpeptidase IV and plasma ($t^{1/2}$ 2.3 and 6.2 h, respectively) whereas Ac-GIP and pGlu-GIP remained intact even after 24 h. Both Ac-GIP and pGlu-GIP were extremely potent ($p<0.001$) at stimulating cAMP production (EC_{50} values 1.9 and 2.7 nmol/l, respectively), almost a tenfold increase compared to native GIP (18.2 nmol/l). Both Ac-GIP and pGlu-GIP (10^{-13}–10^{-8} mmol/l) were more potent at stimulating insulin release compared to the native GIP ($p<0.001$), with 1.3-fold and 1.2-fold increases observed at 10^{-8} mol/l, respectively. Administration of GIP analogues (25 nmol/kg body weight, i.p.) together with glucose (18 mmol/kg) in (*ob/ob*) mice lowered ($p<0.001$) individual glucose values at 60 min together with the areas under the curve for glucose compared to native GIP. This antihyperglycaemic effect was coupled to a raised ($p<0.001$) and more prolonged insulin response after administration of Ac-GIP and pGlu-GIP (AUC, 644±54 and 576±51 ng·ml^{-1}·min, respectively) compared with native GIP (AUC, 257±29 ng·ml^{-1}·min).
Conclusion/interpretation. Ac-GIP and pGlu-GIP, show resistance to plasma dipeptidylpeptidase IV degradation, resulting in enhanced biological activity and improved antidiabetic potential in vivo, raising the possibility of their use in therapy of Type II (non-insulin-dependent) diabetes mellitus. [Diabetologia (2002) 45:1281–1291]

Keywords GIP analogues, antihyperglycaemic effects, insulin secretion, DPP IV stability, BRIN-BD11 cells, obese hyperglycaemic (*ob/ob*) mice.

Received: 25 February 2002 / Revised: 23 April 2002
Published online: 16 July 2002

Corresponding author: Dr. F. P. M. O'Harte, School of Biomedical Sciences, University of Ulster, Coleraine, N. Ireland, UK, BT52 1SA, E-mail: fpm.oharte@ulst.ac.uk
Abbreviations: cAMP, Cyclic adenosine 3′ 5′ monophosphate; DPP IV, Dipeptidylpeptidase IV; GIP, gastric inhibitory polypeptide; GLP-1, glucagon-like peptide-1(7– 36)amide; TFA, trifluoroacetic acid; ESI-MS, electrospray ionisation mass spectrometry; pGlu, N-pyroglutamyl; Ac, N-acetyl; Fmoc, 9-fluorenylmethoxycarbonyl; CHL, Chinese hamster lung fibroblast; DPA, diprotin A; FSK, forskolin; IBMX, isobutylmethylxanthine

Type II (non-insulin-dependent) diabetes mellitus is characterised by a decreased responsiveness of peripheral tissues to insulin and a diminished and delayed pancreatic beta-cell response to glucose [1, 2]. Therefore, novel therapeutic agents that normalise the beta-cell response to glucose are of considerable interest in the treatment of Type II diabetes. Two candidate agents including gastric inhibitory polypeptide (GIP) also called glucose-dependent insulinotropic polypeptide, together with the structurally related glucagon-like peptide-1(7–36)amide (GLP-1), act as major insulin-releasing hormones through the enteroinsular axis

[3, 4]. Considerable interest has already been invested in GLP-1 as a potential therapeutic candidate [4, 5, 6, 7].

Although both GIP and GLP-1 possess important insulinotropic properties [4], controversy exists regarding their relative effectiveness in stimulating insulin release. Some studies have shown that GIP and GLP-1 are equally potent in their capacity to stimulate insulin release [8], whereas others have suggested that GLP-1 possesses greater insulinotropic activity [9, 10]. Another study [11] indicated that GIP and GLP-1 are equally insulinotropic and share the same glucose threshold for activity; however, at the concentrations found postprandially, GIP is likely to be the more important incretin.

Further insight can be gained by examining glucose tolerance in GLP-1 receptor negative and GIP receptor negative animal models. GLP-1 receptor negative (GLP-1R –/–) mice show only modest glucose intolerance [12]. It has been shown that GLP-1R –/– mice have compensatory changes in the enteroinsular axis via increased GIP secretion and enhanced GIP action [12]. Serum GIP concentrations in GLP-1R –/– mice were increased compared with those in GLP-1R +/+ control mice after an OGTT. In contrast, studies with GIP receptor negative (GIPR –/–) mice have shown that these animals have higher blood glucose concentrations with impaired first phase insulin response [13]. The response of GIPR –/– mice to an intraperitoneal glucose tolerance test was similar to GIPR +/+ mice but glucose intolerance was present in the former group after an OGTT [13].

One of the key obstacles in utilising insulinotropic and antihyperglycaemic activity of GIP [14] as a potential therapy for diabetes is the short circulating half-life of the peptide (approximately 3–5 min) in the plasma [15, 16]. As with GLP-1 degradation, this is due mainly to rapid cleavage by a highly specific aminopeptidase, dipeptidyl peptidase IV (DPP IV; EC.3.4.14.5) a member of the prolyl oligopeptidase family of serine proteases [17]. DPP IV is expressed ubiquitously in mammalian tissues and organs [18] with a specificity for removing dipeptides from the amino terminus of a wide range of peptides with penultimate proline, alanine and hydroxyproline residues [19, 20]. DPP IV is in close contact with hormones circulating in the blood, located on endothelial cells of the blood vessels and, moreover, it is found as a soluble enzyme in blood plasma [21]. Thus DPP IV removes the amino-terminal Tyr^1-Ala^2 dipeptide from GIP producing GIP(3–42) [22]. This truncated peptide was initially believed to be biologically inactive; however, current opinion suggests that it could operate as a GIP receptor antagonist, thus preventing normal receptor interaction with the intact hormone [23]. Consistent with these observations, it has been shown that inhibition of DPP IV activity can potentiate the insulinotropic effect of GIP in mammals [24].

Recent studies in our laboratory have shown that N-terminal modification of GIP and GLP-1 by glycation results in resistance to DPP IV and confers an extended plasma half-life [25, 26]. N-terminally modified GIP could have a particularly promising potential as an antihyperglycaemic agent because its glucose lowering and insulin-releasing properties seem to be enhanced by this modification [27]. Our study was designed to investigate the stability and biological activity of two novel N-terminally modified analogues of GIP, namely Ac-GIP and pGlu-GIP. In addition to degradation studies and observations of cyclic AMP production and insulin secretion in vitro, the utility of these analogues has been clearly established in vivo using obese diabetic (*ob/ob*) mice as a commonly used animal model of Type II diabetes having both beta-cell dysfunction and insulin resistance.

Materials and methods

Materials. High-performance liquid chromatography (HPLC) grade acetonitrile was obtained from Rathburn (Walkersburn, Scotland, UK). Sequencing grade trifluoroacetic acid (TFA) was obtained from Aldrich (Poole, Dorset, UK). Dipeptidyl peptidase IV (DPP IV), isobutylmethylxanthine (IBMX), adenosine 3′:5′-cyclic monophosphate (cAMP), adenosine 5′-triphosphate (ATP) were all purchased from Sigma (Poole, Dorset, UK). Fmoc-protected amino acids and diprotin A were from Calbiochem Novabiochem (Beeston, Nottingham, UK). RPMI 1640 and DMEM tissue culture medium, foetal bovine serum, penicillin and streptomycin were all purchased from Gibco (Paisley, Strathclyde, Scotland). The chromatography columns used for cAMP assay, Dowex AG 50 WX and neutral alumina AG7 were obtained from Bio-Rad (Alpha Analytical, Larne, N. Ireland, UK). All water used in these experiments was purified using a Milli-Q, Water Purification System (Millipore, Milford, Mass., USA). All other chemicals used were of the highest purity available.

Synthesis of GIP, Ac-GIP and pGlu-GIP. GIP, Ac-GIP and pGlu-GIP were sequentially synthesised on an Applied Biosystems automated peptide synthesiser (model 432A, Foster City, Calif., USA) using standard solid-phase Fmoc protocols [28], starting from a pre-loaded Fmoc-Gln-Wang resin. The following side chain protected amino acids were used, Fmoc-Gln(Trt)-OH, Fmoc-Thr(Trt)-OH, Fmoc-His(Trt)-OH, Fmoc-Asn(Trt)-OH, Fmoc-Ser(Trt)-OH, Fmoc-Lys(Boc)-OH, Fmoc-Trp(Boc)-OH, Fmoc-Asp(OtBu)-OH, Fmoc-Tyr(OtBu)-OH and Pyr-OH. In the case of Ac-GIP acetic anhydride was added to the growing chain in the final step prior to cleavage from the resin. Deprotection and cleavage of the peptide from the resin was by trifluoroacetic acid:water:thianisole:ethanediol (90:2.5:5:2.5, a total volume of 20 ml/g resin), the resin was removed by filtration and the filtrate volume was decreased under reduced pressure. Dry diethyl ether was slowly added until a precipitate was observed. The precipitate was collected by low-speed centrifugation, resuspended in diethyl ether and centrifuged again, the procedure was carried out five times. The resulting pellets were then dried in vacuo and judged pure by reversed-phase HPLC on a Waters Millennium 2010 chromatography system (Millford, Mass., USA) Software version 2.1.5.

Structural confirmation of GIP and GIP analogues by electrospray ionisation-mass spectrometry (ESI-MS). Intact and degradation fragments of GIP, Ac-GIP and pGlu-GIP were dissolved (approximately 400 pmol/l) in 100 µl of water and applied to an LCQ benchtop LC mass spectrometer (Finnigan MAT, Hemel Hempstead, UK). Samples (20 µl direct loop injection) were applied at a flow rate of 0.2 ml/min, under isocratic conditions in 35% (v/v) acetonitrile/water. Mass spectra were obtained from the quadripole ion trap mass analyser and spectra collected using full ion scan mode over the mass-to-charge (m/z) range 150–2000. The molecular masses of each fragment were calculated using prominent multiple charged ions using the following equation; $M_r=iM_i-iM_h$ (where M_r is molecular mass; M_i is m/z ratio; i is the number of charges; and M_h is the mass of a proton).

Degradation of GIP, Ac-GIP and pGlu-GIP by DPP IV and human plasma. HPLC-purified GIP, Ac-GIP and pGlu-GIP were incubated in vitro at 37°C in 50 mmol/l triethanolamine-HCl, (pH 7.8, final peptide concentration 2 mmol/l) with either DPP IV (5 mU) or pooled human plasma (10 µl) for 0, 2, 4 and 8 h. A 24-h plasma incubation was also carried out for each peptide in the presence of diprotin A (5 mU). The enzymatic reaction was stopped by adding 10 µl of 10% (v/v) TFA/water. The terminated reaction products were then applied to a Vydac C-18 column (4.6×250 mm) and the major degradation fragment GIP(3–42) separated from intact GIP. The column was equilibrated with 0.12% (v/v) TFA/water at a flow rate of 1.0 ml/min. Using 0.1% (v/v) TFA in 70% acetonitrile/water, the concentration of acetonitrile in the eluting solvent was raised from 0% to 28% over 10 min, and from 28% to 42% over 20 min. The absorbance was monitored at 206 nm using a Spectrasystem UV 2000 detector (Thermoquest Limited, Manchester, UK) and peaks were collected manually prior to ESI-MS analysis. The small decline of GIP analogue peak area in some extended incubations, is likely to reflect non-specific binding to the incubation tube.

Cells and cell culture. Chinese hamster lung fibroblast (CHL) cells transfected with human GIP receptor [29] were cultured in DMEM tissue culture medium containing 10% (v/v) foetal bovine serum, 1% (v/v) antibiotics (100 U/ml penicillin, 0.1 mg/ml streptomycin). BRIN-BD11 cells were cultured in sterile tissue culture flasks (Corning, Glass Works, Sunderland, UK) using RPMI-1640 tissue culture medium containing 10% (v/v) foetal calf serum, 1% (v/v) antibiotics (100 U/ml penicillin, 0.1 mg/ml streptomycin) and 11.1 mmol/l glucose. The origin, characteristics and secretory responsiveness of this electrofusion-derived glucose-responsive cell line has been described in detail elsewhere [30]. The cells were maintained at 37°C in an atmosphere of 5% CO_2 and 95% air using a LEEC incubator (Laboratory Technical Engineering, Nottingham, UK). It was confirmed that there was no significant degradation of native GIP in acute incubations with CHL cells or BRIN-BD11 cells under the experimental conditions described below.

Determination of cAMP production in transfected CHL cells. Chinese hamster lung fibroblast (CHL) cells stably transfected with the human GIP receptor were seeded into 12-multiwell plates (Nunc, Roskilde, Denmark) at a density of 1.0×10^5 cells per well [29]. The cells were then allowed to grow for 48 h before being exposed to 2 µCi of tritiated adenine (TRK311, Amersham, Buckinghamshire, UK) in 1 ml DMEM, with 0.5% (w/v) foetal bovine serum, and incubated at 37°C for 5 to 6 h. The cells were then washed twice with Hanks' balanced salt solution (HBSS; 130 mmol/l NaCl, 20 mmol/l HEPES, pH 7.4, 0.9 mmol/l $NaHPO_4$, 0.8 mmol/l $MgSO_4$, 5.4 mmol/l KCl, 1.8 mmol/l $CaCl_2$, 25 mmol/l glucose, 25 µmol/l phenol red). The cells were then exposed to varying concentrations (10^{-12} to 10^{-6} mol/l) of GIP, Ac-GIP, pGlu-GIP or forskolin (FSK) (10 µmol/l) in HBSS, in the presence of 1 mmol/l IBMX, for 10 to 15 min at 37 C. The medium was subsequently removed and the cells lysed with 1 ml of 5% trichloroacetic acid (TCA) containing 0.1 mmol/l unlabelled cAMP and 0.1 mmol/l unlabelled ATP. The intracellular tritiated cAMP was then separated on Dowex and alumina exchange resins as described previously [31].

Acute tests for insulin secretion. Before experimentation, BRIN-BD11 cells were harvested from the surface of the tissue culture flasks with the aid of trypsin-EDTA (Gibco), seeded into 24-multiwell plates (Nunc, Roskilde, Denmark) at a density of 1.0×10^5 cells per well, and allowed to attach overnight at 37°C. Acute tests for insulin release were preceded by 40 min pre-incubation at 37°C in 1.0 ml Krebs Ringer bicarbonate buffer (115 mmol/l NaCl, 4.7 mmol/l KCl, 1.28 mmol/l $CaCl_2$, 1.2 mmol/l KH_2PO_4, 1.2 mmol/l $MgSO_4$, 10 mmol/l $NaHCO_3$, containing 0.5% (w/v) bovine serum albumin, pH 7.4) supplemented with 1.1 mmol/l glucose. Test incubations were carried out (n=8) in 5.6 mmol/l glucose with a range of concentrations (10^{-13} to 10^{-8} mol/l) of GIP, Ac-GIP and pGlu-GIP. After 20 min incubation, the buffer was removed from each well and aliquots (200 µl) were used for measurement of insulin by radioimmunoassay [32].

In vivo biological activities of GIP, Ac-GIP and pGlu-GIP in obese diabetic (ob/ob) mice. Effects of GIP, Ac-GIP and pGlu-GIP on plasma glucose and insulin concentrations were examined using 14 to 18-week-old obese diabetic (*ob/ob*) mice. The genetic background and characteristics of the colony used have been outlined in detail elsewhere [33]. The animals were housed individually in an air-conditioned room at 22±2°C with a 12-h light to 12-h dark cycle. Drinking water and a standard rodent maintenance diet (Trouw Nutrition, Cheshire, UK) were freely available. Plasma glucose and insulin responses were evaluated in 18-h fasted (*ob/ob*) mice after an intraperitoneal (i.p.) injection of saline (0.9% (w/v) NaCl) as control, glucose alone (18 mmol/kg body weight) or in combination with GIP, Ac-GIP or pGlu-GIP (25 nmol/kg). All test solutions were administered in a final volume of 8 ml/kg body weight. Blood samples were collected from the cut tip of the tail of conscious mice into chilled fluoride-heparin microcentrifuge tubes (Sarstedt, Nümbrecht, Germany) immediately before injection (t=0) and at 15, 30 and 60 min after injection. Plasma was separated by centrifugation using a Beckman microcentrifuge (Beckman Instruments, UK; for 30 s at 13 000 g) and stored at –20°C prior to glucose and insulin measurements. The "Principles of Laboratory Animal Care" (NIH publication 1985) were followed and all animal studies were carried out in accordance with the UK Animals (Scientific Procedures) Act 1986.

Assessment of plasma glucose and insulin concentrations. Glucose was assayed by an automated glucose oxidase procedure using a Beckman Glucose Analyser II [34]. Insulin was assessed by dextran-charcoal RIA as described previously [32]. Incremental areas under plasma glucose and insulin curves (AUC) were calculated using a computer generated program (CAREA) using the trapezoidal rule [35] with baseline subtraction.

Statistical analysis. Results are expressed as means ± SEM. Data were compared using the Student's t test or ANOVA, followed by the Student-Newman-Keuls test. Groups of data from

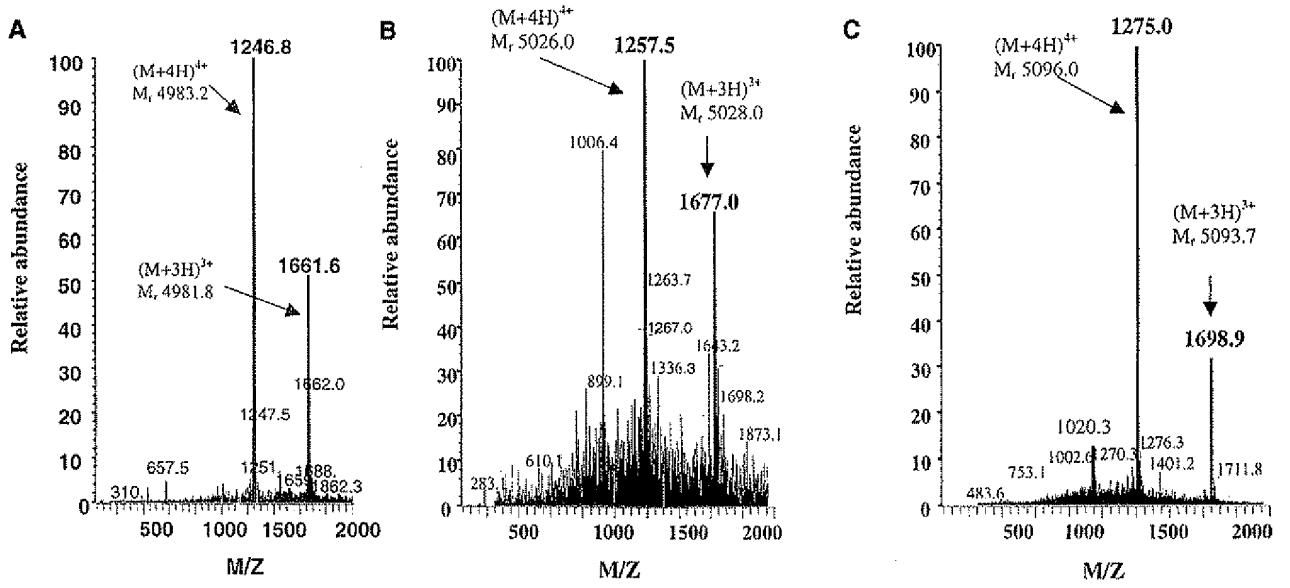

Fig. 1 A–C. Electrospray ionisation mass spectrometry of **A** human GIP(1–42), **B** N-acetyl-GIP and **C** N-pyroglutamyl-GIP, respectively. The peptides were applied by direct loop injection to the LC/MS under isocratic conditions. Spectra were recorded using a quadripole ion trap mass analyser and collected using full ion scan mode over the mass-to-charge (m/z) range 150–2000

both were considered to be significantly different if the p value was less than 0.05.

Results

Structural identification of GIP, Ac-GIP and pGlu-GIP by ESI-MS. GIP, Ac-GIP and pGlu-GIP were produced by solid-phase peptide synthesis using standard Fmoc chemistry protocols. Following further purification on a Vydac C-18 analytical column (4.6×250 mm), the monoisotopic molecular mass of each peptide was calculated using ESI-MS (Fig. 1). After spectral averaging was carried out, prominent multiple charged species $(M+3H)^{3+}$ and $(M+4H)^{4+}$ were detected for GIP at m/z 1661.6 and 1246.8, corresponding to intact M_r 4981.8 and M_r 4983.2 Daltons (Da), respectively (theoretical mass 4980.5 Da) (Fig. 1A). For Ac-GIP, $(M+3H)^{3+}$ and $(M+4H)^{4+}$ were detected at m/z 1677.0 and 1257.5, corresponding to intact molecular masses of M_r 5028.0 and 5026.0 Da, respectively (Fig. 1B), corresponding very closely with the theoretical mass of 5026.2 Da. Similarly, for pGlu-GIP, $(M+3H)^{3+}$ and $(M+4H)^{4+}$ were detected at m/z 1698.9 and 1275.0, corresponding to intact M_r 5093.7 and 5096.0 Da, respectively (Fig. 1C), which corresponds closely with the theoretical mass of 5094.2 Da. Results from the ESI-MS analysis showed that the correct primary structures for GIP and related analogues had been successfully synthesised.

Degradation of GIP, Ac-GIP and pGlu-GIP by DPP IV and plasma. Figures 2, 3 and 4 show typical HPLC peak profiles obtained after separation of the reaction products obtained from the incubation of GIP, Ac-GIP and pGlu-GIP with DPP IV and plasma for 0, 2 and 8 h. The HPLC retention times of GIP, Ac-GIP and pGlu-GIP incubated with DPP IV at t=0 were 21.72, 22.82 and 37.52 min, respectively. Degradation of GIP (Fig. 2A) was evident after just 2 h, which was indicated by a peak with a retention time of 20.81 min, which upon ESI-MS analysis corresponded to GIP(3–42) (observed mass 4748.7 Da compared with theoretical mass 4746.4 Da). After 8 h, GIP (Fig. 2A) was completely degraded. In contrast, Ac-GIP and pGlu-GIP remained intact for more than 8 h (Fig. 3A, Fig. 4A). These peptides remained fully intact even after incubation was prolonged to 24 h. Incubation with DPP IV showed that the relative in vitro half-lives of GIP, Ac-GIP and pGlu-GIP were 2.3 h, >24 and >24 h, respectively.

In plasma degradation studies, retention times for intact GIP (Fig. 2B), Ac-GIP (Fig. 3B) and pGlu-GIP (Fig. 4B) were 21.94, 22.75 and 35.92 min, respectively. Retention times for the major degradation fragment from native GIP, GIP(3–42) was 20.21 min. In general, the degradation with human plasma was not as rapid as with purified DPP IV with 61% of GIP degraded by 8 h (Fig. 2A). The native peptide was completely degraded by 24 h, an effect totally inhibited by DPA. In contrast, Ac-GIP (Fig. 3B) and pGlu-GIP (Fig. 4B) were not degraded by plasma incubation. In human plasma, the estimated half-lives of GIP, Ac-GIP and pGlu-GIP were 6.2 h, >24 h and >24 h, respectively.

Effects of GIP, Ac-GIP and pGlu-GIP on cAMP production. Figure 5 shows the dose-dependent stimulation of cAMP production by GIP, Ac-GIP and pGlu-

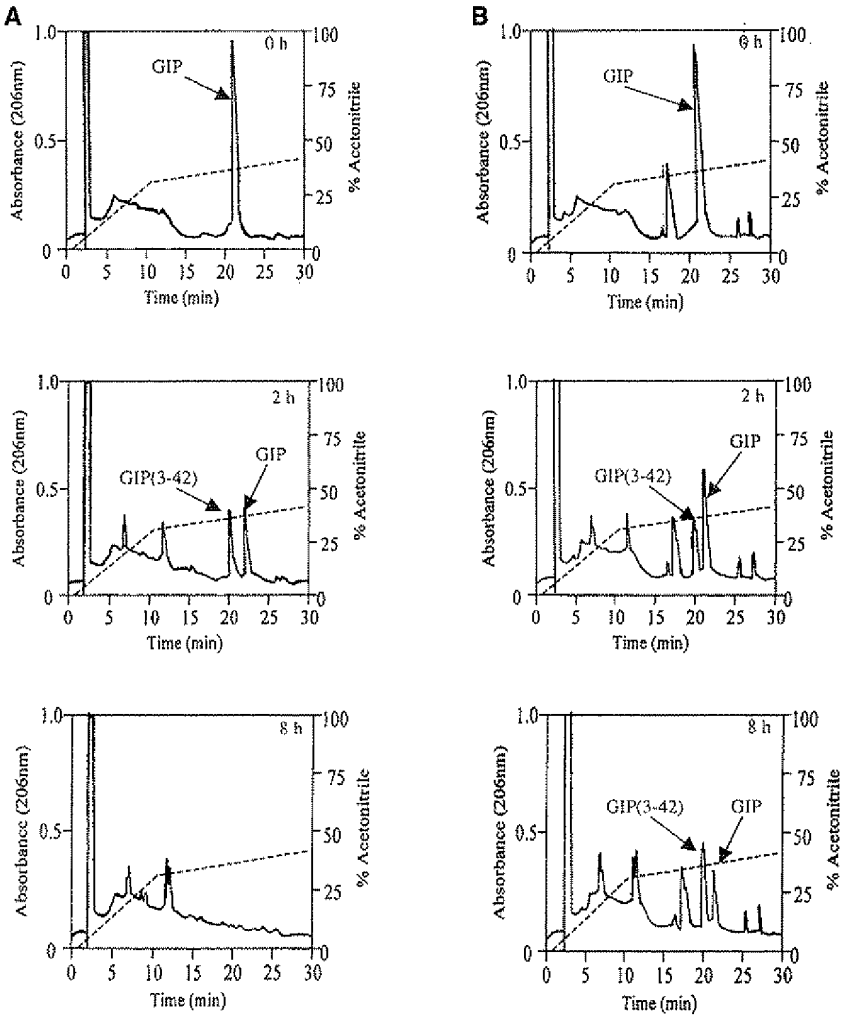

Fig. 2 A, B. Degradation of native GIP by DPP IV and human plasma. Representative HPLC profiles obtained after incubation of native GIP with DPP IV (**A**) and human plasma (**B**) for 0, 2 and 8 h. Reaction products were separated on a Vydac C-18 column. HPLC peaks corresponding to intact GIP and GIP(3–42) are indicated

GIP in CHL cells transfected with human GIP receptors. The calculated EC_{50} values for these peptides were 18.2, 1.9 and 2.7 nmol/l, respectively. The maximal cAMP response of Ac-GIP and pGlu-GIP were 165.7±1.3 and 183.9±5.7%, ($p<0.001$ and $p<0.001$, respectively), compared to native GIP (100%).

Effects of GIP, Ac-GIP and pGlu-GIP on insulin secretion. Figure 6 shows the effect of a range of concentrations (10^{-13} to 10^{-8} mol/l) of GIP, Ac-GIP and pGlu-GIP on insulin secretion from BRIN-BD11 cells. GIP, Ac-GIP and pGlu-GIP stimulated insulin secretion ($p<0.01$ to $p<0.001$) between 10^{-12} and 10^{-8} mol/l by 1.2-fold to 2.5-fold compared to control (5.6 mmol/l glucose alone). The ability of native GIP to stimulate insulin secretion was evident at concentrations of 10^{-11} mol/l or higher. Both Ac-GIP and pGlu-GIP were more potent at stimulating insulin secretion ($p<0.05$ to $p<0.001$) over the entire concentration range tested compared to native GIP. At 10^{-8} mol/l Ac-GIP and pGlu-GIP had a 1.3-fold and 1.2-fold greater stimulatory ability ($p<0.001$) compared to native GIP.

Effects of GIP, Ac-GIP and pGlu-GIP on anti-hyperglycaemic activity in (ob/ob) mice. Plasma glucose responses were evaluated after i.p. injection of saline (0.9% (w/v) NaCl) as a control, glucose alone (18 mmol/kg body weight) or in combination with GIP, Ac-GIP or pGlu-GIP (25 nmol/kg). When saline alone was injected no effect was observed on plasma glucose concentration (Fig. 7A). Administration of glucose alone prompted a high rise (34.4±2.9 mmol/l) in plasma glucose ($p<0.001$) at 15 min compared to basal glucose (5.4±0.5 mmol/l), and the plasma glucose concentration declined over the following 45 min (Fig. 7A). The peak glucose response to native GIP was reduced ($p>0.05$) at 15 min compared to glucose alone and this failed to reach significance in terms of overall glucose excursion as identified by area under the curve (AUC, 0–60 min, Fig 7B). In contrast both

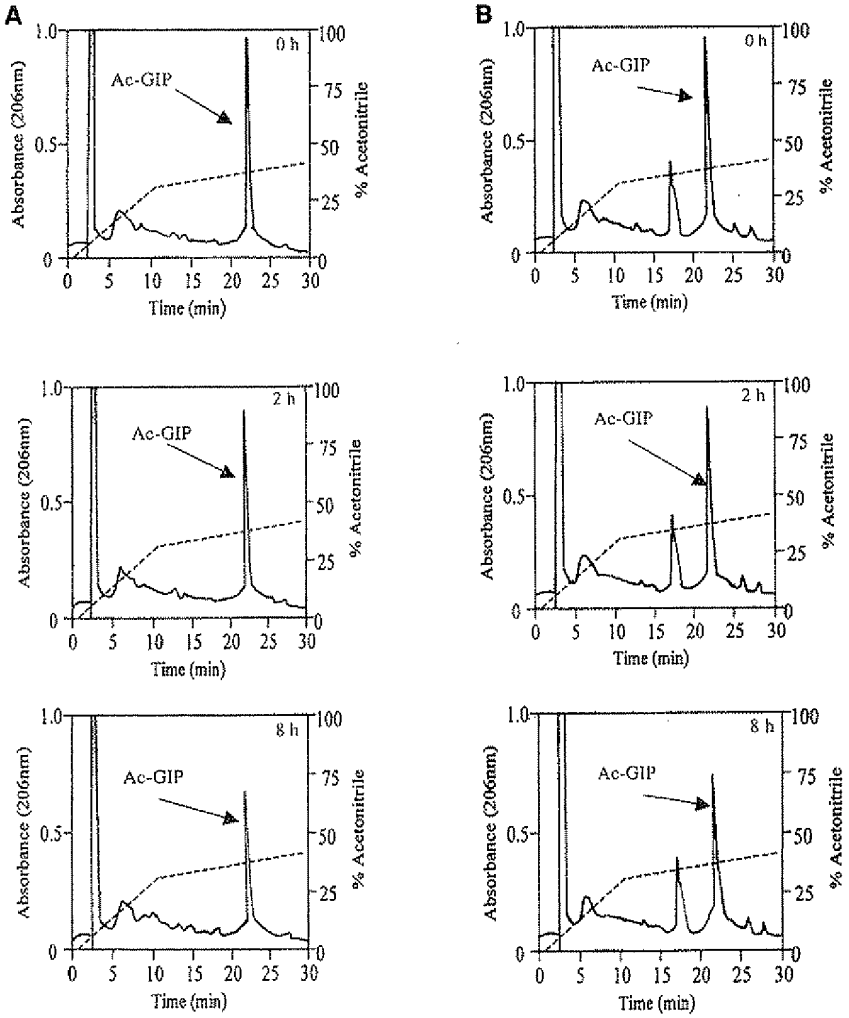

Fig. 3 A, B. Degradation of N-acetyl-GIP by DPP IV and human plasma. Representative HPLC profiles obtained after incubation of Ac-GIP with DPP IV (**A**) and human plasma (**B**) for 0, 2 and 8 h. Reaction products were separated on a Vydac C-18 column. HPLC peaks corresponding to intact Ac-GIP are indicated

Ac-GIP and pGlu-GIP reduced the peak 15 to 30 min glucose excursion compared to glucose alone ($p<0.01$ and $p<0.001$) and also reduced the AUC ($p<0.05$ and $p<0.01$) compared to native GIP.

Effects of GIP, Ac-GIP and pGlu-GIP on insulin-releasing activity in ob/ob mice. Plasma insulin responses to administration of saline, glucose and GIP peptides are shown in Fig. 7. Saline had no effect on plasma insulin concentrations (Fig. 7C). Glucose alone caused a peak (9.0±0.6 ng/ml) in plasma insulin at 15 min compared to basal insulin (2.8±0.5 ng/ml), and the plasma insulin concentration fell over the following 45 min returning to basal values. The insulin response to GIP in the presence of glucose was greater than to glucose alone as shown by the increase AUC values for insulin over 60 min (Fig. 7D, $p<0.05$). The insulinotropic effects of both Ac-GIP and pGlu-GIP were higher than native GIP at 15, 30 and 60 min ($p<0.001$). The AUC values showed a substantial enhancement of insulin releasing activity compared to both glucose alone and native GIP (Fig. 7D, $p<0.001$). It was notable that the insulinotropic effect of these two novel analogues was much more protracted than that of GIP with plasma insulin remaining higher (11.8±0.8 to 10.9±0.9 ng/ml, respectively) at 60 min ($p<0.001$) compared with native GIP (3.8±0.4 ng/ml) (Fig. 7C).

Discussion

In humans, incretin hormones only stimulate glucose-induced insulin release under hyperglycaemic conditions [6, 36, 37] and thus unlike other current non-endogenous insulinotropic agents that are used in the treatment of Type II diabetes, the incretins are not likely to result in hypoglycaemic episodes. It is this unique feature which has led to recent interest in the incretin hormones as a potential therapy for diabetes

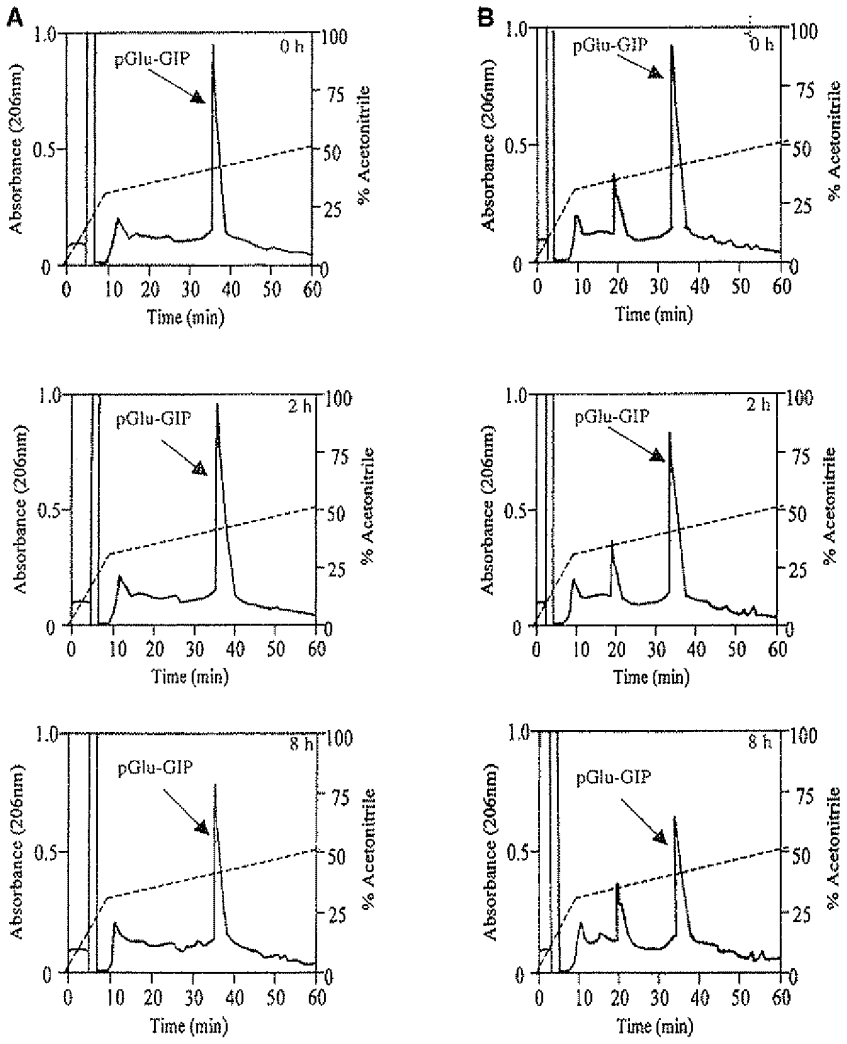

Fig. 4 A, B. Degradation of N-pyroglutamyl-GIP by DPP IV and human plasma. Representative HPLC profiles obtained after incubation of pGlu-GIP with DPP IV (**A**) and human plasma (**B**) for 0, 2 and 8 h. Reaction products were separated on a Vydac C-18 column. HPLC peaks corresponding to intact pGlu-GIP are indicated

[7, 33, 38]. Clinical trials have been restricted to GLP-1 [33] but the administration of long-acting peptide analogues of both GLP-1 [38] and GIP [27], as well as specific inhibition of DPP IV [39, 40], have been shown to improve glucose tolerance in experimental animal studies. Although certain groups of Type II diabetic patients have been suggested to show a de-

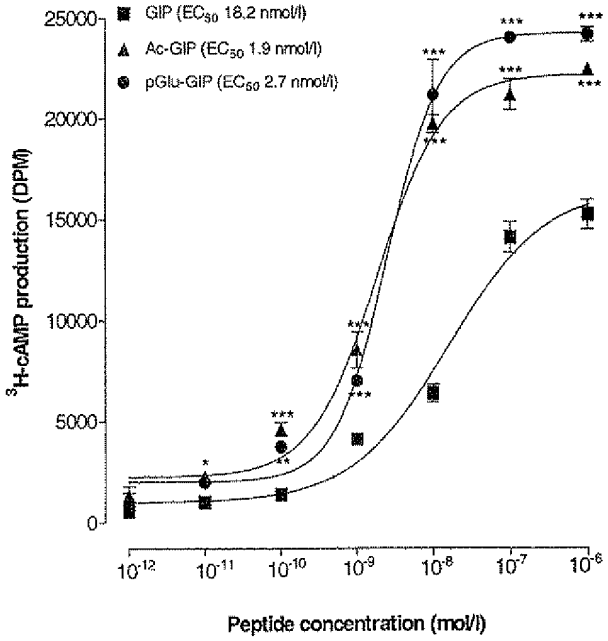

Fig. 5. Dose-dependent production of intracellular cAMP by GIP, N-acetyl-GIP and N-pyroglutamyl-GIP upon binding to CHL fibroblast cells transfected with the human GIP receptor. Each experiment was carried out in triplicate and the data are expressed in absolute values and represent means ± SEM of three independent experiments. The EC_{50} values for cAMP production are shown in parentheses

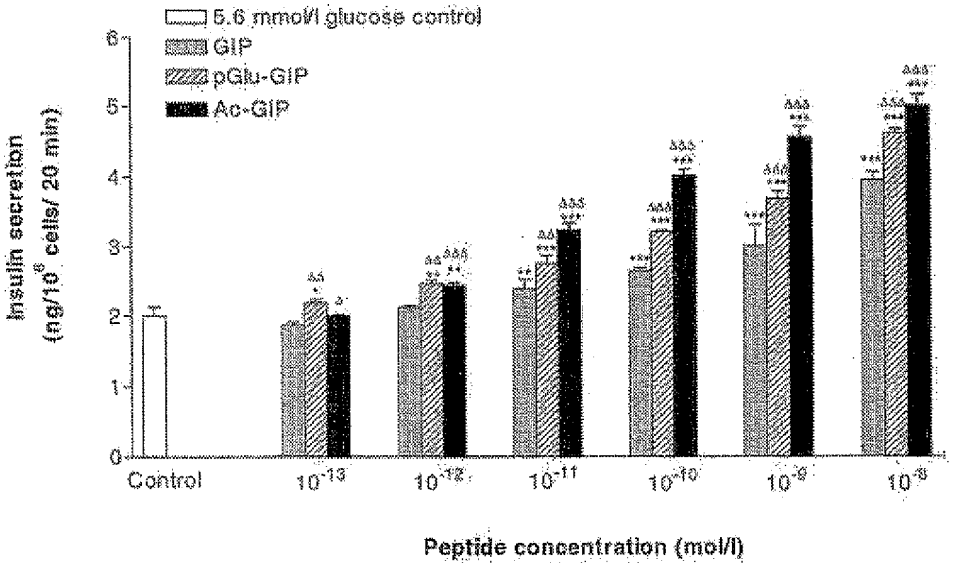

Fig. 6. Dose-dependent effects of GIP, N-acetyl-GIP and N-pyroglutamyl-GIP on insulin secretion from BRIN-BD11 cells. After a pre-incubation of 40 min, the effects of various concentrations of peptide (10^{-13} to 10^{-8} mol/l) were tested on insulin release during a 20 min incubation period. Values are means ± SEM for eight separate observations. *p<0.05, **p<0.01, ***p<0.001 compared to control (5.6 mmol/l glucose alone). $^{\Delta}p$<0.05, $^{\Delta\Delta}p$<0.01, $^{\Delta\Delta\Delta}p$<0.001 compared to GIP at the same concentration

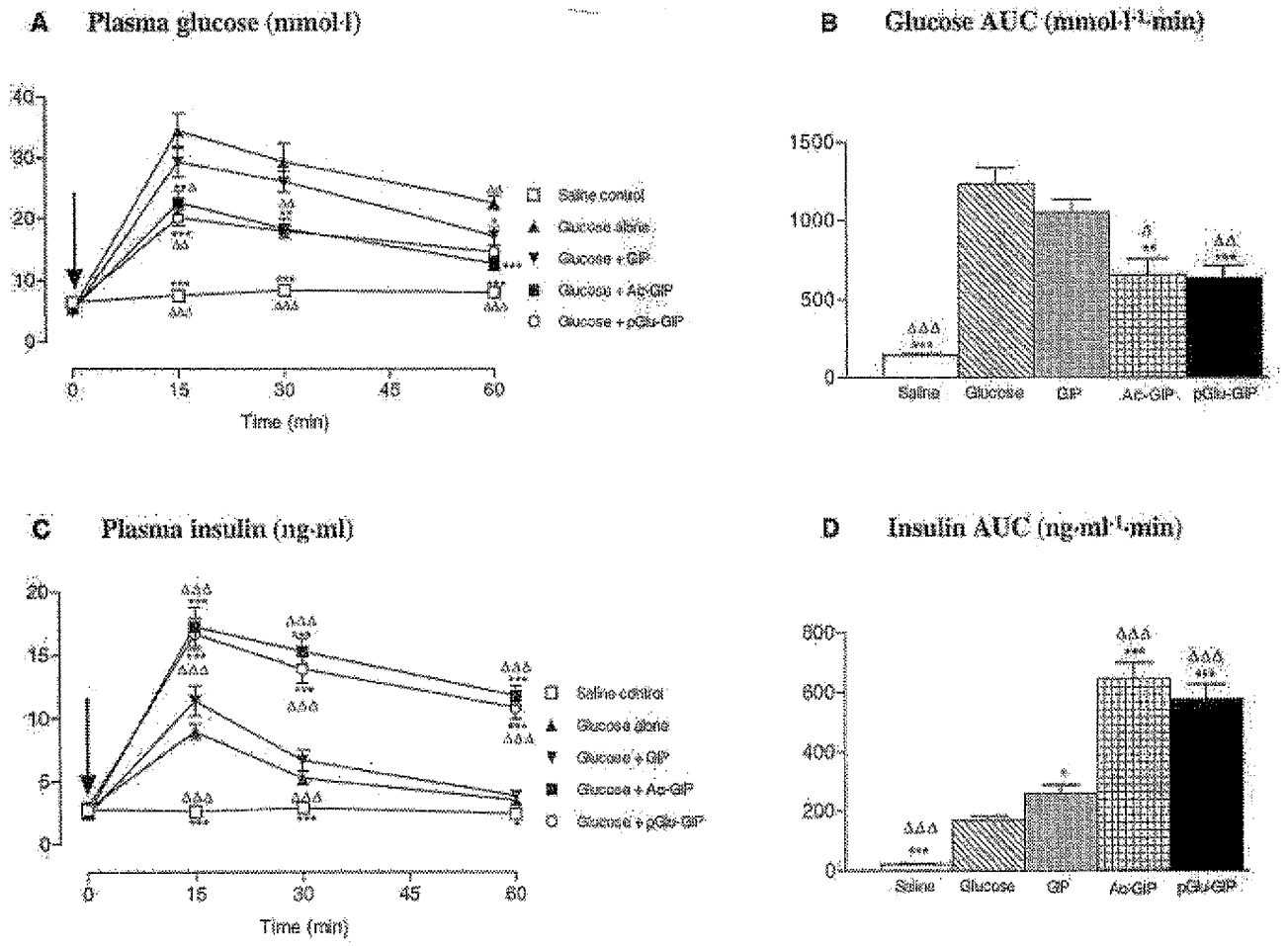

Fig. 7 A–D. Effects of GIP, N-acetyl-GIP and N-pyroglutamyl-GIP on plasma glucose homeostasis and plasma insulin responses in obese diabetic (*ob/ob*) mice. **A** Plasma glucose concentrations were measured prior to and after i.p. administration of saline (0.9% (w/v) NaCl) as control, glucose alone (18 mmol/kg body weight), or in combination with either GIP, Ac-GIP or pGlu-GIP (25 nmol/kg body weight). **B** Plasma glucose AUC values for 0–60 min post-injection. **C** Plasma insulin concentrations were measured prior to and after i.p. administration of saline (0.9% (w/v) NaCl), glucose alone (18 mmol/kg body weight), or in combination with either GIP, Ac-GIP or pGlu-GIP (25 nmol/kg body weight). **D** Plasma insulin AUC values for 0–60 min post-injection. Values are means ± SEM for eight mice. *p<0.05, **p<0.01, ***p<0.001 compared to glucose alone. $^{\Delta}p$<0.05, $^{\Delta\Delta}p$<0.01, $^{\Delta\Delta\Delta}p$<0.001 compared to native GIP

creased beta-cell responsiveness to GIP [41, 42], intracellular pathways triggered by the two incretin hormones seem identical [43]. Mutations of GIP receptors are rare in diabetes [42, 44] and any speculated abnormalities in GIP receptor binding could be overcome by stable and structurally modified analogues of GIP. Therefore, GIP analogues could be useful in the treatment of diabetes, and it is important to explore their actions and potential therapeutic value.

DPP IV has been identified as the key enzyme responsible for inactivation of GIP in serum [24]. This inactivation occurs through the rapid removal (GIP half-life 3–5 min) of the N-terminal dipeptide Tyr^1-Ala^2 giving rise to the major metabolite GIP(3–42). However, DPP IV which has a preference for cleavage after penultimate Pro and Ala residues [19], is responsible for the inactivation of a wide range of other biologically active molecules, such as GLP-1, GLP-2, enterostatin, growth-hormone-releasing factor and neuropeptide Y [20]. Thus inhibitors of DPP IV not only preserve the biological activity of GLP-1 and GIP but also run the risk of adversely affecting many other physiological inactivation processes involving this enzyme [20]. Our study has shown that N-terminal modification of GIP with addition of N-acetyl and N-pyroglutamyl groups confers profound resistance to plasma DPP IV degradation. Thus N-acetyl- and N-pyroglutamyl-GIP were completely stable during in vitro incubations with human serum or purified DPP IV for periods of up to 24 h. As shown elsewhere native GIP was rapidly degraded to GIP(3–42) by a process prevented by DPA, and thus attributable to DPP IV [15, 22, 24, 27]. The current approach to prolonging GIP activity by structurally modifying the peptide by addition of an N-terminal acetyl or pyroglutamyl group therefore seems to be a more subtle and highly effective method of achieving hormone stability, compared with using non-specific DPP IV inhibitors.

The glucose dependency of the insulinotropic action of GIP has been shown in humans [36, 37]. Using the glucose clamp technique in humans, others [37] found that mild hyperglycaemia (at least 1.4 mmol/l above basal levels) was sufficient to initiate the insulinotropic action of GIP. In the perfused rat pancreas, GIP stimulated insulin release at a threshold of 5.5 mmol/l glucose and a maximal response at 16 mmol/l glucose [45]. In our study, the insulinotropic effects of GIP and GIP analogues became apparent at about 10^{-11} mol/l. This is close to the fasting GIP concentration of 5×10^{-11} mol/l, which rises to 2.5×10^{-10} mol/l after ingestion of a mixed meal [46, 47]. Evaluation of the activities of N-acetyl-GIP and N-pyroglutamyl-GIP to increase cAMP showed that these N-terminally modified GIP analogues were up to tenfold more potent than the native hormone. Furthermore, GIP analogues increased insulin secretion up to threefold over glucose alone which compares to a maximal 1.6-fold increase over basal in response to sulphonylureas under similar conditions [48]. This cannot be attributed to differences in the degradation of GIP peptides in acute tests as this was negligible. Thus the results raise the possibility that enhancement of potency at the GIP receptor could overcome any natural impairment of GIP stimulation in diabetes. Of interest, these effects were observed at a physiological glucose concentration of 5.6 mmol/l, providing much encouragement for heightened biological activity in vivo.

Consistent with the in vitro studies, administration of Ac-GIP or pGlu-GIP improved the antihyperglycaemic and insulin-releasing activity of the peptide when administered with glucose to obese diabetic (*ob/ob*) mice. Native GIP only modestly increased plasma insulin and reduced the glycaemic excursion in the diabetic mutant as observed in several studies [49, 50]. However, the N-terminal Tyr^1-modified analogues of GIP increased the insulin-releasing and antihyperglycaemic actions of the peptide by on average 2.4-fold and 1.9-fold, respectively, as estimated from AUC measurements. Detailed kinetic analysis, however, is difficult due to the limitation of sampling times, but the prolonged insulin response after administration of the N-terminal Tyr^1-modified analogues as opposed to GIP is also indicative of a longer half-life. Thus these in vivo results suggest that N-acetyl and N-pyroglutamyl analogues of GIP show resistance to DPP IV degradation while at the same time evoking an enhanced stimulatory insulin secretory response from the beta cell. The former action will impede degradation of the peptide to GIP(3–42), thereby prolonging the half-life and enhancing effective circulating concentrations of the biologically active peptide. It will also decrease circulating concentrations of GIP(3–42) which functions as a highly selective GIP antagonist [51, 52]. Based on these results, it seems that these novel N-terminal Tyr^1-modified analogues of GIP enhance insulin secretion in vivo and improve glycaemic responses in Type II diabetes by conferring DPP IV resistance as well as increased potency at the GIP receptor. Moreover GIP has been proposed to exert various extrapancreatic effects, which could contribute to anthyperglycaemic activity in vivo including stimulation of peripheral glucose uptake [16, 53, 54, 55].

In conclusion, this study shows that the N-terminal Tyr^1-modified analogues of GIP, N-acetyl-GIP and N-pyroglutamyl-GIP, show strong resistance to DPP IV, and thereby have an extended plasma half-life, which in turn contributes to the enhanced biological activity in vitro. This is accompanied by improved antihyperglycaemic activity and raised insulin concentrations in vivo. These observations greatly encourage further investigation of the possible use of stable and biologically enhanced GIP analogues, alongside of those for GLP-1, for the treatment of diabetes and alleviation of its complications.

Acknowledgements. These studies were supported by University of Ulster Research Strategy Funding. The authors wish to thank Professor B. Thorens (University of Lausanne, Switzerland) for kindly providing the transfected Chinese hamster lung fibroblast (CHL) cells.

References

1. Östenson CG (2001) The pathophysiology of Type II diabetes mellitus: an overview. Acta Physiol Scand 171: 241–247
2. Pratley RE, Weyer C (2001) The role of impaired early insulin secretion in the pathogenesis of Type II diabetes mellitus. Diabetologia 44: 929–945
3. Brown JC (1994) Enteroinsular axis. In: Walsh J, Dockray G (eds) Gut peptides biochemistry and physiology. Raven Press, New York, pp 765–784
4. Habener JF (1993) The incretin notion and its relevance to diabetes. Endocrinol Metab Clin North Am 22: 775–794
5. Gutniack M, Ørskov C, Holst JJ, Ahren B, Effendic S (1992) Antidiabetic effect of glucagon-like peptide-1 (7–36)amide in normal subjects and patients with diabetes mellitus. N Eng J Med 326: 1316–1322
6. Holst JJ (2000) Gut hormones as pharmaceuticals. From enteroglucagon to GLP-1 and GLP-2. Regul Pept 93: 45–51
7. Creutzfeldt W (2001) The entero-insular axis in type 2 diabetes-incretins as therapeutic agents. Exp Clin Endocrinol Diabetes 109: S288–S303
8. Suzuki S, Kawai K, Ohashi S, Watanabe Y, Yamashita K (1992) Comparison of the insulinotropic activity of the glucagon-superfamily peptides in rat pancreas perfusion. Horm Metab Res 24: 458–461
9. Shima K, Hirota M, Ohboshi C (1988) Effect of glucagon-like peptide-1 on insulin secretion. Regul Pept 22: 245–252
10. Siegel EG, Schulze A, Schmidt WE, Creutzfeldt W (1992) Comparison of the effect of GIP and GLP-1 (7–36)amide on insulin release from rat pancreatic islets. Eur J Clin Invest 22: 154–157
11. Jia X, Brown JC, Ma P, Pederson RA, McIntosh CHS (1995) Effects of glucose-dependent insulinotropic polypeptide and glucagon-like peptide-1-(7–36) on insulin secretion. Am J Physiol 268: E645–E651
12. Pederson RA, Satkunarajah M, McIntosh CHS et al. (1998) Enhanced glucose-dependent insulinotropic polypeptide secretion and insulinotropic action in glucagon-like peptide 1 receptor –/– mice. Diabetes 47: 1046–1052
13. Miyawaki K, Yamada Y, Yano H et al. (1999) Glucose intolerance caused by a defect in the entero-insular axis: a study in gastric inhibitory polypeptide receptor knockout mice. Proc Nat Acad Sci USA 96: 14843–14847
14. Jones IR, Owens DR, Moody AJ, Luzio SD, Morris T, Hayes TM (1987) The effects of glucose-dependent insulinotropic polypeptide infused at physiological concentrations in normal subjects and Type II (non-insulin-dependent) diabetic patients on glucose tolerance and B-cell secretion. Diabetologia 30: 707–712
15. Kieffer TJ, McIntosh CHS, Pederson RA (1995) Degradation of glucose-dependent insulinotropic polypeptide and truncated glucagon-like peptide 1 *in vitro* and *in vivo* by dipeptidyl peptidase IV. Endocrinology 136: 3585–3596
16. Fehmann HC, Göke R, Göke B (1995) Cell and molecular biology of the incretin hormones glucagon-like peptide-1 and glucose-dependent insulin releasing polypeptide. Endocr Rev 16: 390–410
17. Barrett AJ, Rawlings ND (1992) Oligopeptidases, and the emergence of the prolyl oligopeptidase family. Biol Chem 373: 353–360
18. Wrenger S, Faust J, Mrestani-Klaus C et al. (2000) Down regulation of T-cell activation following inhibition of dipeptidyl peptidase IV/CD26 by the N-terminal part of the thromboxane A2 receptor. J Biol Chem 275: 22180–22186
19. Walter R, Simmons WH, Yoshimoto T (1980) Proline-specific endo-and exopepidases. Mol Cell Biochem 30: 111–127
20. Mentlein R (1999) Dipeptidyl-peptidase IV (CD26)-role in the inactivation of regulatory peptides. Regul Pept 85: 9–24
21. Lojda Z (1979) Studies on dipeptidyl(amino)peptidase IV (glycyl-proline naphthylamidase) II Blood vessels. Histochemistry 59: 153–166
22. Mentlein R, Gallwitz B, Schmidt WE (1993) Dipeptidyl-peptidase IV hydrolyses gastric inhibitory polypeptide, glucagon-like peptide-1(7–36)amide, peptide histidine methionine and is responsible for their degradation in human serum. Eur J Biochem 214: 829–835
23. Maletti M, Carlquist M, Portha B, Kergoat M, Mutt V, Rosselin G (1986) Structural requirements for gastric inhibitory polypeptide (GIP) receptor binding and stimulation of insulin release. Peptides 7: 75–78
24. Deacon CF, Danielsen P, Klarskov L, Olesen M, Holst JJ (2001) Dipeptidyl peptidase IV inhibition reduces the degradation and clearance of GIP and potentiates its insulinotropic and antihyperglycaemic effects in anesthetized pigs. Diabetes 50: 1588–1597
25. O'Harte FPM, Mooney MH, Kelly CM, Flatt PR (2000) Improved glycaemic control in obese diabetic ob/ob mice using N-terminally modified gastric inhibitory polypeptide. J Endocrinol 165: 639–648
26. O'Harte FPM, Mooney MH, Kelly CM, McKillop AM, Flatt PR (2001) Degradation and glycemic effects of His^7-glucitol glucagon-like peptide-1(7–36)amide in obese diabetic ob/ob mice. Regul Pept 96: 95–104
27. O'Harte FPM, Mooney MH, Flatt PR (1999) N-terminally modified gastric inhibitory polypeptide exhibits aminopeptidase resistance and enhanced antihyperglycaemic activity. Diabetes 48: 758–765
28. Fields GB, Noble RL (1990) Solid phase peptide synthesis utilizing 9-fluorenylmethoxycarbonyl amino acids. Int J Pept Protein Res 35: 161–214
29. Gremlich S, Porret A, Hani EH et al. (1995) Cloning, functional expression, and chromosomal localization of the human pancreatic islet glucose-dependent insulinotropic polypeptide receptor. Diabetes 44: 1202–1208
30. McClenaghan NH, Barnett CR, Ah-Sing E et al. (1996) Characterization of a novel glucose-responsive insulin-secreting cell line, BRIN-BD11, produced by electrofusion. Diabetes 45: 1132–1140
31. Bozou JC, Amar S, Vincent JP, Kitabgi P (1986) Neurotensin-mediated inhibition of cyclic AMP formation in neuroblastoma N1E115 cells: involvement of the inhibitory GTP-binding component of adenylate cyclase. Mol Pharmacol 29: 489–496
32. Flatt PR, Bailey CJ (1981) Abnormal plasma glucose and insulin responses in heterozygous lean (ob/+) mice. Diabetologia 20: 573–577
33. Bailey CJ, Flatt PR (1995) Development of antidiabetic drugs. In: Ioannides C, Flatt PR (eds) Drugs, diet and disease: mechanistic approaches to diabetes. Ellis Horwood, London, pp 279–326
34. Stevens JF (1971) Determination of glucose by automatic analyser. Clin Chem Acta 32: 199–201
35. Burington RS (1973) Handbook of mathematical tables and formulas. McGraw-Hill, New York

36. Dupré J, Ross SA, Watson D, Brown JC (1973) Stimulation of insulin secretion by gastric inhibitory polypeptide in man. J Clin Endocrinol Metab 37: 826–828
37. Elahi D, Andersen DK, Brown JC (1979) Pancreatic α and β-cell responses to GIP infusion in normal man. Am J Physiol 237: E185–E191
38. Holst JJ (1999) Glucagon-like peptide-1; a gastrointestinal hormone with pharmaceutical potential. Curr Med Chem 6: 1005–1017
39. Pederson RA, White HA, Schlenzig D, Pauly RP, McIntosh CH, Demuth H-U (1998) Improved glucose tolerance in Zucker fatty rats by oral administration of the dipeptidyl peptidase IV inhibitor isoleucine thiazolidide. Diabetes 47: 1253–1258
40. Pauly RP, Demuth H-U, Rosche F et al. (1999) Improved glucose tolerance in rats treated with the dipeptidyl peptidase IV (CD26) inhibitor ile-thiazolidide. Metabolism 48: 385–389
41. Nauck MA, Heimesaat MM, Ørskov C, Holst JJ, Ebert R, Creutzfeldt W (1993) Preserved incretin activity of glucagon-like peptide 1 [7–36 amide] but not of synthetic human gastric inhibitory polypeptide in patients with type-2 diabetes mellitus. J Clin Invest 91: 301–307
42. Elahi D, McAloon-Dyke M, Fukagawa NK et al. (1994) The insulinotropic actions of glucose dependent insulinotropic polypeptide (GIP) and glucagon-like peptide-1 (7–37) in normal and diabetic subjects. Regul Pept 51: 63–74
43. Ding WG, Gromada J (1997) Protein kinase A-dependent stimulation of exocytosis in mouse pancreatic beta-cells by glucose-dependent insulinotropic polypeptide. Diabetes 46: 615–621
44. Almind K, Ambye L, Urhammer SA et al. (1998) Discovery of amino acid variants in the human glucose-dependent insulinotropic polypeptide (GIP) receptor: the impact on the pancreatic beta cell responses and functional expression studies in Chinese hamster fibroblast cells. Diabetologia 41: 1194–1198
45. Pederson RA, Brown JC (1976) The insulinotropic action of gastric inhibitory polypeptide in the perfused isolated rat pancreas. Endocrinology 99: 780–789
46. Rasmussen H, Zawalich KC, Ganesan S, Calle R, Zawalich WS (1990) Physiology and pathophysiology of insulin secretion. Diabetes Care 13: 655–666
47. Gama R, Norris F, Morgan L, Hampton S, Wright J, Marks V (1997) Elevated post-prandial gastric inhibitory polypeptide concentrations in hypertriglyceridaemic subjects. Clin Sci (Colch) 93: 343–347
48. McClenaghan NH, Ball AJ, Flatt PR (2001) Specific desensitization of sulfonylurea- but not imidazoline-induced insulin release after prolonged tolbutamide exposure. Biochem Pharmacol 61: 527–536
49. Flatt PR, Bailey CJ, Kwasowski P, Page T, Marks V (1984) Plasma immunoreactive gastric inhibitory polypeptide in obese hyperglycaemic (*ob/ob*) mice. J Endocrinol 101: 249–256
50. Flatt PR, Kwasowski P, Howland RJ, Bailey CJ (1991) Gastric inhibitory polypeptide and insulin responses to orally administered amino acids in genetically obese hyperglycemic (ob/ob) mice. J Nutr 121: 1123–1128
51. Deacon CF, Nauck MA, Meier J, Hucking K, Holst JJ (2000) Degradation of endogenous and exogenous gastric inhibitory polypeptide in healthy and in type 2 diabetic subjects as revealed using a new assay for the intact peptide. J Clin Endocrinol Metab 85: 3575–3581
52. Gelling RW, Coy DH, Pederson RA et al. (1997) GIP(6–30amide) contains the high affinity binding region of GIP and is a potent inhibitor of GIP1–42 action in vitro. Regul Pept 69: 151–154
53. Chap Z, Ishida T, Chou J, Lewis R, Hartley C, Entman M, Field JB (1985) Effects of atropine and gastric inhibitory polypeptide on hepatic glucose uptake and insulin extraction in conscious dogs. J Clin Invest 76: 1174–1181
54. Hartmann H, Ebert R, Creutzfeldt W (1986) Insulin-dependent inhibition of hepatic glycogenolysis by gastric inhibitory polypeptide (GIP) in perfused rat liver. Diabetologia 29: 112–114
55. O'Harte FPM, Gray AM, Flatt PR (1998) Gastric inhibitory polypeptide and effects of glycation on glucose transport and metabolism in isolated mouse abdominal muscle. J Endocrinol 156: 237–243

EXHIBIT 7

Degradation, Insulin Secretion, and Antihyperglycemic Actions of Two Palmitate-Derivitized *N*-Terminal Pyroglutamyl Analogues of Glucose-Dependent Insulinotropic Polypeptide

Nigel Irwin,[†] Brian D. Green,[†] Victor A. Gault,*[,†] Brett Greer,[‡] Patrick Harriott,[§] Clifford J. Bailey,[∥] Peter R. Flatt,[†] and Finbarr P. M. O'Harte[†]

School of Biomedical Sciences, University of Ulster, Coleraine BT52 1SA, UK, School of Biology and Biochemistry, Queen's University of Belfast, Belfast BT9 7BL, UK, Department of Pharmaceutical and Medicinal Chemistry, Royal College of Surgeons in Ireland, Dublin, Ireland, and School of Life and Health Sciences, Aston University, Birmingham, B4 7ET, UK

Received September 10, 2004

Exploitation of glucose-dependent insulinotropic polypeptide (GIP) is hindered by its short biological half-life and rapid renal clearance. To circumvent these problems, two novel acylated *N*-terminally modified GIP analogues, *N*-pGluGIP(LysPAL^{16}) and *N*-pGluGIP(LysPAL^{37}), were evaluated. In contrast to native GIP, both analogues were completely resistant to dipeptidyl peptidase IV degradation. In GIP-receptor transfected fibroblasts, *N*-pGluGIP(LysPAL^{16}) and *N*-pGluGIP(LysPAL^{37}) exhibited enhanced stimulation of cAMP production. Insulinotropic responses in clonal beta-cells were similar to native GIP. When administered together with glucose to ob/ob mice, the glycemic excursions were significantly less for both analogues and insulin responses were greater than native GIP. Extended insulinotropic and antihyperglycemic actions were also evident. These data indicate that palmitate-derivitized analogues of *N*-terminal pyroglutamyl GIP represent a novel class of stable, long-acting, and effective GIP analogues for potential type 2 diabetes therapy.

Introduction

Glucose-dependent insulinotropic polypeptide (GIP) is an incretin hormone secreted from the intestinal K-cells in response to oral nutrient absorption.[1] A potent insulin-releasing hormone of the enteroinsular axis,[2] GIP exerts various beneficial effects on pancreatic beta-cell function[3−5] and exhibits antihyperglycemic extrapancreatic effects.[6] These actions and the glucose-dependency of insulin secretion which minimizes the risk of hypoglycemia make GIP very attractive as a potential antidiabetic drug.[7] A spate of recent publications has led to a resurgence of interest in GIP-based antidiabetic therapies. Despite earlier claims,[8,9] it now seems that a reduced GIP-induced insulin secretion in patients with type 2 diabetes is more likely due to a general defect of beta-cell function rather than a specific defect of GIP action.[10,11] Furthermore, GIP does not slow gastric emptying in humans, underlining a major difference between GIP and its sister incretin, glucagon-like peptide-1 (GLP-1).[12]

Dipeptidyl peptidase IV (DPP IV) rapidly hydrolyses GIP at the *N*-terminus to GIP(3−42),[13] rendering the peptide noninsulinotropic[14] and antagonistic of its own receptor.[15] This ubiquitous serine protease has been a major hindrance to the clinical development of GIP; however, various strategies to overcome its degradation by DPP IV are proving successful. For example, several analogues of GIP have been tested that are profoundly resistant to DPP IV and able to overcome any reported unresponsiveness of the beta-cell in type 2 diabetes.[16−21] A small number of these analogues, such as *N*-pGluGIP, appear to be highly effective agonists of the GIP receptor.[17,18] Furthermore, administration of DPP IV inhibitors to dogs and anesthetized pigs increases the proportion of intact GIP significantly and the result is improved insulin release and glucose-lowering action.[22,23]

While there are now a number of publications identifying how GIP may be *N*-terminally modified to prevent degradation by DPP IV, the problem of rapid elimination from the bloodstream by renal filtration has not yet been tackled.[24] Thus, although DPP IV resistant analogues of GIP may improve the short half-life in vivo (7 min),[25] these analogues may not be optimal as they are still subject to clearance by the kidneys. The importance of the kidneys in the final elimination of GIP has been underlined by a study comparing half-lives of GIP and its metabolites in healthy control subjects and patients with chronic renal insufficiency.[24] In healthy control subjects, intact GIP had a half-life of less than 5 min and GIP(3−42) less than 23 min, while patients with renal disease displayed half-lives of 7 and 38 min, respectively.[24]

Various strategies are available to extend the half-life of peptide hormones in the circulation. One such strategy involves the derivitization of peptides with fatty acids, otherwise known as acylation. Acylation facilitates binding to serum proteins, thus reducing renal filtration and prolonging biological activity. This has been successfully applied to extend the action of insulin, through acylation of the ϵ-amino group of Lys^{B29}.[26] Acylated compounds of GIP's sister hormone, GLP-1, have been produced.[27,28] GLP-1 compounds such as

* Corresponding author. Tel: ++44 (0) 28 70 324313. Fax: ++44 (0) 28 70 324965. E-mail: va.gault@ulster.ac.uk.
[†] University of Ulster.
[‡] Queen's University of Belfast.
[§] Royal College of Surgeons in Ireland.
[∥] Aston University.

10.1021/jm049262s CCC: $30.25
Published on Web 02/01/2005

Table 1. Structural Characterization of GIP Peptides by MALDI-TOF Mass Spectrometry[a]

GIP peptide	M_r (Da) theoretical	experimental	difference (Da)
GIP	4982.4	4983.7	1.3
N-pGluGIP(LysPAL^{16})	5332.1	5333.1	1.0
N-pGluGIP(LysPAL^{37})	5332.1	5334.5	2.4

[a] Peptide samples were mixed with α-cyano-4-hydroxycinnamic acid and applied to the sample plate of a Voyager-DE BioSpectrometry workstation, and the mass-to-charge (*m/z*) ratio vs relative peak intensity was recorded.

NN2211, CJC-1131, LY315902, LY307161, and AC2993 display greatly prolonged pharmacokinetic profiles (8−18 h) in humans.[27] However, some acylated GLP-1 analogues are problematic in terms of bioactivity and bioavailability,[28] while others, such as NN2211, have met with side effects such as nausea and dizziness.[29,30] Given the fact that GLP-1 is highly inhibitive of gastric emptying in humans[31] and GIP is not,[12] it is possible that long-acting analogues of GIP would be more attractive therapeutically.

The development and testing of novel GIP analogues with enhanced metabolic stability and reduced renal filtration can potentially be useful treatment of type 2 diabetes. We have previously demonstrated that *N*-terminal pyroglutamyl GIP (*N*-pGluGIP) is a DPP IV resistant GIP agonist that exhibits potent insulinotropic and antihyperglycemic actions in an animal model of type 2 diabetes.[17] In this study, we have synthesized two novel acylated analogues of *N*-terminally modified *N*-pGluGIP, namely *N*-pGluGIP(LysPAL^{16}) and *N*-pGluGIP(LysPAL^{37}). Both GIP analogues contain a C-16 palmitate (PAL) group linked to the ε-amino group of lysine (Lys) at positions 16 or 37. Initially, we investigated their resistance to DPP IV degradation, ability to stimulate cAMP production, and in vitro insulinotropic action. We then undertook a series of in vivo metabolic studies to examine the glucose-lowering and insulin-releasing actions of *N*-pGluGIP(LysPAL^{16}) and *N*-pGluGIP(LysPAL^{37}) in the commonly employed (ob/ob) mouse model of type 2 diabetes.

Results

Structural Identification. Table 1 shows the experimental masses obtained using MALDI-TOF mass spectrometry for purified GIP, *N*-pGluGIP(LysPAL^{16}), and *N*-pGluGIP(LysPAL^{37}). The molecular masses resolved using the mass-to-charge (*m/z*) ratio were 4983.7 Da for native GIP (theoretical mass 4982.4 Da), 5333.1 Da for *N*-pGluGIP(LysPAL^{16}) (theoretical mass 5332.1 Da), and 5334.5 Da for *N*-pGluGIP(LysPAL^{37}) (theoretical mass 5332.1 Da). Experimental masses closely correlated to theoretical masses and thus confirmed successful peptide synthesis.

Degradation by DPP IV. Figure 1 shows the progressive degradation by DPP IV of GIP(1−42) to truncated GIP(3−42). Degradation of native GIP was complete by 8 h, with only truncated GIP(3−42) metabolite remaining. The estimated $t_{1/2}$ following exposure to DPP IV was 2.1 h. Contrastingly, acylated GIP analogues *N*-pGluGIP(LysPAL^{16}) and *N*-pGluGIP(LysPAL^{37}) were fully intact, even following prolonged 24 h incubations (Figure 1).

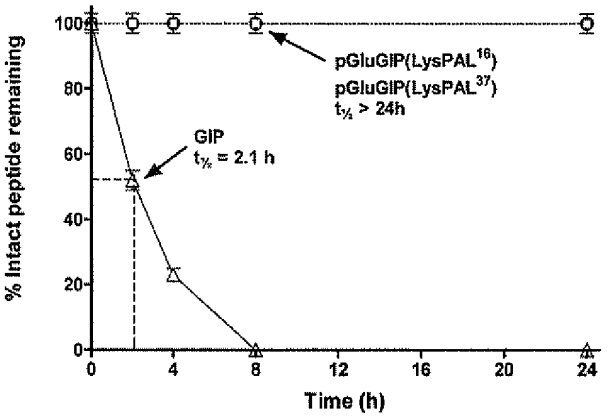

Figure 1. DPP IV degradation profiles for GIP (Δ), *N*-pGluGIP(LysPAL^{16}) (□), and *N*-pGluGIP(LysPAL^{37}) (●). Resistance of each peptide to degradation by DPP IV (5 mU) was measured following 0, 2, 4, 8, and 24 h incubations. Reaction products were subsequently analyzed by HPLC, and degradation was expressed as a percentage of intact peptide relative to the major degradation fragment, GIP(3−42). Values represent means ± SEM for three separate experiments.

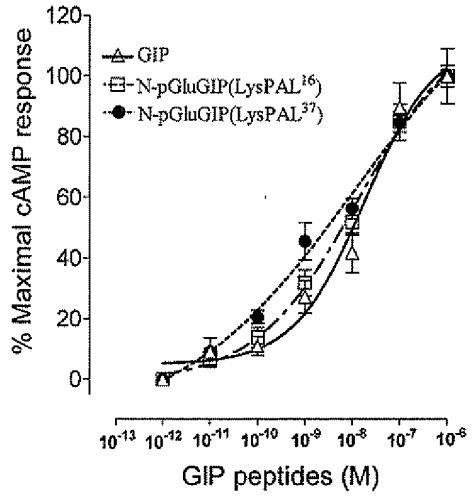

Figure 2. Stimulation of intracellular cAMP production by GIP, *N*-pGluGIP(LysPAL^{16}), and *N*-pGluGIP(LysPAL^{37}). CHL cells stably transfected with the human GIP receptor were exposed to various peptide concentrations for 20 min. Each experiment was performed in triplicate ($n = 3$), and values are expressed (means ± SEM) as a percentage maximum GIP response.

Stimulation of in Vitro cAMP Production. The dose-dependent stimulatory effects of GIP and fatty acid derivatized analogues on intracellular cAMP production following incubation with GIP-receptor transfected CHL fibroblasts are shown in Figure 2. The concentration of GIP, *N*-pGluGIP(LysPAL^{16}), or *N*-pGluGIP(LysPAL^{37}) that produced 50% maximal formation of cAMP (EC_{50}) was approximately 18.2, 3.2, and 2.7 nM, respectively. No significant differences were found between the potency of the three peptides.

Stimulation of in Vitro Insulin Secretion. Figure 3 shows the effect of increasing concentrations of GIP, *N*-pGluGIP(LysPAL^{16}), and *N*-pGluGIP(LysPAL^{37}) on insulin secretion from clonal BRIN-BD11 cells. All peptides stimulated insulin release by up to 2.5-fold in a concentration-dependent manner. There were no apparent differences in potency in vitro.

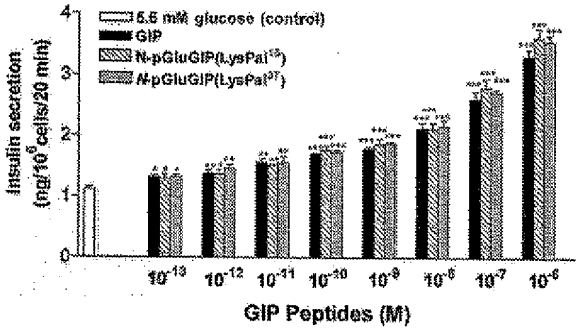

Figure 3. Insulinotopic effects of GIP, *N*-pGluGIP(LysPAL^{16}), and *N*-pGluGIP(LysPAL^{37}) in BRIN-BD11 cells. Cells were exposed to various concentrations of GIP peptides for an acute 20 min period in the presence of 5.6 mM glucose. Values represent means ± SEM for eight separate observations. $^{*}P < 0.05$, $^{**}P < 0.01$, $^{***}P < 0.001$ compared with glucose control.

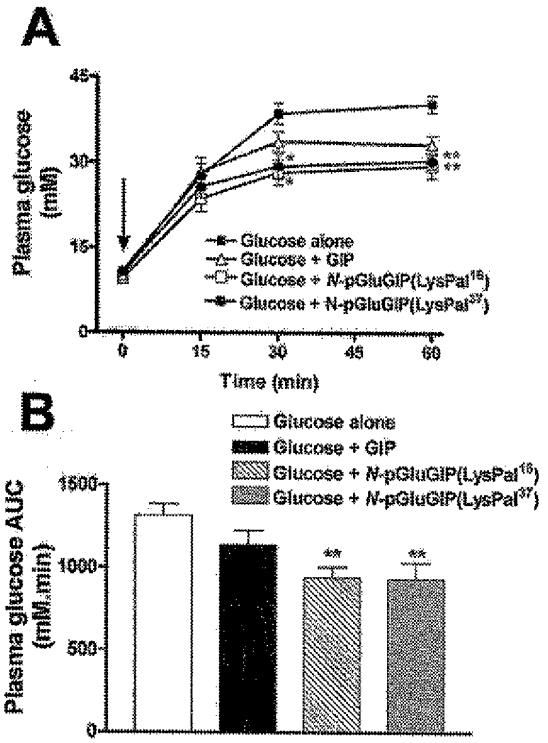

Figure 4. Glucose-lowering effects of GIP, *N*-pGluGIP-(LysPAL^{16}), and *N*-pGluGIP(LysPAL^{37}) in 18-h fasted ob/ob mice. (A) Plasma glucose concentrations were measured prior to and after ip administration of glucose alone (18 mmol/kg of body weight), or in combination with GIP, *N*-pGluGIP(Lys-PAL^{16}), or *N*-pGluGIP(LysPAL^{37}) (25 nmol/kg). The time of injection is indicated by the arrow (0 min). (B) Plasma glucose area under the curve (AUC) values for 0−60 min postinjection. Values represent means ± SEM for eight mice. $^{*}P < 0.05$, $^{**}P < 0.01$ compared to glucose alone.

Antihyperglycemic and Insulin-Releasing Activity in ob/ob Mice. Figure 4A shows the plasma glucose responses to intraperitoneal glucose alone or in combination with GIP, *N*-pGluGIP(LysPAL^{16}), or *N*-pGluGIP-(LysPAL^{37}) (25 nmol/kg of body weight). Injection of glucose alone resulted in a rapid and protracted rise in glucose concentration. The glucose excursion following native GIP was not significantly different at the 15, 30, and 60 min time points. In contrast, glucose concentrations following *N*-pGluGIP(LysPAL^{16}) or *N*-pGluGIP-

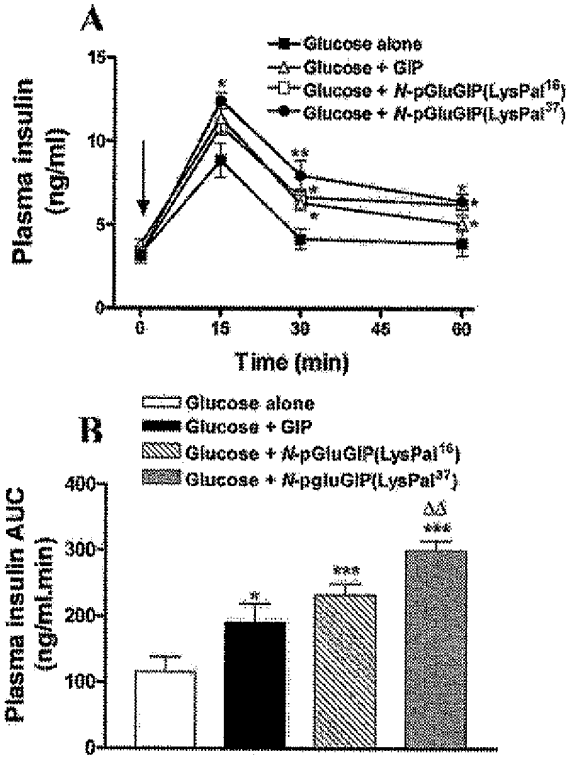

Figure 5. Insulin-releasing effects of GIP, *N*-pGluGIP-(LysPAL^{16}), or *N*-pGluGIP(LysPAL^{37}) in 18-h fasted ob/ob mice. (A) Plasma insulin concentrations were measured prior to and after ip administration glucose alone (18 mmol/kg of body weight) or in combination with GIP, *N*-pGluGIP(LysPAL^{16}), or *N*-pGluGIP(LysPAL^{37}) (25 nmol/kg). The time of injection is indicated by the arrow (0 min). (B) Plasma insulin area under the curve (AUC) values for 0−60 min postinjection. Values represent means ± SEM for eight mice. $^{*}P < 0.05$, $^{**}P < 0.01$, $^{***}P < 0.001$ compared to glucose alone. $^{\Delta\Delta}P < 0.01$ compared to native GIP.

(LysPAL^{37}) were significantly lower after 30 min ($P < 0.05$) and 60 min ($P < 0.01$). Area under the curve (AUC) analysis (0−60 min, Figure 4B) confirmed the significant glucose-lowering actions of *N*-pGluGIP(LysPAL^{16}) and *N*-pGluGIP(LysPAL^{37}) ($P < 0.01$). As shown in Figure 5A,B, these effects were associated with corresponding changes of insulin release. GIP caused significantly greater insulin release than glucose alone ($P < 0.05$). However, the insulin-releasing actions of *N*-pGluGIP(LysPAL^{16}) and *N*-pGluGIP(LysPAL^{37}) were substantially greater ($P < 0.001$) and protracted at 60 min. *N*-pGluGIP(LysPAL^{37}) was the most potent analogue based on overall changes in glucose and insulin concentrations (AUC, Figures 4B and 5B).

Long-Lasting Antihyperglycemic Effects in ob/ob Mice. *N*-pGluGIP(LysPAL^{37}) was selected for further evaluation of long-lasting metabolic effects. As shown in Figure 6, the glucose-lowering action of *N*-pGluGIP-(LysPAL^{37}) was clearly evident when given 4 h before administration of an intraperitoneal glucose load. AUC glucose values were decreased by 21% compared with saline-treated controls ($P < 0.05$; Figure 6B). In contrast, native GIP lacked significant effects on AUC glucose values even when administered simultaneously with glucose (Figure 4B).

Dose-Dependent Metabolic Effects in ob/ob Mice. Dose-dependent studies were conducted using *N*-pGlu-

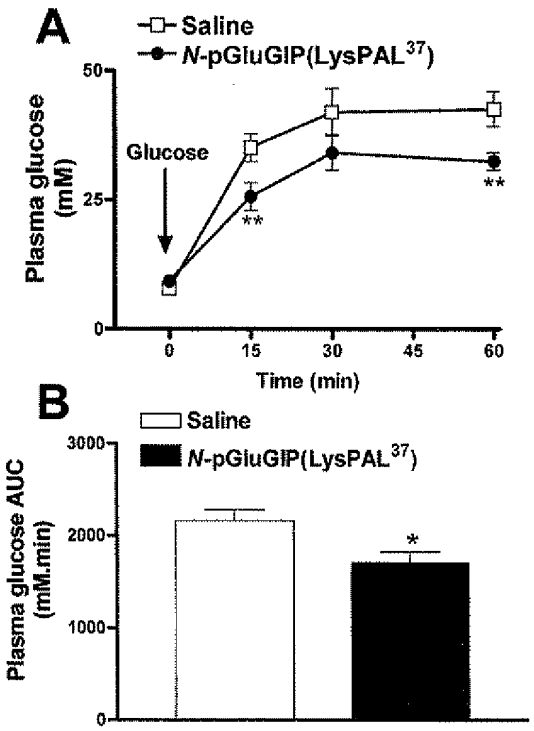

Figure 6. Persistence of glucose-lowering effects of *N*-pGluGIP(LysPAL^{37}) in 18-h fasted ob/ob mice at 4 h after injection. (A) Plasma glucose concentrations were measured prior to and after ip administration of glucose (18 mmol/kg of body weight) in mice injected 4 h previously with *N*-pGluGIP-(LysPAL^{37}) (25 nmol/kg of body weight, ip) or saline. The time of the glucose injection is indicated by the arrow. (B) Plasma glucose area under the curve (AUC) values for 0−60 min postinjection. Values represent means ± SEM for six mice. $^{*}P < 0.05$, $^{**}P < 0.01$ compared mice injected 4 h earlier with saline.

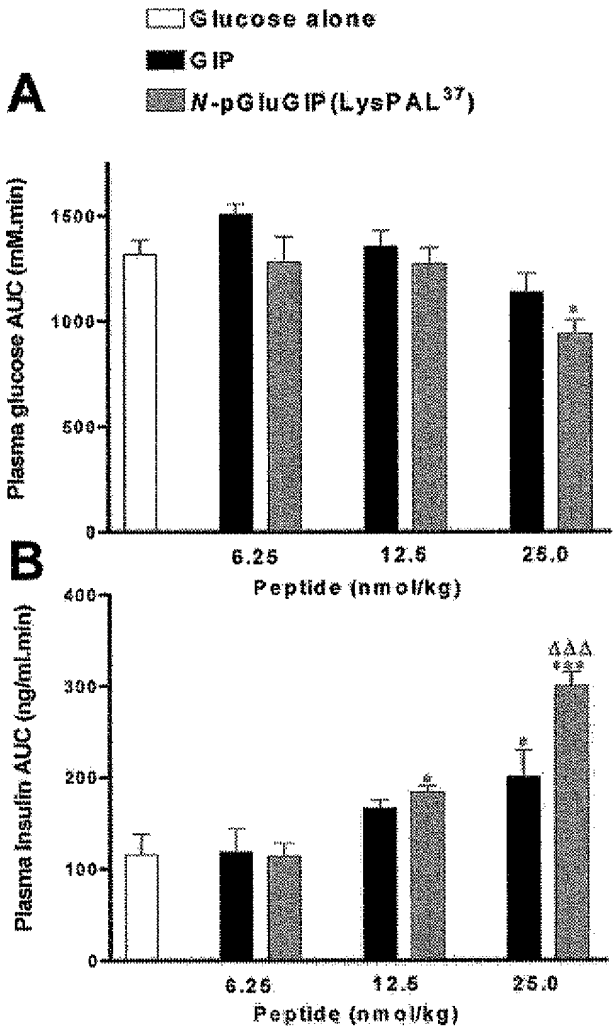

Figure 7. Dose-dependent effects of GIP and *N*-pGluGIP-(LysPal^{37}) on glucose and insulin levels in 18-h fasted ob/ob mice. The incremental area under the curve (AUC; 0−60 min) for (A) glucose and (B) insulin following ip administration of glucose alone (18 mmol/kg of body weight) or with various doses (6.25, 12.5, and 25 nmol/kg) of GIP or *N*-pGluGIP-(LysPal^{37}). Values represent means ± SEM for eight mice. $^{*}P < 0.05$, $^{***}P < 0.001$ compared to glucose alone. $^{\Delta\Delta\Delta}P < 0.01$ compared to native GIP at same dose.

GIP(LysPAL^{37}). Figure 7 shows the AUC values (0−60 min) for plasma glucose and insulin following the administration of glucose alone or in combination with either GIP or *N*-pGluGIP(LysPAL^{37}) at 6.25, 12.5, and 25 nmol/kg of body weight. The maximum glucose-lowering effects of GIP and *N*-pGluGIP(LysPAL^{37}) were observed at the 25 nmol/kg dose. However, only *N*-pGluGIP(LysPAL^{37}) caused significant glucose-lowering (1.4-fold; $P < 0.05$; Figure 7A). Figure 7B shows the equivalent AUC values for plasma insulin. While a 6.25 or 12.5 nmol/kg dose of GIP had no effect on insulin levels, a 25 nmol/kg dose significantly raised overall plasma insulin levels (1.7-fold; $P < 0.05$). In contrast, either a 12.5 or 25 nmol/kg dose of *N*-pGluGIP(Lys-PAL^{37}) caused significant increases in circulating insulin of 1.6-fold ($P < 0.05$) and 2.6-fold ($P < 0.001$), respectively.

Discussion

In recent years, many different GIP analogues have been synthesized and tested for potential antidiabetic properties.[16−21] Until now, the aim has been to *N*-terminally modify GIP to confer it with resistance to DPP IV. So far, this has been very successful with some extremely potent DPP IV-resistant analogues of GIP being developed. Interestingly, some of these analogues (e.g. *N*-pGluGIP) have enhanced insulinotropic and glucose-lowering activities compared with native GIP.[17] However, recent reports indicate the importance of the kidney for the final elimination of GIP from the circulation.[24] As a result, it is predicted that further structural modification of GIP to delay removal of the peptide by renal filtration may prolong bioactivity.

Although the *N*-terminally modified analogue, *N*-pGluGIP, displays profound resistance to DPP IV and strong biological activity,[17] it is still subject to renal clearance. Using an approach already established for insulin and other peptides,[26,27] we have acylated this GIP analogue with palmitate to facilitate binding to plasma proteins, disrupt clearance by the kidney, and ultimately prolong biological activity. The ε-amino group of lysine residues is particularly well-suited for peptide acylation. GIP has four such sites at Lys^{16}, Lys^{30}, Lys^{33}, and Lys^{37}. A computer-generated three-dimensional molecular model has approximated the structure of GIP to be a gently rotating helical chain.[32] Accordingly, we selected the lysine nearest the *N*-terminus and the

lysine nearest the C-terminus as palmitate acylation sites. Thus, in addition to having an *N*-terminal pyroglutamyl group at Tyr^1, the analogues prepared in this study possessed a 16-carbon palmitate group conjugated to the ϵ-amino group of either Lys^{16} or Lys^{37}.

After confirmation of successful synthesis by MALDI-TOF mass spectrometry, the susceptibility of GIP peptides to DPP IV degradation was examined. In contrast to native GIP, which underwent rapid metabolism by DPP IV to the truncated peptide GIP(3−42), *N*-pGluGIP(LysPAL^{16}) and *N*-pGluGIP(LysPAL^{37}) were completely resistant to enzymatic degradation. Thus, as expected, fatty acid derivatization did not affect the established DPP IV resistance of *N*-pGluGIP.[17]

Consistent with previous studies,[18,19] native GIP concentration-dependently stimulated cAMP production with an EC_{50} value of 18.2 nM. Corresponding values for *N*-pGluGIP(LysPAL^{16}) and *N*-pGluGIP(LysPAL^{37}) were approximately 6-fold better than native GIP, but this was not statistically significant. Similarly, native GIP and both fatty acid derivatized pGluGIP analogues induced concentration-dependent stepwise increases of insulin secretion from BRIN-BD11 cells. No significant differences were noted between the potency of the three peptides, indicating that the acylated forms of GIP were at least equally as potent as native GIP in activating the GIP-receptor. This is significant, especially when considering that these analogues will presumably bind appreciably to albumin in the incubation buffers. Thus, the present inability to show significantly greater insulinotropic potency of acylated forms of pGluGIP over native GIP, as noted in previous studies for pGluGIP,[17] may largely reflect lower effective peptide concentrations due to in vitro albumin binding.

In vivo bioactivity of acylated forms of *N*-pGluGIP and native GIP were compared using obese diabetic (ob/ob) mice, a commonly employed animal model of type 2 diabetes.[33] These mice display several characteristics associated with type 2 diabetes; including obesity, insulin resistance, hyperglycemia, hyperinsulinemia, and defective beta-cell function.[33] GIP has been shown previously to have modest antihyperglycemic and insulinotropic activity, when administered to ob/ob mice.[18,19] Although native GIP significantly stimulated insulin release in the present study, this was not accompanied by significant glucose-lowering, reflecting the severe insulin resistance of the ob/ob syndrome at the age tested.[34] However, both *N*-pGluGIP(LysPAL^{16}) and *N*-pGluGIP(LysPAL^{37}) were highly effective in lowering glucose and raising insulin levels, indicating prolonged action and an ability to overcome the insulin resistance and any apparent desensitization of GIP-receptor action.

Although the fatty acid derivatized analogues appeared equipotent in terms of glucose-lowering activities, *N*-pGluGIP(LysPAL^{37}) was substantially more effective and longer acting in stimulating insulin release. The reason behind the increased effectiveness of this C-terminally derivatized peptide to raise plasma insulin is unclear but may include differences in beta-cell stimulation due to differences in effective concentrations as a result of protein binding. Further, lack of reciprocal glucose-lowering effect may suggest that *N*-pGluGIP(LysPAL^{16}) and *N*-pGluGIP(LysPAL^{37}) have different potencies in stimulating glucose disposal in peripheral tissues. The extent to which this reflects changes in the various non-beta-cell and extrapancreatic actions of GIP merits further investigation.[35] However, it is clear from present dose−response studies that *N*-pGluGIP(LysPAL^{37}) was more potent than native GIP, even in acute studies, and more effective over 60 min at doses as low as 12.5 nmol/kg.

Comparison of the present short-term in vivo effects of the two acylated *N*-pGluGIP analogues with previous studies of *N*-pGluGIP [17] suggest quite similar bioactivities of these first- and second-generation analogues. One possible explanation is slower release of fatty acid derivatized GIP into the circulation from the injection site, but further studies are needed to clarify this point. However, such an effect would be more than offset in the longer term by the prolonged biological activity profile of the acylated peptide. Indeed, the persistence of the glucose-lowering actions of *N*-pGluGIP(LysPAL^{37}) even at 4 h after a single injection greatly encourages further studies evaluating the longer term benefits of this *N*-terminally protected palmitate-derivatized GIP analogue in type 2 diabetes.

In conclusion, acylation of DPP IV resistant *N*-terminal analogues of GIP, such as *N*-pGluGIP, with palmitate generates bioactive molecules with the prospect of improved long-term potency and duration of action. *N*-pGluGIP(LysPAL^{37}) appears to be a particularly promising antihyperglycemic, insulin-releasing analogue of GIP for further evaluation. It is hoped that long-acting GIP candidate molecules such as *N*-pGluGIP(LysPAL^{37}) will lead in the future to a once-daily treatment for type 2 diabetes.

Experimental Section

Reagents. High-performance liquid chromatography (HPLC) grade acetonitrile was obtained from Rathburn (Walkersburn, Scotland). Sequencing grade trifluoroacetic acid (TFA), dipeptidylpeptidase IV (DPP IV), isobutylmethylxanthine (IBMX), adenosine 3,5-cyclic monophosphate (cAMP), adenosine 5′-triphosphate (ATP), and α-cyano-4-hydroxycinnamic acid were all purchased from Sigma (Poole, Dorset, UK). Fmoc-protected amino acids were obtained from Calbiochem Novabiochem (Beeston, Nottingham, UK). RPMI 1640 and DMEM tissue culture medium, fetal bovine serum, penicillin, and streptomycin were all purchased from Gibco (Paisley, Strathclyde, Scotland). The chromatography columns used for cAMP assay, Dowex AG 50WX and neutral alumina AG7, were obtained from Bio-Rad (Life Science Research, Alpha Analytical, Larne, N. Ireland). Tritiated adenine (TRK311) was obtained from Amersham Pharmacia Biotech, Bucks, UK. All water used in these experiments was purified using a Milli-Q water purification system (Millipore, Milford, MA). All other chemicals used were of the highest available purity.

Synthesis, Purification, and Characterization of GIP and Related Analogues. GIP, *N*-pGluGIP(LysPAL^{16}), and *N*-pGluGIP(LysPAL^{37}) were sequentially synthesized on an Applied Biosystems automated peptide synthesizer (Model 432A, Applied Biosystems, Foster City, CA) using standard solid-phase Fmoc peptide chemistry.[36] Peptides were synthesized sequentially, starting with a preloaded Fmoc-Gln-Wang resin. The synthetic peptides were judged pure by reversed-phase HPLC on a Waters Millenium (Milford, MA) 2010 chromatography system (Software version 2.1.5) when purity was in excess of 99%. Peptides were characterized by matrix-assisted laser desorption ionization-time-of-flight (MALDI-TOF) mass spectrometry, as described previously.[37]

Degradation of GIP and Related Analogues by DPP IV. GIP, *N*-pGluGIP(LysPAL^{16}), and *N*-pGluGIP(LysPAL^{37}) were incubated in vitro at 37 °C with purified DPP IV (5 mU)

for 0, 2, 4, 8 and 24 h in 50 mM triethanolamine-HCl buffer (pH 7.8; final peptide concentration 2 mM). The enzymatic reactions were terminated by the addition of 15 μL 10% (v/v) TFA/water. The reaction products were then applied to a Vydac C-4 column (4.6 × 250 mm; The Separations Group, Hesparia, CA) and the major degradation fragment, GIP(3–42), was separated from intact GIP. The column was equilibrated with 0.12% (v/v) TFA/water at a flow rate of 1.0 mL/min using 0.1% (v/v) TFA in 70% acetonitrile/water, the concentration of acetonitrile in the eluting solvent was raised from 0% to 40% over 10 min, and from 40% to 75% over 35 min. The absorbance was monitored at 206 nm using a SpectraSystem UV 2000 Detector (Thermoquest Ltd., Manchester, UK), and the peaks were collected manually prior to MALDI-TOF mass spectrometry. HPLC peak area data were used to calculate the percent intact peptide remaining during the incubation.

Cells and Culture. Chinese hamster lung (CHL) fibroblasts transfected with the GIP-receptor[38] were cultured using DMEM tissue culture medium containing 10% fetal bovine serum and 1% (v/v) antibiotics (100 U/mL penicillin and 0.1 mg/mL streptomycin). BRIN-BD11 cells, characterized previously,[39] were cultured using RPMI-1640 tissue culture medium containing 10% fetal bovine serum and 1% (v/v) antibiotics (100 U/mL penicillin, 0.1 mg/mL streptomycin). All cells were maintained in sterile tissue culture flasks (Corning Glass Works, UK) at 37 °C in an atmosphere of 5% CO_2 and 95% air using a LEEC incubator (Laboratory Technical Engineering, Nottingham, UK).

Effects of GIP and Related Analogues on Cyclic AMP Production. CHL fibroblasts were seeded into 12-multiwell plates (Nünc, Roskilde, Denmark) at a density of 1.0×10^5 cells per well. The cells were allowed to grow in culture for 48 h before being preincubated (16 h at 37 °C) in media supplemented with tritiated adenine (2 μCi). The cells were washed twice with cold HBS buffer. The cells were then exposed for 20 min at 37 °C to varying concentrations (10^{-13}–10^{-6} M) of GIP, *N*-pGluGIP(LysPAL^{16}), or *N*-pGluGIP-(LysPAL^{37}) in HBS buffer (estimated albumin concentration 76.5 μM), in the presence of 1 mM IBMX. The medium was subsequently removed and 1 mL of lysis solution added, containing 0.3 mM unlabeled cAMP and 5 mM unlabeled ATP. The intracellular tritiated cAMP was then separated on Dowex and alumina exchange resins as described previously.[40]

Secretion of Insulin and Related Analogues in Vitro. BRIN-BD11 cells were seeded into 24-multiwell plates at a density of 1.0×10^5 cells per well and allowed to attach overnight at 37 °C. Acute tests for insulin release were preceded by 40 min preincubation at 37 °C in 1.0 mL of Krebs Ringer bicarbonate buffer [115 mM NaCl, 4.7 mM KCl, 1.28 mM $CaCl_2$, 1.2 mM KH_2PO_4, 1.2 mM $MgSO_4$, 10 mM $NaHCO_3$, 0.5% (w/v) BSA, pH 7.4] supplemented with 1.1 mM glucose. Test incubations were performed in the presence of 5.6 mM glucose with a range of concentrations (10^{-13}–10^{-6} M) of GIP, *N*-pGluGIP(LysPAL^{16}), and *N*-pGluGIP(LysPAL^{37}). After 20-min incubation, the buffer was removed from each well, and aliquots (200 μL) were used for measurement of insulin.

Effects of GIP and Related Analogues on Glucose-Lowering and Insulin Release in (ob/ob) Mice. The effects of GIP, *N*-pGluGIP(LysPAL^{16}), or *N*-pGluGIP(LysPAL^{37}) on plasma glucose and insulin concentrations were examined in 14–18-week-old obese diabetic (ob/ob) mice. The genetic background and characteristics of the colony used have been outlined in detail elsewhere.[33] The animals were housed individually in an air-conditioned room at 22 ± 2 °C with a 12 h light/12 h darkness cycle. Drinking water and a standard rodent maintenance diet (Trouw Nutrition, Cheshire, UK) were freely available until 18 h before acute tests. In the first series of experiments, mice received an intraperitoneal injection of glucose alone (18 mmol/kg of body weight) or in combination with GIP, *N*-pGluGIP(LysPAL^{16}), or *N*-pGluGIP-(LysPAL^{37}) (each at 25 nmol/kg). In a second series of experiments, glucose (18 mmol/kg) was administered 4 h after *N*-pGluGIP(LysPAL^{37}) (25 nmol/kg) in order to assess longer term duration of action. In a final series of dose-dependent experiments, GIP and the most potent analogue, *N*-pGluGIP-(LysPAL^{37}), were administered at 6.25, 12.5, or 25 nmol/kg in combination with glucose (18 mmol/kg). All test solutions were administered in a final volume of 8 mL/kg of body weight. Blood samples were collected from the cut tip on the tail vein of conscious mice into chilled fluoride/heparin glucose microcentrifuge tubes (Sarstedt, Nümbrecht, Germany) immediately prior to injection and at 15, 30, and 60 min postinjection. Plasma was aliquoted and stored at −20 °C prior to glucose and insulin determinations. No adverse effects were observed following administration of any of the peptides. All animal experiments were carried out in accordance with the UK Animals (Scientific Procedures) Act 1986.

Analyses. Plasma glucose was assayed by an automated glucose oxidase procedure using a Beckman Glucose Analyzer II.[41] Plasma insulin was assayed by dextran-charcoal RIA as described previously.[42] Incremental areas under plasma glucose and insulin curves (AUC) were calculated using a computer-generated program employing the trapezoidal rule[43] with baseline subtraction. Results are expressed as means ± SEM and data compared using the unpaired Student's *t*-test. Where appropriate, data were compared using repeated measures ANOVA or one-way ANOVA, followed by the Student–Newman–Keuls post hoc test. Groups of data from both were considered to be significantly different if $P < 0.05$.

Acknowledgment. These studies were supported by University of Ulster Research Strategy Funding and a project grant from Diabetes UK. The authors thank Professor Bernard Thorens (University of Lausanne, Switzerland) for kindly providing the GIP receptor transfected CHL cells.

References

(1) Brown, J. C. Enteroinsular axis. In *Gut Peptides: Biochemistry and Physiology*; Dockray, G. J., Walsh, J. H., Eds.; Raven Press: New York, 1994; pp 765–784.
(2) Creutzfeldt, W. The entero-insular axis in type 2 diabetes–Incretins as therapeutic agents. *Exp. Clin. Endocrinol. Diabetes* **2001**, *109*, 288–303.
(3) Trumper, A.; Trumper, K.; Trusheim, H.; Arnold, R.; Goke, B,; Horsch, D. Glucose-dependent insulinotropic polypeptide is a growth factor for beta (INS-1) cells by pleiotropic signaling. *Mol. Endocrinol.* **2001**, *15*, 1559–1570.
(4) Trumper, A.; Trumper, K,; Horsch, D. Mechanisms of mitogenic and anti-apoptotic signaling by glucose-dependent insulinotropic polypeptide in beta(INS-1)-cells. *J. Endocrinol.* **2002**, *174*, 233–246.
(5) Ehses, J. A.; Casilla, V. R.; Doty, T.; Pospisilik, J. A.; Winter, K. D.; Demuth, H. U.; Pederson, R. A.; McIntosh, C. H. S. Glucose-dependent insulinotropic polypeptide promotes beta-(INS-1) cell survival via cyclic adenosine monophosphate-mediated caspase-3 inhibition and regulation of p38 mitogen-activated protein kinase. *Endocrinology* **2003**, *144*, 4433–4445.
(6) Morgan, L. M. The metabolic role of GIP: Physiology and pathology. *Biochem. Soc. Trans.* **1996**, *24*, 585–591.
(7) Gault, V. A.; Flatt, P. R.; O'Harte, F. P. M. Glucose-dependent insulinotropic polypeptide analogues and their therapeutic potential for the treatment of obesity–diabetes. *Biochem. Biophys. Res. Commun.* **2003**, *308*, 207–213.
(8) Nauck, M. A.; Heimesaat, M. M.; Orskov, C.; Holst, J. J.; Ebert, R.; Creutzfeldt, W. Preserved incretin activity of glucagon-like peptide 1 [7–36 amide] but not of synthetic human gastric inhibitory polypeptide in patients with type-2 diabetes mellitus. *J. Clin. Invest.* **1993**, *93*, 301–307.
(9) Jones, I. R.; Owens, D. R.; Moody, A. J.; Luzio, S. D.; Morris, T.; Hayes, T. M. The effects of glucose-dependent insulinotropic polypeptide infused at physiological concentrations in normal subjects and type 2 (noninsulin-dependent) diabetic patients on glucose tolerance and B-cell secretion. *Diabetologia* **1987**, *30*, 707–712.
(10) Kjems, L. L.; Holst, J. J.; Volund, A.; Madsbad, S. The influence of GLP-1 on glucose-stimulated insulin secretion: Effects on beta-cell sensitivity in type 2 and nondiabetic subjects. *Diabetes* **2003**, *52*, 380–386.

(11) Meier, J. J.; Nauck, M. A.; Siepmann, N.; Greulich, M.; Holst, J. J.; Deacon, C. F.; Schmidt, W. E.; Gallwitz, B. Similar insulin secretory response to a gastric inhibitory polypeptide bolus injection at euglycemia in first-degree relatives of patients with type 2 diabetes and control subjects. *Metabolism* **2003**, *52*, 1579–1585.
(12) Meier, J. J.; Goetze, O.; Anstipp, J.; Hagemann, D.; Holst, J. J.; Schmidt, W. E.; Gallwitz, B.; Nauck, M. A. Gastric inhibitory polypeptide (GIP) does not inhibit gastric emptying in man. *Am. J. Phys. Endocrinol. Metab.* **2004**, *286*, E621–625.
(13) Kieffer, T. J.; McIntosh, C. H. S.; Pederson, R. A. Degradation of glucose-dependent insulinotropic polypeptide and truncated glucagon-like peptide 1 in vitro and in vivo by dipeptidyl peptidase IV. *Endocrinology* **1995**, *136*, 3585–3596.
(14) Brown, J. C.; Dahl, M.; Kwauk, S.; McIntosh, C. H. S.; Otte, S. C.; Pederson, R. A. Actions of GIP. *Peptides* **1981**, *2*, 241–245.
(15) Gault, V. A.; Parker, J. C.; Harriott, P.; Flatt, P. R.; O'Harte, F. P. M. Evidence that the major degradation product of glucose-dependent insulinotropic polypeptide (GIP), GIP(3–42), is a GIP receptor antagonist in vivo. *J. Endocrinol.* **2002**, *175*, 525–533.
(16) O'Harte, F. P. M.; Mooney, M. H.; Kelly, C. M. N.; Flatt, P. R. Improved glycaemic control in obese diabetic ob/ob mice using *N*-terminally modified gastric inhibitory polypeptide. *J. Endocrinol.* **2000**, *165*, 639–648.
(17) O'Harte, F. P. M.; Gault, V. A.; Parker, J. C.; Harriott, P.; Mooney, M. H.; Bailey, C. J.; Flatt, P. R. Improved stability, insulin-releasing activity and antidiabetic potential of two novel *N*-terminal analogues of glucose-dependent insulinotropic polypeptide: *N*-Acetyl-GIP and pGlu-GIP. *Diabetologia* **2002**, *45*, 1281–1291.
(18) Gault, V. A.; Flatt, P. R.; Bailey, C. J.; Harriott, P.; Greer, B.; Mooney, M. H.; O'Harte, F. P. M. Enhanced cyclic AMP generation and insulin-releasing potency of two novel *N*-terminal Tyr^1-modified enzyme resistant forms of GIP, is associated with significant antihyperglycaemic activity in spontaneous obesity-diabetes. *Biochem. J.* **2002**, *367*, 913–920.
(19) Gault, V. A.; Flatt, P. R.; Harriott, P.; Mooney, M. H.; Bailey, C. J.; O'Harte, F. P. M. Improved biological activity of Gly^2 and Ser^2 substituted analogues of glucose-dependent insulinotropic polypeptide (GIP). *J. Endocrinol.* **2003**, *176*, 133–141.
(20) Hinke, S. A.; Gelling, R. W.; Pederson, R. A.; Manhart, S.; Nian, C.; Demuth, H. U.; McIntosh, C. H. S. Dipeptidyl peptidase IV-resistant [D-Ala^2]glucose-dependent insulinotropic polypeptide (GIP) improves glucose tolerance in normal and obese diabetic rats. *Diabetes* **2002**, *51*, 656–661.
(21) Lindsay, J. R.; Au, S. T. B.; Kelly, C. M. N.; O'Harte, F. P. M.; Flatt, P. R. A novel amino-terminally glycated analogue of glucose-dependent insulinotropic polypeptide (GIP), with a prolonged insulinotropic activity in type 2 diabetes mellitus. *Diabetes* **2002**, *5*, 1394.
(22) Deacon, C. F.; Danielsen, P.; Klarskov, L.; Olesen, M.; Holst, J. J. Dipeptidyl peptidase IV inhibition reduces the degradation and clearance of GIP and potentiates its insulinotropic and antihyperglycemic effects in anesthetized pigs. *Diabetes* **2001**, *50*, 1588–1597.
(23) Deacon, C. F.; Wamberg, S.; Bie, P.; Hughes, T. E.; Holst, J. J. Preservation of active incretin hormones by inhibition of dipeptidyl peptidase IV suppresses meal-induced incretin secretion in dogs. *J. Endocrinol.* **2002**, *172*, 355–362.
(24) Meier, J. J.; Nauck, M. A.; Kranz, D.; Holst, J. J.; Deacon, C. F.; Gaeckler, D.; Schmidt, W. E.; Gallwitz, B. Secretion, degradation, and elimination of glucagon-like peptide 1 and gastric inhibitory polypeptide in patients with chronic renal insufficiency and healthy control subjects. *Diabetes* **2004**, *53*, 654–662.
(25) Deacon, C. F.; Nauck, M. A.; Meier, J.; Hucking, K.; Holst, J. J. Degradation of endogenous and exogenous gastric inhibitory polypeptide in healthy and in type 2 diabetic subjects as revealed using a new assay for the intact peptide. *J. Clin. Endocrinol. Metab.* **2000**, *85*, 3575–3581.
(26) Kurtzhals, P.; Havelund, S.; Jonassen, I.; Kiehr, B.; Larsen, U. D.; Ribel, U.; Markussen, J. Albumin binding of insulins acylated with fatty acids: Characterization of the ligand-protein interaction and correlation between binding affinity and timing of the insulin effect in vivo. *Biochem. J.* **1995**, *312*, 725–731.
(27) Holz, G. G.; Chepurny, O. G. Glucagon-like peptide-1 synthetic analogs: New therapeutic agents for use in the treatment of diabetes mellitus. *Curr. Med. Chem.* **2003**, *10*, 2471–2483.
(28) Green, B. D.; Gault, V. A.; Mooney, M. H.; Irwin, N.; Harriott, P.; Greer, B.; Bailey, C. J.; O'Harte, F. P.; Flatt, P. R. Degradation, receptor binding, insulin secretion and antihyperglycaemic actions of palmitate-derivatised native and Ala^8-substituted GLP-1 analogues. *Biol Chem.* **2004**, *385*, 169–177.
(29) Agersø, H.; Jensen, L. B.; Elbrønd, B.; Rolan, P.; Zdravkovic, M. The pharmacokinetics, pharmacodynamics, safety and tolerability of NN2211, a new long-acting GLP-1 derivative, in healthy man. *Diabetologia* **2002**, *45*, 195–202.
(30) Elbrond, B.; Jakobsen, G.; Larsen, S.; Agerso, H.; Jensen, L. B.; Rolan, P.; Sturis, J.; Hatorp, V.; Zdravkovic, M. Pharmacokinetics, pharmacodynamics, safety, and tolerability of a single-dose of NN2211, a long-acting glucagon-like peptide 1 derivative, in healthy male subjects. *Diabetes Care* **2002**, *25*, 1398–1404.
(31) Nauck, M. A.; Niedereichholz, U.; Ettler, R.; Holst, J. J.; Ørskov, C.; Ritzel, R.; Schmigel, W. H. Glucagon-like peptide-1 inhibition of gastric-emptying outweighs its insulinotropic effects in healthy humans. *Am. J. Physiol.* **1997**, *273*, 981–988.
(32) Hinke, S. A.; Manhart, S.; Pamir, N.; Demuth, H. U.; Gelling, R.; Pederson, R. A.; McIntosh, C. H. Identification of a bioactive domain in the amino-terminus of glucose-dependent insulinotropic polypeptide (GIP). *Biochim. Biophys. Acta* **2001**, *1547*, 143–155.
(33) Bailey, C. J.; Flatt, P. R. Influence of genetic background and age on the expression of the obese hyperglycaemic syndrome in Aston ob/ob mice. *Int. J. Obesity* **1982**, *6*, 11–21.
(34) Flatt, P. R.; Bailey, C. J. Development of glucose intolerance and impaired plasma insulin response to glucose in obese hyperglycaemic (ob/ob) mice. *Horm. Metab. Res* **1981**, *13*, 556–560.
(35) Gault, V. A.; O'Harte, F. P. M.; Flatt, P. R. Glucose-dependent insulinotropic polypeptide (GIP): Anti-diabetic and anti-obesity potential? *Neuropeptides* **2003**, *37*, 253–263.
(36) Fields, G. B.; Noble, R. L. Solid-phase peptide synthesis utilizing 9-fluorenylmethoxycarbonyl amino acids. *Int. J. Pept. Protein Res.* **1990**, *35*, 161–214.
(37) Gault, V. A.; Irwin, N.; Harriott, P.; Flatt, P. R.; O'Harte, F. P. M. DPP IV resistance and insulin releasing activity of a novel di-substituted analogue of glucose-dependent insulinotropic polypeptide, (Ser^2-Asp^{13})GIP. *Cell Biol. Int.* **2003**, *27*, 41–46.
(38) Gremlich, S.; Porret, A.; Hani, E. H.; Cherif, D.; Vionnet, N.; Froguel, P.; Thorens, B. Cloning, functional expression, and chromosomal localization of the human pancreatic islet glucose-dependent insulinotropic polypeptide receptor. *Diabetes* **1995**, *44*, 1202–1208.
(39) McClenaghan, N. H.; Barnett, C. R.; Ah-Sing, E.; Abdel-Wahab, Y. H. A.; O'Harte, F. P. M.; Yoon, T. W.; Swanston-Flatt, S. K.; Flatt, P. R. Characterization of a novel glucose-responsive insulin-secreting cell line, BRIN-BD11, produced by electrofusion. *Diabetes* **1996**, *45*, 1132–1140.
(40) Green, B. D.; Gault, V. A.; Mooney, M. H.; Irwin, N.; Bailey, C. J.; Harriott, P.; Greer, B.; Flatt, P. R.; O'Harte, F. P. M. Novel dipeptidyl peptidase IV resistant analogues of glucagon-like peptide-1(7–36)amide have preserved biological activities in vitro conferring improved glucose-lowering action in vivo. *J. Mol. Endocrinol.* **2003**, *31*, 529–540.
(41) Stevens, J. F. Determination of glucose by an automatic analyser. *Clin. Chem. Acta* **1971**, *32*, 199–201.
(42) Flatt, P. R.; Bailey, C. J. Abnormal plasma glucose and insulin responses in heterozygous lean (ob/+) mice. *Diabetologia* **1981**, *20*, 573–577.
(43) Burington, R. S. *Handbook of Mathematical Tables and Formulae*; McGraw-Hill: New York, 1973.

JM049262S

EXHIBIT 8

Acta Pharm. Nord. 4 (4) 301–308 (1992)

Prodrugs of peptides

19. Protection of the pyroglutamyl residue against pyroglutamyl aminopeptidase by *N*-acyloxymethylation and other means

Judi Møss* and Hans Bundgaard
Royal Danish School of Pharmacy, Department of Pharmaceutical Chemistry, 2 Universitetsparken, DK-2100 Copenhagen, Denmark

The *N*-terminal pyroglutamyl group in several peptides is specifically cleaved by pyroglutamyl aminopeptidase (PAPase I). Whith the aim of protecting this group against enzymatic cleavage by the prodrug approach, various derivatives of L-pyroglutamyl benzylamide, used as a PAPase I sensitive model pyroglutamyl peptide, were prepared and their stability characteristics determined. The derivatives studied included phenoxycarbonyl, phthalidyl, hydroxymethyl and acetoxymethyl derivatives, all formed at the pyroglutamyl NH-moiety. Whereas L-pyroglutamyl benzylamide was rapidly hydrolyzed by PAPase I, all the derivatives were resistant to cleavage by the enzyme. On the other hand, these derivatives, with the exception of the *N*-phenoxycarbonyl derivative, were readily converted to the parent pyroglutamyl benzylamide by spontaneous or plasmacatalyzed hydrolysis, the half-lives of conversion in 80% human plasma being in the range 2.3–8.4 h. The major degradation reaction of the *N*-phenoxycarbonyl derivative in both buffer and plasma solutions was hydrolytic opening of the pyrrolidone ring. The pH-rate profiles for the degradation of the compounds in aqueous solution were obtained and both specific acid and base catalytic reactions as well as a spontaneous reaction were observed. The results suggest that *N*-phthalidylation, *N*-hydroxymethylation and *N*-acyloxymethylation of pyroglutamyl peptides may be useful prodrug approaches to protect such peptides against cleavage by pyroglutamyl aminopeptidase and hence to improve their delivery characteristics.

A major obstacle to the application of peptides as clinically useful drugs is their poor biomembrane penetration, rapid enzymatic degradation and short biological half-lives [1–3]. A possible approach to solve or diminish these delivery problems of peptide drugs is derivatization of the peptides to produce prodrugs or transport forms which are more lipophilic than the parent peptides and capable of protecting these against degradation by enzymes present at the mucosal barrier or in the blood. At the same time, the prodrug derivatives should be capable of releasing the parent peptide spontaneously or enzymatically in the blood following their absorption [4, 5].

Previous studies in our laboratory have demonstrated the usefulness of this prodrug strategy to protect pyroglutamyl-containing peptides against cleavage by pyroglutamyl aminopeptidase [6, 7]. An *N*-terminal pyroglutamyl residue occurs in several peptides such as thyrotropin-releasing hormone (TRH), luteinizing hormone-releasing hormone (LHRH), neurotensin and gastrin and the specific cleavage of this residue is effected by pyroglutamyl aminopeptidase (PAPase I) (EC 3.4.19.3) [8, 9] or, in the case of TRH, by a TRH-specific pyroglutamyl aminopeptidase (PAPase II) as well [10–12]. PAPase I is a cysteine protease that occurs in many different tissues such as liver, kidney and brain, but not in the blood [9, 13]. It cleaves almost all pGlu-peptide bonds, including that in TRH [8–10].

In the previous studies [6, 7], *N*-acylation, *N*-aminomethylation as well as *N*-α-hydroxyalkylation with glyoxylic acid and esters thereof of the pyroglutamyl group of the model peptide L-pyroglutamyl benzylamide (I)

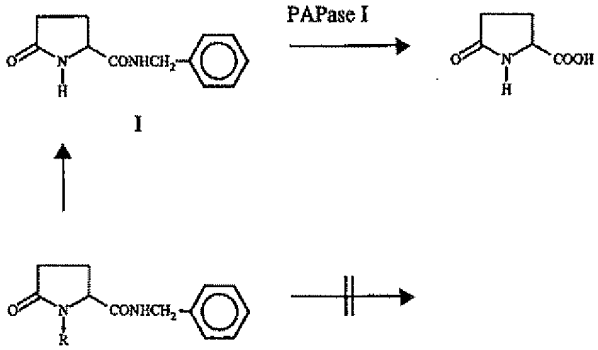

Fig. 1. *L-Pyroglutamyl benzylamide (I) is readily hydrolyzed by pyroglutamyl aminopeptidase (PAPase I) to L-pyroglutamic acid and benzylamine.*
In contrast, *N*-acyl (R = R_1-CO-), *N*-Mannich bases (R = $R_2R_3NCH_2$-) or glyoxylic acid adducts (R = R_4OOC-CH(OH)-) are totally resistant to cleavage by the enzyme, but are capable of being converted to I by spontaneous or plasma-catalyzed hydrolysis [6, 7].

* Correspondence

were shown to give derivatives (Fig. 1) which are completely resistant to attack by PAPase I and at the same time capable of releasing the parent compound I by spontaneous or plasma-catalyzed hydrolysis. The objective of the present work was to explore further prodrug types for the *N*-terminal pyroglutamyl group in peptides. The derivatives studied included a phenoxycarbonyl derivative (II), an *N*-hydroxymethyl derivative (III) and the acetyl ester thereof (IV), as well as a phthalidyl derivative (V), all formed at the pyroglutamyl NH-moiety in the model peptide I.

Experimental

Apparatus

HPLC analysis was performed using a Kontron apparatus consisting of a HPLC pump 420, an UV HPLC detector 432 and a 20 µl loop injection valve (Rheodyne). A deactivated reversed-phase Supelcosil LC-8-DB column (33×4.6 mm) (3-µm particles) equipped with a Supelguard column (purchased from Supelco Inc., U.S.A.) was used. Readings of pH were made at the temperature of study using a Radiometer Type pHM 83 Autocal pH meter. ^{1}H-NMR spectra (200 MHz) were obtained with a Bruker AC-200F spectrometer. Elemental analyses were performed at Leo Pharmaceuticals, Ballerup, Denmark.

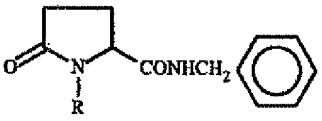

I R = H

II R = 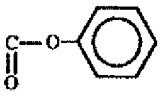

III R = CH_2OH

IV R = 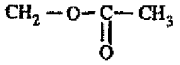

V R = 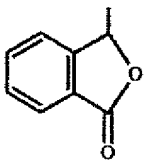

Preparation of the derivatives I–V

L-Pyroglutamyl benzylamide (I)

This compound was prepared by reaction of L-pyroglutamic acid ethyl ester with benzylamine, as previously described [6].

L-1-Phenoxycarbonyl-5-oxoproline benzylamide (II)

To a mixture of compound I (1.09 g, 5 mmol) in acetone (10 ml) and pyridine (0.40 ml, 5 mmol) was added phenyl chloroformate (0.76 ml, 6 mmol). The mixture was refluxed for 3 h and evaporated under reduced pressure. The residue obtained was taken up in water (30 ml) and ethyl acetate (30 ml). The organic phase was separated, washed with 1 M hydrochloric acid, 2% sodium bicarbonate solution and water, dried over anhydrous sodium sulfate and evaporated under reduced pressure. The residue obtained was recrystallized from ethyl acetate-ether-petroleum ether to give 0.95 g of the title compound, m.p. 164–165°C.

Anal.: Calc. for $C_{19}H_{18}N_2O_4$: C, 67.45; H, 5.36; N, 8.28. Found: C, 67.34; H, 5.37; N, 8.28.

L-1-Hydroxymethyl-5-oxoproline benzylamide (III)

A mixture of compound I (1.09 g, 5 mmol), 37% aqueous formaldehyde solution (1.25 ml, 16 mmol) and triethylamine (50 µl) in ethanol (10 ml) was refluxed for 2 h. The solution was evaporated under reduced pressure and the residue taken up in water (20 ml) and ethyl acetate (20 ml). The organic phase was separated, dried over anhydrous sodium sulfate and evaporated under reduced pressure to leave a residue which crystallized from ethanol-ether-petroleum ether to give the title compound in a yield of 75%, m.p. 134–135°C.

Anal.: Calc. for $C_{13}H_{16}N_2O_3$: C, 62.89; H, 6.50; N, 11.28. Found: C, 62.96; H, 6.59; N, 11.14.

L-1-Acetoxymethyl-5-oxoproline benzylamide (IV)

A mixture of compound III (166 mg, 0.7 mmol), acetic anhydride (0.5 ml) and pyridine (5 ml) was stirred at room temperature for 29 h and evaporated under reduced pressure. The solid residue obtained was recrystallized from ethyl acetate-ether to give compound IV in a yield of 65%, m.p. 125–126°C.

Anal.: Calc. for $C_{15}H_{18}N_2O_4$: C, 62.06; H, 6.25; N, 9.65. Found: C, 62.17; H, 6.40; N, 9.59.

L-1-Phthalidyl-5-oxoproline benzylamide (V)

The compound was prepared using the general procedure described by Wheeler *et al.* [14]. A mixture of equimolar amounts of compound I and phthalaldehydic acid was kept at 130°C for 4 h. The solid obtained upon cooling to room temperature was washed with an aqueous sodium bicarbonate solution and recrystallized from ethanol-water, m.p. 203–204°C. The compound is most likely a mixture of diastereomers. In HPLC analysis only one peak was seen.

Anal.: Calc. for $C_{20}H_{18}N_2O_4$: C, 68.56; H, 5.18; N, 8.00. Found: C, 68.36; H, 5.26; N, 7.95.

All new compounds (II–V) showed ^{1}H NMR spectra in agreement with their structures. No racemization in the L-

pyroglutamyl benzylamide moiety occurred during the synthesis of the derivatives, as shown in the following manner: The derivatives were degraded in alkaline aqueous solution at 37°C. An aliquot of the solutions containing pyroglutamyl benzylamide was then incubated at pH 7.4 with pyroglutamyl aminopeptidase as described below. With all compounds (II–V) it was found that the pyroglutamyl benzylamide formed upon their hydrolysis was hydrolyzed completely by the enzyme and at exactly the same rate as authentic L-pyroglutamyl benzylamide. D-pyroglutamyl derivatives are not hydrolyzed by pyroglutamyl aminopeptidase [8, 9] and therefore these experiments show unequivocally that the pyroglutamyl benzylamide produced from the derivatives is the L-isomer.

HPLC analysis

Reversed-phase HPLC procedures were used for the quantitative determination of the compounds I–V. A deactivated Supelcosil column was eluted with mobile phases consisting of mixtures of acetonitrile and 0.1% v/v phosphoric acid, the concentration of acetonitrile (5–30%) being adjusted for each compound to give an appropriate retention time. The flow rate was 1.0 ml min^{-1} and the column effluent was monitored at 215 nm. Quantitation of the compounds was done from measurements of the peak heights in relation to those of standards chromatographed under the same conditions.

Kinetic measurements

Degradation studies in aqueous solutions. The hydrolysis of the compounds was studied in aqueous buffer solutions at 37 or 60 ± 0.2°C. The buffers used were hydrochloric acid, acetate, phosphate, borate and carbonate buffers; the total buffer concentration used was generally 0.02 M and a constant ionic strength (μ) of 0.5 was maintained for each buffer by adding a calculated amount of potassium chloride. The reactions were initiated by adding 100 μl of a stock solution of the derivatives in acetonitrile to 10 ml of preheated buffer solution, the final concentration of the compunds being about 10^{-4} M. The solutions were kept in a water-bath at 37 or 60°C and at appropriate intervals samples were taken and analyzed by HPLC as described above. Pseudo-first-order rate constants for the degradation were determined from the slopes of linear plots of the logarithm of residual derivative against time.

Degradation studies in human plasma. The compounds were incubated at 37°C in human plasma diluted to 80% with 0.05 M phosphate buffer of pH 7.4. The initial concentration of the derivatives was about 10^{-4} M. The mixtures were kept in a waterbath at 37°C and at appropriate intervals samples of 250 μl were withdrawn and added to 500 μl of a 2% solution of zinc sulfate in methanol-water (1:1 v/v) in order to deproteinize the samples. After mixing and centrifugation for 3 min at 13,000 rpm, 20 μl of the clear supernatant was analyzed by HPLC as described above.

Degradation studies in the presence of pyroglutamyl aminopeptidase. The stability of the compounds I–V in the presence of pyroglutamyl aminopeptidase (PAPase I) (a calf liver preparation obtained from Boehringer, Mannheim, F.R.G.) was examined at 37°C under conditions similar to those previously described for compound I [6]. At appropriate intervals samples were withdrawn and immediately chromatographed as described above for the degradation studies in buffer solutions.

Results and discussion

L-Pyroglutamyl benzylamide (I) was used as a model for the pyroglutamyl residue in pyroglutamyl-containing peptides. As previously reported [6], this compound is a good substrate for pyroglutamyl aminopeptidase (PAPase I). Thus, at pH 7.4 and 37°C and using a 0.1 M phosphate buffer solution containing the enzyme in a concentration of 0.011 U/ml, disodium edetate (1 mM) and dithiothreitol (0.5 mM), compound I was hydrolyzed according to first-order kinetics with a rate constant of 0.049 min^{-1}, corresponding to a half-life of 14 min. In aqueous buffer solutions without the enzyme, as well as in 80% human plasma (pH 7.4), the compound is completely stable [6, 7].

Stability of the prodrug derivatives in aqueous solution

The kinetics of degradation of the prodrug derivatives II–V was studied in aqueous solution at 37°C over a wide pH range. At constant pH and temperature, the disappearance of the derivatives displayed strict first-order kinetics over several half-lives and all reactions proceeded to completion. No significant catalysis by the buffers used was observed.

The influence of pH on the rate of hydrolysis of compound II–V is shown in Figs. 2 and 3, in which the logarithms of the observed pseudo-first-order constants (k_{obs}) are plotted against pH. The pH-rate profiles

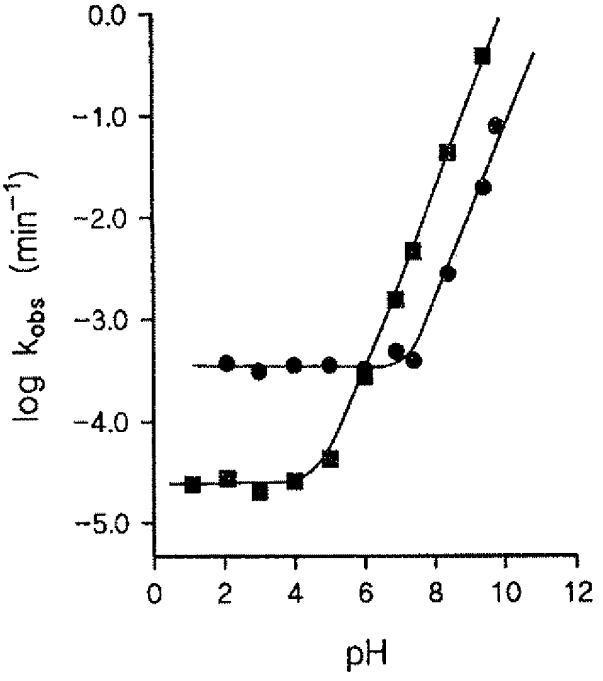

Fig. 2. *The pH-rate profiles for the degradation of compound II (■) and V (●) in aqueous solution at 37°C (μ = 0.5).*

obtained indicate that the overall degradation can be described in terms of a water-catalyzed or spontaneous reaction and specific acid- and base-catalyzed reactions according to the following rate expression:

$$k_{obs} = k_0 + k_H a_H + k_{OH}\, a_{OH} \quad (1)$$

where a_H and a_{OH} refer to the hydrogen ion and hydroxide ion activity, respectively. Values of the second-order rate constants k_H and k_{OH} and the first-order rate constant for spontaneous hydrolysis (k_0) were determined from the pH-rate profiles and Eqn. 1, and are listed in Table 1. In Figs. 2 and 3, the solid curves were constructed from these constants and Eqn. 1. The half-lives of hydrolysis of the compounds at pH 7.4 and 37°C are given in Table 2.

In neutral and alkaline solutions the hydrolysis of the *N*-phenoxycarbonyl derivative II was shown to follow two parallel pathways, giving either the parent compound (I) or the *N*-phenyl carbamate of glutamic acid α-benzylamide which was subsequently hydrolyzed to glutamic acid benzylamide and phenol (Scheme 1). HPLC analysis of the reaction solutions (pH 6–9) revealed that compound I was only formed in an amount of 10%, indicating the predominance of the k_2-pathway. Similar simultaneous ring opening and hydrolysis has previously been observed for various *N*-acyl derivatives of pyroglutamyl benzylamide [6].

The degradation of the *N*-hydroxymethyl derivative III was studied at 37°C in the pH range 6.0–9.8 and at 60°C in the pH range 1.2–6.0. As seen from the pH-rate profiles obtained (Fig. 4), the degradation was subject to both specific acid and base catalysis as well as to a spontaneous reaction. At all pH values studied, the derivative was quantitatively converted to compound I (and formaldehyde).

The stability of the analogous *N*-hydroxymethyl derivative of pyrrolidone has previously been reported and at pH 7.4 and 37°C its half-life of decomposition, leading to pyrrolidone and formaldehyde, was estimated to be

Table 1. *Rate data for the hydrolysis of compounds II–V in aqueous solution at 37°C and μ = 0.5.*

Compound	k_H (M^{-1} min^{-1})	k_0 (min^{-1})	k_{OH} (M^{-1} min^{-1})
II	–	2.5×10^{-5}	8.0×10^{3}
III	–	–	1.8×10^{3}
	2.0×10^{-3}[a]	2.0×10^{-5}[a]	2.2×10^{4}[a]
IV	0.25	1.0×10^{-4}	8.0×10^{1}
V	–	3.5×10^{-4}	3.8×10^{2}

[a] At 60°C.

Table 2. *Half-lives ($t_{1/2}$) of degradation of compound I–V in various media at pH 7.4 and 37°C.*

Compound	$t_{1/2}$ (h) 0.1 M Phosphatebuffer	80% human plasma	PAPase I solution[a]
I	stable	stable	14 min
II	2.5	0.2	3.7
III	9.8	2.3	7.9
IV	72.9	2.3	41.5
V	21.4	8.4	17.5

[a] These data are half-lives for the degradation in buffer solution (pH 7.4) containing calf liver pyroglutamyl aminopeptidase (0.011 U ml^{-1}).

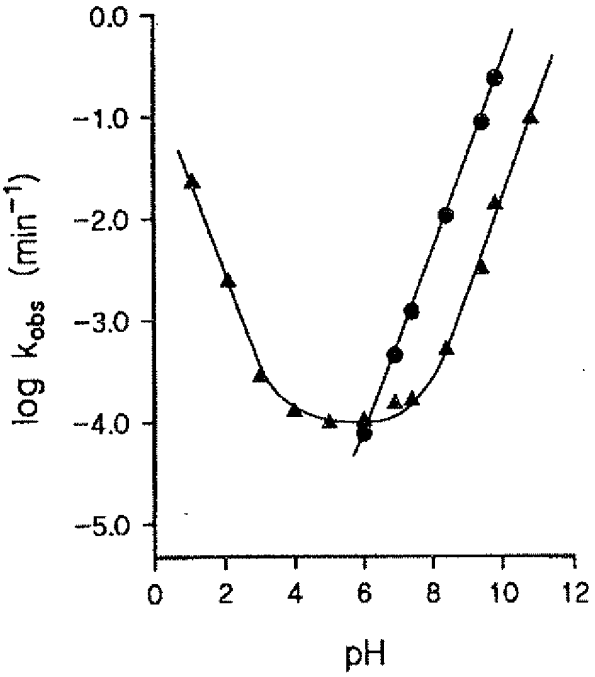

Fig. 3. *The pH-rate profiles for the degradation of compound III (●) and IV (▲) in aqueous solution at 37°C (μ = 0.5).*

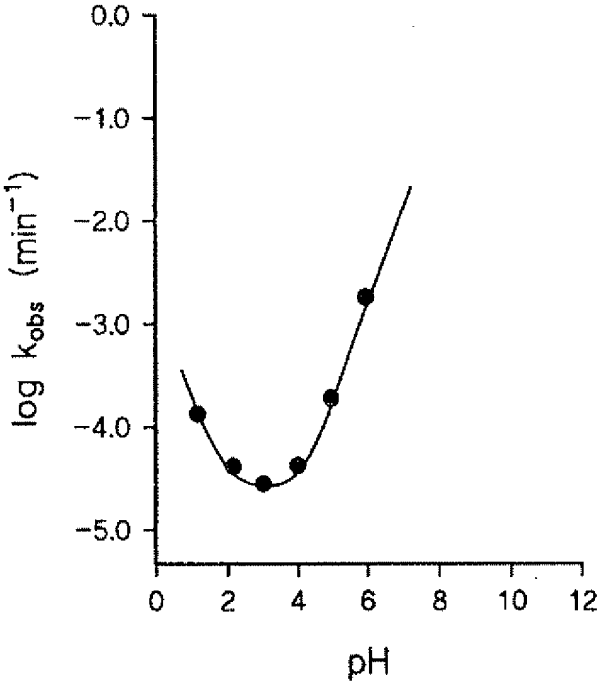

Fig. 4. *The pH-rate profile for the degradation of compound III in aqueous solution at 60°C (μ = 0.5).*

6×10^3 h [7]. The reactivity of compound III is seen to be about 600 times higher than that of *N*-(hydroxymethyl)-2-pyrrolidone, its half-life being 9.8 h at pH 7.4 and 37° (Table 2). The reactivity of *N*-hydroxymethyl derivatives of NH-acidic compounds such as carboxamides and imides has been found to increase with increasing acidity of the NH-group [15, 16] and, accordingly, the increased reactivity of compound III relative to *N*-(hydroxymethyl)-2-pyrrolidone can be ascribed to this factor. The benzylamide group in III is strongly electron-withdrawing and should lead to an increased acidity of the neighbouring NH-group. Using the relationship previously established between pK_a of the NH-acidic compound and reactivity of *N*-hydroxymethyl derivatives [16], a pK_a value of 14.4 can be calculated for compound III. This value appears to be quite reasonable [15]. The decomposition of the *N*-acetoxymethyl derivative IV proceeded with the quantitative formation of the *N*-hydroxymethyl derivative III, which subsequently decomposed to the parent compound I and formaldehyde, as depicted in Scheme 2. This was shown by HPLC analysis of reaction solutions of pH less than about 6, where the rate of hydrolysis of compound IV is higher than the rate of degradation of compound III (*cf.* Fig. 3). An example of a product analysis at pH 5.95 and 60°C is shown in Fig. 5. Under these conditions, compounds III and IV degraded with half-lives of 462 and 410 min, respectively. As can be seen from Fig. 5, the *N*-hydroxymethyl derivative III is produced in quantitative amounts, the rate of formation following first-order kinetics with no occurrence of any lag period.

The spontaneous (pH-independent) decomposition of *N*-acyloxymethyl derivatives of acyclic, secondary amides like *N*-methylbenzamide and *N*-alkyl benzylcarbamates has recently been shown to proceed by a unimolecular elimination-addition process, with the formation of a transient *N*-acyliminium ion intermediate as depicted in Scheme 3 [17, 18]. In this mechanism the

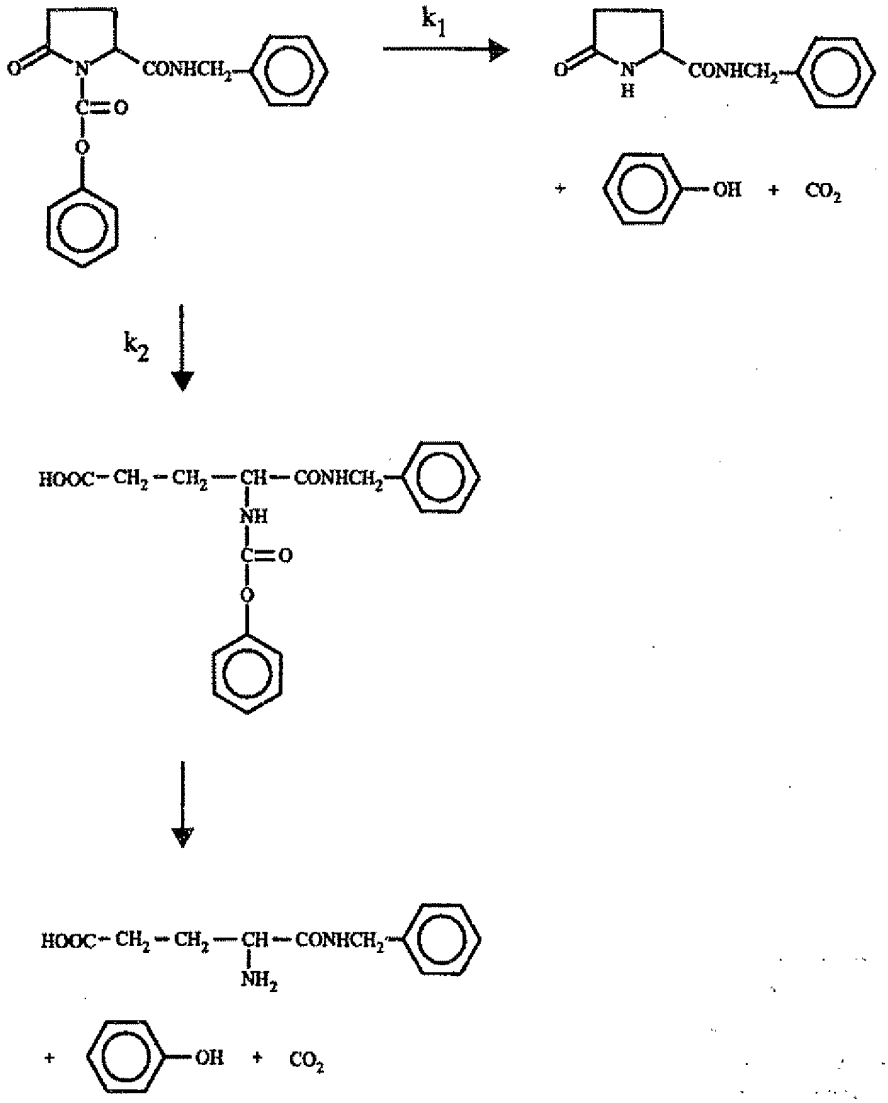

Scheme 1

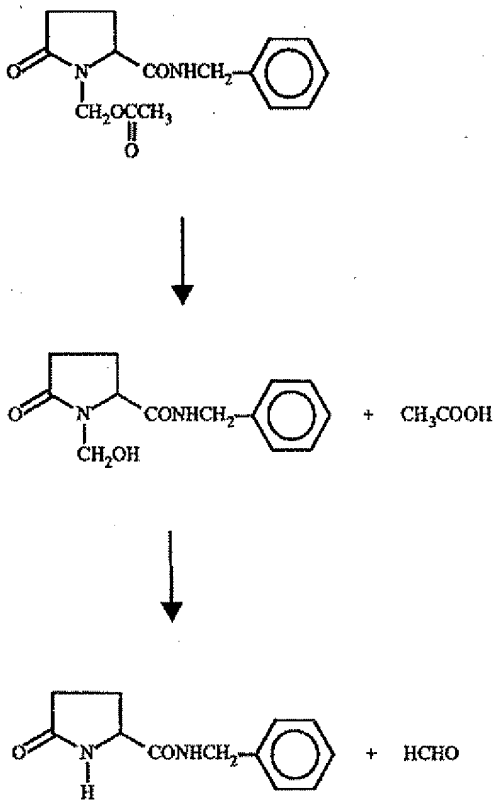

Scheme 2

rate-determining step involves elimination of a carboxylate anion to give an iminium ion, which in a subsequent fast step undergoes attack by hydroxide ions, giving the *N*-hydroxymethyl amide.

The k_0-value for compound IV is 25 times less than for the decomposition of the *N*-acetoxymethyl derivative of *N*-benzyloxycarbonylglycine benzylamide (VI) under similar reaction conditions [18]. This considerably higher stability of compound IV indicates that a normal ester hydrolysis mechanism involving acyl-oxygen bond cleavage is primarily involved and not a S_N1 reaction as for compound VI. The k_0-value for compound IV is similar to those for *N*-acetoxymethyl derivatives of 5-fluorouracil [19] and phenytoin [20] and it therefore appears, contrary to previous speculations [18], that the mechanism of decomposition and hence stability of *N*-acyloxymethyl derivatives formed with a secondary-CONH-moiety depends on whether this moiety is part of an acyclic or cyclic structure.

The degradation of the *N*-phthalidyl derivative V in aqueous solution proceeded with the quantitative formation of the parent compound I and phthalaldehydic acid, as revealed by HPLC analysis of the reaction solutions. As has been described earlier for *N*-phthalidyl derivatives of various amides [21], the mechanism of degradation most likely involves hydrolytic opening of the lactone ring as the rate-determining step to give an *N*-α-hydroxybenzyl derivative which rapidly decomposes to the amide and phthalaldehydic acid (Scheme 4).

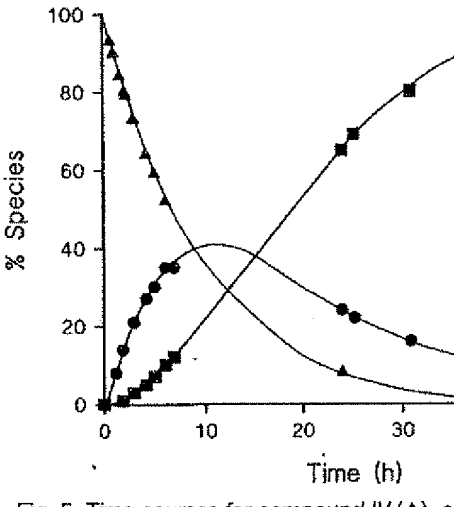

Fig. 5. *Time courses for compound IV (▲), compound III (●) and compound I (■) during degradation of compound IV in 0.02 M phosphate buffer solution of pH 5.95 at 60°C.*

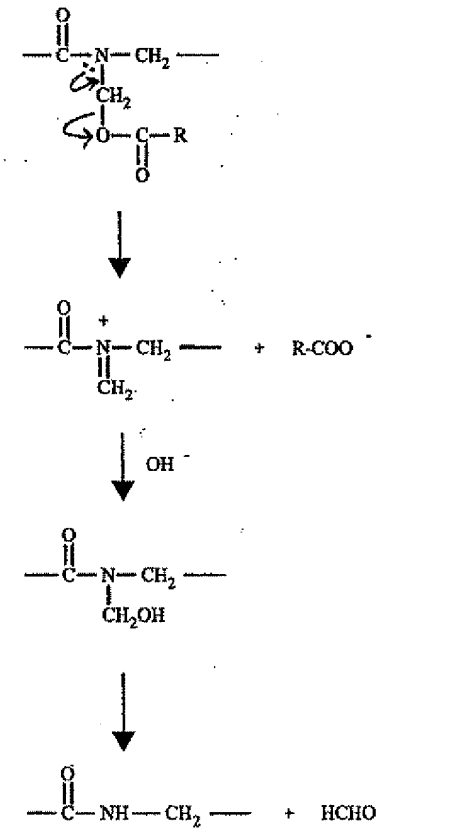

Scheme 3

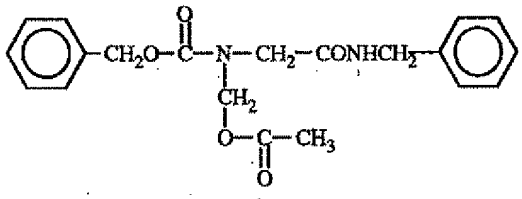

VI

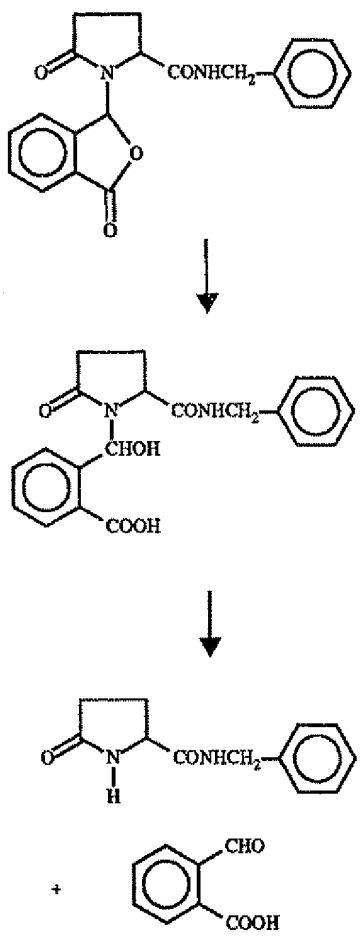

Scheme 4

Stability in plasma

The rates of decomposition of compounds II–V were determined in 80% human plasma (pH 7.4) at 37°C and the half-lives obtained are shown in Table 2. The data show that the degradation of all compounds is catalyzed by plasma, especially the *N*-acetoxymethyl derivative IV. The catalytic effect on compounds IV and V is certainly due to plasma esterases, catalyzing the hydrolysis of the ester groups in these compounds. HPLC analysis of the reaction solutions showed that compound I was formed quantitatively from compounds III–V, whereas only 8% was formed from compound II. Thus, plasma appears to catalyze both the k_1- and k_2-pathways of degradation of compound II (Scheme 1).

The slight but significant catalytic effect of plasma on the decomposition of the *N*-hydroxymethyl derivative III is difficult to rationalize on the basis of the mechanism involved in the decomposition of such compounds [15] but a similar catalytic effect has also been observed for other *N*-hydroxymethyl derivatives [22]. Whether the effect is due to protein-binding phenomena or to a true enzymatic action [23] is not known. The first possibility appears most likely, however, since a similar half-life of decomposition of compound III was observed in both heat-treated (60°C for 2 h) plasma and in fresh plasma.

Stability toward pyroglutamyl aminopeptidase

As stated above, the parent pyroglutamyl benzylamide (I) is rapidly hydrolyzed to pyroglutamic acid and benzylamine in the presence of PAPase I, the half-life being 14 min at the conditions specified. Under the same conditions, none of the derivatives II–V were found to be attacked by the enzyme. As seen from the results in Table 2, the rates of degradation of the derivatives in the presence of the enzyme were much slower than that of compound I and in the same order as those occurring in buffer solutions without the enzyme. The slightly higher rates observed for the ester derivatives IV and V in the PAPase I solution as compared with the buffer solutions without the enzyme, may be due to the existence of a small esterase activity in the enzyme preparation used.

As stated above, compound V is most likely a mixture of diasteromers. It showed only one peak in HPLC and this peak disappeared in all cases (buffer and enzyme solutions and plasma) according to strict first-order kinetics. Thus, if the peak represents a mixture of diasteromers, each species has the same reactivity.

Conclusions

The results described suggest that *N*-phthalidylation, *N*-acyloxymethylation and *N*-hydroxymethylation of pyroglutamyl peptides may be useful approaches to obtain prodrug derivatives which, on the one hand, are stable against PAPase I and on the other hand are readily bioreversible, releasing the parent pyroglutamyl peptide by spontaneous degradation at physiological pH or by a plasma esterase-catalyzed reaction. In contrast, *N*-acylation of the pyroglutamyl moiety by reaction with a chloroformate appears to be a less useful approach as the *N*-alkoxycarbonyl derivatives thereby obtained may undergo a plasma-catalyzed hydrolytic opening of the pyroglutamyl ring, resulting in a non-quantitative formation of the parent pyroglutamyl peptide. The rate-determining step in the bioconversion of *N*-acyloxymethyl derivatives like compound IV to the parent pyroglutamyl peptide is decomposition of the *N*-hydroxymethyl derivative. Since the latter has a relatively high lability, contrary to previous predictions [7], *N*-acyloxymethylation may be a particularly useful prodrug approach. Thus, by varying the acyl group it may be possible to control the lipophilicity of the derivatives.

Acknowledgements

This work has been supported by the Danish Medical Research Council and PharmaBiotec Research Centre.

References

1. Humphrey M. J. and Ringrose P. S. (1986) Peptides and related drugs: a review of their absorption, metabolism, and excretion. *Drug Metab. Rev. 17,* 283–310
2. Lee V. H. L. and Yamamoto A. (1990) Penetration and enzymatic barriers to peptide and protein absorption. *Adv. Drug Delivery Rev. 4,* 171–207
3. Lee V. H. L. (Ed.) (1991) *Peptide and Protein Drug Delivery.* Marcel Dekker, New York
4. Bundgaard H. (1992) Prodrugs as a means to improve the delivery of peptide drugs. *Adv. Drug. Delivery Rev. 8,* 1–38
5. Bundgaard H. (1992) The utility of the prodrug approach to improve peptide absorption. *J. Control. Release 21,* 63–72
6. Bundgaard H. and Møss J. (1989) Prodrugs of peptides. IV. Bioreversible derivatization of the pyroglutamyl group by *N*-acylation and *N*-aminomethylation to effect protection against pyroglutamyl aminopeptidase. *J. Pharm. Sci. 78,* 122–126
7. Møss J. and Bundgaard H. (1989) Prodrugs of peptides. 5. Protection of the pyroglutamyl residue against pyroglutamyl aminopeptidase by bioreversible derivatization with glyoxylic acid derivatives. *Int. J. Pharm. 52,* 255–263
8. Orlowski M. and Meister A. (1971) Enzymology of pyrrolidone carboxylic acid. In Boyer P. D. (Ed), *The Enzymes, Vol. IV,* Academic Press, New York, pp 123–151
9. Abraham G. N. and Podell D. N. (1981) Pyroglutamic acid. Nonmetabolic formation, function in proteins and peptides, and characteristics of the enzymes effecting its removal. *Mol. Cell. Biochem. 38,* 181–190
10. Wilk S. (1989) Inhibitors of TRH-degrading enzymes. *Ann. N. Y. Acad. Sci. 553,* 252–264
11. Møss J. and Bundgaard H. (1990) Kinetics and pattern of degradation of thyrotropin-releasing hormone (TRH) in human plasma. *Pharm. Res. 7,* 751–755
12. Bundgaard H. and Møss J. (1990) Prodrugs of peptides. 6. Bioreversible derivatives of thyrotropin-releasing hormone (TRH) with increased lipophilicity and resistance to cleavage by the TRH-specific serum enzyme. *Pharm. Res. 7,* 885–892
13. Szewczuk A. and Kwiatkowska J. (1970) Pyrrolidonyl peptidase in animal, plant and human tissues. Occurrence and some properties of the enzyme. *Eur. J. Biochem. 15,* 92–96
14. Wheeler D. D., Young D. C. and Erley D. S. (1957) Reactions of phthalaldehydic acid. *J. Org. Chem. 22,* 547–556
15. Johansen M. and Bundgaard H. (1979) Pro-drugs as drug delivery systems. VI. Kinetics and mechanism of the decomposition of *N*-hydroxymethylated amides and imides in aqueous solution and assessment of their suitability as possible pro-drugs. *Arch. Pharm. Chemi. Sci. Ed. 7,* 175–192
16. Bundgaard H. and Johansen M. (1980) Prodrugs as drug delivery systems. VIII. Bioreversible derivatization of hydantoins by *N*-hydroxymethylation. *Int. J. Pharm. 5,* 67–77
17. Iley J., Moreira R. and Rosa E. (1991) Acyloxymethyl as a drug-protecting group. Kinetics and mechanism of the hydrolysis of *N*-acyloxymethylbenzamides. *J. Chem. Soc., Perkin Trans. 2,* 563–570
18. Bundgaard H. and Rasmussen G. J. (1991) Prodrugs of peptides. 11. Chemical and enzymatic hydrolysis kinetics of *N*-acyloxymethyl derivatives of a peptide-like bond. *Pharm. Res. 8,* 1238–1242
19. Buur A., Bundgaard H. and Falch E. (1985) Prodrugs of 5-fluorouracil. IV. Hydrolysis kinetics, bioactivation and physicochemical properties of various *N*-acyloxymethyl derivatives of 5-fluorouracil. *Int. J. Pharm. 24,* 43–60
20. Varia S. A., Schuller S. and Stella V. J. (1984) Phenytoin prodrugs. IV. Hydrolysis of various 3-(hydroxymethyl)phenytoin esters. *J. Pharm. Sci. 73,* 1074–1080
21. Bundgaard H., Buur A., Hansen K. T., Larsen J. D., Møss J. and Olsen L. (1988) Prodrugs as drug delivery systems. 77. Phthalidyl derivatives as prodrug forms for amides, sulfonamides, carbamates and other NH-acidic compounds. *Int. J. Pharm. 45,* 47–57
22. Bundgaard H. and Rasmussen G. J. (1991) Prodrugs of peptides. 9. Bioreversible *N*-α-hydroxyalkylation of the peptide bond to effect protection against carboxypeptidase or other proteolytic enzymes. *Pharm. Res. 8,* 313–322
23. Bundgaard H. and Kahns A. H. (1991) Chemical stability and plasma-catalyzed dealkylation of peptidyl-α-hydroxyglycine derivatives – intermediates in peptide α-amidation. *Peptides 12,* 745–748

Received May 4, 1992
Revised edition accepted July 20, 1992

EXHIBIT 9

DRUG DEVELOPMENT RESEARCH 46:219–234 (1999)

Research Overview

Conotoxins and Their Potential Pharmaceutical Applications

David J. Adams,[1]* Paul F. Alewood,[2] David J. Craik,[2] Roger D. Drinkwater,[3] and Richard J. Lewis[1,2]

[1]*Department of Physiology and Pharmacology, University of Queensland, Brisbane, QLD, Australia*
[2]*Centre for Drug Design and Development, and* [3]*CSIRO, Gehrmann Laboratories, University of Queensland, Brisbane, QLD, Australia*

Strategy, Management and Health Policy				
Venture Capital Enabling Technology	Preclinical Research	Preclinical Development Toxicology, Formulation Drug Delivery, Pharmacokinetics	Clinical Development Phases I-III Regulatory, Quality, Manufacturing	Postmarketing Phase IV

ABSTRACT The neurotoxins isolated from cone shell venoms are a diverse group of small, disulfide-rich peptides. Most of the active peptides isolated to date have been shown to specifically target various components of neural transmission, and have generally demonstrated high specificities for ion channel and receptor types and subtypes. The specificity of conotoxins is one of the attributes that make them valuable diagnostic tools in the characterisation of neural pathways, as therapeutic agents in medicine, and potentially as biodegradable toxic agents in agroveterinary applications. The number of novel, active peptides within the numerous *Conus* species is considered to be enormous. Currently, however, relatively few peptides have been characterised. In this article, we review current research on conotoxins with a focus on drug potential being developed at the University of Queensland, Australia. Drug Dev. Res. 46:219–234, 1999.

Key words: ion channels; sodium channel; acetylcholine; nicotinic receptor; synaptic transmission; peptide; gene cloning; NMR spectroscopy; crystal structure

INTRODUCTION: ION CHANNELS AS DRUG TARGETS

Voltage-dependent ion channels are intrinsic membrane proteins that play an important role in fast communication in excitable cells. A short stretch of amino acids, the pore region, is the sole determinant of cation selectivity and also forms the binding site for many channel blockers. Toxins that interact intimately with this region can be used as structural templates to deduce the spatial organisation of the pore region of the ion channels. These models of pore structure are valuable for understanding the mechanisms of ion permeation, and ultimately may be useful for the rational design of drugs that modify the function of ion channels in clinical conditions such as stroke, pain, or epilepsy.

Broadly, ion channels have structural and functional similarities, but even within a class of ion channels there are significant differences that can be targeted in drug applications. The diversity and distribution of ion channel types and subtypes being uncovered through the use of molecular biology and toxin probes present an exciting opportunity for the discovery of new therapeutics which are specific for channel subtypes involved in disease states. The various ion channels to be considered will be examined briefly in turn.

Nicotinic Acetylcholine Receptor-Channels

The nicotinic acetylcholine receptor (nAChR) is part of the ligand-gated ion channel superfamily, which includes the $GABA_A$, serotonin, and glutamate (NMDA,

Contract grant sponsors: DIST and the Australian Research Council; Contract grant number: 96/ARCL244G.

*Correspondence to: Professor David J. Adams, Department of Physiology and Pharmacology, University of Queensland, St. Lucia, QLD 4072, Australia. E-mail: dadams@plpk.uq.edu.au

AMPA, kainate) receptors. All ligand-gated ion channels are large, membrane-bound pentamers with various subunit compositions. These receptors have several conserved features. Ligand-gated ion channels are pentamers, with each subunit containing four transmembrane helices (M1 to M4), with the M2 helix lining the ion channel lumen and providing it selectivity. Binding of an endogenous ligand to a large, extracellular domain remote to the M2 helix brings about a conformational change in the M2 helices that causes the pore to open. Due to the size of these receptors (~290 kDa), the only direct structure determinations have been of low resolution (~9 Å) using electron microscopy [Unwin, 1998].

Nicotinic ACh receptors are found throughout the central and peripheral nervous systems, with distinct genes encoding the nAChR subunits which form a heteropentameric ion channel complex selective for cations. The muscle-subtype nAChR has been well characterised due to the availability of specific probes (e.g., α-bungarotoxin) and has the subunit composition $(\alpha 1)_2\beta 1\delta\gamma$ or ε in mature muscle. In mammalian central and autonomic neurones and adrenal medulla, the neuronal nAChRs are composed of α and β subunits only. At least seven different α subunits (α2–α7 and α9) and three β subunits (β2–β4) have been identified and it has been shown that α2, α3, and α4 can combine with β2 or β4 to form functional channels in the *Xenopus* oocyte expression system [McGehee and Role, 1995]. In addition, α7 and α9 subunits can be expressed as functional homooligomers in this system, with the α7 gene product being α-bungarotoxin-sensitive and highly permeable to Ca^{2+} [Colquhoun and Patrick, 1997]. Although these neuronal nAChR subunits are homologous with one another, each functional subunit combination is physiologically and pharmacologically distinct. This may account for the diversity of neuronal nAChRs observed in vivo. For example, the α5 subunit appears to participate in nAChRs expressed in heterologous systems and primary neurones and contributes to the pore lining of functionally unique nAChRs. Recent studies using single cell RT-PCR analysis of nAChR gene transcripts indicate that multiple nAChR subtypes are expressed by individual rat intracardiac neurones and that the combination of subtypes expressed varies among cells [Poth et al., 1997]. The development of specific pharmacological probes for neuronal nAChR subunits will provide new insight into the structural composition and functional role of the different neuronal nAChRs subtypes.

Activation of distinct subtypes of these presynaptic nAChRs by nicotinic agonists can selectively regulate the release of different neurotransmitters, including dopamine, norepinephrine, glutamate, and acetylcholine [Kulak et al., 1997; Kaiser et al., 1998; Picciotto et al., 1998]. Such receptors have also been implicated in the pathophysiology of several neuropsychiatric disorders, including schizophrenia, Alzheimer's disease, Parkinson's disease, and Tourette's syndrome [Kulak et al., 1997]. Despite their importance, few of the nicotinic receptor antagonists identified to date are highly selective between the multiple neuronal nAChR subtypes. Thus, the ability of recently discovered α-conotoxins — small (12–19 amino acids), rigid, highly disulfide-bonded peptides isolated from marine snails of the genus *Conus* — to target neuronal nAChR subunits with high specificity has considerable significance for both basic neuroscience and potential drug development.

Sodium Channels

Sodium channels consist of three separate and biochemically separable protein subunits, the α plus β-1 and β-2 auxiliary subunits, which comprise the channel in a 1:1:1 stoichiometry. The α-subunit is a transmembrane glycoprotein of approximately 260 kDa molecular weight that binds a diverse range of neurotoxins at specific positions on its surface (six or seven sites are currently identified). The two β-subunits have smaller molecular weights (~30 kDa each) and are integral membrane glycoproteins. Numerous models of sodium channel α-subunit structure have appeared, based on primary sequence data [Noda et al., 1984]. All show four highly homologous regions of sequence domains, labeled I–IV, with each domain containing six transmembrane helices, denoted S1–S6. The S5 and S6 segments of each domain are highly nonpolar, the S1, S2, and S3 segments are relatively nonpolar, with just a few charged sidechains, but the S4 segments within each domain have the distinctive feature that every third residue is positively charged (mostly arginines). The S4 segments are believed to move upward on depolarisation to open the activation gate (m gate) and allow the selective influx of sodium ions. In the process, voltage-dependent movement of an IFM particle to interact with adjacent intracellular loops is facilitated and inactivation occurs, blocking the further flow of ions (Fig. 1).

There is considerable structural homology among the three types of brain Na^+ channel α-subunits (I, II, and III), the μ1-sodium channel α-subunit from adult skeletal muscle, and the h1 sodium channel α-subunit from heart and denervated muscle. Despite these similarities, considerable pharmacological diversity exists. For example, tetrodotoxin (TTX) blocks the brain types I, II, and III at nanomolar concentrations, and the h1 form from the heart at micromolar concentrations.

Until recently, there was no hard evidence to indicate that pharmacologically distinct forms of neuronal sodium channels are expressed in sensory neurons, and thus no evidence that a specific Na^+ channel pathway could be modulated to control particular diseases. The

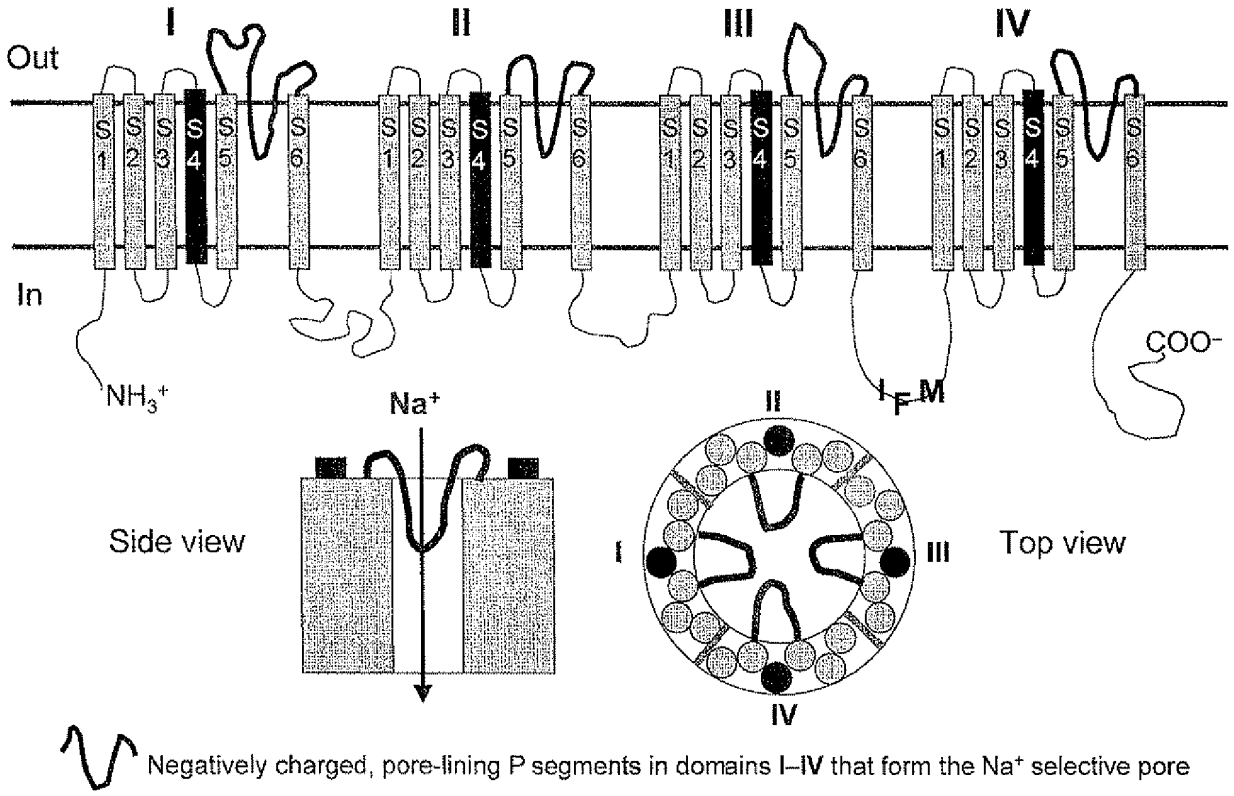

Fig. 1. Transmembrane segments of the sodium channel and a model of their construction into the α-subunit that forms the pore of the channel. The repeating nature of the transmembrane domains is emphasised, as is the IFM particle that acts as the inactivation gate. The nature of the residues comprising the activation gate is presently not known. Interestingly, the calcium channel has the same general structure.

newly discovered TTX-insensitive sodium channel, named PN3 or SNS [Sangameswaran et al., 1996], which is located specifically in sensory neurons, represents one of a number of potential Na^+ channel targets for drug discovery. Additional neuronal pathways for therapeutic intervention may also be uncovered using conopeptides such as μ-conotoxin PIIIA, the first conopeptide to distinguish amongst neuronal TTX-sensitive Na^+ channels [Shon et al., 1998; Watson et al., 1998].

Calcium Channels

Structurally, the calcium channels are closely related to sodium channels, with the main difference being the positioning and nature of the residues that line the selectivity filter in the pore of the channel. There are at least six pharmacologically distinct calcium channels types, including L-, N-, P/Q-, T, and R-type calcium channels, and within each group are multiple subtypes that are presently less easy to distinguish. In the nervous system, several types of ion channels may contribute to processes such as neurotransmitter release, with the ratio and role for each type varying among different nervous tissues [Olivera et al., 1994]. This situation provides the possibility for selective modulation of nerve function with type and subtype selective modulators that may allow the selective treatment of conditions such as pain and stroke. The ω-conotoxins have been of enormous importance as physiological tools, with currently one peptide (MVIIA or Ziconitide) in clinical trials for pain and stroke.

Potassium Channels

There are numerous types of potassium channel, each with its own distinctive electrophysiological and pharmacological properties; what they all have in common is that they tend to stabilise the membrane potential at the K^+ equilibrium potential. DNA sequencing reveals that the potassium channels encoded by *Drosophila* and vertebrate genes all resemble a single domain of the voltage-dependent sodium channel [Jan and Jan, 1997]. Voltage-dependent potassium channels are tetrameric homo-oligomers organised in axial fourfold symmetry around the K^+-selective pore. Analogous to voltage-dependent sodium and calcium channels, the S4 transmembrane segment carries a cluster of positively charged residues and is thought to act as the voltage sen-

sor for channel activation. Site-directed mutagenesis studies, coupled with the use of selective toxins, have proved invaluable in unraveling which residues of the potassium channel protein are functionally important. Recently, the crystal structure of a K^+ channel has been determined [Doyle et al., 1998]. The pore structure determined previously from toxin binding interaction studies has proved to be remarkably predictive [Miller, 1995], though it lacks the structural detail obtained by X-ray crystallography. κ-Conotoxin PVIIA is a new structural class of K^+ channel blocking peptide that binds in a voltage-sensitive manner to the outer vestibule of the channel [Scanlon et al., 1997].

DISCOVERY AND CHARACTERISATION OF NOVEL CONOTOXINS

Tropical waters, especially in coral reef ecosystems, house an extraordinary diversity of invertebrate species, many of whom use novel bioactive compounds as part of defensive or prey capture strategies. The cone shells which comprise a group of some 500+ predatory molluscs are the most specialised, with venoms that target fish, worms, and other molluscs. The venom is injected through a harpoon-like apparatus and contains a complex mix of small, constrained peptides which contain 10–40 amino acids and up to five disulfide bonds [Myers et al., 1993]. This cocktail of peptides targets a diverse range of voltage-sensitive sodium, calcium, and potassium channels and *N*-methyl-d-aspartate, glutamate, vasopressin, serotonin, and acetylcholine receptors, which leads to an immediate and efficient immobilisation of the prey. The conotoxins present in the venom have been divided into a number of major classes based on their pharmacological activity and cysteine frameworks (Table 1). Their high potency and specificity, and convenient chemical synthesis, also make the conotoxins attractive leads in drug design programs. In addition to the conotoxins being among the smallest bioactive peptides, they are unusual in containing a high density of cysteine residues and posttranslation modifications, including hydroxylation, carboxylation, amidation, sulphation, and bromination. These features often complicate their chemical characterisation and occasionally their chemical synthesis.

All major classes of conotoxins have been identified through initial in vitro or in vivo functional assays [Olivera et al., 1990]. Screening based on receptor-binding displacement of radiolabeled ligands is also playing a major role. At the 3D Centre, University of Queensland, sensitive ^{125}I-GVIA and ^{125}I-MVIIC assays have been established for rat and human brain preparations to allow for the isolation of new ω-conotoxins. More recently, other chemical and molecular biology approaches have facilitated the identification and primary structure determination of new conotoxins. In practice, all of these approaches are used in concert to discover new conotoxins.

The realisation that most if not all conotoxins were biologically active led us to establish chemical approaches to rapidly identify new conotoxins and confirm the presence of known conotoxins. The starting source of venom was either from the dissected venom ducts of Conidae or from the milked venom of captive species. The venom paste was then extracted with varying amounts of acetonitrile acidified with 0.1% trifluoroacetic acid. This procedure efficiently extracts most of the conotoxins present. Early research findings at the 3D Centre revealed considerable inter- and intraspecies variability in the components in cone shell venoms and also that most species contained in excess of 100 different peptides [Bingham et al., 1996]. This analysis was facilitated by the application of Ionspray mass spectrometry, which dramatically reduced the time and quantity of venom required to characterise the components of these complex mixtures [Lewis et al., 1994; Bingham et al., 1996; Jones et al., 1996]. An example of an LC/MS analysis of the peptides present in the crude venom from *Conus geographus* is given in Figure 2. From analyses of more than 30 species, it is evident that the 60+ conotoxins reported to date represent less than 0.1% of the peptides present in the venoms of Conidae.

HPLC/electrospray mass spectrometry analysis is generally complemented with a suite of chemical techniques to rapidly "mass profile" each crude venom. The tagging of each molecular component has facilitated the subsequent isolation and characterisation of novel peptides. Fractionation of the venom is often directed by the mass and number of disulfide bonds present in the peptide. Posttranslational modifications, which are common in cone shell venoms, are usually identified by MS/MS, enzymatic degradation/MS studies, amino acid analysis, and Edman chemistry [Loughnan et al., 1998]. Fortunately, most conopeptides are not N-terminally blocked.

The determination of disulfide bond connectivity for many conotoxins remains challenging. Classical approaches using enzymic degradation often fail, as most conotoxins are resistant to proteolysis, even with high levels of enzyme present. Success has been achieved using a reductive alkylation/Edman sequence strategy [Gray, 1993]. However, this approach occasionally fails, as the alkylation step is performed under basic conditions where scrambling may occur. Recently, we developed a more general approach that employs both mass spectrometry and Edman chemistry [Jones et al., 1996]. Briefly, the conotoxin is sequentially reduced and alkylated under acidic conditions with mass spectrometric/HPLC analysis and Edman sequencing. For smaller peptides (e.g., the α-conotoxins), the differentially alkylated products need only be subjected to collision-induced dis-

TABLE 1. Six Major Classes of Conopeptides and Their Disulfide Connectivity

α-conopeptides (2 loop framework peptides that inhibit nicotinic acetylcholine receptors)		
GI	E C C N – P A C G R H Y S – – C*	
GIA	E C C N – P A C G R H Y S – – C G K*	
GII	E C C H – P A C G K H F S – – C*	
MI	G R C C H – P A C G K N Y S – – C*	
SI	I C C N – P A C G P K Y S – – C*	
SIA	Y C C H – P A C G K N F D – – C*	C C..C...C
SII	G C C C N O A C G P B Y G – – C G T S C S	
PnIA	G C C S L P P C A A N N P D Y C*	
PnIB	G C C S L P P C A L S N P D Y C*	
ImI	G C C S D P R C A W R – – – – C*	
EI	R D O C C Y H P T C N M S N P Q I C*	
MII	G C C S N P V C H L E H S N L C*	
EpI	G C C S D P R C N M N N P D Y (SO_4)C*	
AuIB	G C C S Y P P C F A T N P D – C	
μ-conopeptides (3 loop framework that block sodium channels)		
GIIIA	R D C C T O O K K C K D R Q C K O Q R C C A*	C C.C...C.C C
GIIIB	R D C C T O O R K C K D R R C K O M K C C A*	
GIIIC	R D C C T O O K K C K D R R C K O L K C C A*	
PIIIA	R L C C G F O K S C R S R Q C K O H R C C*	
ω-conopeptides (4 loop framework peptides that block calcuim channels)		
GVIA	C K S O G S S C S O T S Y N C C – R S C N O Y T K R C Y	
GVIB	C K S O G S S C S O T S Y N C C – R S C N O Y T K R C Y G*	
GVIC	C K S O G S S C S O T S Y N C C – R S C N O Y T K R C*	
SVIA	C R S S G S O C G V T S I – C C G R – C – – Y R G K C T*	
SVIB	C K L K G Q S C R K T S Y D C C S G S C G R S – G K C*	C...C..CC.C..C
GVIIA	C K S O G T O C S R G M R D C C – – S C L L Y S N K C R R Y*	
GVIIB	C K S O G T O C S R G M R D C C T – S C L S Y S N K C R R Y*	
MVIIA	C K G K G A K C S R L M Y D C C T G S C R S – – G K C*	
MVIIB	C K G K G A S C H R T S Y D C C T G S C N R – – G K C*	
MVIIC	C K G K G A P C R K T M Y D C C S G S C G R R – G K C*	
MVIID	C Q G R G A S C R K T M Y N C C S G S C N R – – G R C*	
TVIA	C L S O G S S C S O T S Y N C C – R S C N O Y S R K C Y*	
δ-conopeptides (4 loop framework peptides that delay inactivation of sodium channels)		
TxVIA	W C K Q S G E M C N L L D Q N C C D G Y – C I V L V C T	
TxVIB	W C K Q S G E M C N L L D Q N C C D G Y – C I V F V C T	C...C..CC.C..C
GmVIA	V K P C R K E G Q L C D P I F Q N C C R G W N C – V L F C V	
NgVIA	S K C F S O G T F C G I K O G L C C S V R – C F S L F C I S F E	
PVIA	E A C Y A P G T F C G I K O G L C C S E F – C L P G V C F G*	
κ-conopeptides (4 loop framework pepetide that blocks Shaker potassium channels)		
PVIIA	C R I O N Q K C F Q H L D D C C S R K C N R F N K C V	C...C..CC.C..C
conantokins (helical peptides that inhibit the NMDA-glutamate receptor)		
Con-G	G E Z Z L Q Z N Q Z L I R Z K S N	
Con-T	G E Z Z Y Q K M L Z N L R Z A E V K K N A	

Amino acid sequences shown with cysteines (bold) aligned within each structural framework.
*Processed carboxyl terminal; O = hydroxyproline residue, Z = γ-carboxyglutamic acid residue. Letter prefixes indicate conopeptides from the fish hunters *C. magus* (M), *C. geographus* (G), *C. tulipa* (T), *C. striatus* (S), *C. purpurascens* (P), and *C. ermineus* (E); the mollusc hunters *C. textile* (Tx), *C. episcopatus* (Ep), *C. gloriamaris* (Gm), *C. nigropunctatus* (Ng), and *C. aulicus* (Au); and the worm hunter *C. imperialis* (Im).

sociation to locate the labeled cysteine residues and hence deduce the disulfide bond connectivity pattern.

Conotoxins are synthesised by cone shells from mRNA templates derived from toxin genes, and expressed in the venom ducts as precursor peptides. There are now numerous gene cloning techniques that can be used to isolate and characterise the precursor molecules, as a prelude to predicting the composition of the mature peptide. The mRNA can be isolated and converted to either single-stranded (ss) or double-stranded (ds) complementary DNA (cDNA). Cloning of the ds-cDNA produces a venom duct library, which can be screened with DNA probes from known toxin mature peptide sequence or precursor peptide sequence to find closely related clones. This strategy was successfully used to isolate and define the precursor structure of the ω-conotoxin GVIA from a *C. geographus* library [Colledge et al., 1992]. An alternative approach is to make use of polymerase chain reaction (PCR) technologies. In this method, oligonucleotide primers homologous to known mature peptide sequence

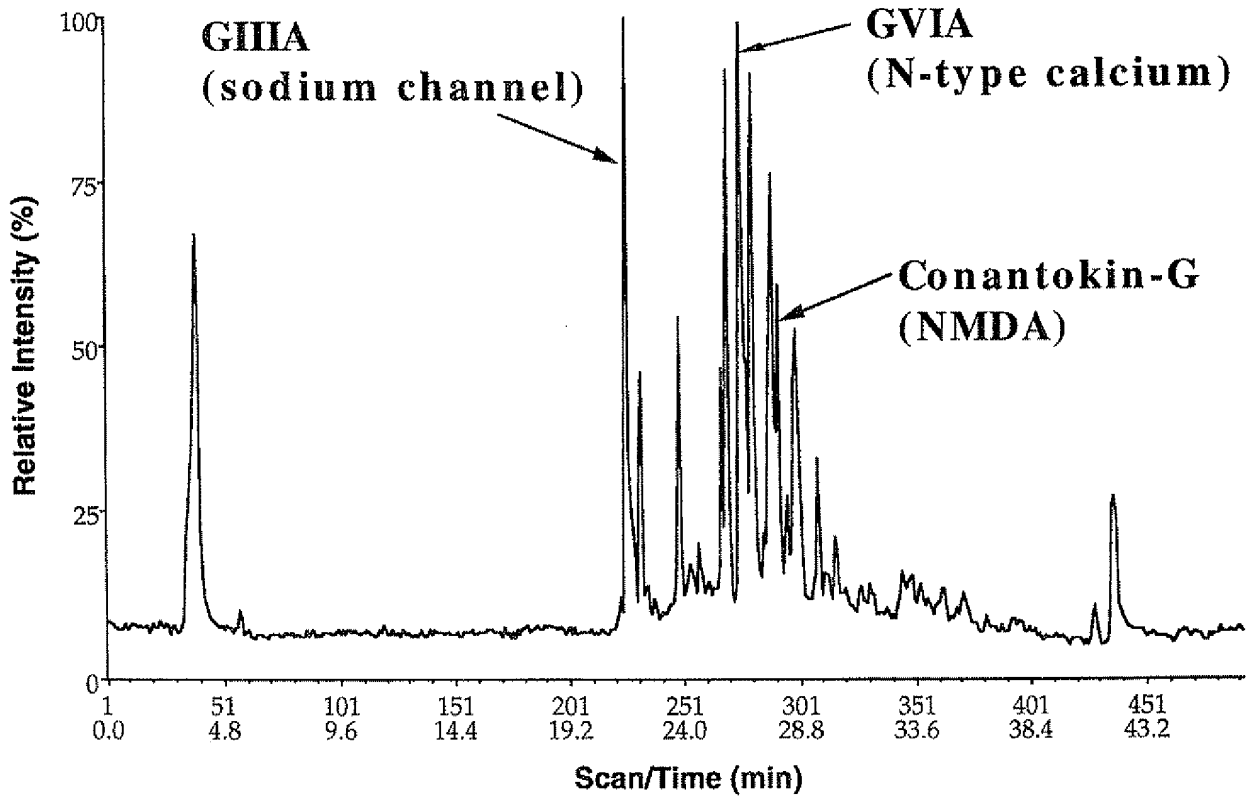

Fig. 2. LC-MS chromatogram of *Conus geographus* venom. Reverse-phase HPLC/mass spectrometry profile of the crude venom from *Conus geographus* collected on the Great Barrier Reef, Australia. Conotoxins which target sodium channels (GIIIA), N-type calcium channels (GVIA), and the NMDA receptor (conantokin G) are indicated.

can be used to derive 5′ leader propeptide and untranslated sequence using adaptor ligated ds-cDNA (5′RACE). This sequence can then be used to identify conserved regions in the precursor leader sequences in which to position oligonucleotide primers that are specific to conopeptide families. PCR using these specific primers in conjunction with a 3′ anchor primer on venom duct ss-cDNA will produce amplified copies of the expressed peptides in that particular family (3′ RACE). Cloning and sequencing will produce the full peptide sequence, from which the mature peptide region can be predicted. Apart from the targeted approaches of the library and PCR strategies, the complete screening of venom duct cDNA libraries in a manner similar to an EST (expressed sequence tag) strategy is quite feasible and very productive. Most conopeptide sequences are less than 1,000 nucleotides, allowing complete sequencing of each peptide gene simply by using primer sites based on the vector sequence of the clones. While the molecular cloning methods of conotoxin isolation does have a number of distinct benefits in comparison to assay directed fractionation of whole venom, they have the disadvantage of not being able to predict posttranslational modifications of the mature peptides. Conopeptides can be highly and unusually modified, such as the alpha peptide EpI, which has a sulphated tyrosine [Loughnan et al., 1998]. These modifications provide chemical alterations that may well be important in the activity of the conopeptide at the receptor target. At present, the gene structures that combine to produce a toxin peptide precursor mRNA transcript are not known. The identification of these genes and the mRNA splicing pathways that ultimately produce the highly variable toxin peptides will provide a much better understanding of toxin peptide evolution in the *Conus* species, and will undoubtedly lead to more effective strategies for library-based and PCR-based toxin peptide isolation.

CONOTOXIN SYNTHESIS, FOLDING, AND PURIFICATION

All conotoxins described to date, with the exception of the conantokins, contain multiple disulfide bonds. Unlike studies on other animal toxins (e.g., snakes, scorpions), both the complexity of the venom and the small quantities available (usually micrograms) preclude in-depth studies on the native material. Solid phase pep-

tide synthesis has been the most successful approach in providing significant quantities of these peptides for biological and structural studies. Most often this has been achieved through synthesis of the fully reduced polypeptide before "folding" under oxidative conditions. Although this approach yields the desired peptide, in many instances it is present in a mixture of other "wrongly" or partially folded isomers. The nonnative isomers differ solely in the connectivity of their disulfide bridges and can be difficult to separate from the native material, leading to reduced yields of pure conopeptide.

Directed Folding

Conotoxin GI is part of the α-conotoxin family and contains 13 residues with two intramolecular disulfide bridges. Various oxidative techniques on fully reduced α-conotoxin GI yield mixtures of all three potential isomers with the native isomer α-CTX GI(2-7;3-13) generally predominating. We recently described an on-resin "directed-disulfide" strategy to gain access to each isomer [Alewood, 1998]. This is illustrated in the directed synthesis of the native isomer (Fig. 3). The orthogonal protecting groups acetomidomethyl (Acm) and fluorenylmethyl (Fm) were chosen to allow stepwise regiospecific disulfide formation on the resin. Chain assembly was performed using standard Boc chemistry [Schnölzer et al., 1992] on *p*-methylbenzhydrylamine resin. The Fm group was removed and oxidised with piperidine-DMF. Deprotection and oxidation of the Acm group by iodine in DMF led to the formation of the second disulfide bond. Final HF cleavage led to deprotected "crude" conotoxin containing minor amounts of polymer. Reversed-phase

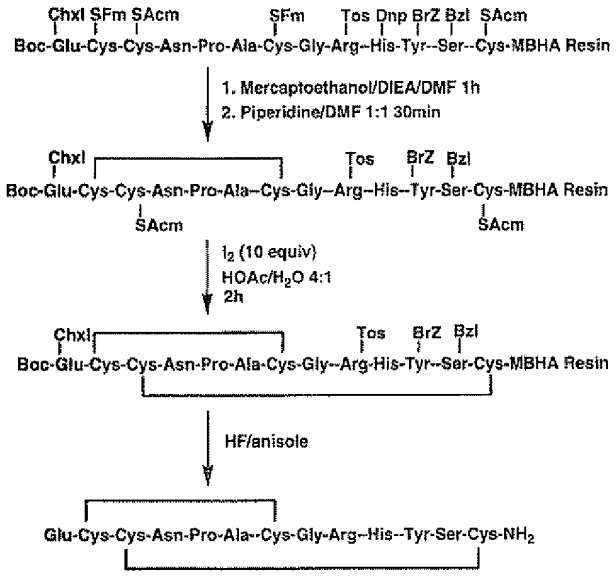

Fig. 3. Directed folding of α-conotoxin GI.

HPLC analysis confirmed that only the native isomer was formed. The two nonnative isomers of α-conotoxin GI were made employing a similar strategy.

Rapid Solid Phase Peptide Synthesis (SPPS)

A bottleneck in structure–function studies of the conotoxins has been the availability of the desired mutants within a reasonable time frame. The small number of such studies reflects, in part, the difficulties in the synthesis and folding of these cysteine-rich frameworks. As such there is a pressing need to develop faster, more efficient chemistry.

In recent years, there have been efforts [Schnölzer et al., 1992; Alewood et al., 1997] by several groups to improve the speed and efficiency of SPPS. The introduction of HBTU/in situ neutralisation chemistry has allowed routine synthesis where three residues per hour are incorporated in the growing peptide chain. The further development of improved acylating agents such as HATU has opened up the possibility of more rapid synthetic procedures using HATU/Boc in situ neutralization [Alewood et al., 1997]. This is illustrated by the rapid chain assembly of the A10L mutant of PnIA conotoxin from *Conus pennaceus*, which blocks the nicotinic acetylcholine receptor. The conotoxin was assembled in a little over 1 h, worked up, and oxidised to give fully folded homogeneous material within a day.

Conotoxin Folding

Most reduced forms of native conotoxins are capable of folding efficiently. The folding/oxidation thus remains a matter of probing sufficient "folding" space so that the desired conotoxin forms uniquely or as the predominant product. Whereas many laboratories have the capacity to isolate quantities of the reduced purified precursors, their efforts at the "folding" stage have often been inadequate. This may be a direct result of not having access to native material for comparison. This is particularly important in cases where the disulfide bond connectivity of the conotoxin has not been unambiguously determined.

More specifically, the folding of ω-conotoxins has caused difficulties in several laboratories where nonnative isomers have formed a significant proportion of the oxidised products. This is readily illustrated in the folding of the N-type neuronal calcium channel blocker, GVIA (Fig. 4), where the selection of inappropriate though commonly used folding conditions (trace E) led exclusively to nonnative products. Moreover, the selection of "appropriate" folding conditions (trace A) yielded almost exclusively the correctly folded native conotoxin.

STRUCTURE DETERMINATION OF CONOTOXINS BY NMR

NMR spectroscopy is now a well-established method for structure determination of peptides and pro-

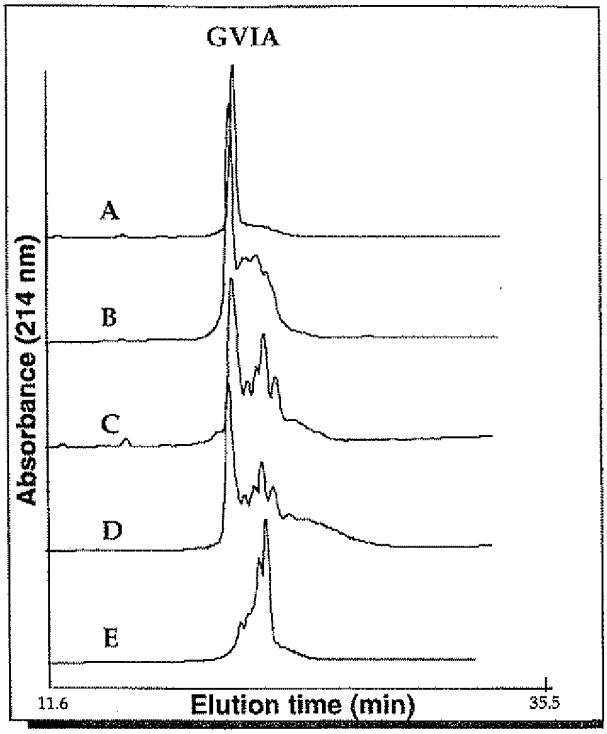

Fig. 4. Folding of ω-conotoxins GVIA under different oxidation conditions.

	Buffer	Peptide Conc (mM)	GSH/GSSG	pH
A	NH_4Oac/GnHCl (0.33M/0.5M)	0.05	100:10	7.8
B	NH_4Oac/GnHCl (0.33M/0.5M)	0.05	–	7.8
C	NH_4Oac/GnHCl (0.33M/0.5M)	0.19	100:10	7.8
D	NH_4Oac/GnHCl (0.33M/0.5M)	0.19	–	7.8
E	NaOAc (50mM)	0.05	–	7.5

*Note that the buffer used in A gave the best results and buffer E was poorest.

teins. The method relies on the measurement of a large number of distance restraints between pairs of protons. These restraints are used in a simulated annealing protocol to calculate a family of structures consistent with both the input restraints and with a force-field defining covalent geometry of atoms. Distance restraints are often supplemented with restraints on peptide backbone and sidechain dihedral angles. The distance restraints are derived from NOESY spectra and the dihedral restraints from a combination of coupling constant and NOE data. Depending on the size of the protein being studied and the complexity of the spectra, 2D, 3D, or 4D NMR methods may be required. The higher dimensional spectra (i.e., 3D or 4D) generally require uniform labeling of the protein with ^{15}N and/or ^{13}C isotopes so that spectral overlap may be resolved using the additional frequency dimensions associated with these NMR active nuclei, as well as the usual proton chemical shift axis.

An assumption inherent in the NMR structure determination method is that the peptide or protein adopts predominantly a single conformation in solution. For linear peptides comprising fewer than approximately 30 amino acid residues this is often not the case, with such small peptides being extremely flexible and adopting a myriad of conformations in solution. Thus, for these peptides only qualitative conclusions can be drawn about solution conformations. However, peptides which are cross-linked by disulfide bonds are more restrained in their conformations and are very suitable for quantitative structure determination by NMR. As indicated above, the conotoxins are rich in disulfide bonds and are hence particularly amenable to conformational analysis by NMR.

An additional advantage of conotoxins is that their small size (generally less than 30 residues) means that spectral overlap is generally not a problem, and 2D rather than 3D or 4D NMR methods are sufficient for spectral assignment and structure determination. Because isotopic labeling is not required for such studies, it is in principle possible to determine structure from native peptides extracted from venom ducts. However, in practice the amounts of material required (~1 mg) generally means that it is more convenient to synthesise the conotoxins using the methods described above.

Over the last few years we have determined the structures of more than 30 conotoxins (from all the known classes and from novel ones as yet unreported) and are using these structures in several drug design programs. From these studies, and from studies by colleagues in the literature, it has become clear that conotoxin structures fall into a limited number of families. Representatives of these structural families are summarised in Figure 5.

From these structures it can be seen that the α-conotoxins adopt a fold such that the N- and C-termini are brought into close proximity by the internal disulfide bonds, and that a short helical segment is present. By contrast, the structures of the μ-, κ-, and ω-conotoxins are dominated by a series of loops which are superimposed on a core comprising well-defined elements of secondary structure. For the μ-conotoxins these secondary structure elements include a helical region and a β-hairpin, while the κ- and ω-conotoxins contain a triple-stranded β-sheet. The conantokins have no disulfide bonds, but adopt helical structures [Skjaerbaek et al.,

Fig. 5. Three-dimensional structures of several classes of conotoxins recently determined in our laboratory. The backbone folds are represented by tubular ribbons, with sidechains shown in stick form. Nitrogen sidechain atoms are shown in blue, oxygen atoms are in red, and the sulfur atoms of cysteine residues are in yellow.

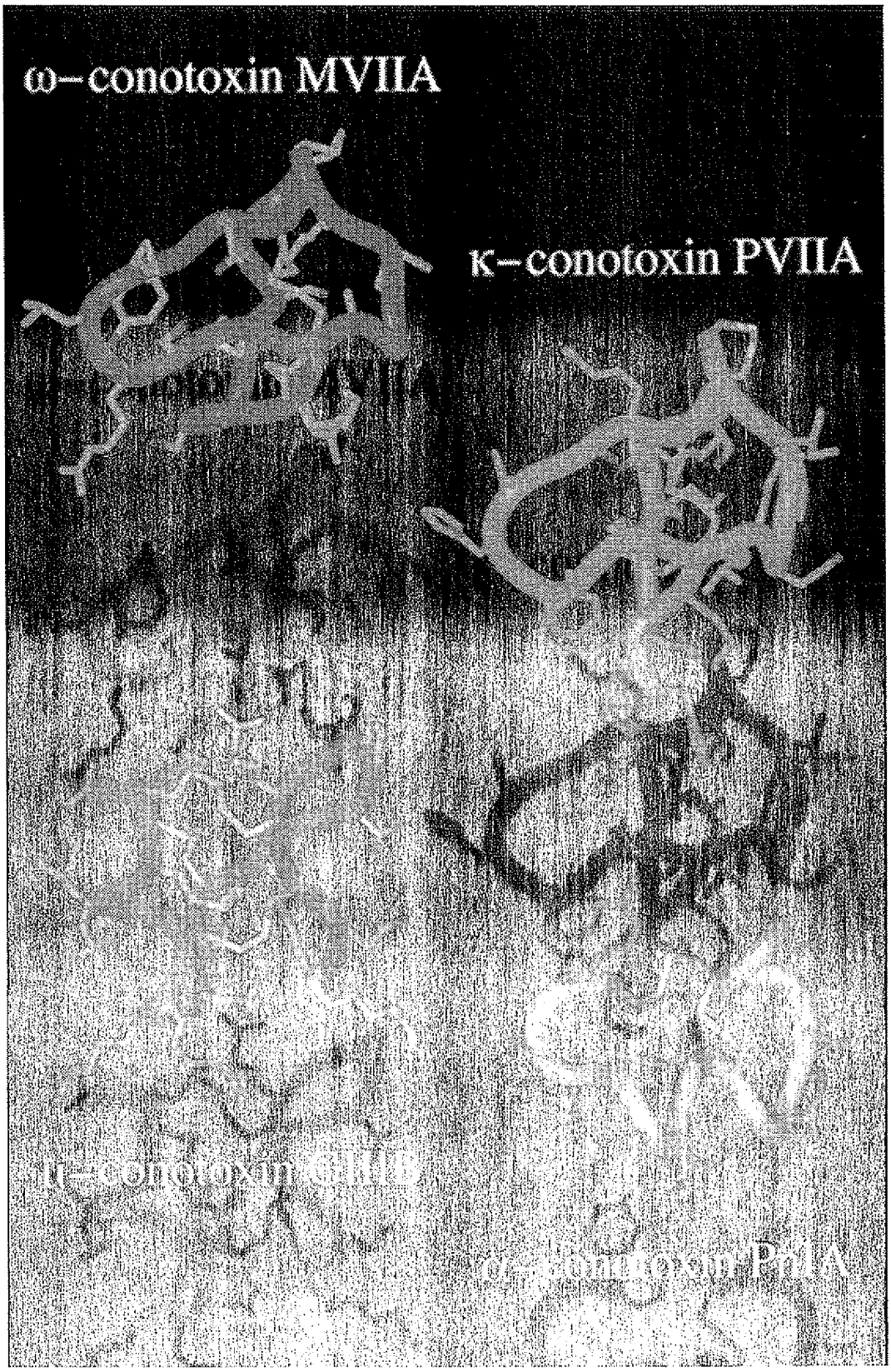

Figure 6.

1997]. We return later to a more extensive discussion of specific details of some of these structures, but emphasise here that the conotoxins clearly may be regarded as "mini-proteins" and adopt well-defined solution structures with all of the features of larger proteins. The defined presentation of amino acids on the surface of the frameworks in Figure 5 accounts for the specificity of their binding interactions and the small size of the molecules makes them valuable lead compounds in drug design applications.

Conotoxins Which Block the Nicotinic ACh Receptor

There are several classes of ligands that bind to the nAChR. These comprise small molecules, such as the endogenous ligand agonist acetylcholine, small peptides, including the lophotoxins and α-conotoxins, and large peptide toxins isolated from snake venoms (e.g., α-bungarotoxin). The α-conotoxins are widespread in the venoms of cone snails and have been isolated from piscivorous, molluscivorous, and vermivorous species [Gray et al., 1981; McIntosh et al., 1982, 1994; Zafaralla et al., 1988; Myers et al., 1991; Ramilo et al., 1992; Fainzilber et al., 1994; Martinez et al., 1995; Loughnan et al., 1998]. These toxins are valuable ligands for probing structure–function relationships of various nAChR subtypes as they are potent antagonists and exhibit marked selectivity between the peripheral and neuronal forms of the receptor. Typically, the α-conotoxins are 12–18 residues in length and are characterised by the presence of two conserved disulfide bonds and two loops in the peptide backbone between the cysteines. The number of amino acids in these two intra-cysteine loops varies, giving rise to the α3/5, α4/7, and α4/3 subclasses of α-conotoxins.

The affinity of a given α-conotoxin depends both on the species and the subtype of nAChR present. The first α-conotoxins discovered were found to bind to the muscle-type nAChR (e.g., α-conotoxin GI) through a highly selective interaction at the α–δ over the α–γ subunit interface [Hann et al., 1994; Groebe et al., 1995]. Recent studies have described the isolation and characterisation of α-conotoxins selective for *neuronal* nAChRs and the molecular basis of the interaction of these α-conotoxins with the nAChR is beginning to be revealed. For example, α-conotoxin ImI selectively targets the homomeric α7 and α9 subtypes of neuronal nAChR [Johnson et al., 1995], whereas α-conotoxin MII was found to potently block α3β2 nAChRs expressed in *Xenopus* oocytes with an IC_{50} of 0.5 nM [Cartier et al., 1996; Harvey et al., 1997]. The structure of MII differs significantly from the other α-conotoxins; however, the disulfide bonding is conserved and it has the α 4/7 spacing like α-conotoxins PnIA, PnIB, and EpI. α-Conotoxins PnIA and PnIB from *C. pennaceus* have been reported to have a different phylogenic specificity compared to the other α-conotoxins, in that they block neuronal nAChRs in molluscs [Fainzilber et al., 1994]. However, in preliminary experiments on dissociated rat parasympathetic neurones, we found that α-conotoxins PnIA[A10L] and PnIB (0.1–1 μM) inhibit the α-bungarotoxin-sensitive component of the ACh-evoked current [Hogg et al., 1999], and identified EpI as a new selective neuronal nAChR antagonist [Loughnan et al., 1998]. We believe that the growing diversity of α-conotoxins in terms of their selectivity, not only between muscle and neuronal nAChR subtypes but between neuronal α subunits, will provide the molecular tools needed to probe and distinguish between neuronal nAChR subtypes so that their distinct function(s) can be understood.

As a result of recent studies in our laboratories, X-ray crystal structures have been determined for GI [Guddat et al., 1996], PnIA [Hu et al., 1996], and PnIB [Hu et al., 1997], EpI [Hu et al., 1998], ImI and SII (unpublished structures). Combined with NMR solution structures of a similar range of α-conotoxins, they provide initial insights into the putative binding surface of these peptides. Comparison of the published structures of the α-conotoxins indicates that their backbones are superimposable. This structural consensus allows us to model differences in specificity and potency for AChRs with differences in the position of exposed sidechains in the α-conotoxins. From this analysis we will identify residues important for selectivity, allowing us to design new selective α-conotoxins. To illustrate recent work from our laboratory in this class of conotoxins, we describe studies on conotoxin GI, the first and one of the smallest α-conotoxins to be discovered, and on MII, a recently discovered member of the family with selectivity of neuronal nAChRs. The sequence and characteristics of these peptides are given in Table 2.

Conotoxin GI

Our interest in GI has focused on its use as a model to explore conformational diversity resulting from disulfide bond engineering. As already noted, conotoxins are characterised by their particularly high content of cysteine, with the cysteine residues almost invariably connected in pairs to form disulfide bonds. In peptide toxins, even more so than in larger proteins, these disulfide bonds have a crucial bearing on three-dimensional structure and function. As the number of cysteine residues in a peptide increases, the number of ways of connecting the cysteines in disulfide bonds increases dramatically, leading to a large number of potential isomers. It is interesting and highly significant that invariably only one of the possible isomers occurs naturally, i.e., venoms do not nor-

TABLE 2. α-Conotoxin Sequences and Specificities

Name	Sequence	Loop sizes	Species	Prey	nAChR target	Reference
GI	ECCNPACGRHYSC-NH_2	3:5	*C. geographus*	fish	α/δ	Gray et al., 1981; Groebe et al., 1997
GIA	ECCNPACGRHYSCGK-NH_2	3:5	*C. geographus*	fish		Gray et al., 1981
GII	ECCHPACGKHFSC-NH_2	3:5	*C. geographus*	fish		Gray et al., 1981
MI	G RCCHPACGKNYSC-NH_2	3:5	*C. magus*	fish	α/δ	McIntosh et al., 1982; Groebe et al., 1995
SIA	YCCHPACGKNFDC-NH_2	3:5	*C. striatus*	fish		Ramilo et al., 1992
SI	ICCNPACGPKYSC-NH_2	3:5	*C. striatus*	fish	α/δ	Zafaralla et al., 1988; Groebe et al., 1995
SII	GCCCNPACGPNYGCGTSCS	3:5:3	*C. striatus*	fish		Ramilo et al., 1992
ImI	GCCSDPRCAWRC-NH_2	4:3	*C. imperialis*	worm	α7	McIntosh et al., 1994
MII	GCCSNPVCHLEHSNLC-NH_2	4:7	*C. magus*	fish	α3β2	Cartier et al., 1997; Harvey et al., 1997
EI	RD OCCYHPTCNMSNPQIC-NH_2	4:7	*C. ermineus*	fish		Martinez et al., 1995
AulA	GCCSYPPCFATNSDYC-NH_2	4:7	*C. aulicus*	mollusc	α3β4	Luo et al., 1998
AulB	GCCSYPPCFATNPDC-NH_2	4:6	*C. aulicus*	mollusc	α3β4	Luo et al., 1998
AulC	GCCSYPPCFATNSGYC-NH_2	4:7	*C. aulicus*	mollusc	α3β4	Luo et al., 1998
EpI	GCCSDPRCNMNNPDY (SO_4)C-NH_2	4:7	*C. episcopatus*	mollusc	α3β; α3β4	Loughnan et al., 1998
PnIA*	GCCSLPPCAANNPDYC-NH_2	4:7	*C. pennaceus*	mollusc		Fainzilber et al., 1994
PnIB*	GCCSLPPCALSNPDYC-NH_2	4:7	*C. pennaceus*	mollusc	α7	Fainzilber et al., 1994
αA-PIVA	GCCGSYONAACHOCSCKDROSYCGQ-NH_2	7:2:1:6	*C. purpurascens*	fish	α/δ; α/γ	Hopkins et al., 1995
αA-EIVA	GCCGPYONAACHOCGCKVGROOYCDROSGG-NH_2	7:2:1:7	*C. ermineus*	fish	α/δ; α/γ	Jacobsen et al., 1997
αA-EIVB	GCCGKYONAACHOCGCTVGROOYCDROSGG-NH_2	7:2:1:7	*C. ermineus*	fish	α/δ; α/γ	Jacobsen et al., 1997

*PnIA and PnIB have been shown to target neuronal nAChRs of molluscs and, more recently, PnIA[A10L] and PnIB have been reported to block the mammalian α7 nAChR subunit [Hogg et al., 1999].

mally contain different isomers of the same conotoxins with different connections of the disulfide bonds. However, using solid phase chemical methods it is possible to selectively produce each of the individual disulfide bond isomers. As noted in a section above, we used this approach to synthesise all three possible disulfide bond isomers of the α-conotoxin GI and have determined their structures [Gehrmann et al., 1998]. We refer to the three isomers as GI(2-7;3-13), GI(2-13;3-7), and GI(2-3;7-13).

The structural findings may be summarised by noting that the native connectivity of the four constituent cysteine residues produces a significantly more stable and well defined structure than either of the two alternative arrangements of the disulfide bonds [Gehrmann et al., 1998]. A single solution conformation was detected for the native isomer, GI(2-7;3-13), which consists primarily of a distorted 3_{10} helix from residues 5 to 11. The two nonnative forms exhibit multiple conformations in solution, with the major populated forms being different in structure both from each other and with the native form. We concluded that the disulfide bonds in GI play a major role in determining both the structure and stability of the peptide. A trend for increased conformational flexibility was observed in the order GI(2-7;3-13) < GI(2-13;3-7) < GI(2-3;7-13).

Interest in making nonnative isomers arises because peptide analogues are widely regarded as valuable drug leads, and in recent years there has been much effort directed towards the development of peptide libraries. It has been of particular interest to develop methods to increase the surface variability of peptides because the diversity of peptide libraries are, to some extent, limited by the use of the 20 natural amino acids. The study described above shows that the use of alternative disulfide bond connectivities provides another way of altering molecular conformations without modifying the sequence.

Conotoxin MII

The recently identified α-conotoxin MII from *C. magus* belongs to the α4/7 subclass and is a potent and highly specific blocker of mammalian neuronal nAChRs composed of α3β2 subunits. MII was first reported by Cartier et al. [1996] following the electrophysiological screening of RP-HPLC fractions of duct venom against cloned nAChRs expressed in *Xenopus* oocytes. We independently isolated and characterised MII as part of a comprehensive study of the milked venom of *C. magus* and recently reported its three-dimensional structure [Hill et al., 1998].

The molecule folds into a highly compact globular structure consisting of a central region of α-helix and a series of overlapping β-turns at the N- and C-termini. The α-helix comprising residues 6–12 exhibits two turns and is amphipathic, with Cys8, His9, Glu11, and His12 on one side and Pro6, Val7, and Leu10 on the other. Remarkably, the hydrophobic residues of the α-helix are more exposed to the solvent than the charged/hydrophilic residues. However, this is consistent with the fact that MII is more hydrophobic when oxidised than in the reduced form. Hydrophilic residues on the surface include Ser4, Asn5, and residues Glu11, His12, Ser13, and Asn14. The latter patch, comprising residues with both polar and charged groups (Glu11-Asn14), may be responsible for initial recognition by the nAChR, with further stabilisation of binding provided by the proximal hydrophobic residues. Analysis of the solvent accessibility of individual residues provides support for Pro6, Val7, Leu10, Glu11, and Asn 14 as potential residues for interaction with the nAChR as they are highly solvent exposed [Hill et al., 1998].

Sodium Channel Binding Conotoxins

The piscivorous cone snail, *C. geographus*, produces polypeptide neurotoxins that specifically inhibit skeletal muscle and eel electroplax sodium channels [Sato et al., 1983; Cruz et al., 1985; Yanagawa et al., 1988; Moczydlowski et al., 1986]. These toxins, the μ-conotoxins and conotoxin GS, are attractive probes of sodium channel structure because of their high binding affinity and ability to discriminate between the skeletal muscle and neuronal and cardiac channel isoforms [Yanagawa et al., 1988; Moczydlowski et al., 1986; Ohizumi et al., 1986; Chen et al., 1992]. It is remarkable that while these peptides belong to the same pharmacological class they have different structural frameworks, as illustrated in Table 1.

The μ-conotoxins, a family of highly basic 22-residue polypeptides (GIIIA, GIIIB, and GIIIC), contain six cysteine residues which are paired in a 1–4, 2–5, 3–6 pattern to form three intramolecular disulfide bonds and a three-loop framework. Conotoxin GS has a strikingly different sequence and is 50% larger than the μ-conotoxins. This polypeptide contains six cysteine residues arranged in a similar 1–4, 2–5, 3–6 pattern [Nakao et al., 1995]; however, differences in the spacings between cysteine residues results in a four-loop framework rather than a three-loop framework. Despite the low sequence identity, conotoxin GS binds competitively with μ-conotoxin GIIIA, suggesting overlapping binding sites on the extracellular surface of skeletal muscle and eel electroplax sodium channels [Yanagawa et al., 1988].

Conotoxin GIIIB

GIIIB adopts a compact structure [Hill et al., 1996] consisting of a distorted 3_{10}-helix, a small β-hairpin, a cis-hydroxyproline, and several turns. The molecule is stabilised by three disulfide bonds, two of which connect the helix and the β-hairpin, forming a structural core with similarities to the CSαβ motif [Cornet et al., 1995].

This motif is common to several families of small proteins, including scorpion toxins and insect defensins. Other structural features of GIIIB include the presence of eight arginine and lysine sidechains that project into the solvent in a radial orientation relative to the core of the molecule. These cationic sidechains form potential sites of interaction with anionic sites on sodium channels. The global fold is similar to that reported for μ-conotoxin GIIIA, and together the structures provide a basis for further understanding of the structure–activity relationships of the μ-conotoxins and for their binding to skeletal muscle sodium channels.

Conotoxin GS

The three-dimensional structure of conotoxin GS [Hill et al., 1997] consists of a compact, disulfide-bonded core from which several loops and the C-terminus project. The main element of secondary structure is a double-stranded antiparallel β-sheet comprising residues 17–20 and 26–29 connected by a turn involving residues 21–25 to give a β-hairpin structure. A further peripheral β-strand involving residues 7–9 is almost perpendicular to the β-hairpin, with only Ser7 hydrogen-bonded to the central β-strand forming an isolated β-bridge.

GS is unusual in that it contains the posttranslationally modified residue γ–carboxy glutamic acid. To investigate the role of Gla32 in this polypeptide, an analog [Glu32]conotoxin GS was synthesised and the NMR spectra compared with those of conotoxin GS. The chemical shift differences for the backbone Hα and NH protons of conotoxin GS and [Glu32]conotoxin GS were small (≤0.05 ppm), suggesting that the backbone conformation of the two peptides is essentially identical. Several other parameters, including the observed NOEs, $^3J_{NH\text{-}H\alpha}$ coupling constants and amide exchange rates are similar, providing further evidence of conserved structure in these peptides. This suggests that the Gla residue does not play a role in modulating the three-dimensional structure of conotoxin GS.

As the sequence and structure of conotoxin GS is quite different from the μ-conotoxins, it provides a valuable new probe for further characterisation of sodium channel geometry. The structure of conotoxin GS will facilitate the design of analogues to define the binding surface and to undertake complementary mutagenesis on the sodium channel to identify the interacting residues. These experiments with conotoxins may prove as useful in modeling the outer vestibule of sodium channels as the peptide toxins from scorpions have been for potassium channels.

Calcium Channel Blocking Conotoxins

The ω-conotoxins are a set of structurally related peptides that have a wide range of specificities for different subtypes of the voltage-sensitive calcium channel (VSCC). To understand their VSCC subtype differentiation, we studied the structure of two naturally occurring ω-conotoxins, MVIIA (specific to N-type VSCCs) and SVIB (specific to P/Q-type) and a synthetic hybrid, SNX-202, which has altered specificities to both VSCC subtypes [Nielsen et al., 1996]. The secondary structures of the three peptides are almost identical, consisting of a triple-stranded β-sheet and several turns. The three-dimensional structures of SVIB and MVIIA are likewise quite similar, but some subtle differences are manifested as orientational differences between two key loops.

A remarkable feature of the six cysteine / four-loop framework exemplified by the ω-conotoxins is the presence of a cystine knot within the structures. This motif consists of an embedded loop in the structure formed by two of the disulfide bonds and their connecting backbone segments. This loop is penetrated by the third disulfide bond in a remarkable example of Nature's engineering designs.

Although the structural rigidity of the core of MVIIA is apparently assured by the knotted disulfide structure, we used NMR to probe for possible conformational flexibility in the exposed loops. As indicated above, it is important be aware of potential conformational changes that might affect receptor binding. In the case of MVIIA, the H^{α} shifts were found to be similar in a range of solvents, indicating that there are no solvent-induced changes in structure.

From the above structural studies and a large number of other studies of molecules within this family it is apparent that the ω-conotoxins form a consensus structure despite differences in sequence and VSCC subtype specificity. This indicates that the ω-conotoxin macrosites for the N/P/Q-subfamily of VSCCs are related, with specificity for receptor targets being conferred by the positions of functional sidechains on the surface of the peptides.

As mentioned earlier, the ω-conotoxins have attracted the most interest for potential pharmaceutical applications. Indeed, conotoxin MVIIA is currently in clinical trial for the treatment of chronic pain. Structural studies of the type described above are likely to lead to the development of second-generation analogues which may overcome some of the side effects of MVIIA itself.

Potassium Blocking Conotoxins

κ-PVIIA is a 27-residue polypeptide isolated from the venom of *C. purpurascens* and is the first member of a new class of conotoxins that block potassium channels. By comparison to other ion channels of eukaryotic cell membranes, voltage-sensitive potassium channels are relatively simple and methodology has been developed for mapping their interactions with small peptide toxins. PVIIA, therefore, is a valuable new probe of potassium channel structure. In a recent study, we determined the solution

structure and mode of channel binding of PVIIA [Scanlon et al., 1997] and this forms the basis for mapping the interacting residues at the conotoxin–ion channel interface.

The three-dimensional structure of PVIIA resembles the triple-stranded β-sheet / cystine knot motif formed by a number of toxic and inhibitory peptides, including the ω-conotoxins and conotoxin GS, as described above. Subtle structural differences, however, predominantly in loops 2 and 4, are observed between PVIIA and other conotoxins with similar structural frameworks. Electrophysiological binding data suggest that PVIIA blocks K^+ channel currents by binding in a voltage-sensitive manner to the external vestibule and occluding the pore. Comparison of the electrostatic surface of PVIIA with that of the well-characterised potassium channel blocker charybdotoxin suggested a likely binding orientation for PVIIA. Although the structure of PVIIA is considerably different from that of the αK scorpion toxins, it has a similar mechanism of channel blockade. On the basis of a comparison of the structures of PVIIA and charybdotoxin, we suggested that Lys 19 of PVIIA is the residue responsible for physically occluding the pore of the potassium channel.

Common Structural Frameworks.

From the studies described above it has become clear that conotoxins with the six cysteine / four-loop framework are the most abundant group of peptides isolated from *Conus* venoms so far. This structural class encompasses at least five known pharmacological classes: ω-conotoxin calcium channel blockers, δ-conotoxins which inhibit the inactivation of sodium channels, κ-conotoxin PVIIA which blocks potassium channels, the sodium channel blocker conotoxin GS, and two peptides recently found in *C. marmoreus* that affect both sodium and calcium currents [Myers et al., 1993; Cruz, 1996; Terlau et al., 1996]. The solution structures of several of these classes have now been determined, including the ω-conotoxins, κ-conotoxin, and GS, and all contain a triple-stranded antiparallel β-sheet with $+2x$, -1 topology and cystine knot motif common to that observed in a number of toxic and inhibitory peptides [Pallaghy et al., 1994; Narasimhan et al., 1994].

Thus, there are now many examples where one structural framework is associated with different pharmacological activities. Interestingly, the converse also occurs; that is, the same pharmacological activity may be associated with completely different structural frameworks, as demonstrated, for example, with the studies described above on the μ-conotoxins and conotoxin GS.

CONCLUSIONS

Conotoxins provide a vast library of peptides with unique abilities to discriminate among types and subtypes of ion channels in a manner that is unmatched by the typical small molecule drugs which dominate the pharmaceutical industry. In addition, cone venom peptides are small and inherently stable, making them ideal leads for peptide therapeutics, especially ion channel therapeutics. The high structural resolution now obtained with modern NMR spectroscopy and X-ray crystallography provides emerging opportunities to use conotoxins as templates for the design of smaller peptidomimetics that incorporate the selectivity and potency of conotoxins. Because of its selectivity and potency, ω-conotoxin MVIIA (Ziconotide) is being developed as a drug for the treatment of chronic pain. Conotoxins continue to be discovered that define new pharmacological targets. With improvement in methods of delivering peptides, it is anticipated that conopeptides can be modified for effective oral delivery.

ACKNOWLEDGMENTS

DJC is an Australian Research Council Professorial Fellow. We thank our colleagues at the University of Queensland who were involved in various aspects of these studies: Michael Dooley, John Gehrmann, Justine Hill, Kathy Nielsen, Martin Scanlon, Marion Loughnan, Trudy Bond, Linda Thomas, Alun Jones, Denise Adams, Elka Palant (3D Centre), Javier Cuevas, Ron Hogg, and Michael Watson (Dept. of Physiology and Pharmacology).

REFERENCES

Alewood PF. 1998. Conotoxins as molecular templates for drug design. In: Ramage R, Epton R, editors. Peptides. Bodwin, UK: Mayflower Scientific. p 183–186.

Alewood PF, Alewood D, Miranda L, Love S, Meutermans W, Wilson D. 1997. Rapid *in situ* neutralization protocols for Boc and Imoc solid phase chemistries. Methods Enzymol 289:14–29.

Bingham J-P, Jones A, Lewis RJ, Andrews PR, Alewood PF. 1996. *Conus* venom peptides (conopeptides): inter-species, intra-species and within individual variation revealed by ionspray mass spectrometry. In: Lazarovici P et al., editors. Biochemical aspects of marine pharmacology. Alaken Inc., Colorado. p 13–27.

Cartier GE, Yoshikami D, Gray WR, Luo S, Olivera BM, McIntosh JM. 1996. A new α-conotoxin which targets α3β2 nicotinic acetylcholine receptors. J Biol Chem 271:7522–7528.

Chen L-Q, Chahine M, Kallen RG, Barchi RL, Horn R. 1992. Chimeric study of sodium channels from rat skeletal and cardiac muscle. FEBS Lett 309:253–257.

Colledge CJ, Hunsperger JP, Imperial JS, Hillyard DR. 1992. Precursor structure of ω-conotoxin GVIA from a cDNA clone. Toxicon 30:111–1116.

Colquhoun LM, Patrick JW. 1997. Pharmacology of neuronal nicotinic acetylcholine receptor subtypes. Adv Pharmacol 39:191–220.

Cornet B, Bonmatin J-M, Hetru C, Hoffman JA, Ptak M, Vovelle F. 1995. Refined three-dimensional solution structure of insect defensin A. Structure 3:435–448.

Cruz LJ. 1996. Primary structural motifs of *Conus* peptides. In: Singh BR, Tu AT, editors. Natural toxins II. New York: Plenum Press. p 155–167.

Cruz LJ, Gray WR, Olivera BM, Zeikus RD, Kerr L, Yoshikami D, Moczydlowski E. 1985. *Conus geographus* toxins that discriminate between neuronal and muscle sodium channels. J Biol Chem 260:9280–9288.

Doyle DA, Cabral JM, Pfuetzner RA, Kuo A, Gulbis JM, Cohen SL, Chait BT, MacKinnon R. 1998. The structure of the potassium channel: molecular basis of K^+ conduction and selectivity. Science 280:69–77.

Fainzilber M, Hasson A, Oren R, Burlingame AL, Gordon D, Spira ME, Zlotkin E. 1994. New mollusc-specific alpha-conotoxins block *Aplysia* neuronal acetylcholine receptors. Biochemistry 33:9523–9529.

Gray WR. 1993. Disulfide structures of highly bridged peptides: a new strategy for analysis. Protein Sci 2:1732–1748.

Gray WR, Luque A, Olivera BM, Barrett J, Cruz LJ. 1981. Peptide toxins from *Conus geographus* venom. J Biol Chem 256: 4734–4740.

Gehrmann J, Alewood PF, Craik DJ. 1998. Structure determination of the three disulfide bond isomers of α-conotoxin GI: a model for the role of disulfide bonds in structural stability. J Mol Biol 278:401–415.

Groebe DR, Dumm JM, Levitan ES, Abramson SN. 1995. α-Conotoxins selectively inhibit one of the two acetylcholine binding sites of nicotinic receptors. Mol Pharmacol 48:105–111.

Guddat LW, Martin JL, Shan L, Edmundson AB, Gray WR. 1996. Three-dimensional structure of the α-conotoxin GI at 1.2 Å resolution. Biochemistry 35:11329–11335.

Hann RM, Pagon OR, Eterovic VA. 1994. The α-conotoxins GI and MI distinguish between the nicotinic acetylcholine receptor agonist sites while SI does not. Biochemistry 33:14058–14063.

Harvey SC, McIntosh JM, Cartier GE, Maddox FN, Luetje CW. 1997. Determinants of specificity for α-conotoxin MII on α3β2 neuronal nicotinic receptors. Mol Pharmacol 51:336–342.

Hill JM, Alewood PF, Craik DJ. 1996. Three-dimensional solution structure of μ-conotoxin GIIIB, a specific blocker of skeletal muscle sodium channels. Biochemistry 35:8824–8835.

Hill JM, Alewood PF, Craik DJ. 1997. Solution structure of the sodium channel antagonist conotoxin GS: a new molecular caliper for probing sodium channel geometry. Structure 5:571–583.

Hill JM, Oomen CJ, Miranda LP, Bingham J-P, Alewood PF, Craik DJ. 1998. Three-dimensional solution structure of α-conotoxin MII by NMR spectroscopy: effects of solution environment on helicity. Biochemistry 37:15621–15630.

Hogg RC, Lewis RJ, Adams DJ. 1999. α-Conotoxin analogue, PnIA[A10L], and α-bungarotoxin block the same component of nicotinic ACh-induced current in rat parasymapthetic neurons. Proc Aust Neurosci Soc 10:152.

Hopkins C, Grilley M, Miller C, Shon K-J, Cruz LJ, Gray WR, Dykert J, Rivier J, Yoshikami D, Olivera BM. 1995. A new family of *Conus* peptides targed to the nicotinic acetylcholine receptor. J Biol Chem 270:22361–22367.

Hu S-H, Gehrmann J, Guddat LW, Alewood PF, Craik DJ, Martin JL. 1996. The 1.1 Å crystal structure of the neuronal acetylcholine receptor antagonist, α-conotoxin PnIA from *Conus pennaceus*. Structure 4:417–423.

Hu S-H, Gehrmann J, Alewood PF, Craik DJ, Martin JL. 1997. Crystal structure at 1.1 Å resolution of α-conotoxin PnIB: comparison with α-conotoxins PnIA and GI. Biochemistry 36:11323–11330.

Hu S-H, Loughnan M, Miller R, Weeks CM, Blessing RH, Alewood PF, Lewis RJ, Martin JL. 1998. The 1.1 Å resolution crystal structure of [Tyr^{15}]EpI, a novel α-conotoxin from *Conus episcopatus*, solved by direct methods. Biochemistry 37:11425–11433.

Jacobsen R, Yoshikami D, Ellison M, Martinez J, Gray WR, Cartier GE, Shon K-J, Groebe DR, Abramson SN, Olivera BM, McIntosh JM. 1997. Differential targeting of nicotinic acetylcholine receptors by novel αA-conotoxins. J Biol Chem 272:22531–22537.

Jan LY, Jan YN. 1997. Cloned potassium channels from eukaryotes and prokaryotes. Annu Rev Neurosci 20:91–123.

Johnson DS, Martinez J, Elgoyhen AB, Heinemann SF, McIntosh JM. 1995. α-Conotoxin ImI exhibits subtype-specific nicotinic acetylcholine receptor blockade: preferential inhibition of homomeric α7 and α9 receptors. Mol Pharmacol 48:194–199.

Jones A, Bingham J-P, Gehrmann J, Bond T, Loughnan M, Atkins A, Lewis RJ, Alewood PF. 1996. Isolation and characterisation of conopeptides by high-performance liquid chromatography combined with mass spectrometry and tandem mass spectrometry. Rapid Commun Mass Spectrom 10:138–143.

Kaiser SA, Soliakov L, Harvey SC, Luetje CW, Wonnacott S. 1998. Differential inhibition by α-conotoxin-MII of the nicotinic stimulation of [^{3}H]dopamine release from rat striatal synaptosomes and slices. J Neurochem 70:1069–1076.

Kulak JM, Nguyen TA, Olivera BM, McIntosh JM. 1997. α-Conotoxin MII blocks nicotine-stimulated dopamine release in rat striatal synaptosomes. J Neurosci 17:5263–5270.

Lewis RJ, Bingham J-P, Jones A, Alewood PF. 1994. Analysis of *Conus* venoms by ionspray mass spectrometry. Australasian Biotech 4:298–300.

Loughnan M, Bond T, Atkins A, Cuevas J, Adams DJ, Broxton NM, Livett BG, Down JG, Jones A, Alewood PF, Lewis RJ. 1998. α-Conotoxin EpI, a novel sulfated peptide from *Conus episcopatus* that selectively targets neuronal nicotinic acetylcholine receptors. J Biol Chem 273:15667–15674.

Luo S, Kulak JM, Cartier GE, Jacobsen RB, Yoshikami D, Olivera BM, McIntosh JM. 1998. α-Conotoxin AuIB selectively blocks α3β4 nicotinic acetylcholine receptors and nicotine-evoked norepinephrine release. J Neurosci 18:8571–8579.

Martinez JS, Olivera BM, Gray WR, Craig AG, Groebe DR, Abramson SN, McIntosh JM. 1995. α-Conotoxin EI, a new nicotinic acetylcholine receptor antagonist with novel selectivity. Biochemistry 34:14519–14526.

McGehee DS, Role LW. 1995. Physiological diversity of nicotinic acetylcholine receptors expressed by vertebrate neurons. Annu Rev Physiol 57:521–546.

McIntosh JM, Cruz LJ, Hunkapiller MW, Gray WR, Olivera BM. 1982. Isolation and structure of a peptide toxin from the marine snail *Conus magus*. Arch Biochem Biophys 218:329–334.

McIntosh JM, Yoshikami D, Mahe E, Nielsen DB, Rivier JE, Gray WR, Olivera, BM. 1994. A nicotinic acetylcholine receptor ligand of unique specificity, α-conotoxin ImI. J Biol Chem 269:16733–16739.

Miller C. 1995. The charybdotoxin family of K^+-channel blocking peptides. Neuron 15:5–10.

Moczydlowski E, Olivera BM, Gray WR, Strichartz GR. 1986. Discrimination of muscle and neuronal Na-channel subtypes by binding competition between [^{3}H]saxitoxin and μ-conotoxins. Proc Natl Acad Sci USA 83:5321–5325.

Myers RA, Zafaralla GC, Gray WR, Abbott J, Cruz LJ, Olivera BM. 1991. α-Conotoxins, small peptide probes of nicotinic acetylcholine receptors. Biochemistry 30:9370–9377.

Myers RA, Cruz LJ, Rivier JE, Olivera BM. 1993. *Conus* peptides as

chemical probes for receptors and ion channels. Chem Rev 93:1923–1936.

Nakao M, Nishiuchi Y, Nakata M, Watanabe TX, Kimura T, Sakakibara S. 1995. Synthesis and disulfide structure determination of conotoxin GS, a γ-carboxyglutamic acid-containing neurotoxic peptide. Lett Pept Sci 2:17–26.

Narasimhan L, Singh J, Humblet C, Guruprasad K, Blundell T. 1994. Snail and spider toxins share a similar tertiary structure and 'cystine motif.' Nat Struct Biol 1:850–852.

Nielsen KJ, Thomas L, Lewis RJ, Alewood PF, Craik DJ. 1996. A consensus structure for ω-conotoxins with different selectivities for voltage-sensitive calcium channel subtypes: comparison of MVIIA, SVIB and SNX-202. J Mol Biol 263:297–310.

Noda M, Shimizu S, Tanabe T, Takai T, Kayano T, Ikeda T, Takahashi H, Nakayama H, Kanaoka Y, Minamino N, Kangawa K, Matsuo H, Raftery MA, Hirose T, Inayama S, Hayashida H, Miyata T, Numa S. 1984. Primary structure of *Electrophorus electricus* sodium channel deduced from cDNA sequence. Nature 312:121–127.

Ohizumi Y, Nakamura H, Kobayashi J, Catterall WA. 1986. Specific inhibition of [^{3}H]saxitoxin binding to skeletal muscle sodium channels by geographutoxin II, a polypeptide channel blocker. J Biol Chem 261:6149–6152.

Olivera BM, Rivier J, Clark C, Ramilo C, Corpuz GP, Abogadie FC, Mena EE, Woodward SR, Hillyard DR, Cruz LJ. 1990. Diversity of *Conus* neuropeptides. Science 249:257–263.

Olivera BM, Miljanich G, Ramachandran J, Adams ME. 1994. Calcium channel diversity and neurotransmitter release: the ω-conotoxins and ω-agatoxins. Annu Rev Biochem 63:823–867.

Pallaghy PK, Nielsen KJ, Craik DJ, Norton RS. 1994. A common structural motif incorporating a cystine knot and a triple-stranded β-sheet in toxic and inhibitory polypeptides. Protein Sci 3:1833–1839.

Picciotto MR, Zoli M, Rimondini R, Léna C, Marubio LM, Pich EM, Fuxe K, Changeux J-P. 1998. Acetylcholine receptors containing the β2 subunit are involved in the reinforcing properties of nicotine. Nature 391:173–177.

Poth K, Nutter TJ, Cuevas J, Parker MJ, Adams DJ, Luetje CW. 1997. Heterogeneity of nicotinic receptor class and subunit mRNA expression among individual parasympathetic neurons from rat intracardiac ganglia. J Neurosci 17:586–596.

Ramilo CA, Zafaralla GC, Nadasdi L, Hammerland LG, Yoshikami D, Gray WR, Kristipati R, Ramachandran J, Miljanich G, Olivera BM, Cruz LJ. 1992. Novel α- and ω-conotoxins from *Conus striatus* venom. Biochemistry 31:9919–9926.

Sangameswaran L, Delgado SG, Fish LM, Koch BD, Jakeman LB, Stewart GR, Sze P, Hunter JC, Eglen RM, Herman RC. 1996. Structure and function of a novel voltage-gated, tetrodotoxin-resistant sodium channel specific to sensory neurons. J Biol Chem 271:5953–5956.

Sato S, Nakamura H, Ohizumi Y, Kobayashi J, Hirata Y. 1983. The amino acid sequences of homologous hydroxyproline-containing myotoxins from the marine snail *Conus geographus* venom. FEBS Lett 155:277–280.

Scanlon MJ, Naranjo D, Thomas L, Alewood, PF, Lewis RJ, Craik DJ. 1997. The structure of novel potassium channel toxin, κ-conotoxin PVIIA, from the venom of *Conus purpurascens*: implications for the mechanism of channel block. Structure 5:1585–1597.

Schnölzer M, Alewood P, Jones A, Alewood D, Kent SBH. 1992. *In situ* neutralization in Boc-chemistry solid phase peptide synthesis. Int J Pept Protein Res 40:180–193.

Shon K-J, Olivera BM, Watkins M, Jacobsen RB, Gray WR, Floresca CZ, Cruz LJ, Hillyard DR, Brink A, Terlau H, Yoshikami D. 1998. μ-Conotoxin PIIIA, a new peptide for discriminating among tetrodotoxin-sensitive Na channel subtypes. J Neurosci 18:4473–4481.

Skjaerbaek N, Nielsen KJ, Lewis RJ, Alewood P, Craik DJ. 1997. Determination of the solution structures of conantokin-G and conantokin-T by CD and NMR spectroscopy. J Biol Chem 272:2291–2299.

Terlau H, Shon K-J, Grilley M, Stocker M, Stühmer W, Olivera BM. 1996. Strategy for rapid immobilisation of prey by a fish-hunting marine snail. Nature 381:148–151.

Unwin N. 1998. The nicotinic acetylcholine receptor of the *Torpedo* electric ray. J Struct Biol 121:181–190.

Watson MJ, Lewis RJ, Adams DJ. 1998. Effects of synthetic μ-conotoxins on voltage-dependent sodium currents in rat sensory neurones. Proc Aust Physiol Pharmacol Soc 29:326P.

Yanagawa Y, Abe T, Satake M, Odani S, Suzuki J, Ishikawa K. 1988. A novel sodium channel inhibitor from *Conus geographus*: purification, structure, and pharmacological properties. Biochemistry 27:6256–6262.

Zafaralla GC, Ramilo C, Gray WR, Karlstrom R, Olivera BM, Cruz LJ. 1988. Phylogenetic specificity of cholinergic ligands: α-conotoxin SI. Biochemistry 27:7102–7105.

EXHIBIT 10

ELSEVIER

Toxicon 39 (2001) 7–14

TOXICON

www.elsevier.com/locate/toxicon

Conotoxins, in retrospect

Baldomero M. Olivera[a,*], Lourdes J. Cruz[a,b]

[a]*Department of Biology, University of Utah, Salt Lake City, UT, USA*
[b]*Marine Science Institute, University of the Philippines, Diliman, Quezon City, 1101, Philippines*

Received 2 May 2000; accepted 4 May 2000

This review is dedicated to the memory of Craig Clark.

1. Introduction

It is now over 20 years since the first conotoxin was biochemically characterized, establishing for the first time that an active component of a *Conus* venom was a small, disulfide-rich peptide. This review is a retrospective that looks back at the last two decades of conotoxin research and provides a somewhat idiosyncratic personal history. In addition, we outline a few insights that have emerged, which provide a conceptual framework and technological platform that should make further exploration of the neuropharmacological resource which is the sum total of *Conus* venom peptides much more facile. It is now clear that there are potentially ~50,000 different conotoxins present in the venoms of living species in the genus *Conus* (this may even be a conservative estimate) — unquestionably, there is much more to be done.

2. A brief history

2.1. First phase: why picking up a cone snail can be fatal

Undoubtedly, what initially motivated the investigation of cone venoms was that the stings of these molluscs were known to cause human fatality. Pioneering work done by Alan Kohn, who first discovered that cone snails hunted fish, and by Robert Endean and his co-workers in Australia, who documented the pharmacology of crude venoms in the 1970s, demonstrated that different cone snail venoms must have different biologically active components (Kohn, 1956; Kohn et al., 1960; Endean et al., 1974, 1976, 1977). An early attempt to purify peptides from cone snail venoms carried out by an Australian group (Spence, et al., 1977) resulted in an amino acid composition of a peptide which can be unambiguously identified today as a μ-conotoxin.

The first *Conus* peptide for which a complete amino acid sequence was established, and subsequently confirmed by chemical synthesis, was α-conotoxin GI, a 13-amino acid peptide with two disulfide bonds from *Conus geographus* venom (Cruz et al., 1978; Gray et al., 1981). This was followed by the characterization of the μ-conotoxins, the other major group of paralytic peptides that affect mammals (Stone and Gray, 1982; Nakamura et al., 1983; Sato et al., 1983; Cruz et al., 1985a). The presence of these two peptides in the venom of *C. geographus* explained why stings of this snail were so deadly. With both a potent nicotinic antagonist (α-conotoxin), acting like α-neurotoxins from snake venoms such as α-bungarotoxin and cobratoxin, as well as a sodium channel blocker (μ-conotoxin) acting much like tetrodotoxin or saxitoxin (Moczydlowski, et al., 1986), a toxinological rationale could

* Corresponding author.

PII: S0041-0101(00)00157-4

be made for the 70% fatality rate of untreated human stinging cases by *C. geographus* (Cruz and White, 1995). Thus, the characterization of peptides which potently affected mammalian neuromuscular transmission provided a kind of closure to observations on human fatality from cone snail stings, first reported by Rumphius 300 years ago (Rumphius, 1705).

2.2. Second phase: giving creative undergraduates free rein

The next advance in conotoxin research could probably have happened only at a university, since the key ingredient was the creativity of curious students who do not necessarily have to do mission-oriented research. A young 18-year-old undergraduate named Craig Clark came to work with us at the University of Utah right after he finished high school. He got (what was in retrospect) the truly inspired idea of injecting venom fractions directly into the central nervous system of mammals, instead of using the i.p. injections already standard in our laboratory (Clark, et al., 1981). When *Conus* venom fractions were tested by i.p. injection into mice, a very small proportion gave symptoms that could readily be scored. However, when the same fractions were injected intracranially, the true pharmacological diversity of *Conus* venoms was revealed by the amazing array of different behavioral phenotypes elicited in the mice (Olivera et al., 1990, 1999a).

Craig Clark himself initially recorded the many diverse symptoms elicited in mice by various venom fractions. He decided to purify a "sleeper" fraction, which put mice that were less than 14 days old into a sleep-like state (Olivera, et al., 1985b). Two other undergraduates, David Johnson and Aryan Azimi, later discovered that if the same fraction was injected into mice that were 21 days old, a hyperactivity syndrome where the mice would constantly climb the sides of their cages and run from corner to corner was observed. This venom component was referred to as the "sleeper/climber" peptide, with the behavior elicited in mice dependent on their age.

A group of talented students purified other peptides that elicited distinctive behavioral symptomatology. Most notable was Michael McIntosh, an undergraduate recruited by Craig Clark into our labs. Michael had planned to spend his summer after high school touring with a company doing musical theater, but decided at the last minute to do research instead — he purified a "shaker" peptide (Olivera, et al., 1984) that caused characteristic tremors when injected intracranially into mice (more about this peptide is given below). A "sluggish" peptide was purified by David Griffin (Craig et al., 1999a), another undergraduate in our laboratories. This simple assay, injection into the central nervous system of mice, also resulted in the characterization of a "spasmodic" peptide (Lirazan et al., 2000), a "scratcher" peptide (Cruz et al., 1987) and many others.

What has actually happened to the initial set of peptides first purified by those young undergraduates in the early to mid 1980s is a testimony to the unpredictability of what basic research might lead to. The shaker peptide originally purified by Michael McIntosh from *C. magus* (Olivera et al., 1985a), together with another shaker peptide found in *C. geographus* venom (Olivera et al., 1984), was shown soon afterwards by Doju Yoshikami and collaborators to inhibit calcium currents *and* synaptic transmission at the frog neuromuscular junction (Kerr and Yoshikami, 1984; Feldman et al., 1987). Once Doju Yoshikami realized that these peptides inhibited both; he predicted that they probably targeted a novel type of calcium channel that controlled neurotransmitter release. At that time, new calcium currents were being characterized using electrophysiological techniques by Richard Tsien's laboratory at Yale (Nowycky et al., 1985), and a collaboration was arranged to determine whether any of these were affected by the "shaker peptides"; it was found that a novel Ca conductance, the N-type calcium current, was potently and specifically inhibited by the shaker peptides (McCleskey et al., 1987).

Today, these shaker peptides are known as ω-conotoxins GVIA and MVIIA (Olivera et al., 1985a). Next to tetrodotoxin, ω-conotoxin GVIA has probably become the most widely used toxin in neuroscience, since it is useful both for inhibiting synaptic transmission and for assessing whether N-type Ca currents are present (Olivera et al., 1994). The original shaker peptide purified by Michael McIntosh, ω-conotoxin MVIIA, may become a therapeutic drug with the generic name Ziconotide this year; it has been through Phase III clinical trials as an analgesic for intractable pain, and the clinical data have been incorporated into a new drug application which is currently under final review (Heading, 1999).

The "sleeper/climber peptide," first purified by Craig Clark (Olivera et al., 1985b), has had an equally interesting history. Now called conantokin-G, and known to be an NMDA receptor antagonist, this is one of the few *Conus* peptides that does not contain disulfide crosslinks. Michael McIntosh showed that this 17-amino acid peptide has five residues of an unusual post-translationally modified amino acid, γ-carboxyglutamate (McIntosh et al., 1984), the first documented occurrence of this modified amino acid in any invertebrate system (it was previously thought to occur only in mammalian blood clotting factors). Edward Mena, then at Pfizer, suggested to us, from the behavioral symptomatology elicited in mice, that the peptide might be an NMDA receptor antagonist; several tests

confirmed his suggestion (Mena et al., 1990; Hammerland et al., 1992). Other members of the conantokin family have since been characterized (Haack et al., 1990). Using animal models, this peptide family was recently shown to have therapeutic potential for epilepsy, and clinical trials will be initiated this year (White et al., 2000).

The "sluggish peptide," purified by David Griffin, was recently shown to be an agonist of the neurotensin receptor (Craig et al., 1999b). This peptide, now known as contulakin-G, has an unusual post-translational modification. Anthony Craig of the Salk Institute both recognized the homology between the sluggish peptide and neurotensin, and elucidated the structure of the *O*-glycan modification. Contulakin-G was shown to be a potent analgesic in animal models, and is now the lead compound for a commercial analgesia program.

Another peptide that gave a striking phenotype upon intracranial injection is now called conopressin-G. This 9-amino acid peptide from *C. geographus* venom, which proved to be the first invertebrate vasopressin/oxytocin neuropeptide family member (Cruz et al., 1987), elicited an intense scratching syndrome in the injected mice. For many of the peptides that were biochemically characterized because of the distinctive behavioral symptomatology they caused, the underlying molecular mechanism remains unknown (an example is the "spasmodic peptide"). Nevertheless, it now seems clear that the original idea of a creative undergraduate has yielded, and will continue to yield, a bonanza of pharmaceutical reagents for neuroscience and novel therapeutic leads for medicine.

2.3. Third phase: from learning to milk snails to the nirvana cabal

Most cone venoms used in research are venom duct extracts. For many interesting species, not enough venom from ducts is available. This was the case for the purple cone, *C. purpurascens*, a fish-hunting species from the Eastern Pacific; a few live specimens were occasionally brought to us by a famous marine photographer, Alex Kerstitch, who works in the Sea of Cortez, but dissecting these would not yield sufficient venom to do a proper biochemical study. However, if we could keep the snails in captivity and "milk" them, much more venom could be collected. For several years, we tried to recruit a student to milk cone snails.

Chris Hopkins, an undergraduate student, seemed completely unfazed when we suggested the snail milking project to him. He said he wanted to think about it for a few days, came back and asked for a little cash. He returned with a box of condoms and started blowing one up. He rubbed the inflated condom against a goldfish and then lowered it into a tank filled with hungry *Conus striatus* buried under the aquarium sand. Several came up from the sand, and one harpooned the condom with such force that Chris let go in surprise. The condom floated up with the snail still attached to it through its harpoon and proboscis. The sight of an inflated condom floating at the surface, with a tethered snail swinging like a pendulum below it, was one of those moments that should have been recorded with a camera.

Chris quickly adapted his first success into a routine method for milking several fish-hunting *Conus* species, and his major focus was on *C. purpurascens*. He found that by taking an Eppendorf tube, coring out the cover, putting both a membrane and a bit of fish fin between the cored cover and the tube, he could induce the snails to routinely harpoon the tube and eject their venom (Hopkins et al., 1995); *C. purpurascens* typically gave 3–5 μl per milking; several milliliters of *C. purpurascens* venom were tediously accumulated in this way.

By maintaining the colony of *C. purpurascens* for milking, we saw fish being stung many times. A good strike by *C. purpurascens* led to the fish jerking violently, followed by an immediate tetanic paralysis. Even a large fish would be immobilized in a spastic posture less than a second after being harpooned. Chris Hopkins initiated the purification of *C. purpurascens* venom components. Later, Ki-Joon Shon, a post-doctoral fellow, decided to systematically characterize all large peaks from HPLC chromatography of *C. purpurascens* venom. With the help of Rick Jacobsen, an undergraduate, and another post-doc, Michelle Grilley, all major components from the venom were biochemically characterized and several were chemically synthesized (Shon et al., 1995, 1997, 1998a, 1998b).

From several fish-hunting *Conus* venoms, we had purified multiple components that caused paralysis in fish; this proved to be true for *C. purpurascens* venom as well. All fish-hunting cone venoms have peptides targeted to nicotinic receptors at the endplate of neuromuscular junctions. In addition, peptides which target muscle sodium channels and presynaptic calcium channels are generally present — these are all individually paralytic to fish. Every fish-hunting snail venom has three or more such paralytic components which interfered with neuromuscular transmission.

However, the venom components that individually caused paralysis in fish did not account for the very rapid immobilization of prey observed when live *C. purpurascens* actually stung a fish. Ki-Joon Shon and Michelle Grilley discovered that by combining two different venom fractions, they could elicit the immediate tetanic paralysis observed right after a fish had been stung (Terlau et al., 1996). These results gave rise to the concept of toxin cabals. We realized that cone venoms seemed to be organized into groups of peptides working together for the same physiological end-point

(Olivera, 1997). The term cabal, from secret societies plotting to overthrow the government, seemed consistent with the effects of these groups of toxins on injected prey.

Thus, in *C. purpurascens*, there is a "motor cabal" of peptides which potently abolishes neuromuscular transmission; all the individually paralytic peptides fall into this category. However, there is a second cabal of toxins which causes an almost immediate tetanic immobilization of prey, which we call the "lightning-strike cabal." At a minimum, this requires a peptide, δ-conotoxin, which inhibits inactivation of voltage-gated Na^+ channels, as well as a second peptide, κ- or κA-conotoxin, which inhibits voltage-gated K^+ channels (Shon et al., 1995; Terlau, et al., 1996; Shon, et al., 1998b). The lightning-strike cabal causes a massive depolarization of axonal fibers near the venom injection site, resulting in the immediate tetanic paralysis — in effect, the fish are electrically shocked.

Prey capture by fish-hunting snails like *C. purpurascens*, therefore, requires two toxin cabals, each comprising different sets of venom peptides that act synergistically after venom injection. The lightning-strike cabal causes immediate tetantic immobilization which gives time for the motor cabal of toxins to spread through the body of the prey, reach motor axons and neuromuscular junctions, and cause an irreversible neuromuscular paralysis. The concept of toxin cabals is a useful organizing principle in dissecting function of venom components. Defining the physiological end-point achieved by a cabal provides a framework for reasonable hypotheses regarding likely targets and molecular mechanisms of individual peptides comprising that cabal.

Understanding prey capture in one *Conus* species in mechanistic terms provided a baseline for comparison to other *Conus* venoms. In particular, the contrast between *C. geographus* and *C. purpurascens* has been specially illuminating. *C. geographus* also has a set of venom components comprising a motor cabal. In striking contrast to *C. purpurascens* venom, however, *C. geographus* does not appear to have a lightning-strike cabal of toxins. In order to rationalize this, observing the live snails in an aquarium has been instructive. In the wild, *C. geographus* may go after schools of smaller fish hiding in reefs at night. This species engulfs prey with its huge, highly distensible mouth, which it uses effectively as a net. Only after the fish are already engulfed in its mouth does the snail inject its venom.

In place of a lightning-strike cabal, this species appears to have a set of toxins that deaden the sensory circuitry; it may even release some venom into its mouth when fish are engulfed before actually stinging. Once fish are within the mouth of the snail, they seem sedated, and the sudden violent jerking routinely observed when fish are harpooned by *C. purpurascens* is never seen. We suggest that instead of having a lightning-strike cabal of toxins, *C. geographus* has a "nirvana cabal," resulting in the fish appearing to be in a relaxed and sedated state. The venom of *C. geographus* seems to be enriched in peptides that lower the activity of neuronal circuitry. Among these are the sleeper/climber peptide (conantokin-G) and the sluggish peptide (contulakin-G), two of the venom components originally purified by undergraduates from their behavioral symptomatology.

The fact that the snail appears to use these and other venom components to quiet down the neuronal circuitry led to the idea of systematically exploring whether the peptides of the nirvana cabal might quiet down pathologically active neuronal circuits in humans (which as might occur in epilepsy, or intractable pain states). Several members of the nirvana cabal are being actively explored for these types of potential pharmacological applications. These commercial drug development efforts with conopeptides have recently been reviewed (Jones and Bulaj, 2000).

2.4. Fourth phase: molecular conotoxinology

As with all other areas of biology, conotoxin research is significantly impacted by the rapid changes in molecular biology. The analysis of mRNA, as well as genes encoding *Conus* peptides revealed an underlying family and superfamily organization based on conserved sequence elements. There are probably only 5–10 major conotoxin gene superfamilies that encode over 80% of all *Conus* peptides. Over the genus, superfamilies have differentiated functionally and structurally into discrete families, each with a defined pharmacological targeting specificity.

The sweeping developments in molecular neuroscience have resulted in most potential receptor and ion channel targets of conotoxins being cloned and expressed. Thus, it has become possible to test venoms, or individual conotoxins on potential cloned targets. This approach was pioneered by Michael McIntosh (the former undergraduate who purified ω-conotoxin MVIIA, now a member of the Psychiatry and Biology faculties of the University of Utah). He systematically analyzed one group of conotoxins, the α-conotoxins, for functional effects on their corresponding target ion channel family, the nicotinic acetylcholine receptors (Martinez et al., 1995; Cartier et al., 1996; Jacobsen et al., 1997; Luo et al., 1998; McIntosh et al., 1999). A certain symmetry has emerged: an α-conotoxin family member specifically targets a corresponding nicotinic acetylcholine receptor isoform.

The analysis of both the conotoxins and their potential target receptors and ion channels by advanced molecular techniques is extremely powerful. Increasing progress will undoubtedly be made through more and

more sophisticated matching of cone snail venom genes with information from genomics regarding their targets, an emerging field we refer to as "conotoxinomics."

3. *Conus* venoms 2000: a conceptual framework

Although the last two decades have brought significant biochemical, pharmacological, electrophysiological and molecular information regarding cone snail venoms, the extent of our ignorance is all too apparent; only a miniscule fraction of the 50,000 or so peptides present in these venoms has been characterized even minimally. Despite this, formulating a reasonable overview for these venoms is now feasible.

It has become well-established that the major biologically active principles of *Conus* venoms are small, structured peptides, and that the venom from any one *Conus* species contains a large number of such peptides. At what level, and when an individual peptide is expressed, may vary considerably, but the total repertoire of peptides that can be expressed in the venom of a single species is probably of the order of 100–300. Every conotoxin serves as a highly specific ligand, each with a particular molecular target; binding of the peptide ligand to its target leads to a biologically relevant change in physiological function. Most targets that we know of are ion channels, either voltage-gated or ligand-gated, and in a few cases, G-protein-linked receptors. Thus, when venom is injected, the general strategy is to change nervous system function in the injected animal by using a set of diverse, potent neuropharmacological agents. The venom is organized into cabals, groups of toxins acting together to achieve a specific physiological end-point.

Each *Conus* peptide is encoded by a single mRNA and biosynthesis occurs through normal ribosomal translation mechanisms. The initial translation product is a prepropeptide precursor with a characteristic organization. The precursor, usually between 70 and 120 amino acids in length, has an N-terminal signal sequence (~20 AA), an intervening pro region and the mature toxin (usually 10–30 AA) encoded at the C-terminal end, always in a single copy (Hillyard et al., 1989; Olivera et al., 1990; Walker et al., 1999). *Conus* peptides are post-translationally modified to varying extents, and some have the highest post-translational modification density of any polypeptide gene products known (Craig et al., 1997; Jimenez et al., 1997; Craig et al., 1999a). We suspect that disulfide crosslinks form with the aid of specialized cellular components in specific secretory pathways for each peptide superfamily. The highly conserved signal sequences of each superfamily may play a specialized role in targeting each peptide to the appropriate secretory pathway.

From molecular analyses of *Conus* genes, it appears that the different segments of the prepropeptide precursor evolve at extremely different rates. Signal sequences of peptides within the same superfamily are extraordinarily conserved; in marked contrast, the mature toxin regions are hypermutated (Olivera et al., 1999b; Walker et al., 1999). In some superfamilies at least, the signal sequence, pro region and mature toxin region are each encoded by different small exons, separated from each other by large introns. We have suggested elsewhere that the large intronic sequences could modulate replication or recombination events (and potentially even more unusual mechanisms such as RNA editing) to yield the observed accelerated evolution in the C-terminal part of the precursor, and in striking juxtaposition, the unique conservation of N-terminal signal sequences (Olivera et al., 1999b).

The snails generate molecular diversity in venom peptides primarily by hypermutating the mature toxin region. In effect, the snails are using a combinatorial library strategy over an evolutionary time scale to generate novel peptide sequences in their venoms, while conserving the basic structural frameworks (primarily the arrangement of disulfide crosslinks). Thus, acquisition of recognition signals for post-translational modification enzymes in the "pro" region of the precursor could generate another dimension to the molecular diversity of mature *Conus* peptides. Recently, it was shown that recognition signal sequences for one of the well-characterized post-translational modifications of *Conus* peptides are found in the pro region of the precursor (Bandyopadhyay et al., 1998).

Venom is clearly the major weapon used by cone snails for prey capture. The venom may also be used for other biological purposes (defense against predators, competitive interactions). In many ways, the contents of a venom provide a biochemical reflection of the biotic interactions critical to the success or failure of that species. In the ecological niche in which a particular species successfully competes, there is presumably continuing natural selection for the various individual venom components. As new species evolve, perhaps because of a sudden change in the environment, the changing spectrum of prey, predators and competitors would presumably generate new and powerful selective pressures for other venom components. Under these unstable conditions, components of the venom can apparently be hypermutated such that in a relatively short period of time, new species emerge with a new spectrum of venom peptides to fit the altered ecological niche (Olivera et al., 1995). Consequently, *Conus* has arguably become the most species-rich of all the marine invertebrate genera. Through this expansion into hundreds of species, the

basic strategy of the venom remains the same: small, structured peptides, derived by diversification of a few gene superfamilies, potently affecting the nervous systems of potential prey, predators and competitors.

Acknowledgements

The work of the authors has been continuously supported by the National Institute of General Medical Sciences (GM48677). This research was a continuous collaboration with W.R. Gray and D.R. Hillyard, University of Utah, and J. Rivier, Salk Institute. We would like to acknowledge the general contributions of Gloria Corpuz, Cecilia Ramilo and Julita Imperial to our research.

Appendix A.1. Nomenclature of Conus peptides

As the first peptides from *C. geographus* were discovered in the 70s, different names for the same peptides were given by various research groups. To ease the confusion, a nomenclature was proposed in 1985 (Cruz et al., 1985b) and minor modifications were introduced a few years later (Gray et al., 1988). Recent development of sensitive and rapid technologies has greatly accelerated *Conus* peptide discovery and revealed the existence of several new superfamilies. Peptides in the same superfamily share a characteristic arrangement of cysteine residues (see Table A.1) and a highly conserved signal sequence in their precursors (McIntosh et al., 1999).

The final name of a conotoxin with a known mechanism consists of a Greek letter to designate its pharmacological action, followed by a hyphen before the word conotoxin, a one- or two-letter code to indicate the *Conus* species, a Roman numeral to indicate the Cys pattern of the peptide, then a capital letter to indicate a specific peptide variant. For example, ω-conotoxin GVIA is a *C. geographus* peptide that blocks voltage sensitive calcium channels and has a class VI Cys pattern. δ-Conotoxin TxVIA is a peptide from *C. textile*, which delays inactivation of sodium channels and has a class VI Cys pattern. A list of codes to designate the species can be found in the website http://conus.biology.utah.edu.

The name of a peptide of unknown mechanism of action does not have a Greek letter. It consists only the species code in lower case letter(s), an Arabic numeral to designate the Cys pattern and a small letter to indicate a particular variant, e.g., tx5a. The corresponding clone encoding tx5a is designated as Tx5.2, with the name of the species beginning with a capital letter followed by the Arabic number to designate the Cys patterns and a number after the dot to designate the clone variant (Tx5.1 was the first characterized clone encoding a different peptide with a class 5 Cys pattern). Should the peptide turn out to have a novel mode of action, its final name might be τ-conotoxin TxVA.

Specific Cys patterns are designated by numbers and the modes of action are indicated mainly by Greek letters. For peptides with the same mode of action but a different disulfide framework, the Greek letter is followed by a capital letter. Peptides with the same Cys pattern and mode of action are differentiated by capital letters.

Non-conotoxin families, those with one or no disulfide bond, are named differently; they are usually less

Table A.1
Conotoxin superfamilies

Superfamily	Class of cysteine arrangement		Pharmacological family	
	Pattern	Designation	Designation	Action
A	CC–C–C	I or 1	α	Competitive antagonist of ACh receptor
	CC–C–C–C–C	IV or 4	αA	Competitive antagonist of ACh receptor
	CC–C–C–C–C	IV or 4	κA	Inhibits K^+ channels (VSPC)
M	CC–C–C–CC	III or 3	μ	Blocks Na^+ channels (VSSC) at site I
	CC–C–C–CC	III or 3	Ψ	Noncompetitive antagonist of ACh receptor
O	C–C–CC–C–C	VI or 6	ω	Blocks Ca^{++} channels (VSCC)
	C–C–CC–C–C	VII or 7	ω	Blocks Ca^{++} channels (VSCC)
	C–C–CC–C–C	VII or 7	κ	Inhibits K^+ channel
	C–C–CC–C–C	VI or 6	δ	Delays inactivation of VSSC by binding to site VI
	C–C–CC–C–C	VI or 6	μO	Blocks VSCC; does not compete with TTX and STX
P	–C–C–C–C–C–C–	IX or 9		Unknown
S	C–C–C–C–C–C–C–C–C–C	VIII or 8	σ	5-HT_3 receptor
T	–CC–CC–	V or 5		Unknown

diverse and found in fewer species. These conopeptides are given a name, followed by a one- or two-letter code for the species (conopressin-S, contryphan-R and contulakin-G from *C. striatus*, *C. radiatus* and *C. geographus*, respectively). Larger polypeptides (>70 AA) are similarly designated (e.g., conodipine-M).

References

Bandyopadhyay, P.K., Colledge, C.J., Walker, C.S., Zhou, L.-M., Hillyard, D.R., Olivera, B.M., 1998. Conantokin-G precursor and its role in γ-carboxylation by a vitamin K-dependent carboxylase from a *Conus* snail. J. Biol. Chem. 273, 5447–5450.

Cartier, G.E., Yoshikami, D., Gray, W.R., Luo, S., Olivera, B.M., McIntosh, J.M., 1996. A new α-conotoxin which targets α3β2 nicotinic acetylcholine receptors. J. Biol. Chem. 271, 7522–7528.

Clark, C., Olivera, B.M., Cruz, L.J., 1981. A toxin from *Conus geographus* venom which acts on the vertebrate central nervous system. Toxicon 19, 691–699.

Craig, A.G., Bandyopadhyay, P., Olivera, B.M., 1999a. Post-translationally modified peptides from *Conus* venoms. European J. Biochem. 264, 271–275.

Craig, A.G., Jimenez, E.C., Dykert, J., Nielsen, D.B., Gulyas, J., Abogadie, F.C., Porter, J., Rivier, J.E., Cruz, L.J., Olivera, B.M., McIntosh, J.M., 1997. A novel post-translational modification involving bromination of tryptophan: identification of the residue, L-6-bromotryptophan, in peptides from *Conus imperialis* and *Conus radiatus* venom. J. Biol. Chem. 272, 4689–4698.

Craig, A.G., Norberg, T., Griffin, D., Hoeger, C., Akhtar, M., Schmidt, K., Low, W., Dykert, J., Richelson, E., Navarro, V., Macella, J., Watkins, M., Hillyard, D., Imperial, J., Cruz, L.J., Olivera, B.M., 1999b. Contulakin-G, an *O*-glycosylated invertebrate neurotensin. J. Biol. Chem. 274, 13752–13759.

Cruz, L.J., de Santos, V., Zafaralla, G.C., Ramilo, C.A., Zeikus, R., Gray, W.R., Olivera, B.M., 1987. Invertebrate vasopressin/oxytocin homologs. Characterization of peptides from *Conus geographus* and *Conus striatus* venoms. J. Biol. Chem. 262, 15821–15824.

Cruz, L.J., Gray, W.R., Olivera, B.M., 1978. Purification and properties of a myotoxin from *Conus geographus* venom. Arch. Biochem. Biophys. 190, 539–548.

Cruz, L.J., Gray, W.R., Olivera, B.M., Zeikus, R.D., Kerr, L., Yoshikami, D., Moczydlowski, E., 1985a. *Conus geographus* toxins that discriminate between neuronal and muscle sodium channels. J. Biol. Chem. 260, 9280–9288.

Cruz, L.J., Gray, W.R., Yoshikami, D., Olivera, B.M., 1985b. *Conus* venoms: a rich source of neuroactive peptides. J. Toxicol. — Toxin Rev. 4, 107–132.

Cruz, L.J., White, J., 1995. Clinical toxicology of *Conus* snail stings. Journal, 117–127.

Endean, R., Gyr, P., Surridge, J., 1977. The pharmacological actions on gunea-pig ileum of crude venoms from the marine gastropods *Conus striatus* and *Conus magus*. Toxicon 15, 327.

Endean, R., Parrish, G., Gyr, P., 1974. Pharmacology of the venom of *Conus geographus*. Toxicon 12, 131.

Endean, R., Williams, H., Gyr, P., Surridge, J., 1976. Some effects on muscle and nerve of crude venom from the gastropod *Conus striatus*. Toxicon 14, 267.

Feldman, D., Olivera, B.M., Yoshikami, D., 1987. ω-*Conus geographus* toxin: a peptide that blocks calcium channels. FEBS Lett. 214, 295–300.

Gray, W.R., Luque, A., Olivera, B.M., Barrett, J., Cruz, L.J., 1981. Peptide toxins from *Conus geographus* venom. J. Biol. Chem. 256, 4734–4740.

Gray, W.R., Olivera, B.M., Cruz, L.J., 1988. Peptide toxins from venomous *Conus* snails. Ann. Rev. Biochem. 57, 665–700.

Haack, J.A., Rivier, J., Parks, T.N., Mena, E.E., Cruz, L.J., Olivera, B.M., 1990. Conantokin T: a γ-carboxyglutamate-containing peptide with *N*-methyl-D-aspartate antagonist activity. J. Biol. Chem. 265, 6025–6029.

Hammerland, L.G., Olivera, B.M., Yoshikami, D., 1992. Conantokin-G selectively inhibits NMDA-induced currents in *Xenopus oocytes* injected with mouse brain mRNA. Eur. J. Pharmacol. 226, 239–244.

Heading, C., 1999. Ziconotide. Curr. Opin. CPNS Invest. Drugs 1, 153–166.

Hillyard, D.R., Olivera, B.M., Woodward, S., Gray, W.R., Corpuz, G.P., Ramilo, C.A., Cruz, L.J., 1989. A molluscivorous *Conus* toxin: conserved frameworks in conotoxins. Biochemistry 28, 358–361.

Hopkins, C., Grilley, M., Miller, C., Shon, K., Cruz, L.J., Gray, W.R., Dykert, J., Rivier, J., Yoshikami, D., Olivera, B.M., 1995. A new family of *Conus* peptides targeted to the nicotinic acetylcholine receptor. J. Biol. Chem. 270, 22361–22367.

Jacobsen, R., Yoshikami, D., Ellison, M., Martinez, J., Gray, W.R., Cartier, G.E., Shon, K., Groebe, D.R., Abramson, S.N., Olivera, B.M., McIntosh, J.M., 1997. Differential targeting of nicotinic acetylcholine receptors by novel αA-conotoxins. J. Biol. Chem. 272, 22531–22537.

Jimenez, E.C., Craig, A.G., Watkins, M., Hillyard, D.R., Gray, W.R., Gulyas, J., Rivier, J.E., Cruz, L.J., Olivera, B.M., 1997. Bromocontryphan: post-translational bromination of tryptophan. Biochemistry 36, 989–994.

Jones, R.M., Bulaj, G., 2000. Conotoxins — new vistas for peptide therapeutics. Current Pharmaceutical Design, in press.

Kerr, L.M., Yoshikami, D., 1984. A venom peptide with a novel presynaptic blocking action. Nature 308, 282–284.

Kohn, A.J., 1956. Piscivorous gastropods of the genus *Conus*. Proc. Natl. Acad. Sci. USA 42, 168–171.

Kohn, A.J., Saunders, P.R., Wiener, S., 1960. Preliminary studies on the venom of the marine snail *Conus*. Ann. N.Y. Acad. Sci. 90, 706–725.

Lirazan, M.B., Hooper, D., Corpuz, G.P., Ramilo, C.A., Bandyopadhyay, P., Cruz, L.J., Olivera, B.M., 2000. The spasmodic peptide defines a new conotoxin superfamily. Biochemistry 39, 1583–1588.

Luo, S., Kulak, J.M., Cartier, G.E., Jacobsen, R.B., Yoshikami, D., Olivera, B.M., McIntosh, J.M., 1998. α-Conotoxin AulB selectively blocks α3β4 nicotinic acetylcholine receptors and nicotine-evoked norepinephrine release. J. Neurosci. 18, 8571–8579.

Martinez, J.S., Olivera, B.M., Gray, W.R., Craig, A.G., Groebe, D.R., Abramson, S.N., McIntosh, J.M., 1995. α-Conotoxin EI, a new nicotinic acetylcholine receptor-targeted peptide. Biochemistry 34, 14519–14526.

McCleskey, E.W., Fox, A.P., Feldman, D., Cruz, L.J., Olivera, B.M., Tsien, R.W., Yoshikami, D., 1987. ω-Conotoxins: Direct and persistent blockade of specific types of calcium channels in neurons but not muscle. Proc. Natl. Acad. Sci. USA 84, 4327–4331.

McIntosh, J.M., Olivera, B.M., Cruz, L.J., Gray, W.R., 1984. γ-Carboxyglutamate in a neuroactive toxin. J. Biol. Chem. 259, 14343–14346.

McIntosh, J.M., Santos, A.D., Olivera, B.M., 1999. *Conus* peptides targeted to specific nicotinic acetylcholine receptor subtypes. Annu. Rev. Biochem. 68, 59–88.

Mena, E.E., Gullak, M.F., Pagnozzi, M.J., Richter, K.E., Rivier, J., Cruz, L.J., Olivera, B.M., 1990. Conantokin-G: a novel peptide antagonist to the *N*-methyl-D-aspartate acid (NMDA) receptor. Neurosci. Lett. 18, 241–244.

Moczydlowski, E., Olivera, B.M., Gray, W.R., Strichartz, G.R., 1986. Discrimination of muscle and neuronal Na-channel subtypes by binding competitition between [3H]saxitoxin and μ-conotoxins. Proc. Natl. Acad. Sci. USA 83, 5321–5325.

Nakamura, H., Kobayashi, J., Ohizumi, Y., Hirata, Y., 1983. Isolation and amino acid compositions of geographutoxin I and II from the marine snail *Conus geographus* Linné. Experientia (Basal) 39, 590–591.

Nowycky, M.C., Fox, A.P., Tsien, R.W., 1985. Three types of neuronal calcium channel with different calcium agonist specificity. Nature 316, 440–443.

Olivera, B.M., 1997. E.E. Just Lecture, 1996. *Conus* venom peptides, receptor and ion channel targets and drug design: 50 million years of neuropharmacology. Mol. Biol. Cell 8, 2101–2109.

Olivera, B.M., Cruz, L.J., Yoskikami, D., 1999a. Effects of *Conus* peptides on the behavior of mice. Curr. Op. Neurobiol. 9, 772–777.

Olivera, B.M., Gray, W.R., Zeikus, R., McIntosh, J.M., Varga, J., Rivier, J., de Santos, V., Cruz, L.J., 1985a. Peptide neurotoxins from fish-hunting cone snails. Science 230, 1338–1343.

Olivera, B.M., Hillyard, D.R., Marsh, M., Yoshikami, D., 1995. Combinatorial peptide libraries in drug design: lessons from venomous cone snails. Tibtech 13, 422–426.

Olivera, B.M., McIntosh, J.M., Clark, C., Middlemas, D., Gray, W.R., Cruz, L.J., 1985b. A sleep-inducing peptide from *Conus geographus* venom. Toxicon 23, 277–282.

Olivera, B.M., McIntosh, J.M., Cruz, L.J., Luque, F.A., Gray, W.R., 1984. Purification and sequence of a presynaptic peptide toxin from *Conus geographus* venom. Biochemistry 23, 5087–5090.

Olivera, B.M., Miljanich, G., Ramachandran, J., Adams, M.E., 1994. Calcium channel diversity and neurotransmitter release: the ω-conotoxins and ω-agatoxins. Ann. Rev. Biochem. 63, 823–867.

Olivera, B.M., Rivier, J., Clark, C., Ramilo, C.A., Corpuz, G.P., Abogadie, F.C., Mena, E.E., Woodward, S.R., Hillyard, D.R., Cruz, L.J., 1990. Diversity of *Conus* neuropeptides. Science 249, 257–263.

Olivera, B.M., Walker, C., Cartier, G.E., Hooper, D., Santos, A.D., Schoenfeld, R., Shetty, R., Watkins, M., Bandyopadhyay, P., Hillyard, D.R., 1999b. Speciation of cone snails and interspecific hyperdivergence of their venom peptides: potential evolutionary significance of introns. Ann. N.Y. Acad. Sci. 870, 223–237.

Rumphius, G.E., 1705. D'Amboinsche Rariteikamer. Fr. Halma, Amsterdam.

Sato, S., Nakamura, H., Ohizumi, Y., Kobayashi, J., Hirata, Y., 1983. The amino acid sequences of homologous hydroxyproline containing myotoxins from the marine snail *Conus geographus* venom. FEBS Lett. 155, 277–280.

Shon, K., Grilley, M., Jacobsen, R., Cartier, G.E., Hopkins, C., Gray, W.R., Watkins, M., Hillyard, D.R., Rivier, J., Torres, J., Yoshikami, D., Olivera, B.M., 1997. A non-competitive peptide inhibitor of the nicotinic acetylcholine receptor from *Conus purpurascens* venom. Biochemistry 31, 9581–9587.

Shon, K., Grilley, M.M., Marsh, M., Yoshikami, D., Hall, A.R., Kurz, B., Gray, W.R., Imperial, J.S., Hillyard, D.R., Olivera, B.M., 1995. Purification, characterization and cloning of the lockjaw peptide from *Conus purpurascens* venom. Biochemistry 34, 4913–4918.

Shon, K., Olivera, B.M., Watkins, M., Jacobsen, R.B., Gray, W.R., Floresca, C.Z., Cruz, L.J., Hillyard, D.R., Bring, A., Terlau, H., Yoshikami, D., 1998a. μ-Conotoxin PIIIA, a new peptide for discriminating among tetrodotoxin-sensitive Na channel subtypes. J. Neurosci. 18, 4473–4481.

Shon, K., Stocker, M., Terlau, H., Stühmer, W., Jacobsen, R., Walker, C., Grilley, M., Watkins, M., Hillyard, D.R., Gray, W.R., Olivera, B.M., 1998b. κ-Conotoxin PVIIA: a peptide inhibiting the Shaker K^+ channel. J. Biol. Chem. 273, 33–38.

Spence, I., Gillessen, D., Gregson, R.P., Quinn, R.J., 1997. Characterization of the neurotoxic constituents of *Conus geographus* (L) venom. Life Sci. 21, 1759–1770.

Stone, B.L., Gray, W.R., 1982. Occurence of hydroxyproline in a toxin from the marine snail *Conus geographus*. Arch. Biochem. Biophys. 216, 756–767.

Terlau, H., Shon, K., Grilley, M., Stocker, M., Stühmer, W., Olivera, B.M., 1996. Strategy for rapid immobilization of prey by a fish-hunting cone snail. Nature 381, 148–151.

Walker, C., Steel, D., Jacobsen, R.B., Lirazan, M.B., Cruz, L.J., Hooper, D., Shetty, R., DelaCruz, R.C., Nielsen, J.S., Zhou, L., Bandyopadhyay, P., Craig, A., Olivera, B.M., 1999. The T-superfamily of conotoxins. J. Biol. Chem. 274, 30664–30671.

White, H.S., McCabe, R.T., Armstrong, H., Donevan, S., Cruz, L.J., Abogadie, F.C., Torres, J., Rivier, J.E., Paarman, I., Hollmann, M., Olivera, B.M., 2000. In vitro and in vivo characterization of conantokin-R, a selective NMDA antagonist isolated from the venom of the fish-hunting snail *Conus radiatus*. J. Pharmacol. Exp. Therap. 292, 425–432.

EXHIBIT 11

The Journal of Neuroscience, June 15, 1998, 18(12):4473–4481

μ-Conotoxin PIIIA, a New Peptide for Discriminating among Tetrodotoxin-Sensitive Na Channel Subtypes

Ki-Joon Shon,[1] Baldomero M. Olivera,[2] Maren Watkins,[3] Richard B. Jacobsen,[2] William R. Gray,[2] Christina Z. Floresca,[2,4] Lourdes J. Cruz,[2,4] David R. Hillyard,[3] Anette Brink,[5] Heinrich Terlau,[5] and Doju Yoshikami[2]

[1]Department of Physiology and Biophysics, Case Western Reserve University, Cleveland, Ohio 44106, Departments of [2]Biology and [3]Pathology, University of Utah, Salt Lake City, Utah 84112, [4]Marine Science Institute, University of the Philippines, Quezon City, 1101 Philippines, and [5]Molekulare Biologie Neuronaler Signale, Max-Planck-Institut für experimentelle Medizin, D-37075 Göttingen, Germany

We report the characterization of a new sodium channel blocker, μ-conotoxin PIIIA (μ-PIIIA). The peptide has been synthesized chemically and its disulfide bridging pattern determined. The structure of the new peptide is:

where *Z* = pyroglutamate and *O* = 4-*trans*-hydroxyproline.

We demonstrate that Arginine-14 (Arg^{14}) is a key residue; substitution by alanine significantly decreases affinity and results in a toxin unable to block channel conductance completely. Thus, like all toxins that block at Site I, μ-PIIIA has a critical guanidinium group.

This peptide is of exceptional interest because, unlike the previously characterized μ-conotoxin GIIIA (μ-GIIIA), it irreversibly blocks amphibian muscle Na channels, providing a useful tool for synaptic electrophysiology. Furthermore, the discovery of μ-PIIIA permits the resolution of tetrodotoxin-sensitive sodium channels into three categories: (1) sensitive to μ-PIIIA and μ-conotoxin GIIIA, (2) sensitive to μ-PIIIA but not to μ-GIIIA, and (3) resistant to μ-PIIIA and μ-GIIIA (examples in each category are skeletal muscle, rat brain Type II, and many mammalian CNS subtypes, respectively). Thus, μ-conotoxin PIIIA provides a key for further discriminating pharmacologically among different sodium channel subtypes.

Key words: Na channels; μ-conotoxin; tetrodotoxin; neuromuscular transmission; ion channel subtype; peptide

Several potent toxins target voltage-gated sodium channels; the different sites of binding and modes of activity of these toxins have been described (Catterall, 1992). These ligands have been indispensable for investigating the structure and function of these ion channels, which play a key role in excitable tissues. The demonstration (Narahashi et al., 1964) that tetrodotoxin specifically inhibited voltage-gated sodium currents without effect on potassium currents provided crucial experimental support for the Hodgkin–Huxley formulation of the action potential. Sodium channel toxins continue to be important pharmacological tools for neuroscientists.

Channel blockers, notably the guanidinium toxins saxitoxin and tetrodotoxin, target a site generally postulated to be at the extracellular end of the channel pore (Site I). Only one family of polypeptide toxins, the μ-conotoxins, has been shown to act at this site and functionally affect voltage-gated sodium currents. These were isolated originally from the venom of the marine snail *Conus geographus* (Stone and Gray, 1982; Sato et al., 1983; Cruz et al., 1985; Olivera et al., 1985).

Received July 29, 1997; revised March 27, 1998; accepted March 31, 1998.

This work was supported by Grant PO1 GM 48677 from the United States Public Health Service (USPHS), grants from the SFB Synaptische Interaktionen in neuronalen Zellverbänden (A.B. and H.T.), DOST-ESEP, Philippines (C.Z.F.), and USPHS Grant GM 54710 (K.S.). Rat Type II Na channel mRNA was prepared by Dr. M. Stocker. Some of the binding experiments were performed by J. S. Imperial.

Correspondence should be addressed to Dr. Baldomero M. Olivera, Department of Biology, University of Utah, Salt Lake City, Utah 84112.

Other families of *Conus* peptides (notably the ω-conotoxins, which target calcium channels, and the α-conotoxins, which target nicotinic acetylcholine receptors) have been found in the venoms of many *Conus* species that have been examined. Members within a given family of peptides from different *Conus* species have homologous structures but show extreme sequence hypervariability, and comparison of their activities has provided insightful structure–function information. In particular, the wide diversity among natural toxins within each family has been instrumental in identifying new subclasses of receptors (Olivera et al., 1990, 1994). By contrast, because the μ-conotoxins so far have been described only from the venom of *C. geographus*, most structure–function information for this peptide family has come from experiments with synthetic analogs.

In this report we describe the first new member of the μ-conotoxin peptide family to be characterized in over a decade, μ-conotoxin PIIIA from *Conus purpurascens*, an Eastern Pacific fish-hunting species. As expected, the new μ-conotoxin shows considerable sequence divergence from the μ-conotoxins of *Conus geographus*. In addition to a comprehensive biochemical characterization of the peptide, we provide electrophysiological and binding data, which demonstrate that μ-conotoxin PIIIA has considerable potential, both as a novel pharmacological tool for electrophysiology of the neuromuscular junction and for distinguishing among different tetrodotoxin-sensitive Na channel subtypes in the CNS.

(A)

```
--- GAA AAG AGA CAA CGA CTG TGT TGC GGT TTT CCG AAG AGT TGC AGA
    Glu Lys Arg Gln Arg Leu Cys Cys Gly Phe Pro Lys Ser Cys Arg
                ↑

TCC CGA CAA TGC AAA CCT CAT AGG TGT TGC GGA CGA TAA ---
Ser Arg Gln Cys Lys Pro His Arg Cys Cys Gly Arg OCH
```

(B)

```
          (1)     (2)          (3)   (4)
           ↓       ↓            ↓     ↓
---EKRQRLCCGFPKSCRSRQCKPHRCCGR
```

⇓

ZRLCCGFOKSCRSRQCKOHRCC-NH_2

Figure 1. *A*, The nucleic acid sequence derived by analyzing cDNA clones from a *Conus purpurascens* venom duct library. The sequence encoding the inferred C-terminal end of an open reading frame is shown. The pattern of Cys residues suggests that the encoded C-terminal peptide might be a μ-conotoxin. The *arrow* indicates the predicted site of proteolytic cleavage to generate the mature toxin: a -Lys-Arg- sequence is the most common motif for proteolytic cleavage of conotoxin precursors. *B*, The predicted sequence of the post-translationally processed mature peptide. The amino acid sequence shown in *A* would be predicted to be post-translationally processed at the four indicated sites as follows: the encoded glutamine residue would be converted to pyroglutamate after proteolysis (site *1*), proline would be hydroxylated to 4-*trans*-hydroxyproline (sites *2* and *3*), and the C-terminal -Cys-Gly-Arg- sequence would be processed by an exopeptidase and amidation enzymes to a -Cys-NH_2 moiety (site *4*). These post-translational processing events would yield the indicated *bold* sequence, where *Z* = pyroglutamate and *O* = 4-*trans*-hydroxyproline.

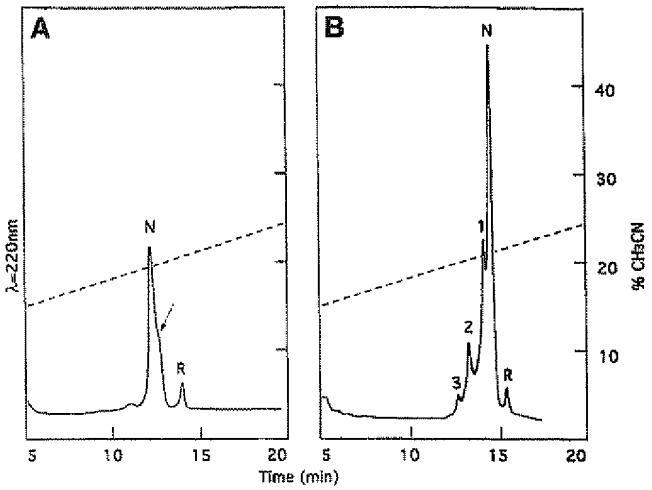

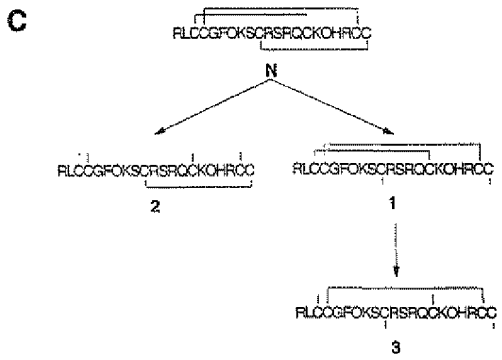

Figure 2. Disulfide bridge analysis. Reverse-phase HPLC chromatograms (12–30% acetonitrile gradient in 30 min; flow rate = 1 ml/min) of native (*N*), fully reduced (*R*), and partially reduced μ-PIIIA[2–22] after incubation with 20 mM TCEP, pH 3. *A*, Before iodination, the partially reduced species is indicated with an *arrow* (1 min incubation at 65°C). *B*, After mono-iodination of His residue, intermediates are labeled *1–3* (5 min incubation at room temperature). *C*, Schematic diagrams of disulfide connectivity in fully oxidized and partially reduced peptides, as labeled in *B*.

MATERIALS AND METHODS

Molecular cloning. *Conus purpurascens* venom ducts were collected, and mRNA was prepared by methods previously described (Woodward et al., 1990; Colledge et al., 1992; Hopkins et al., 1995). The analysis of cDNA clones from *Conus* venom ducts was performed as detailed previously (Colledge et al., 1992; Hillyard et al., 1992; McIntosh et al., 1995).

Solid-phase peptide synthesis. The peptide was built without the N-terminal pyroglutamate on Rink amide resin, using standard Fmoc chemistry. All amino acids were purchased from Bachem (Torrance, CA), and side chains were protected as follows: Arg(pmc), His(trt), Hyp(t-bu), Lys(Boc), Ser(t-bu), Gln(trt), and Cys(trt). Peptide bond coupling was performed with equimolar amounts of amino acid, dicyclohexylcarbodimide (DCC), and hydroxybenzotriazole (HOBT) on an ABI model 430A synthesizer. The terminal Fmoc group was removed by treatment with 1:4 piperidine/*N*-methylpyrrolidone (NMP) (v/v). To complete the predicted sequence of the peptide, we manually coupled pyroglutamate to portions of the resin before peptide cleavage. Resin (50 mg) was deprotonated by treatment with 1 ml of piperidine (20% in NMP) for 1 min and washed three times each with alternating methanol and NMP. Pyroglutamate (0.5 mmol) was activated in 1 ml of 1 M diisopropylcarbodimide (DIC)/1 M hydroxybenzotriazole (HOBT) in NMP for 30 min; the solution was added to the deprotonated resin, and the reaction mixture was stirred for 2.5 hr. Then the resin was centrifuged and washed with NMP five times, followed by three washes with methanol. Pyroglutamate was not protected with Fmoc, and so further deprotection was not necessary. The final resin was subjected to peptide cleavage as described previously (Shon et al., 1995). The cleavage mixture was filtered into tert-butyl methyl ether at −10°C. The peptide immediately precipitated, and the solution was centrifuged to separate the pellet, which was washed once with the ether. The pellet dissolved in 60% acetonitrile (ACN)/0.1% trifluoroacetic acid (TFA) in H_20 and was purified by HPLC on a Vydac C_{18} preparative column (2.5 cm; flow = 20 ml/min). The linear peptide was oxidized with glutathione as described previously (Dudley et al., 1995) and yielded a mixture of isomers. The major isomer, accounting for 20–30% of the total absorbance, proved to be biologically active. After preparative purification, this isomer was purified to homogeneity, using a Vydac C_{18} semi-preparative column (7.0 mm × 240 cm; flow = 3 ml/min). All HPLC was done by using a 12–30% linear gradient of ACN in 0.1% TFA and water. Analysis of the purified, biologically active peptide by electrospray mass spectrometry gave a monoisotopic MH^+ = 2604.05 (calculated MH^+ = 2604.12).

The same methods were used to obtain the R14A analog of μ-PIIIA. To obtain the unblocked analog, μ-PIIIA[2–22], we performed the same cleavage and oxidation procedures with resin to which pyroglutamate was not coupled manually.

Disulfide bridge analysis. The disulfide connectivity of μ-PIIIA was analyzed by the partial reduction strategy of Gray (1993), using an analog without the N-terminal pyroglutamate and the mono-iodohistidine derivative of the same peptide (see Results). As detailed in Shon et al. (1995), peptides were partially reduced, using tris (2-carboxyethyl) phosphine (TCEP), and then alkylated with iodoacetamide. Yields of partially alkylated peptide were low. To avoid further loss of peptide, we performed amino acid sequencing with the remaining disulfide bonds intact, using automated Edman degradation on an ABI Model 477A instrument. All purification was done with a Vydac C_{18} analytical HPLC column (218TP54; 4.6 × 250 mm), and peptides were eluted under the conditions previously described above in Solid-Phase Peptide Synthesis.

Iodination of μ-conotoxin PIIIA[2–22]. Peptide solution (5–10 nmol in ~700 μl of HPLC eluant) was combined with an equal volume of 0.1 M Tris, pH 8. Iodine in methanol (2 mM) was added to make a final iodine concentration of 20 μM. After a 10 min incubation at room

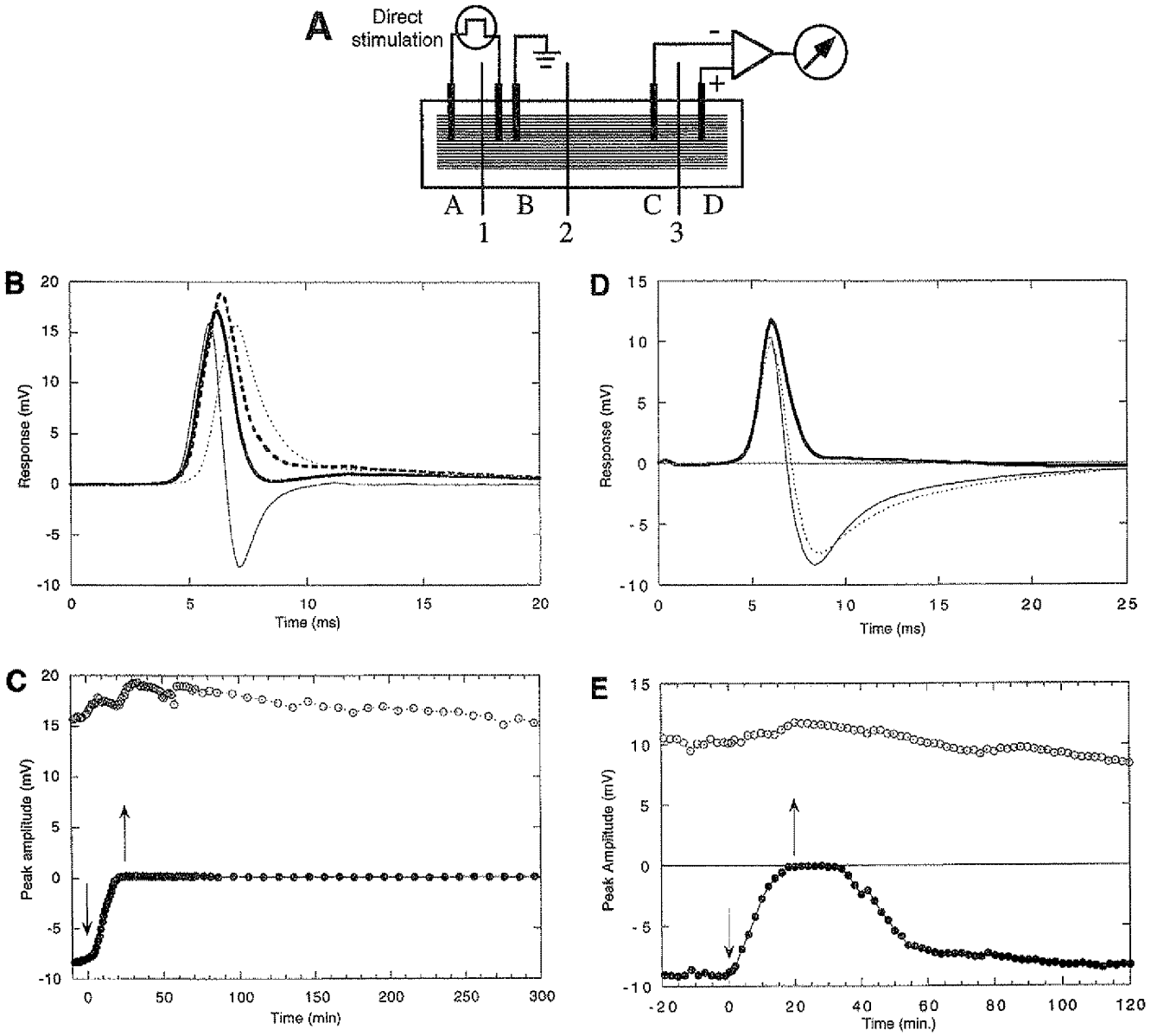

Figure 3. *A*, Sketch of electrophysiological recording chamber for testing toxin on frog's cutaneous pectoris muscle response to direct electrical stimulation. The rectangular SYLGARD trough (~4 × 16 × 1 mm) was partitioned into four compartments (*A–D*) by three Mylar sheets (*1–3*). The sheets were inserted into slots in the wall of the trough after the muscle had been pinned to the floor of the trough. Two Mylar strips (~1 × 55 × 0.1 mm) were placed on either side of the muscle to serve as stops to prevent the partitions from cutting into the muscle. The cutaneous end of the muscle was located in *A*, and the xiphisternum (cartilage) was in *D*. Stimulating electrodes were in *A* and *B*, and a ground electrode was in *B*. The recording electrode in *C* was connected to the negative input, and that in *D* was connected to the positive input of a differential AC preamplifier. Compartment *D* served as the test chamber; only the muscle segment in this compartment was exposed to toxin. All compartments contained Ringer's solution, and all electrodes were bare platinum wires. *B*, PIIIA (1 μM) blocks directly evoked action potentials in frog muscle. Shown are superimposed traces of responses before, during, and after exposure to toxin. Stimulus was applied at $t = 0$. *Thin solid curve*, Control response; *bold solid curve*, response after exposure to toxin for 23 min and just before toxin was washed out; *bold dashed curve*, response 20 min after toxin washout; *thin dashed curve*, response after >4.5 hr of washing. Toxin was placed only in compartment *D* (see *panel A*), which contained the portion of the muscle that produced the negative phase of the response in the control trace. *C*, Time course of the block of the directly evoked action potentials. Maximum amplitudes of the positive phase (*open circles*) and negative phase (*filled circles*) of the response are plotted as a function of time. The solution in compartment *D* was replaced with 1 μM PIIIA at time *0* (*downward arrow*), and the toxin was washed out 23 min later (*upward arrow*). *D*, μ-Conotoxin GIIIA (5 μM) reversibly blocks directly evoked action potentials in frog muscle. Shown are superimposed traces of responses before, during, and after exposure to toxin. *Thin solid curve*, Control response; *bold solid curve*, response after 20 min of exposure to toxin; *dashed curve*, response 45 min after toxin is washed out. Experimental conditions were essentially the same as those for Figure 4*A*, except that GIIIA instead of PIIIA was used and that the experiment was conducted with a different cutaneous pectoris muscle preparation. *E*, Time course of the block of the directly evoked action potentials by μ-conotoxin GIIIA. Maximum amplitudes of the positive phase (*open circles*) and of the negative phase (*filled circles*) of responses are plotted as a function of time. The solution in compartment *D* was replaced by 5 μM toxin at $t = 0$ (*downward arrow*), and the toxin was washed out 20 min later (*upward arrow*). Responses behaved essentially the same as those obtained with exposure to μ-conotoxin PIIIA (see Fig. 4*B*), except that here the effect of the toxin GIIIA was reversible.

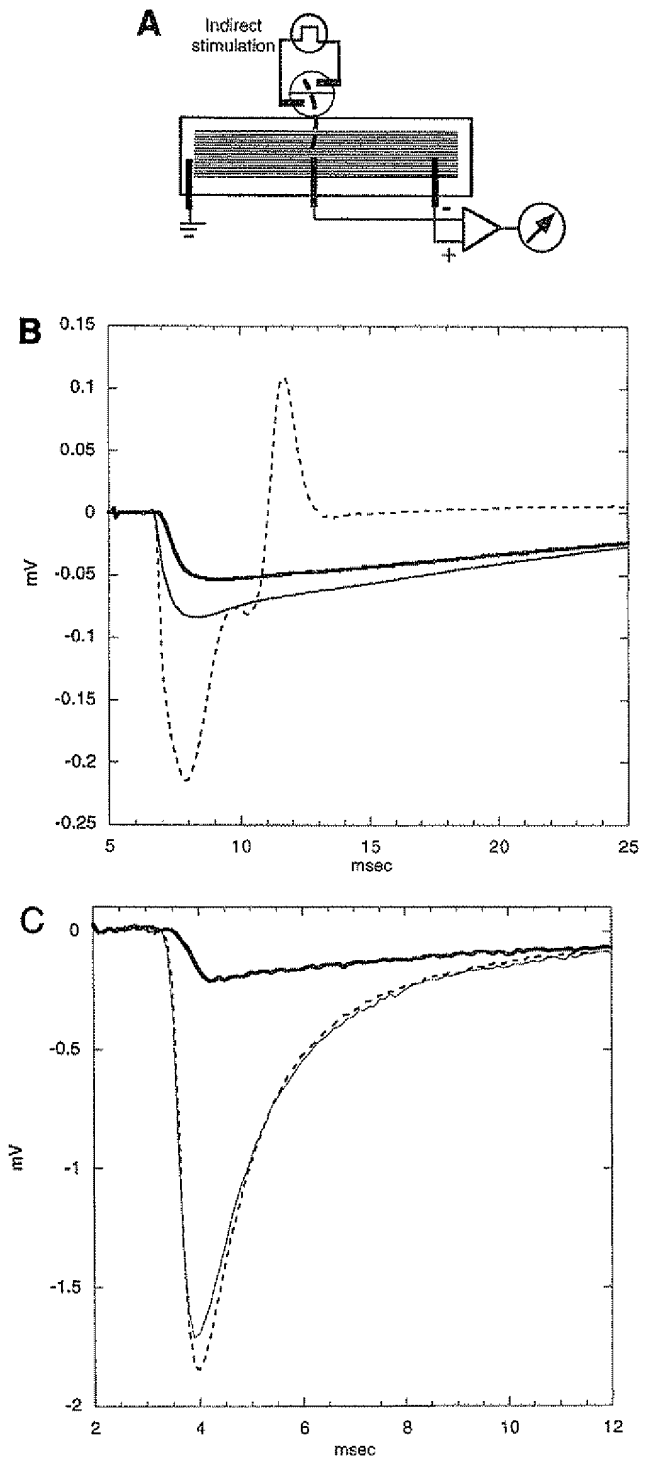

Figure 4. *A*, Sketch of recording chamber for indirect stimulation. For indirect stimulation the frog motor nerve (*bold dashed line*) was draped into a circular, two-compartment well adjoining the trough in which the muscle resided. The compartments of the well contained stimulating electrodes, and the wire recording electrodes that are illustrated were used to acquire the extracellular responses shown in *B*. The trough contained no partitions so that the entire muscle could be exposed to toxin. *B*, Extracellularly recorded responses before, during, and after exposure to 5 μM PIIIA. The motor nerve was stimulated at $t = 5$ msec while the response was recorded with a wire electrode from the endplate region of a population of muscle fibers. The "before" trace (*dashed*) has an early negative and late positive phase, the former having contributions from both action and synaptic potentials and the latter consisting of the propagated action potential. The "during" (*bold*) and "after" (*thin solid*) responses have only a negative phase, indicating that only the endplate current remains after treatment with toxin. Note that the latency of the response is reversibly increased by the peptide, suggesting that PIIIA reversibly reduces the conduction velocity of the action potential of the motor nerve. PIIIA also reversibly attenuates the postsynaptic response, an action reminiscent of the effect of focal tetrodotoxin application (Katz and Miledi, 1968). *C*, Extracellular synaptic currents recorded before, during, and after exposure to ~20 μM PIIIA. The motor nerve was stimulated (at $t = 2$ msec) every minute, and the responses were recorded with a focal extracellular electrode, the tip of which was placed near the endplate of a fiber of a muscle that previously had been exposed to ~2 μM PIIIA for 15 min, to preblock the sodium channels of the muscle irreversibly; then it was washed. Each trace represents the average of five evoked responses acquired before toxin exposure (*dashed curve*), after the preparation had been exposed to 20 μM PIIIA for 15 min (*bold curve*), or 50 min after the washout of toxin was initiated (*solid curve*). The response was mainly from a single endplate; hence, its time course was briefer than the synaptic responses in *B*. As in *B*, the toxin reversibly attenuated the amplitude of the response, albeit more strongly, and reversibly increased its latency.

temperature, the reaction was quenched by the addition of 0.75 M ascorbic acid (1:100 by volume). The mixture was applied to an analytical column and eluted by using the HPLC conditions described above. The mono- and di-iodo derivatives of μ-PIIIA[2–22] eluted as discrete peaks ~1.5 and 3 min after the noniodinated form, using a gradient of 0.6% ACN increase per minute. The expected masses of the iodinated derivatives were confirmed by electrospray mass spectrometry.

Electrophysiology. The cutaneous pectoris muscle dissected from ~7 cm of *Rana pipiens* frogs was trimmed longitudinally so that only the lateral one-quarter of muscle remained (Yoshikami et al., 1989). The trimmed muscle was pinned flat on the bottom of a shallow trough fabricated from SYLGARD (a silicone elastomer, Dow Chemical, Midland, MI). To examine the response of the muscle to direct electrical stimulation, we partitioned the trough as illustrated in Figure 3*A*. Current was injected into the muscle across partition 1; the stimulating electrodes were connected to a stimulus isolation unit, and supramaximal 1-msec-long rectangular pulses were used to elicit action potentials in the muscle directly. Stimuli were applied at a frequency of 1/min or less. The recording electrodes monitored the potential across partition 3 (partition 2 served to isolate the recording electrically from the stimulating electrodes). When the action potential propagated into chamber C, a positive response was recorded by the preamplifier, and the further propagation of the action potential into chamber D was recorded as a negative response. Thus, the extracellularly recorded action potential from the population of fibers in the muscle was recorded as a biphasic response, with the phases separated from each other by only a few milliseconds (see Fig. 3*B*). To examine the effect of the toxin, we replaced the normal frog Ringer's solution in chamber D by one containing toxin. If the toxin blocked sodium channels, attenuation of only the late negative phase should be observed. The early positive phase should remain mainly unaltered, reflecting the fact that portions of the muscle not exposed to toxin remained normal. Thus, there are two advantages of exposing only the solution in chamber D to toxin: one, this allows the response in chamber C to serve as an internal control for the overall vitality of the muscle preparation as well as to insure that the stimulus remains supramaximal; two, the volume of toxin solution necessary is reduced, and in these experiments 25 μl sufficed.

To examine synaptically evoked responses, we used an arrangement similar to that previously described (Yoshikami et al., 1989) (see Fig. 4*A*). The trough was similar to that used for direct stimulation but had no partitions, and the motor nerve was draped into a two-compartment well adjacent to the trough. Both compartments of the well were filled with Ringer's solution. The portions of the nerve exposed to air were covered with Vaseline. Each compartment of the well had an electrode to allow for electrical stimulation (0.1 msec rectangular pulses) of the nerve. The recording and ground electrodes were essentially the same as those for direct stimulation, except that the negative recording electrode was centered near the middle of the muscle where the endplates were located. This placement of the electrodes allowed the extracellular endplate currents from the population of fibers to be

←

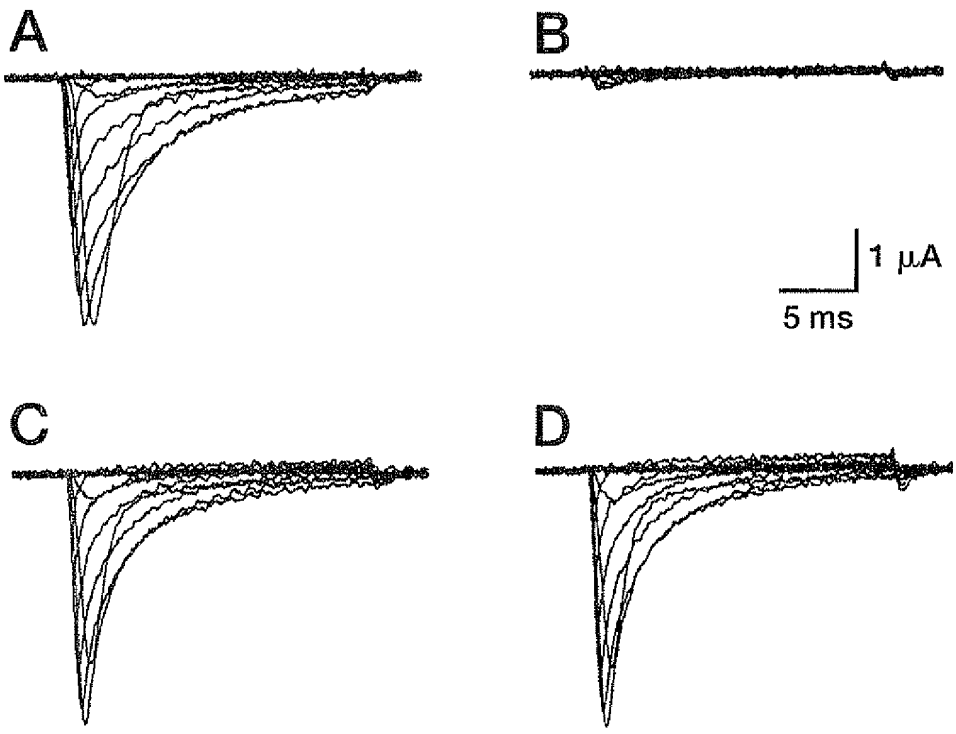

Figure 5. μ-PIIIA blocks rat Type II Na channel expressed in *Xenopus* oocytes. *A*, Whole-cell current recorded from an oocyte expressing rat Type II Na channels. Voltage steps ranging from −80 to + 60 mV, in 10 mV increments, were generated from a holding potential of −100 mV. *B*, The addition of 2 μM μ-PIIIA to the bath solution resulted in a profound block of the currents. *C*, Wash with frog Ringer's solution. *D*, The addition of 2 μM μ-GIIIA did not block the sodium currents.

recorded readily (Yoshikami et al., 1989) (see also Fig. 4*B*). When the action potentials of the muscle were blocked irreversibly with PIIIA, no muscle movement occurred when the nerve was stimulated, so an extracellular recording microelectrode could be placed close to the endplate of a selected fiber to record more focal extracellular synaptic currents (see Fig. 4*C*).

Recording from cloned channels in oocytes. Oocytes from *Xenopus laevis* were prepared as described previously (Stühmer, 1992). cRNA encoding rat Type II sodium channel α-subunit (Noda et al., 1986) or rat μ1 skeletal muscle Na channel (Trimmer et al., 1989) was injected into stage VI oocytes (30–50 ng/oocyte). The vitelline membranes of the oocytes were removed mechanically with fine forceps, and currents were recorded in frog Ringer's solution 2–6 d after injection under two-electrode voltage-clamp control with a Turbo-Tec amplifier (NPI Elektronik, Tamm, Germany) driven by the Pulse+PulseFit software package (HEKA Elektronik, Lambrecht, Germany). Intracellular electrodes were filled with 2 M KCl and had a resistance between 0.6 and 0.8 MΩ. Current records were low-pass-filtered at 3 kHz and were sampled at 10 kHz. Leak and capacitive currents were corrected on-line by using a P/N method. To estimate the IC_{50} for the block of PIIIA, we measured whole-cell currents of oocytes expressing rat Type II or μ1 Na channels, and we successively increased the toxin concentrations in the bath. The peak inward current was measured and plotted against the toxin concentration. Dose–response curves were fit by using the equation: $y = (1 + (T/IC_{50})^n)^{-1}$, where T is the toxin concentration and n is the Hill coefficient.

Binding experiments. [^{3}H]Saxitoxin binding to rat brain membranes was performed by the protocol of Doyle et al. (1993) except that the assays were scaled down to a volume of 0.25 ml, and 1 mM phenylmethylsulfonyl fluoride (PMSF), 1 μM leupeptin, and 1 μM pepstatin were present. Electric eel membranes were prepared as described by Becker et al. (1989) except that the homogenizing buffer used was (in mM) 10 HEPES-Tris, 10 EDTA, 10 EGTA, and 1 PMSF plus 1 μM leupeptin and pepstatin, pH 7.0.

RESULTS

Identification of a cDNA clone from *Conus purpurascens* encoding a putative μ-conotoxin: chemical synthesis

The feasibility of discovering new *Conus* peptides from the predicted amino acid sequences encoded by cDNA clones was demonstrated previously with ω-conotoxins (Hillyard et al., 1992). As part of a comprehensive program to characterize the toxins in the venom of *Conus purpurascens* systematically, a large number of cDNA clones derived from the mRNA of the venom duct of *C. purpurascens* have been sequenced. Several cDNA clones contain the nucleotide sequence shown in Figure 1; the predicted amino acid sequence from this nucleotide sequence strongly suggests that the clone might encode a μ-conotoxin. There are a number of important features similar to those of the previously characterized μ-conotoxins (μ-GIIIA, μ-GIIIB, and μ-GIIIC from *Conus geographus*), despite the significant sequence divergence: the pattern of Cys residues, the high net positive charge, and the apparent conservation of the critical Arg residue (residue 14 of the predicted mature peptide) believed to be essential for μ-conotoxin function (Sato et al., 1991; Becker et al., 1992).

We therefore synthesized the predicted 22-residue peptide, incorporating post-translational modifications modeled on other related peptides: (1) Gln^1 to pyroglutamate (all glutamines at the termini of *Conus* peptides so far have been found as pyroglutamates), (2) prolines to hydroxyproline (all prolines in known μ-conotoxins are hydroxylated), and (3) C-terminal -Cys.Cys.Gly.Arg- to -Cys.Cys.NH_2 (the presence of -Gly.Arg- is

a signal for C-terminal amidation). This predicted peptide is referred to as μ-conotoxin PIIIA (μ-PIIIA), based on the physiological evidence detailed below. A detailed description of the chemical synthesis and oxidation of μ-PIIIA is given under Materials and Methods. The pure synthetic peptide caused flaccid paralysis in both mice and fish, as expected for a μ-conotoxin (Cruz et al., 1985).

Disulfide bridge analysis

The putative mature peptide has a pyroglutamate residue at the N terminus. Because disulfide bridge analysis requires that the partially reduced intermediates be sequenced by Edman degradation, each blocked intermediate would need to be unblocked enzymatically. Instead, we analyzed the analog lacking the N-terminal pyroglutamate. This was readily available from cleavage of the resin before the final addition of pyroglutamate. The major μ-conotoxin PIIIA[2–22] peptide obtained after the Cys residues were oxidized was bioassayed and proved to cause paralysis in fish. A comparison of the efficacy of the two peptides on frog skeletal muscle (see Electrophysiology Using Amphibian Muscle, below) also shows that both peptides blocked muscle action potentials, with no recovery after toxin washout for at least 3 hr in both cases. This strongly indicated that the major oxidation product of both the original peptide and the analog shares the same disulfide pattern.

Partial reduction of μ-PIIIA[2–22] produced only one species that could be separated from the fully oxidized peptide (indicated by the *arrow* in Fig. 2*A*). Alkylation and sequence analysis revealed that this peptide had a single intact disulfide bridge (shown as sequence 2 in Fig. 2). A second reduction intermediate was required to determine the remaining disulfide linkages. Repeated attempts to obtain another intermediate under the reaction conditions in Figure 2*A* were unsuccessful; however, partial reduction of the mono-iodohistidine derivative of μ-PIIIA[2–22] produced three species, as shown in Figure 2*B*, that could be separated from the oxidized peptide in quantities sufficient for analysis. Each peak in Figure 2*B* is numbered to show the corresponding peptide structure in Figure 2*C*, as revealed by alkylation and sequence analysis. These data reveal that μ-conotoxin PIIIA has the same disulfide pattern as μ-conotoxin GIIIA as well as the following structure:

where *Z* = pyroglutamate and *O* = 4-*trans*-hydroxyproline.

Electrophysiology using amphibian muscle

The effects of the peptide on the response of the frog muscle to direct electrical stimulation were investigated with the recording chamber illustrated in Figure 3*A*. A control response before toxin addition is shown in Figure 3*B*. The progression of the action potential between muscle segments in compartments C and D is readily apparent; the biphasic waveform that was generated represents the propagation of the action potential from C to D. When μ-PIIIA was added to segment D, the action potential clearly propagated into segment C, causing the voltage change characteristic of the first half of the biphasic waveform in Figure 3*B*; however, the negative phase was abolished completely, indicating that propagation in segment D of the muscle was abolished. These results are consistent with inhibition of voltage-gated sodium channels in the muscle plasma membrane.

On exposure to toxin, the positive phase initially becomes larger as the counteracting negative phase is attenuated. The initial rising phase of the positive phase also is delayed slightly after exposure to toxin; this is thought to be attributable to leakage of the toxin into compartment C with an attendant decrease in the propagation velocity of the action potential in that compartment. The leak of toxin into compartment C is also thought to be responsible for the decrement in the amplitude of the positive phase as well as delayed time to peak observed in the response taken >4.5 hr later.

The peaks of the responses as a function of time before, during, and after toxin addition are shown in Figure 3*C*. The negative phase is completely and irreversibly obliterated by exposure to μ-conotoxin PIIIA, whereas the positive phase remains mainly intact, indicating that no untoward systemic changes occurred. Even with washing for many hours in the absence of toxin, no recovery was observed in segment D, although action potential propagation to segment C was essentially normal (a slight rundown was observed with time). Similar results also were observed with the μ-PIIIA[2–22] analog of the toxin (results not shown).

The results are consistent with the activity of a μ-conotoxin; the homologous peptides from *Conus geographus* previously have been shown to be highly specific for the skeletal muscle Na channel subtype in peripheral systems. Although μ-GIIIA and μ-PIIIA selectively inhibit skeletal muscle action potentials, a notable difference is that the latter peptide appears to act much more irreversibly in the frog neuromuscular preparation (see Fig. 3*D,E* for the results with μ-GIIIA).

Indirect stimulation experiments

Synaptically evoked responses also were examined (Fig. 4). When the frog motor nerve was stimulated electrically, a muscle twitch was observed and muscle action potential was recorded. After exposure to μ-conotoxin PIIIA, muscle twitches and action potentials were abolished completely; in contrast, endplate currents still were observed. Thus, the propagation of action potentials in the motor axon is not blocked, although action potentials in the muscle were abolished.

However, in the presence of high concentrations of PIIIA, an effect on the excitatory postsynaptic response was observed. The latency of the response was increased, and its amplitude was attenuated. These effects on the synaptic response, unlike the block of the action potential of the muscle, were reversible. The attenuation of the synaptic response was greater during exposure to 20 than to 5 μM PIIIA (Fig. 4*B,C*). At lower concentrations of toxin (~1 μM) the muscle action potential still could be abolished irreversibly, but the delay in response latency was barely detectable (data not shown). These changes in the synaptic response are presumed to be a presynaptic effect of PIIIA. They clearly require a relatively high concentration of toxin and are reversible, as compared with the irreversible high-affinity effects of the toxin on the muscle action potential.

The new peptide, μ-PIIIA, should serve as a most convenient pharmacological agent for irreversibly preventing muscle twitching when the synaptic electrophysiology of amphibian neuromuscular junctions is investigated. Application of the toxin, followed by washout, yields a frog motor nerve/skeletal muscle preparation with muscle action potentials selectively blocked, an ideal preparation for examining synaptic events.

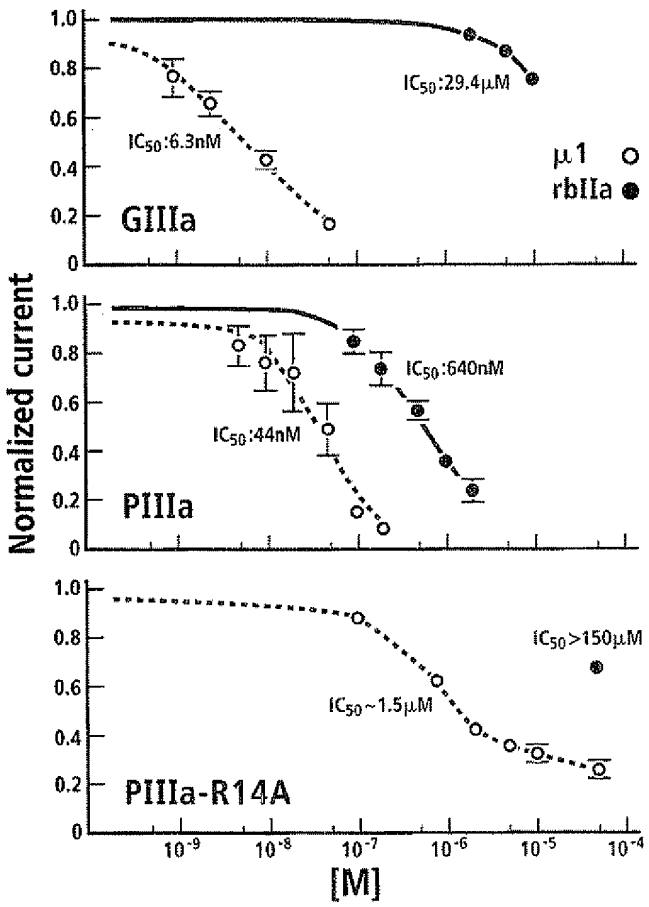

Figure 6. Inhibition of sodium currents by μ-conotoxin PIIIA and the R14A analog. Shown are dose–response curves for the block of μ-conotoxin GIIIA (*top panel*) and PIIIA (*middle panel*) on skeletal muscle sodium channels (*open circles*) and on rat brain IIA sodium currents (*filled circles*). *Bottom panel*, Block of rat skeletal muscle sodium currents by the analog μ-PIIIA[R14A]. For the R14A analog tested on the rat brain IIA sodium channel only, the data point for 50 μM is given, which blocked the currents by only ~30%.

Effect of μ-PIIIA on two different mammalian Na channel subtypes

We investigated whether μ-conotoxin PIIIA could affect voltage-gated sodium channels in the mammalian CNS. The effect of the toxin was tested on a major subtype of voltage-gated sodium channels found in central neurons expressed in *Xenopus* oocytes, the tetrodotoxin (TTX)-sensitive Type II voltage-gated sodium channels (Fig. 5*A–C*). μ-PIIIA blocked Type II Na channels from rat; the presence of μ-PIIIA (2 μM) in the bath solution abolished nearly all Na current, but in a reversible manner (Fig. 5*B,C*). Under the same conditions μ-GIIIA did not affect Na currents (Fig. 5*D*). A comparison of the dose–response for the two toxins is shown in Figure 6; the inhibition by μ-GIIIA is incomplete even at the highest concentration tested. The data indicate that μ-PIIIA has a ~50-fold greater affinity for the channel than does μ-GIIIA.

The effects of μ-conotoxins PIIIA and GIIIA on a cloned mammalian skeletal muscle sodium channel subtype expressed in *Xenopus* oocytes also were evaluated; a comparison between the muscle and Type II subtypes is shown for both μ-GIIIA and μ-PIIIA in Figure 6 (*top* and *middle panels*); both toxins block the conductance of this cloned channel. The affinity of μ-PIIIA for the mammalian muscle sodium channel is higher than for the CNS Type II subtype (IC_{50} ~44 vs 640 nM); however, the affinity of μ-PIIIA for the mammalian muscle channel does not seem to be as high as for fish and amphibian channels of the same subtype. Although both toxins are high-affinity antagonists when tested on the skeletal muscle Na channel subtypes from a variety of vertebrate systems, μ-PIIIA binds more irreversibly in the amphibian system, whereas μ-GIIIA is the more potent toxin for the mammalian skeletal muscle subtype.

Structure–activity studies: effects of mutations in a critical arginine residue

Structure–activity studies done on μ-conotoxins from *Conus geographus* suggested that the guanidinium group of a critical Arg residue is responsible for occluding the ion channel pore. Although μ-conotoxin PIIIA is highly divergent in sequence from μ-conotoxins from *Conus geographus*, the alignment of conserved cysteine residues suggests that Arginine-14 (Arg^{14}) is homologous to the critical Arg defined in the *Conus geographus* μ-conotoxins. We therefore evaluated the effects of an alanine substituted for the Arg residue in this position. The R14A-μ-conotoxin PIIIA homolog was tested first on the Type II rat brain sodium channel; no effects on channel conductance were seen at concentrations >10-fold greater than the K_D of the wild-type toxin for the Type II sodium channel. Although we did not have sufficient toxin to carry out a complete curve, an extrapolation suggests that the μ-PIIIA[R14A] homolog has a IC_{50} >150 μM for antagonizing the Type II rat brain sodium channel (Fig. 6, *bottom panel*).

The μ-PIIIA[R14A] homolog also was evaluated, using rat skeletal muscle sodium channel subtype expressed in oocytes (Fig. 6, *bottom panel*). Clearly, the homolog has a lower affinity for this cloned channel than does the wild-type toxin. However, the data in Figure 6 do not fit a simple monotonic inhibition curve; it appears that, even at 100 μM μ-PIIIA[R14A], significant conductance is still detected (>20% of the control). Thus, although an apparent IC_{50} of ~1.5 μM is obtained in this experiment, the data suggest that a sodium channel bound by the μ-PIIIA[R14A] homolog has significantly reduced but measurable conductance. These data are qualitatively similar to results obtained with the R13Q homolog of μ-conotoxin GIIIA (French et al., 1996). Thus, the R14A substitution caused a decrease in the affinity of the toxin for the μ1 rat muscle sodium channel and resulted in a channel with some residual conductance even when toxin was bound.

Binding experiments

Binding displacement experiments were performed with [^{3}H]saxitoxin as the radiolabeled ligand and with *Electrophorus electricus* electric organ membranes as the source of the receptors (Fig. 7). The electric organ has a high density of Na channels more closely resembling a skeletal muscle subtype than the neuronal Na channel subtypes. As expected, μ-conotoxin PIIIA completely displaced [^{3}H]saxitoxin ([^{3}H]STX) binding to electric organ membranes. Clearly, μ-conotoxin PIIIA has a high affinity (IC_{50} ~3×10^{-9} M) for the STX binding site of *Electrophorus* electric organ.

In contrast, it was found that μ-PIIIA displaced only a fraction (>50%) of specific [^{3}H]STX binding to crude membranes from rat brain. A comparison of μ-PIIIA and μ-GIIIA displacement of specific [^{3}H]STX binding to rat brain sites is shown in Figure 7. These data indicate that μ-PIIIA displaces more than one-half of the [^{3}H]STX high-affinity sites in rat brain; in contrast, μ-GIIIA

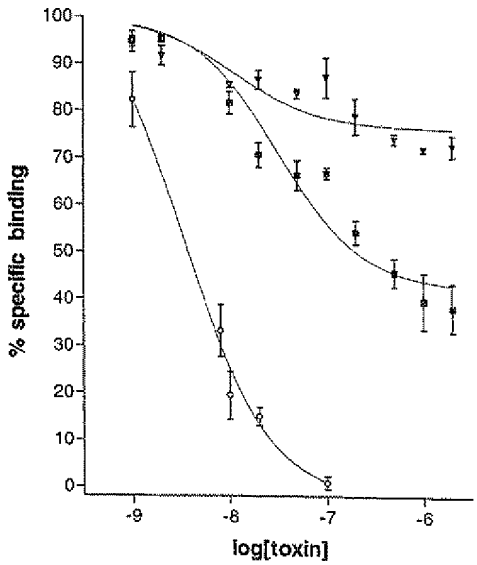

Figure 7. Binding competition experiments with [^{3}H]saxitoxin. The displacement of specific [^{3}H]STX binding by μ-conotoxin in rat brain and in eel electroplax was determined as described in Materials and Methods. Specific binding was determined by subtracting the nonspecific binding of [^{3}H]saxitoxin from the total binding; the nonspecific binding was measured by using 12 μM TTX to displace [^{3}H]saxitoxin binding. *Open circles*, μ-PIIIA displacement for eel electroplax sites; *squares*, μ-PIIIA displacement for rat brain sites; *triangles*, μ-GIIIA displacement for rat brain sites. Error bars indicate SEM.

displaces ~20% of specific [^{3}H]STX binding at the same concentrations. These results suggest the presence of a significant number of μ-PIIIA-sensitive, μ-GIIIA-resistant Na channels in the mammalian CNS.

DISCUSSION

The studies above establish that *Conus purpurascens* venom ducts express a μ-conotoxin. Although this peptide, μ-conotoxin PIIIA, has clear structural homology with the three previously characterized μ-conotoxins from *Conus geographus* venom, it exhibits significant sequence divergence. There are many parallels between this work and previous work on the Ca channel blocker ω-conotoxin MVIIC ((Hillyard et al., 1992; Olivera et al., 1994). Both peptides were synthesized directly from predicted sequences of cDNA clones and were not purified from venom. Both peptides, although being relatively specific, exhibited somewhat broader target specificity than their previously characterized homologs (ω-conotoxin GVIA in the case of ω-MVIIC and μ-conotoxin GIIIA for μ-PIIIA).

The peptide from *Conus purpurascens*, μ-conotoxin PIIIA, like the μ-conotoxins from *Conus geographus* (Table 1) is highly positively charged and has the same disulfide framework. Of the 16 noncysteine amino acids in μ-conotoxin PIIIA, only five are identical in all four peptides (Arg^2, Hyp^8, Arg^{14}, Lys^{17}, and Hyp^{18}). Some of the most divergent substitutions involve the replacement of the two aspartic acid residues by Leu^3 and Ser^{13}. Sato et al. (1991) reported that individual replacements of these aspartate residues by Ala increased the potency of μ-GIIIA analogs in rat diaphragm muscle two- to threefold. Of great significance is the conservation of Arg^{14}, the amino acid residue previously reported to be critical for activity (Sato et al., 1991; Becker et al., 1992). We have demonstrated that the R14A analog of μ-PIIIA has much lower affinity for muscle Na channels expressed in oocytes and, even at saturating concentrations, is unable to block channel conductance completely. A detailed model of μ-GIIIA with its homologous Arg residue placed within the vestibule of the sodium channel has been published (Dudley et al., 1995); our results with the R14A homolog are consistent with this postulated role for Arg^{14}.

Potentially, some of the most useful results of the present study arise from the differences in affinity and Na channel subtype specificity between μ-conotoxin PIIIA and μ-GIIIA. In amphibians, the inhibition of muscle action potentials by μ-GIIIA is reversible, whereas that by μ-PIIIA is essentially irreversible (see Fig. 3). At high concentrations PIIIA appears to have presynaptic effects analogous to the reduction and delay of transmitter release produced by the focal application of TTX to the presynaptic nerve terminal (Katz and Miledi, 1968). Thus, our working assumption is that high concentrations of PIIIA can attenuate the action potential in the nerve terminal. If the reduction in the endplate current is used as an index of the potency of PIIIA in

Table 1. Comparison of sequence of μ-PIII to previously known μ-conotoxins

	↓
μ-PIIIA	ZRL**C**C**G**FOKS**C**RSRQ**C**KOHR**C**C*
	5 10 15 20
	↓
μ-GIIIA	RD**C**C**T**OOKK**C**KDRQ**C**KOQR**C**C**A***
μ-GIIIB	RD**C**C**T**OORK**C**KDRR**C**KOMK**C**C**A***
μ-GIIIC	RD**C**C**T**OOKK**C**KDRR**C**KOLK**C**C**A***

Disulfide Bonding

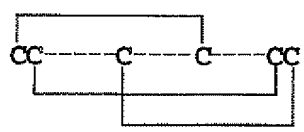

Z = pyroglutamate; O = 4-*trans*-hydroxyproline. Arrow, Arg residue postulated to be critical for biological activity. Asterisk indicates amidated C terminus; the amidation for GIIIC was not directly determined but is inferred by homology.

this regard, it can be estimated from the data in Figure 4 that the IC_{50} of the toxin is ~10 μM. These effects of PIIIA, unlike its block of the muscle action potential, are reversible, however. This makes μ-PIIIA a most convenient pharmacological tool for studying synaptic events at the amphibian neuromuscular junction—it is the only known agent to inhibit muscle Na channels irreversibly (and therefore muscle action potential and attendant muscle twitching) in a selective manner.

Compared with μ-GIIIA, μ-conotoxin PIIIA appears to target a wider spectrum of mammalian voltage-gated sodium channel subtypes in the mammalian CNS. μ-PIIIA reversibly blocked the TTX-sensitive rat brain Type II Na channel with an IC_{50} of 0.64 μM; in contrast, this channel was relatively μ-GIIIA-resistant (IC_{50} ~29.4 μM). In addition, μ-conotoxin PIIIA was able to displace a larger fraction of specific [^{3}H]STX binding to high-affinity rat brain sites than could μ-GIIIA. However, not all [^{3}H]STX binding sites could be displaced by μ-PIIIA even at high peptide concentrations, suggesting that μ-PIIIA discriminates among different classes of [^{3}H]STX binding sites in the mammalian CNS.

At the present time, voltage-gated sodium channels are distinguished primarily *in situ* by their tetrodotoxin sensitivity. The discovery and characterization of μ-conotoxin PIIIA described above provide the basis for subdividing the tetrodotoxin-sensitive sodium channels into three categories, distinguishable by their differential sensitivity to two μ-conotoxins:

(1) Voltage-gated sodium channels that are sensitive to both μ-PIIIA and μ-GIIIA. An example of this subtype is the skeletal muscle subtype in both frog and mammalian systems. The binding data in Figure 7 are suggestive that there are CNS sodium channels that also may fit into this category, but this would represent only a minor fraction of the total STX/TTX-sensitive voltage-gated sodium channels present in adult rat brain.

(2) Voltage-gated sodium channels that are sensitive to both TTX and μ-PIIIA but that are significantly more resistant to μ-GIIIA. Rat brain Type II sodium channels apparently belong to this category.

(3) Finally, both the binding and electrophysiological data strongly suggest that a significant fraction of tetrodotoxin-sensitive sodium channels will be resistant to both μ-PIIIA and μ-GIIIA at micromolar concentrations of these toxins. The binding data indicate that a major fraction of the total CNS sodium channels falls into this category.

The discovery of μ-conotoxin PIIIA suggests that the μ-conotoxin peptide family may be broadly distributed in *Conus* species. Different μ-conotoxin sequence variants that remain to be discovered in the ~500 species of *Conus* may be expected to exhibit different affinities for the various subtypes of voltage-gated sodium channels. The μ-conotoxins should prove to be a useful class of ligands for dissecting the role of Na channel subtypes in neurons or circuits when multiple molecular forms of voltage-gated Na channels are present.

REFERENCES

Becker S, Atherton E, Gordon RD (1989) Synthesis and characterization of μ-conotoxin IIIA. Eur J Biochem 185:79–84.

Becker S, Prusak-Sochaczewski E, Zamponi G, Beck-Sickinger AG, Gordon RD, French RJ (1992) Action of derivatives of μ-conotoxin GIIIA on sodium channels. Single amino acid substitutions in the toxin separately affect association and dissociation rates. Biochemistry 31:8229–8238.

Catterall WA (1992) Cellular and molecular biology of voltage-gated sodium channels. Physiol Rev 72:S15–S48.

Colledge CJ, Hunsperger JP, Imperial JS, Hillyard DR (1992) Precursor structure of ω-conotoxin GVIA determined from a cDNA clone. Toxicon 30:1111–1116.

Cruz LJ, Gray WR, Olivera BM, Zeikus RD, Kerr L, Yoshikami D, Moczydlowski E (1985) *Conus geographus* toxins that discriminate between neuronal and muscle sodium channels. J Biol Chem 260:9280–9288.

Doyle DD, Guo Y, Lustig SL, Satin J, Rogart RB, Fozzard HA (1993) Divalent cation competition with [^{3}H]saxitoxin binding to tetrodotoxin-resistant and -sensitive sodium channels. J Gen Physiol 101:153–182.

Dudley SC, Todt H, Lipkind G, Fozzard HA (1995) A μ-conotoxin-insensitive Na channel mutant: possible localization of a binding site at the outer vestibule. Biophys J 69:1657–1665.

French RJ, Prusak-Sochaczewski E, Zamponi GW, Becker S, Kularatna AS, Horn R (1996) Interactions between a pore-blocking peptide and the voltage sensor of the sodium channel: an electrostatic approach to channel geometry. Neuron 16:407–413.

Gray WR (1993) Disulfide structures of highly bridged peptides: a new strategy for analysis. Protein Sci 2:1732–1748.

Hillyard DR, Monje VD, Mintz IM, Bean BP, Nadasdi L, Ramachandran J, Miljanich G, Azimi-Zoonooz A, McIntosh JM, Cruz LJ, Imperial JS, Olivera BM (1992) A new *Conus* peptide ligand for mammalian presynaptic Ca^{2+} channels. Neuron 9:69–77.

Hopkins C, Grilley M, Miller C, Shon K-J, Cruz LJ, Gray WR, Dykert J, Rivier J, Yoshikami D, Olivera BM (1995) A new family of *Conus* peptides targeted to the nicotinic acetylcholine receptor. J Biol Chem 270:22361–22367.

Katz B, Miledi R (1968) The effect of local blockage of motor nerve terminals. J Physiol (Lond) 199:729–741.

McIntosh JM, Hasson A, Spira ME, Li W, Marsh M, Hillyard DR, Olivera BM (1995) A new family of conotoxins which block sodium channels. J Biol Chem 270:16796–16802.

Narahashi T, Moore JW, Scott WR (1964) Tetrodotoxin blockage of sodium conductance increase in lobster giant neurons. J Gen Physiol 47:965–974.

Noda M, Ikeda T, Kayano T, Suzuki H, Takeshima H, Karusaki M, Takahashi H, Numa S (1986) Existence of distinct sodium channel messenger RNAs in rat brain. Nature 320:188–191.

Olivera BM, Gray WR, Zeikus R, McIntosh JM, Varga J, Rivier J, de Santos V, Cruz LJ (1985) Peptide neurotoxins from fish-hunting cone snails. Science 230:1338–1343.

Olivera BM, Hillyard DR, Rivier J, Woodward S, Gray WR, Corpuz G, Cruz LJ (1990) Conotoxins: targeted peptide ligands from snail venoms. In: Marine toxins: origin, structure and molecular pharmacology (Hall S, Strichartz G, eds), pp 256–278. Washington, DC: American Chemical Society.

Olivera BM, Miljanich G, Ramachandran J, Adams ME (1994) Calcium channel diversity and neurotransmitter release: the ω-conotoxins and ω-agatoxins. Annu Rev Biochem 63:823–867.

Sato K, Ishida Y, Wakamatsu K, Kato R, Honda H, Ohizumi Y, Nakamura H, Ohya M, Lancelin J-M, Kohda D, Inagaki F (1991) Active site μ-conotoxin GIIIA, a peptide blocker of muscle sodium channels. J Biol Chem 266:16989–16991.

Sato S, Nakamura H, Ohizumi Y, Kobayashi J, Hirata Y (1983) The amino acid sequences of homologous hydroxyproline containing myotoxins from the marine snail *Conus geographus* venom. FEBS Lett 155:277–280.

Shon K, Grilley MM, Marsh M, Yoshikami D, Hall AR, Kurz B, Gray WR, Imperial JS, Hillyard DR, Olivera BM (1995) Purification, characterization, and cloning of the lockjaw peptide from *Conus purpurascens* venom. Biochemistry 34:4913–4918.

Stone BL, Gray WR (1982) Occurrence of hydroxyproline in a toxin from the marine snail *Conus geographus*. Arch Biochem Biophys 216:756–767.

Stühmer W (1992) Electrophysiological recordings from *Xenopus* oocytes. Methods Enzymol 207:319–339.

Trimmer JS, Cooperman SS, Tomiko SA, Zhou J, Crean SM, Boyle MB, Kallen RG, Sheng Z, Barchi L, Sigworth FJ, Goodman RH, Agnew WS, Mandel G (1989) Primary structure and functional expression of a mammalian skeletal muscle sodium channel. Neuron 3:33–49.

Woodward SR, Cruz LJ, Olivera BM, Hillyard DR (1990) Constant and hypervariable regions in conotoxin propeptides. EMBO J 1:1015–1020.

Yoshikami D, Bagabaldo Z, Olivera BM (1989) The inhibitory effects of omega-conotoxins on calcium channels and synapses. Ann NY Acad Sci 560:230–248.

EXHIBIT 12

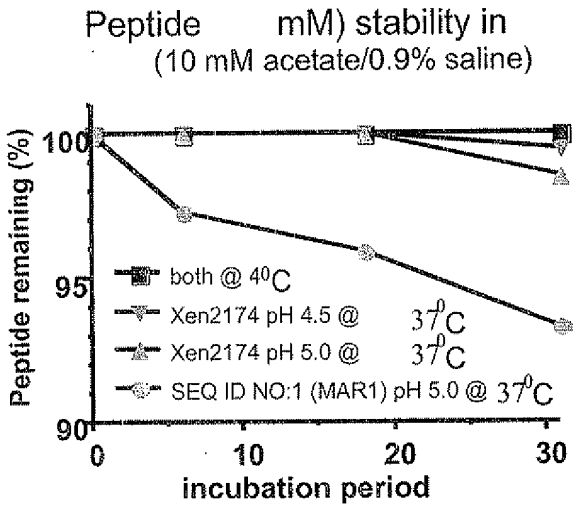

Figure 1: Chemical stability in buffer (10 mM acetate/0.9% saline) of Xen2174 and SEQ ID NO: 1 (also known as Mar1 or χ-MrIA). The stability was determined at 4°C and 37°C (the temperature that an implanted pump would adopt).

EXHIBIT 13

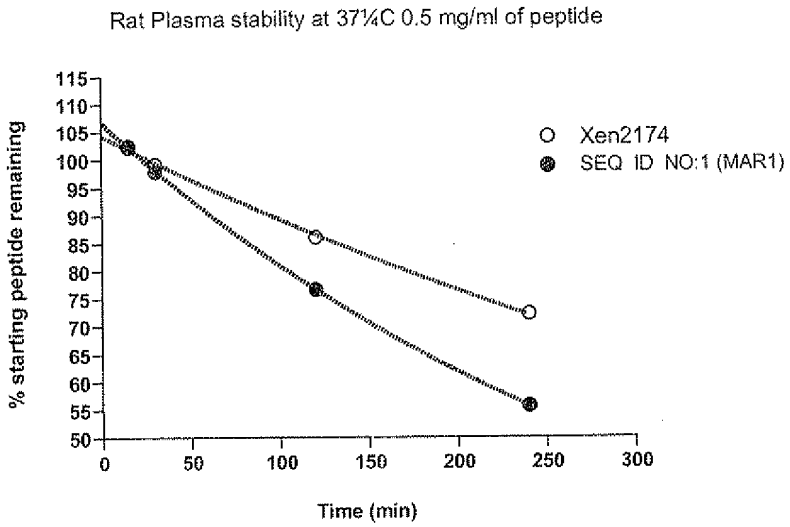

	Xen2174	SEQ ID NO:1 (MAR1)
One phase exponential decay		
Best-fit values		
SPAN	100.0	100.0
K	0.001631	0.002986
PLATEAU	4.311	6.733
HalfLife	425.1	232.1
Std. Error		
K	4.181e-005	1.888e-005
PLATEAU	0.4026	0.1392
95% Confidence Intervals		
K	0.001451 to 0.001810	0.002905 to 0.003068
PLATEAU	2.579 to 6.044	6.134 to 7.332
HalfLife	382.9 to 477.8	226.0 to 238.6
Goodness of Fit		
Degrees of Freedom	2	2
R squared	0.9991	1.000
Absolute Sum of Squares	0.4884	0.04981
Sy.x	0.4942	0.1578
Constraints		
SPAN	SPAN = 100.0	SPAN = 100.0
K	K > 0.0	K > 0.0

Figure 2: Rat plasma stability – comparing Xen2174 and SEQ ID NO: 1 (also known as Mar1 or χ-MrIA) at a concentration of 0.5 mg/mL at 37°C.

EXHIBIT 14

Table 1: Summary of animal efficacy and side effect data in a CCI rat model of neuropathic pain. Peptides delivered as a single bolus intrathecal dose.

Peptide	In vitro potency c.f. Mar1	In vivo dose	Therapeutic window	Comments
SEQ ID NO: 11 where Xaa1 refers to D-arg, Xaa3 refers to 4-hydroxyproline (rGVCCGYKLCHOC-NH_2)	≈ x 5	1nmol	narrow	The antiallodynic effects of i.t. SEQ ID NO: 11 where Xaa1 refers to D-arg, Xaa3 refers to 4-hydroxyproline (1 nmol) in CCI-rats peaked at 0.75 h and lasted > 3 h. In the contralateral paw antinociception peaked at 0.25 h and lasted around 3 h. Side-effects included an arched back posture, a brief period of intermittent grooming behaviour, very brief head twitching in one rat, intermittent staring behaviour and sedation. Apnoea was also observed in one of three rats tested. Although the apparent potency of SEQ ID NO: 11 where Xaa1 refers to D-arg, Xaa3 refers to 4-hydroxyproline appears to be higher than that of SEQ ID NO:1 (also known as Mar1 or χ-MrIA) (new batch) and with a longer duration of action, the side-effect profile was inferior. Based on these findings, SEQ ID NO: 1 (also known as Mar1 or χ-MrIA) appears to have a superior therapeutic window relative to SEQ ID NO: 11 where Xaa1 refers to D-arg, Xaa3 refers to 4-hydroxyproline.
SEQ ID NO: 11 where Xaa1 refers to D-asn, Xaa3 refers to 4-hydroxyproline (nGVCCGYKLCHOC-NH_2)	X 1.0	1nmol	narrow	SEQ ID NO: 11 where Xaa1 refers to D-asn, Xaa3 refers to 4-hydroxyproline administered in an i.t. dose of 1 nmol produced moderate levels of pain relief in CCI-rats in the ipsilateral hindpaw that had a relatively slow onset of action (peak response at 1 h post-dosing) and a relatively long duration of action (≈ 3 h). The anti-allodynic potency in the ipsilateral hindpaw is greater than the antinociceptive potency in the contralateral hindpaw, which is a desirable attribute for a potential therapeutic treatment for the alleviation of neuropathic pain. The side-effect profile produced by SEQ ID NO: 11 where Xaa1 refers to D-asn, Xaa3 refers to 4-hydroxyproline indicates that SEQ ID NO: 1 (also known as Mar1 or χ-MrIA) has a superior therapeutic window, when these compounds are given in equi-effective doses by the i.t. route.
SEQ ID NO: 11 where Xaa1 refers to norleucine, Xaa3 refers to 4-hydroxyproline ([NLE]GVCCGYKLCHOC-NH_2)	X 3	1nmol	narrow	SEQ ID NO: 11 where Xaa1 refers to norleucine, Xaa3 refers to 4-hydroxyproline administered in an i.t. dose of 1 nmol produced relatively high levels of pain relief in CCI-rats in the ipsilateral hindpaw that peaked at 5 min post dosing and had a short duration of action (≈ 0.5 h). Low levels of antinociception were produced in the contralateral hindpaw of the same rats with peak antinociception observed at 5 min post-dosing and a duration of action of approx. 0.5 h. The side-effect profile produced by SEQ ID NO: 11 where Xaa1 refers to norleucine, Xaa3 refers to 4-hydroxyproline indicates that SEQ ID NO: 1 (also known as Mar1 or χ-MrIA) has a superior therapeutic window.
Xen2174 ([Glp]GVCCGYKLCHOC-NH_2)	X 1.0	1nmol	High (~30)	Xen2174 administered in an i.t. dose of 1 nmol produced relatively high levels of pain relief in CCI-rats in the ipsilateral hindpaw that peaked at 30 min post dosing and had a relatively long duration of action (> 3 h). Although relatively high levels of antinociception were produced in the contralateral hindpaw of the same rats, there was a higher apparent potency in the ipsilateral hindpaw; this is desirable. Xen2174 appears to have a therapeutic window appears similar to that of SEQ ID NO: 1 (also known as Mar1 or χ-MrIA).

EXHIBIT 15

Table 2: Comparison of hNET binding affinities of chi to peptide Q819.

Peptide Name	**Sequence**	**Ki (μM)**
SEQ ID NO: 1 (Mar1, MrIA)	NGVCCGYKLCHOC-NH_2	2.2
Xen2174 (C-term amidated SEQ ID NO: 4)	UGVCCGYKLCHOC-NH_2	3.0
Q819 (SEQ ID NO: 6)	QTCCGYRMCVPCR-NH_2	> 100
Q819 with Glp at N-terminus	UTCCGYRMCVPCR-NH_2	> 100